STUDIES ON INFLUENZA A VIRUS PB1-F2 PROTEIN

Sandra Vater

A Thesis Submitted for the Degree of PhD
at the
University of St. Andrews

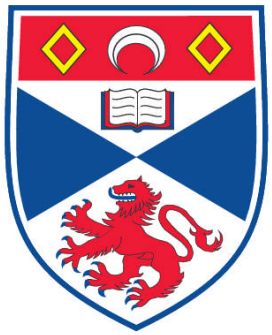

2011

STUDIES ON INFLUENZA A VIRUS PB1-F2 PROTEIN

SANDRA VATER

Biomedical Sciences Research Complex
University of St. Andrews
St Andrews, UK

Submitted for the degree of Doctor of Philosophy in Molecular Virology

August 2011

Abstract

The influenza A virus genome codes for up to 12 proteins. Segment 2 encodes three proteins, the polymerase subunit PB1, a small protein PB1-F2 and an N-terminally truncated version of PB1 called N40. Different functions have been reported for PB1-F2 such as induction of apoptosis, regulation of the viral polymerase activity, enhancement of secondary bacterial infections and modulation of the innate immune system. So far, no function has been ascribed to N40.

To study PB1-F2 in more detail, its coding sequence was deleted from its original position and inserted downstream of the PB1 (segment 2), NA (segment 6) or M (segment 7) open reading frames (ORF) employing different strategies, including the use of an overlapping Stop-Start cassette, a duplicated promoter sequence and the self-cleaving 2A peptide derived from foot-and-mouth disease virus. Viruses with bicistronic segments were rescued and tested for their ability to express PB1-F2. Whereas no expression of PB1-F2 was detected from bicistronic segments 2 and 7, expression of PB1-F2 from segment 6 was observed in high levels. However, the phenotype of all these viruses was similar to that of viruses lacking PB1-F2 which made mutational analysis of PB1-F2 not worthwhile.

Previously, the function of PB1-F2 was mainly studied using a virus deficient in PB1-F2 production but showing increased N40 expression. In the present study, recombinant WSN viruses lacking either PB1-F2 or N40, or both proteins were engineered and the effects of these mutations on the viral life cycle were examined. Viruses deficient for PB1-F2 that overexpressed N40 showed the most attenuated phenotype, whereas the loss of PB1-F2 alone did not obviously affect virus replication. Reduced viral polymerase activity was observed for viruses lacking N40, however attenuation *in vivo* was only seen in combination with the loss of PB1-F2. Neither the loss of PB1-F2 nor N40 alone had a great impact, but changes in the expression level of both proteins were disadvantageous for the virus. Increased levels of N40 shifted the polymerase activity towards replication, suggesting a new function for N40.

Thus, it was shown that the segment 2 gene products and their expression level influence viral replication and pathogenicity, and a careful design of mutant recombinant viruses is vital for determining the experimental outcome.

Declarations

I, **Sandra Vater**, hereby certify that this thesis (which is approximately **50,000** words in length, excluding bibliography) has been written by me, that it is the record of work carried out by me, and that it has not been submitted in any previous application for a higher degree.

Date .....Signature of candidate .....

I was admitted as a research student in September 2007 as a candidate for the degree of **Doctor of Philosophy (PhD) in Molecular Virology**; the higher study for which this is a record and was carried out at the University of St. Andrews between 2007 and 2011.

Date ..... Signature of candidate .....

I hereby certify that the candidate has fulfilled the conditions of the Resolution and Regulations appropriate for the degree of Doctor of Philosophy at the University of St. Andrews, and that the candidate is qualified to submit this thesis in application for that degree.

Date ..... Signature of supervisor .....

Prof. R.M. Elliott

In submitting this thesis to the University of St Andrews I understand that I am giving permission for it to be made available for use in accordance with the regulations of the University Library for the time being in force, subject to any copyright vested in the work not being affected thereby. I also understand that the title and the abstract will be published, and that a copy of the work may be made and supplied to any *bona fide* library or research worker, that my thesis will be electronically accessible for personal or research use unless exempt by award of an embargo as requested below, and that the library has the right to migrate my thesis into new electronic forms as required to ensure continued access to the thesis. I have obtained any third-party copyright permissions that may be required in order to allow such access and migration, or have requested the appropriate embargo below.

The following is an agreed request by candidate and supervisor regarding the electronic publication of this thesis:
Access to printed copy and electronic publication of thesis through the University of St Andrews.

Date ..... Signature of candidate .....

Date ..... Signature of supervisor .....
Prof. R.M. Elliott

Acknowledgements

Most importantly, I would like to thank my supervisor Professor Richard Elliott, for all his advice, support, patience and stimulating discussions and for having an open door at any time.

Thanks to Marieke Hoeve at the University of Edinburgh for her assistance with the macrophage assay and the flow cytometry and to Bernadette Dutia and her lab at the University of Edinburgh for their help with all the mouse experiments.

Also a special thank to all members of the RME lab, past and present, for their invaluable practical help and the supportive supply of coffee and chocolate in our office: Agnieszka, Angela, Basma, Ben, Beryl, Charlie, Daisy, Elina, Gjon, Ing, Jill, Laura, Ping, Sophie, Steve and Xiaohong.

My deepest thanks go to my parents, my sister and my friends for their emotional help, encouragement and unwavering belief in me. And Markus: you provided the best motivation to complete this work.

This work was funded by ICHAIR (Interdisciplinary Centre for Human & Avian Influenza Research) and the BBSRC.

Contents

List of Figures

List of Tables

Abbreviations

293FT	Highly transfectable clone derived from human embryonal kidney cells
A549	Adenocarcinomic human alveolar basal epithelial cell line
aa	Amino acid
ADV	Adenovirus
AEV	Avian encephalomyelitis virus
Ala	Alanine (A)
ANT	Adenine nucleotide translocator
AP	Alkaline Phosphatase
APV	Avian pneumovirus
Arg	Arginine (R)
ASFV	African swine fever virus
Asn	Asparagine (N)
Asp	Aspartic acid (D)
Bak	Bcl-2 homologous antagonist killer
Bax	Bcl-2associated X protein
Bcl-2	B-cell lymphoma 2
Bcl-xL	B-cell lymphoma-extra large
BCV	Baculovirus
BLV	Bovine leukemia virus
BM2	Influenza B virus matrix protein 2
BSA	Bovine serum albumin
CAT	Chloramphenicol acetyltransferase
CARD	Caspase activation and recruitment domains
Cardif	CARD adaptor inducing IFN-β
cDNA	Complementary DNA
CMV	Cytomegalovirus
cRNA	Complementary RNA

CRS	Caspase recognition site
CTD	C-terminal domain of the cellular RNA polymerase II
Cys	Cysteine (C)
DMEM	Dulbecco's modified Eagle medium
DIs	Defective interfering particles
dNTP	Deoxyribonucleotide triphosphate
dpi	Days post infection
dsDNA	Double stranded DNA
EBNA	Epstein-Barr nuclear antigen
EBV	Epstein-Barr virus
E.coli	*Eschericia coli*
EDTA	Ethylenediaminetetraacetic acid
Env	Envelope glycoprotein complex
FBS	Fetal bovine serum
FCV	Feline calicivirus
FMDV	Foot-and-mouth disease virus
FPV	Fowlpox virus
GFP	Green fluorescent protein
Glu	Glutamic acid (E)
Gln	Glutamine (Q)
Gly	Glycine (G)
GM-CSF	Granulocyte-macrophage colony stimulating factor
GUS	β-glucuronidase
γ**HV-68**	γ-Herpesvirus 68
HA	Hemagglutinin
HBV	Hepatitis B virus
HBx	HBV X protein
HCV	Hepatitis C virus
HHV-8	Human herpesvirus 8
His	Histidine (H)
HIV-1	Human immunodeficiency virus 1
hpi	Hours post infection
HPN	Herpesvirus pan
HPO	Herpesvirus papio
HPR	Horseradish peroxidase
HPV	Human papillomavirus
HTLV-1	Human T lymphotropic virus 1

hvPR8	High-virulent variant of A/PR/8/34
HVS	Herpesvirus saimiri
IAV	Influenza A virus
IFN	Interferon
IL	Interleukin
Ile	Isoleucine (I)
IMDM	Iscove's Modified Dulbecco's Medium
IPS-1	Interferon-β promoter stimulator 1
IRF-3	Interferon regulatory factor 3
JAK	Janus Kinase
JUNV	Junin Virus
kbp	Kilo base pair
kDa	Kilodalton
KSBcl-2	Kaposi sarcoma Bcl-2
LB	Luria-Bertani medium
LCMV	Lymphocytic choriomeningitis virus
Leu	Leucine (L)
lvPR8	Low-virulent variant of A/PR/8/34
Lys	Lysine (K)
M1	Matrix protein 1
M2	Matrix protein 2
MAVS	Mitochondrial antiviral signaling
M-CSF	Macrophage colony-stimulating factor
MDCK	Madin-Darby Canine Kidney epithelial cell line
Met	Methionine (M)
MMP	Mitochondrial membrane permeabilisation
MOI	Multiplicity of infection
MTOC	Microtubule-organizing center
mRNA	Messenger RNA
MXV	Myxoma virus
NaCl	Sodium chloride
NA	Neuraminidase
$NaHCO_3$	Sodium bicarbonate
NAT	N-acetyl trypsin
NEP	Nuclear export protein
NeuAcα2,3Gal	N-acetylneuraminic acid linked to galactose by α2,3-linkage

NeuAcα2,6Gal	N-acetylneuraminic acid linked to galactose by α2,6-linkage
NFκB	Nuclear factor kappa-light-chain-enhancer of activated B cells
NP	Nucleoprotein
NS1	Nonstructural protein 1
o/n	Overnight
ORF	Open reading frame
P	Phosphoprotein P
PA	Polymerase acidic protein
PAMPs	Pathogen-associated molecular patterns
PB1	Polymerase basic protein 1
PB2	Polymerase basic protein 2
PBS	Phosphate-buffered saline
PCR	Polymerase chain reaction
pfu	Plaque-forming unit
Phe	Penylalanine (F)
pi	Post-infection
PI	Propidium iodide
PLV	Poliovirus
PPVO	Parapoxvirus ORF virus
Pro	Proline (P)
PTPC	Permeability transition pore complex
PVM	Pneumovirus of mice
RAW/W	Mouse leukaemic monocyte macrophage cell line
RdRp	Viral RNA-dependent RNA polymerase
RHDV	Rabbit haemorrhagic disease virus
RID	Receptor internalization and degradation complex
RIG-I	Retinoic acid inducible gene I
RNA	Ribonucleic acid
RNAPII	Cellular DNA-dependent RNA polymerase II
RNP	Ribonucleprotein
rpm	Revolutions per minute
RSV	Respiratory syncytial virus
SARS-CoV	Severe acute respiratory syndrome coronavirus
SDS	Sodium Dodecyl Sulfate
Ser	Serine (S)

SOCS	Suppressor of cytokine signaling
STAT	Signal Transducer and Activator of Transcription
StSt	Overlapping Stop-Start pentanucleotide UAAUG
T4 PNK	T4 Polynucleotide Kinase
TAE	Tris-acetate-EDTA
TBE	Tris-borate-EDTA
Thr	Threonine (T)
TGF-β	Transforming Growth Factor β
TRIM	TRIpartite interaction Motif
Trp	Tryptophane (W)
Tyr	Tyrosine (Y)
Udo	Influenza A virus A/Udorn/72
VACV	Vaccinia virus
Val	Valine (V)
VDAC	Voltage-dependent anion channel
vIAPs	Viral inhibitor of apoptosis proteins
vICA	Viral inhibitor of caspase-8 activation
VISA	Virus-induced signaling adaptor
vMAP	Viral mitochondrial antiapoptotic protein
VP0c	VP0 protein of Mengo virus
Vpr	Viral protein R
vRNA	Viral RNA
VSV	Vesicular stomatitis virus
v/v	Volume per volume
WDSV	Walleye dermal sarcoma virus
WNV	West Nile virus
WSN	Influenza A virus A/WSN/33
WT	Wild type
w/v	Weight per volume

Chapter 1

INTRODUCTION

Aims of Chapter 1

This chapter provides an introduction on influenza A viruses (IAV), including some general aspects such as virus structure, genome organisation and viral life cycle. More specifically, it contains information about PB1-F2, however, this particular part only covers the knowledge until 2007, when this project was started. This is because the recent findings on PB1-F2 and the discovery of a 12th protein expressed by influenza A viruses changed the project in certain ways. Therefore, recent findings on IAV segment 2 made after 2007 can be found in the individual results Chapters and in Chapter 7 (Conclusions). Furthermore, an overview of reverse genetics is given, as this provides the foundation of the presented work.

1.1 General information on influenza A viruses

1.1.1 *Orthomyxoviridae*: Classification and taxonomy

The name *Orthomyxoviridae* originates from the Greek words *orthos*, meaning ”standard” or ”straight”, and *myxa* meaning ”mucus”. The spherical to pleomorphic shaped virions possess a helical nucleocapsid, which is enveloped by a host cell membrane-derived lipid layer. The International Committee on Taxonomy of Viruses (ICTVdB, 2009) lists 5 genera of vertebrate viruses in the family *Orthomyxoviridae*: three genera of influenza viruses (*Influenza virus A*, *B* and *C*), *Thogotovirus* (Leahy et al., 1997; Pringle, 1996) and *Isavirus* (Krossøy et al., 1999). A number of other viruses was suggested to be part of the *Orthomyxoviridae* family (Silva et al., 2005; Presti et al., 2009). All members have a linear negative single-stranded RNA genome composed of six to eight segments (Table 1.1). Replication takes place in the nucleus of infected cells.

Genus	Species	Segments
Influenzavirus A	***Influenza A virus***	8
Influenzavirus B	***Influenza B virus***	8
Influenzavirus C	***Influenza C virus***	7
Thogotovirus	***Thogoto virus***	6
	Dhori virus	7
Isavirus	***Infectious Salmon Anemia virus***	8

Table 1.1: *Orthomyxoviridae*: Summary of the characterised genera and their species and numbers of genome segments. The type species of each genus is shown in bold.

The classification of influenza viruses into three types (A, B and C) is made on antigenic features of the matrix protein M1 and the nucleoprotein (Knipe et al., 2001). Influenza A viruses are further divided into subtypes due to the antigenic characteristics of the two surface glycoproteins hemagglutinin (HA) and neuraminidase (NA). So far, 16 HA and nine NA subtypes are known (Fouchier et al., 2005; Laver et al., 1984). Influenza viruses are able to exchange segments (reassortment) following dual

infection of the same cell, which can lead to the development of new subtypes. Influenza A viruses can infect a broad range of host species, however, aquatic birds are the natural reservoir. Influenza B viruses are only found in humans and seals (Osterhaus et al., 2000). Although no different subtypes for influenza B viruses exist, they are also capable for reassortment in nature to form different strains (McCullers et al., 1999). Influenza C viruses possess only 7 RNA segments due to the nature of the glycoprotein hemagglutinin-esterase (HEF), which combines three functions: receptor-binding (hemagglutination), receptor-destroying (esterase) and fusion (Herrler et al., 1988). Antigenic and sequence differences are not sufficient to separate this genus into subtypes. The *Thogotovirus* genus contains two species: Thogoto virus and Dhori virus. They are insect-borne viruses that infect both insects and vertebrates. The genome of Thogoto viruses consist of 6 segments whereas Dhori viruses contain 7 segments. No protein analogs for neuraminidase or non-structural protein (NS) have been found (Macken et al., 2001). Infectious salmon anemia virus is the only known species in the genus *Isavirus*. The virus infects Atlantic salmon (*Salmo salar*) and has therefore a great negative financial impact in aqua culture (Scheel et al., 2007).

1.1.2 Structure of influenza A viruses

Influenza A virus is one of the major human pathogens with the capability to cause epidemics and pandemics. According to the World Health Organisation (WHO) it is believed that influenza A viruses infect about 5-15% of the world's population every year and 300,000 - 500,000 people worldwide die as a consequence of the infection (Kamps, 2006). Due to a high mutation rate of the low fidelity viral polymerase and the ability to reassort, antigenically novel influenza A viruses can emerge. If they encounter an immunologically naïve population the morbidity and mortality rate can be much higher (Digard et al., 2009).

The spherical to filamentous virus particles have an average diameter of 100 nm, but can be up to 20-30 µm in length (Roberts and Compans, 1998; Simpson-Holley et al., 2002). Each virus comprises 8 segments of negative sense RNA (Figure 1.1). The viruses are enclosed by a lipid envelope that derives from the host cell. Embedded within this envelope are the two viral glycoproteins, hemagglutinin and neuraminidase, and the matrix protein 2

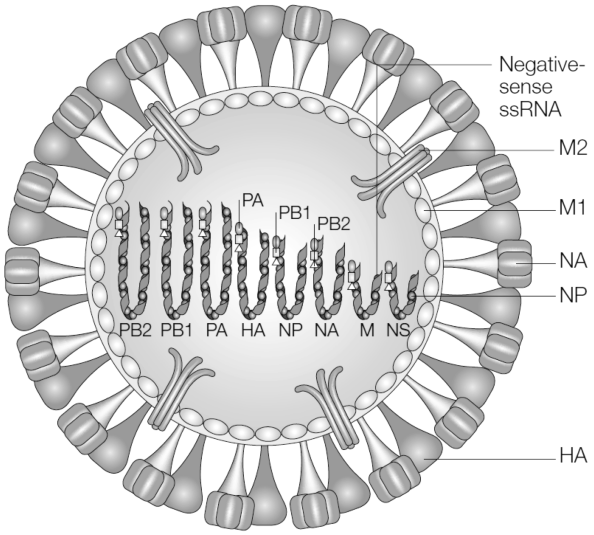

Figure 1.1: Schematic diagram of an influenza virus particle: In the center of the virion are the eight negative sense RNA segments. Each segment is covered by a number of copies of the nucleoprotein and one copy of each polymerase subunit. These so-called RNPs are surrounded by a layer of matrix protein 1 and a lipid envelope that derives from the host cell. Within this lipid envelope the two viral glycoproteins, hemagglutinin and neuraminidase, are incorporated as well as the matrix protein 2. Picture taken from Horimoto and Kawaoka (2005).

(Zebedee et al., 1985; Lamb et al., 1985; Cox et al., 2005). M2 is an ion channel protein and is required for acidification of the virus particle during cell entry (Pinto et al., 1992). Below the lipid envelope is a layer of the matrix protein 1 (Ruigrok et al., 1989). In the center of the virion are the so-called ribonucleoproteins (RNPs), each consisting of one RNA segment. The RNA is covered by a number of nucleoprotein molecules. Also attached to each segment is a polymerase complex, which is composed of the three polymerase subunits PB2, PB1 and PA. RNPs represent the minimal infectious unit, since it is necessary for negative sense RNA viruses to provide their own RNA-dependent RNA polymerase (RdRp) for replication and transcription (Huang et al., 1990; Honda et al., 2002). When looking at serially sectioned virus particles using transmission electron microscopy, the eight segments appear in an organised structure. Seven segments are in a circular array surrounding one segment in the center (Noda et al., 2006). It is not known if the middle one is a specific segment or if this varies. The ends of each RNA segment are complementary and highly conserved and are proposed to interact to form a panhandle or a ”corkscrew” structure (Hsu et al., 1987; Flick et al., 1996).

1.1.3 Influenza A virus genome and gene products

Depending on the strain, up to 12 proteins are expressed from the influenza A virus genome (Figure 1.2) (Wise et al., 2009). Hence, some of the segments encode more than one protein (Table 1.2). Whereas segment 1 and 3 to 6 are monocistronic, segments 2, 7 and 8 encode two or three proteins each.

Segment	Protein	Abbreviation
1	Polymerase basic protein 2	PB2
2	Polymerase basic protein 1	PB1
	PB1-Frame 2	PB1-F2
	N40	N40
3	Polymerase acidic protein	PA
4	Hemagglutinin	HA
5	Nucleoprotein	NP
6	Neuraminidase	NA
7	Matrix protein 1	M1
	Matrix protein 2	M2
8	Non-structural protein 1	NS1
	Nuclear export protein	NEP

Table 1.2: Influenza A virus (A/WSN/33): Segments and encoded proteins of each segment.

Segment 1 encodes one of the basic polymerase protein, PB2. PB2 is, like the two other polymerase subunits PB1 and PA, an essential part of the viral RNA-dependent RNA polymerase complex. During viral infection short 5' cap structures are cleaved from cellular pre-mRNAs and are used for initiation of viral transcription (Plotch et al., 1981). This process is known as 'cap-snatching'. One of the involved polymerase proteins is the PB2 subunit. It was shown to possess cap recognition and binding activity (Blaas et al., 1982). PB2 also plays a role in host range restriction. One confirmed

contributing amino acid is at position 627 (Subbarao et al., 1993b). In order to ”jump” from an avian host to a human host, changes of amino acid 627 from glutamic acid to lysine often occur, as seen in the recent H5N1 outbreaks in Hong Kong (Hatta et al., 2001) or with a Dutch patient infected with H7N7 (Fouchier et al., 2004).

The basic polymerase protein 1 (PB1), encoded by segment 2, is the core subunit of the polymerase complex. It binds to PB2 and PA to form an active heterotrimer. It is responsible for initiation and elongation during transcription and replication (Braam et al., 1983). PB1 recognises and binds, therefore, to the promoter region of the viral RNA (González and Ortín, 1999). By a process called leaky ribosomal scanning up to two other proteins are expressed from segment 2 mRNA. The 87 - 90 aa short pro-apoptotic protein PB1-F2 is translated from an alternative +1 ORF from most influenza A virus strains (Chen et al., 2001), and an N-terminally truncated form of the PB1 protein, called N40, is observed in infected cells (Wise et al., 2009). Segment 2 will be described in more detail in Section 1.2, as well as in Chapters 3 and 6.

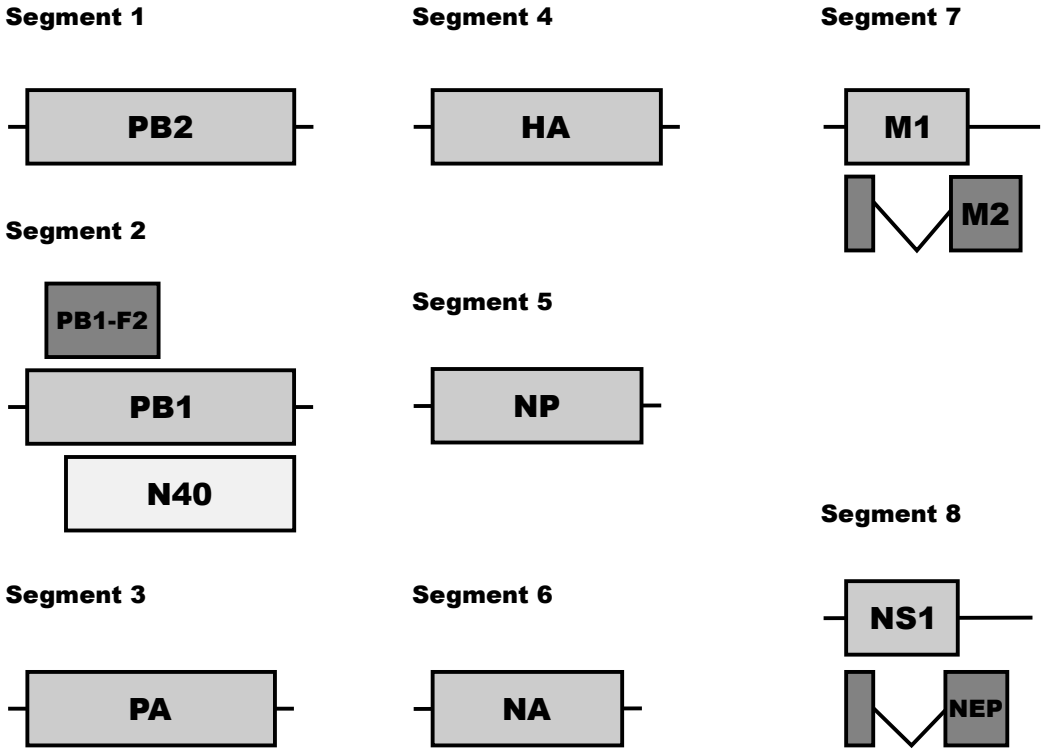

Figure 1.2: Schematic map of the influenza A virus genome: The linear segmented negative sense RNA genome encodes up to 12 proteins.

PA is the acidic polymerase subunit encoded by the third largest viral segment. In 2009 the endonuclease activity for the ”cap-snatching” process was mapped to the N-terminus of the PA subunit (Dias et al., 2009; Yuan et al., 2009).

One of the viral glycoproteins, hemagglutinin, is encoded by segment 4. HA is one of the most abundant viral proteins and it is distributed evenly on the viral surface as a homotrimer (Wiley et al., 1977). The protein facilitates binding to the cell surface by interacting with sialic acid-containing receptors. Cleavage of the HA0 precursor into two subunits, HA1 and HA2, by cellular proteases is required for infectivity (Garten and Klenk, 1983). After binding to the host cell membrane and internalisation of the particle by endocytosis, the cleaved hemagglutinin mediates membrane fusion between the endosomal membrane and the virus membrane in order to release the vRNPs into the cytoplasm (Skehel and Wiley, 2000).

The nucleoprotein, encoded on segment 5, is the most abundant protein of the ribonucleocapsid. The RNA-binding groove is composed of a number of highly conserved basic residues that are spread over the primary sequence of NP but cluster between the head and the body domain of the folded protein (Ye et al., 2006). The RNA is believed to wrap around NP which acts as a scaffold. Several signals on the nucleoprotein regulate the import and export of vRNPs into the nucleus (O'Neill et al., 1995; Neumann et al., 1997). Whereas the protein localises to the nucleus early in infection, localisation is mainly cytoplasmic late in infection. This process is regulated by phosphorylation of NP (Neumann et al., 1997; Bullido et al., 2000).

The second viral glycoprotein is neuraminidase, which is encoded on segment 6. Beside HA, NA is the major antigen of the influenza A virus. The protein forms a homotetramer on the virus surface and is responsible for the release of progeny virus particles from the cell by its sialidase activity.

Segment 7 encodes the two matrix proteins 1 and 2. M1 is the most abundant protein in the virus particle that, amongst other factors, determines the morphology of the virion (Roberts et al., 1998b; Bourmakina and García-Sastre, 2005). M1 was also shown to be important for the nuclear export of vRNPs (Whittaker et al., 1996). It functions as a bridge between vRNPs and the lipid envelope by interacting with both (Gregoriades, 1980; Sakaguchi et al., 2003). The small ion channel protein M2 is translated from a spliced mRNA transcribed from the same segment. It forms a homotetramer and localises to the lipid envelope (Holsinger and Lamb,

1991; Lamb et al., 1985). M2 is activated by low pH in the late endosome and permits protons to enter the virus particle, which leads to a process known as uncoating (Pinto et al., 1992; Sugrue et al., 1990).

The smallest viral segment is, like segment 7, bicistronic. The non-structural protein NS1 is the major virulence factor. Although it is small, it is a multifunctional protein, but it mainly functions as an interferon (IFN) antagonist (García-Sastre et al., 1998; Hale et al., 2008). It inhibits the export and splicing of host-cell mRNAs, which leads to host cell protein shut-off (Alonso-Caplen et al., 1992; Chen and Krug, 2000; Krug et al., 2003). NS1 maintains all these functions by a large number of interactions with host cell proteins. The second protein expressed from segment 8 is called NEP and is translated from spliced mRNA. It contains a nuclear export signal (NES) and deletion of the protein causes retention of RNPs in the nucleus. Therefore, it was suggested that NEP functions as a nuclear export protein for RNPs by binding to them via the matrix protein M1 (O'Neill et al., 1998; Shimizu et al., 2011). Further, it was proposed that NEP is involved in transcription and replication because it was shown to alter the levels of viral RNA species synthesised in a ribonucleoprotein reconstitution assay (Robb et al., 2009).

1.1.4 Influenza A virus life cycle

Human influenza viruses establish disease primarily in the upper respiratory tract in epithelial cells. The specificity of HA to bind to host cell receptors differs amongst influenza A viruses. Human viruses prefer N-acetylneuraminic acid linked to galactose by α2,6-linkage (NeuAcα2,6Gal) which is present on bronchial epithelial cells in the upper respiratory tract (Shinya et al., 2006). Avian influenza viruses in contrast preferentially bind to sialic acids containing NeuAcα2,3Gal linkages present in the intestine of birds and in the lower respiratory tract of humans (Rogers et al., 1983; Rogers and Paulson, 1983; van Riel et al., 2006). After binding to the host cell membrane by the hemagglutinin the virus is taken up by the cell via endocytosis (Matlin et al., 1981). By lowering the endosomal pH, the host cell attempts to denature the viral particles. However, instead of destroying the virus, this lower pH helps the virus to translocate the vRNPs from the endosome into the cytoplasm. A conformational change in the hemagglutinin protein leads to the fusion of the viral and the endosomal

membrane (Skehel et al., 1982). Acidification of the virus particle mediated by the M2 ion channel results in the release of the vRNPs into the cytoplams (Pinto et al., 1992; Wharton et al., 1994).

Replication and transcription of the influenza A viral genome takes place in the nucleus of infected cells (Herz et al., 1981). Because of this, some of the newly expressed viral proteins, such as the viral RdRp, have to be located to the nucleus to fulfil their tasks. The three subunits form a heterotrimer to function as a polymerase (Detjen et al., 1987). PB1 is believed to be the central subunit, interacting with PB2 and PA, however more recently an interaction of PB2 and PA was also confirmed (Toyoda et al., 1996; González et al., 1996; Hemerka et al., 2009). After translation of viral proteins in the cytoplasm, the three subunits have to be transported into the nucleus. Different models have tried to explain the mechanism of translocating the subunits into the nucleus (Deng et al., 2005, 2006a; Naito et al., 2007). The most recent ones suggest dimerisation of the PB1 and PA subunits in the cytoplasm and transport of the heterodimer into the nucleus, whereas PB2 localises to the nucleus as a monomer. Formation of the trimer takes place in the nucleus (Huet et al., 2010). A possible involvement of heat shock protein 90 (Hsp90) and RanBP5 in transport and trimerisation were reported (Deng et al., 2006a; Naito et al., 2007).

Viral membrane proteins, HA, NA and M2, are synthesised at membrane-bound ribosomes and translocated into the lumen of the ER, where post-translational modification, such as glycosylation and palmitoylation, and oligomerisation takes place. Viral membrane proteins are subsequently transported via the Golgi apparatus to the apical plasma membrane (Doms et al., 1993; Holsinger et al., 1995). The progeny vRNPs are transported to the same site of the cell membrane, where finally virus assembly and budding takes place (Figure 1.3) (Cox et al., 2005). vRNP transport was not well understood for a long time. Recent findings suggest the involvement of the protein Rab11 (Bruce et al., 2010; Eisfeld et al., 2011; Amorim et al., 2011). After replication of the individual segments in the nucleus, vRNAs are assembled into vRNPs and, by interaction with M1 and the nuclear export protein NEP, they are transported into the cytoplasm. They accumulate near the microtubule-organizing centre (MTOC) and via interaction with Rab11 they are transported to the apical membrane along the microtubule network (Eisfeld et al., 2011; Amorim et al., 2011). The process of assembly of the individual components may be

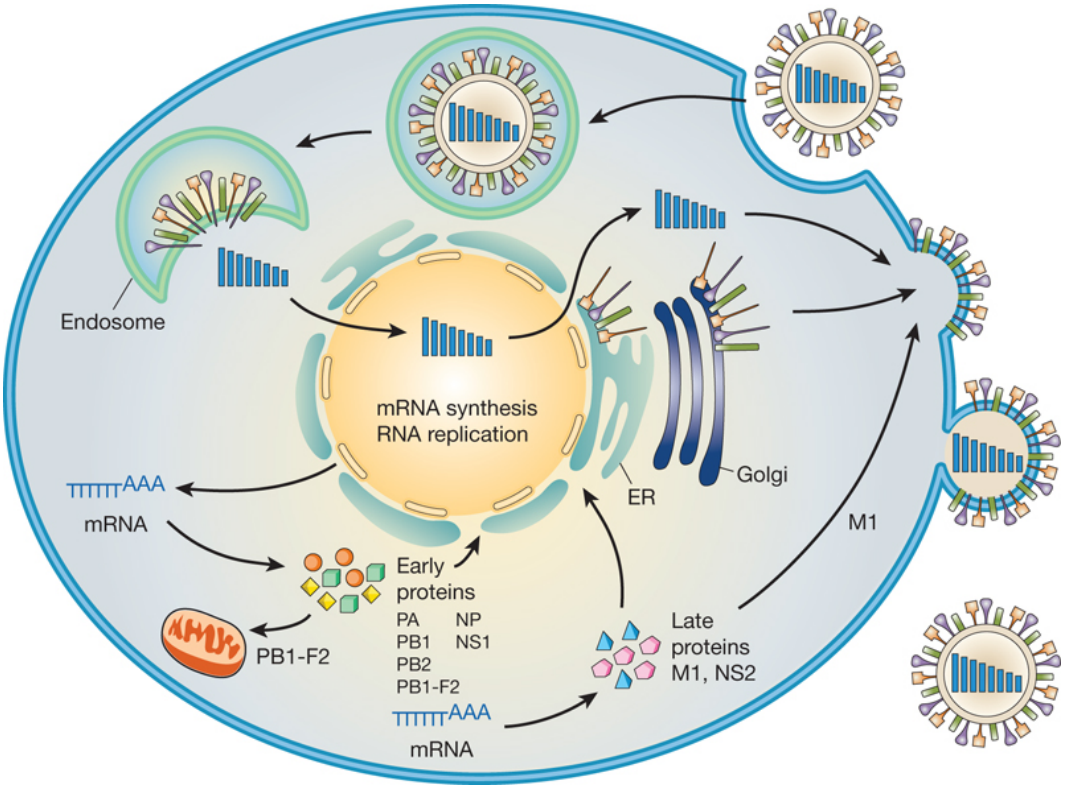

Figure 1.3: Influenza A virus replication cycle: Viruses attach to sialic acid containing receptors on the host cell surface. After endocytosis of virus particles, the viral genome is released into the cytoplasm and vRNPs are transported to the nucleus, where transcription and replication occur. Viral mRNAs are translocated to the cytoplasm for translation of viral proteins. Early in infection, the produced proteins are mainly involved in replication and are therefore transported back to the nucleus. Structural proteins required for virus particles and newly synthesised vRNPs are translocated to the cell membrane, where virus assembly and budding takes place. The non-structural proteins PB1-F2 and NS1 are made early in infection. PB1-F2 interacts with mitochondria and NS1 is involved in interfering with the host cell immune response. Picture taken from Neumann et al. (2009).

triggered by protein-protein interactions as well as RNA-RNA interactions of the segments. Although it is an evolutionary advantage to have a segmented genome, the virus has to make sure that each segment is incorporated once (at least) into a virus particle. How this is maintained is not fully understood, however findings suggest a specific mechanism (Fujii et al., 2003; Hutchinson et al., 2010). Assembly of the segments in combination with interactions between the cytoplasmic tails of HA, NA and M2 with the vRNPs via M1 is thought to induce the process known as budding, which includes the formation, growth and release of the progeny virion (Nayak et al., 2009; Hutchinson et al., 2010).

1.1.5 Viral transcription and replication

The minimal complex for viral replication is the vRNP, which consists of the negative sense RNA, one copy of the polymerase complex and a number of nucleoprotein molecules. The vRNPs are the starting point for viral transcription and replication. Whereas the initiation of transcription depends on a primer, synthesis of cRNA and vRNA are primer-independent processes (Figure 1.4).

Cap-snatching is required for initiating viral mRNA synthesis. The viral RdRp binds to cellular RNA polymerase II (RNAPII), more specifically to the C-terminal domain in its Ser5-phosphorylated stage (Engelhardt et al., 2005). RNAPII is the polymerase responsible for the synthesis of cellular mRNA. Its CTD gets differentially phosphorylated throughout the transcription process, and binding of the viral RdRp to the form that is engaged in the initiation of cellular transcription was thought be bring the viral RdRp in close proximity to newly made 5' capped mRNAs (Engelhardt et al., 2005). The polymerase subunit PB2 was shown to recognise and bind to the 5' cap and cleavage is performed by the PA subunit (Blaas et al., 1982; Braam et al., 1983; Dias et al., 2009; Yuan et al., 2009). Although it was first reported that no base-pairing is needed between the primer and the 3' end of the vRNA, recent reports suggest a preference of complementary sequences both *in vitro* and *in vivo* (Krug et al., 1980; Geerts-Dimitriadou et al., 2011a,b). The non-translated regions of each segment are partially complementary and form a stable complex (Figure 1.5). Two models have been proposed: the panhandle and the "corkscrew" model (Hsu et al., 1987; Flick et al., 1996). The interaction of the 3' and 5' end of the viral RNA are thought to be important for transcription and replication (Fodor et al., 1994; Flick and Hobom, 1999a; Azzeh et al., 2001). After binding of the viral polymerase complex to the promoter region and cap snatching, the PB1 subunit starts transcription at the penultimate cytosine in the vRNA (Caton and Robertson, 1980; Beaton and Krug, 1981). PB1 contains conserved motifs that are characteristic for RNA-dependent RNA polymerases (Argos, 1988; Biswas and Nayak, 1994).

After elongation of viral mRNA by PB1, a poly(A) tail is attached in a process that is different to cellular polyadenylation (Fodor et al., 2001). Synthesis of mRNA is halted when the polymerase reaches the 5-7 uridine stretch near the 5' end of the vRNA (Robertson et al., 1981). The polymerase complex is believed to be stably bound to the 5' end of the vRNA and the loop of

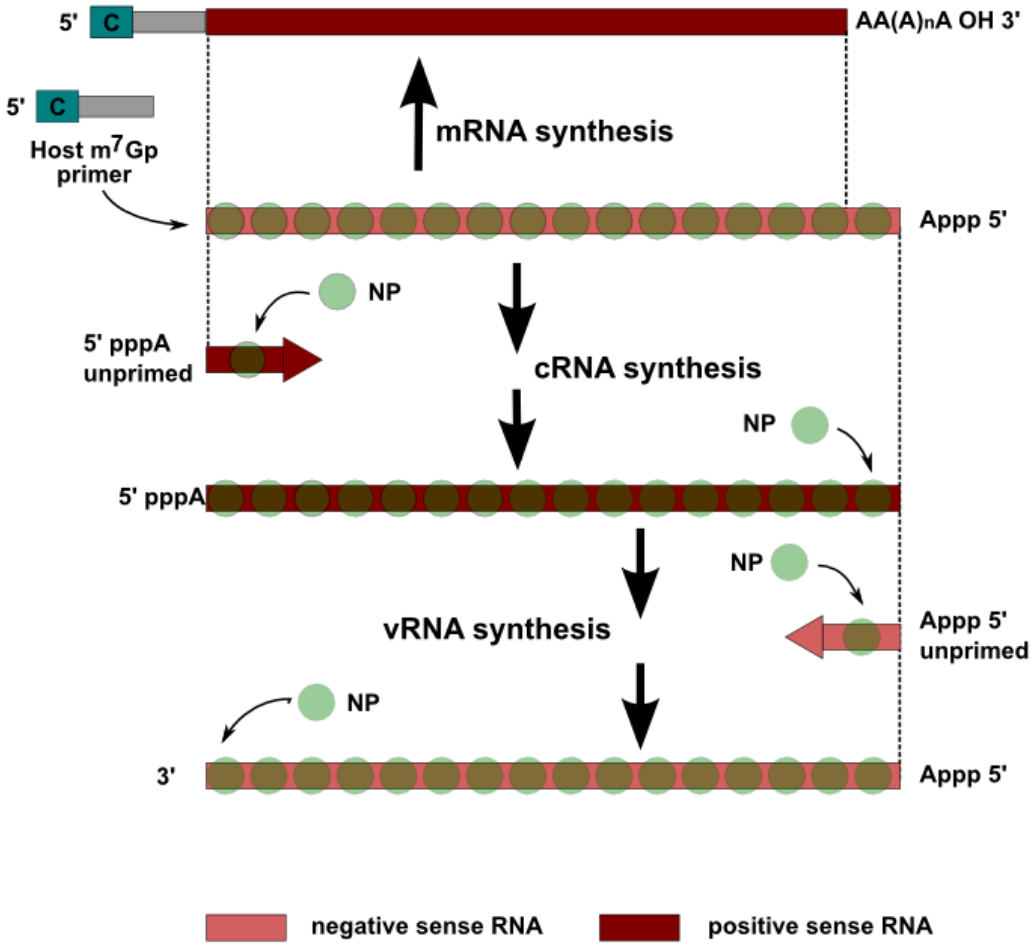

Figure 1.4: Schematic overview of influenza A virus transcription and replication: The viral RNA genome is the starting point for mRNA synthesis and cRNA synthesis. cRNA is used as a template for vRNA synthesis. mRNA synthesis is primed by a short capped primer that derives from host mRNA. The product is about 15-22 nucleotides shorter than the vRNA template and polyadenylated. cRNA and vRNA are synthesised without the use of a primer. The products are covered with nucleoprotein molecules to form RNPs.

remaining template that still needs to be transcribed gets shorter throughout the process (Figure 1.5). Eventually, the complex provides a physical barrier that results in stuttering of the polymerase at the uridine stretch (Luo et al., 1991; Li and Palese, 1994; Tiley et al., 1994; Fodor et al., 1994; Poon et al., 1999).

When the uridine stretch was mutated into an adenine stretch, the viral mRNA contained a poly(U) tail, supporting the model of a stuttering RdRp (Poon et al., 1999). Also, tight binding of the RdRp to the 5' end is crucial for polyadenylation (Tiley et al., 1994; Fodor et al., 1994; Pritlove et al., 1998).

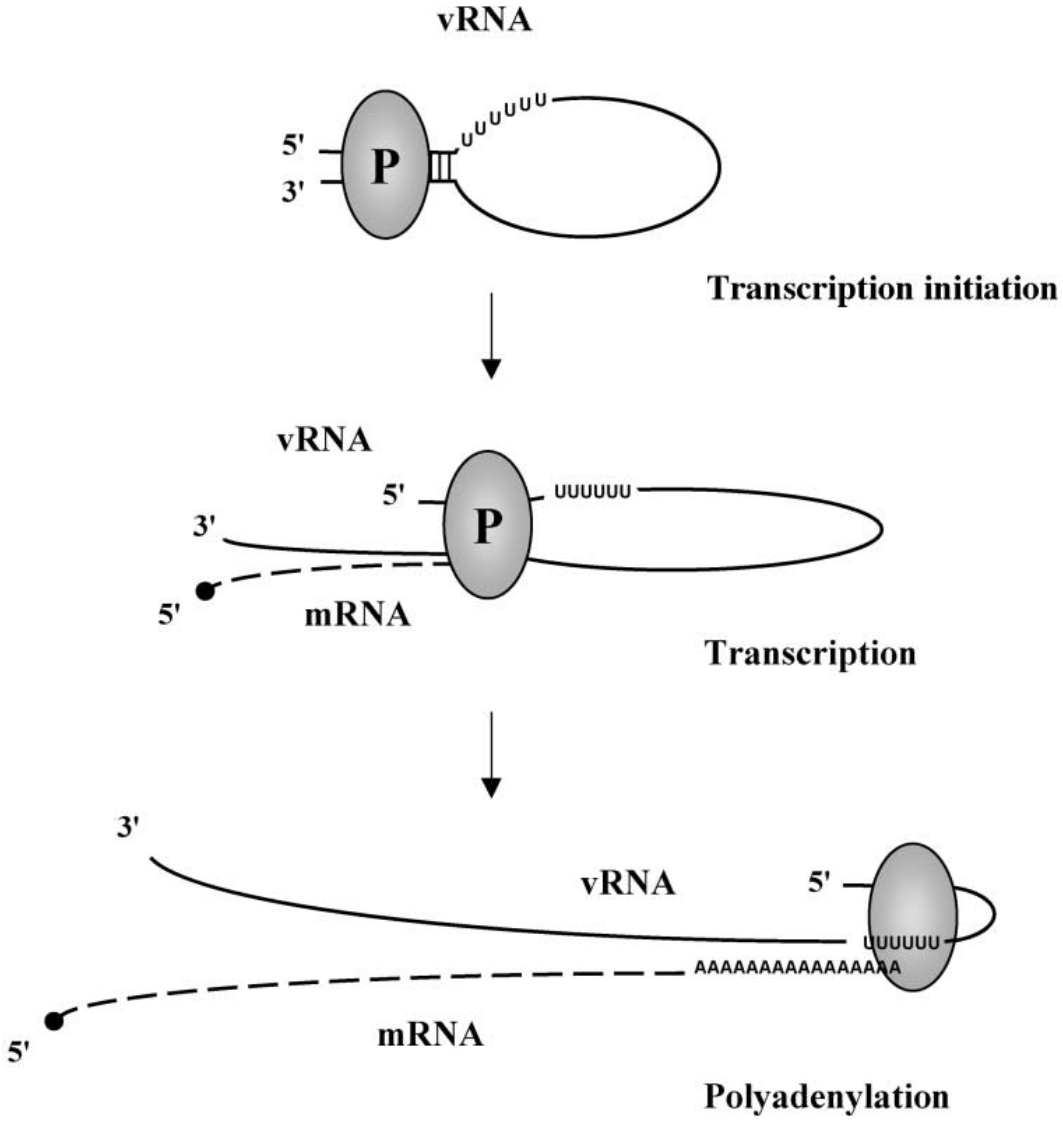

Figure 1.5: Proposed model for influenza A virus transcription initiation, elongation and polyadenylation: The viral polymerase complex binds the 5' and 3' termini of each segment and starts transcription in a primer-dependent manner. The viral RdRp is bound to the 5' end throughout the transcription process. When the polymerase complex reaches the Uridine stretch, it stutters due to steric hindrance, which leads to the polyadenylation of the viral mRNA (Tiley et al., 1994; Fodor et al., 1994; Poon et al., 1999). Picture taken from Fodor et al. (2001).

Replication of the viral genome is divided into two steps. Before new genomes can be made, an intermediate of positive sense full-length RNA is produced. This antigenome is complementary to the vRNA and is therefore called cRNA (Figure 1.4). In contrast to mRNA synthesis, the process of cRNA and vRNA synthesis is primer-independent (Shapiro and

Krug, 1988). Initiation of cRNA and vRNA are reported to differ between each other (Figure 1.6). Two models have been proposed for the initiation of cRNA synthesis. Deng et al. hypothesised that the synthesis of a pppApG dinucleotide starts at the terminal 3' end of the vRNA promoter and proceeds directly into elongation (Figure 1.6(A)) (Deng et al., 2006b). A newer model by Zhang et al. suggests that the *de novo* synthesis of cRNA starts internally at the second nucleotide and an external nucleotide (preferably a purine) is added by a cellular ribonucleotidyl transferase (Zhang et al., 2010b). A model for the *de novo* synthesis of vRNA is shown in Figure 1.6(B). Initiation starts internally at nucleotide 4 and 5 leading to the synthesis of a dinucleotide pppApG (Deng et al., 2006b). The RdRp is thought to pause at the following uridine residues, which causes the polymerase to realign at the 3' end of the cRNA template (Zhang et al., 2010b). The dinucleotide serves as a primer to initiate full length vRNA synthesis.

Synthesis of both mRNA and cRNA starts from a vRNA template. Different models have been proposed to explain the switch from transcription to replication, however this remains an open question. NP was shown to interact with the viral RdRp and with the RNA to form c/vRNPs (Kobayashi et al., 1994; Biswas et al., 1998). Temperature sensitive mutants with lesions in NP were shown to be defective in replication and/or transcription (Mena et al., 1999) and the depletion of NP abolished c/vRNA synthesis (Beaton and Krug, 1986). The mechanism of this is not well understood. A model proposed by Vreede et al. suggested that no regulation towards transcription or replication exists *per se*, but newly synthesised cRNA gets degraded within the cell unless it is covered and protected by NP molecules (Vreede et al., 2004; Vreede and Brownlee, 2007). A study titrating increasing amounts of NP to cells infected with influenza A viruses however did not support this model (Mullin et al., 2004). Levels of mRNA and vRNA were not different regardless the transfected amount of plasmids to express NP. Alternatively, NP could alter the structure of the promoter region to favour transcription or replication, or it could influence the replicase or transcriptase function of the viral polymerase by binding to it (Fodor et al., 1994; Newcomb et al., 2009).

Additional factors have been described that are involved in this process of switching from transcription to replication. High levels of capped cellular mRNAs were shown to support transcription, whereas high levels of viral

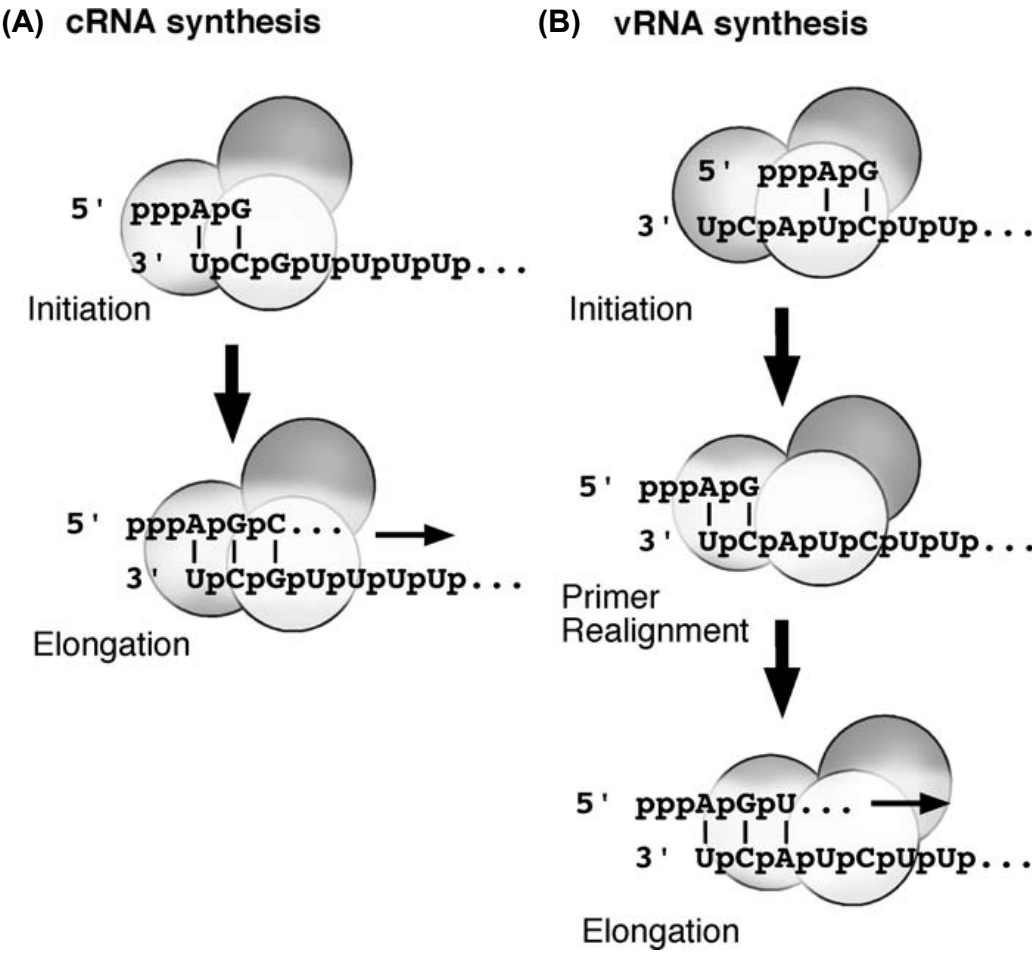

Figure 1.6: Proposed model for initiation of cRNA and vRNA synthesis: (A) Synthesis of cRNA was proposed to start at the very end of the 3' end of vRNA templates by ATP. The addition of a second nucleotide triggers elongation of the cRNA synthesis (Deng et al., 2006b). **(B)** Synthesis of vRNA initiates also with ATP to produce a pppApG dinucleotide. However, this happens at positions 4 and 5 and the dinucleotide translocates back to the 3' end to realign and inititate vRNA synthesis from this short dinucleotide primer ("internal initiation and realignment model") (Deng et al., 2006b; Zhang et al., 2010b). Picture taken from Digard et al. (2009).

RdRp and 5' end vRNA promote viral replication (Olson et al., 2010). The latter report is in line with a recent finding by Perez et al., suggesting that small viral RNAs corresponding to the 5' end of each vRNA switch the viral RdRp towards a replicase (Perez et al., 2010). However, the exact mechanism has yet to be determined. It cannot be ruled out that additional viral factors influence the switch, such as NEP (Robb et al., 2009) and that the process of regulating viral transcription and replication depends on multiple effectors.

1.1.6 Viral pathogenicity and the involvement of host cell proteins

Several factors have to act together so that viruses can infect a host and induce disease. These include effects the virus has on the host cell, e.g. during viral replication, and aspects the host contributes itself, e.g. via the immune response. The degree of pathogenicity is thereby determined by this interplay. Are specific receptors available on the host cell and is the virus able to bind to them? Is the virus able to hijack the transcription and translation machinery within the host cell? How effective is the immune system to counteract the viral infection and what mechanisms does the virus have to escape or modulate these host defence systems?
These aspects have a great influence on the success of the viral infection and are key issues for the development of viral pandemics. Aquatic birds are the natural hosts of influenza A viruses. Frequently viruses cross the species barrier from an avian host to humans or other mammals. In order to be able to replicate in a mammalian host, the virus needs to adapt to it. Different factors have been described that are important for this to happen. One way to cross the species barrier is by direct introduction of an avian strain into the human population followed by accumulation of mutations that change the virus' specificity. The 1918 pandemic is believed to have been directly transmitted from birds to humans (Taubenberger and Morens, 2006). Several viral proteins were shown to be involved in the process of adaptation and virulence, such as HA, polymerase subunits, NS1 and PB1-F2 (Kobasa et al., 2004; Watanabe et al., 2009; McAuley et al., 2007). Since 1997, continued interspecies transmissions of H5N1 viruses have been reported (Smith et al., 2006). A second possibility to cross the species barrier is by reassortment between an avian and a human strain. Because of the segmented nature of the viral genome, this can happen when one cell gets infected by two virus strains. In this context, swine are believed to be good "mixing vessels", because they have both receptors recognised by human and avian viruses (Ma et al., 2008). Such an event most likely did happen with the last pandemic virus from 2009 (Smith et al., 2009). However a new virus is introduced into the human population, further adaptations within the viral proteins are needed for efficient replication and transmission. Two main reasons for this are:
(1) Replication of the viral genome depends largely on the interaction of viral proteins with cellular proteins.

(2) Host cell immune responses are induced by viral infection which the virus has to counteracted in order to replicate efficiently.

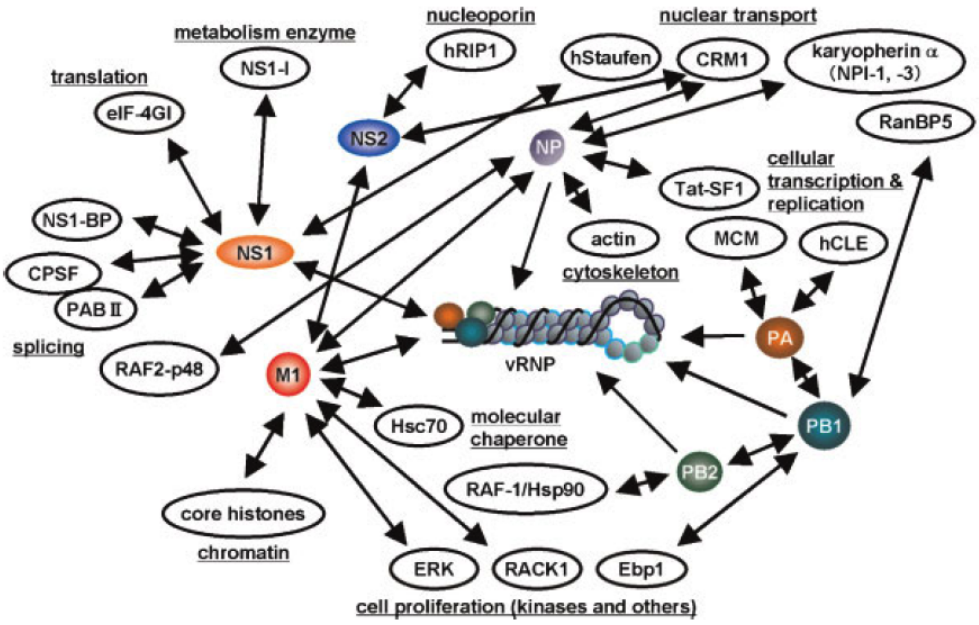

Figure 1.7: Interaction map of cellular and viral proteins involved in viral replication and transcription: A large number of cellular proteins were identified as interaction partners for viral proteins. Proteins shown in this map are involved in viral replication and transcription. The cellular factors can be categorised in groups involved in nuclear transport, nucleoporins, metabolic enzymes, translation, splicing factors, chromatin, molecular chaperones, cell proliferation, cytoskeleton and transcription and translation. Picture taken from Nagata et al. (2008).

Figure 1.7 shows some of the identified cellular proteins that interact with viral proteins, specifically those who are involved in viral replication and transcription. With the use of new techniques such as RNAi screenings, even more interactions have been identified (Hao et al., 2008; Karlas et al., 2010; Stertz and Shaw, 2011). Some of the shown proteins are involved in the nuclear transport of vRNPs and viral proteins, such as CRM1 and RanBP5 (Elton et al., 2001; Deng et al., 2006a). Other interactions help transcribing and processing viral mRNAs. The viral RdRp was found to bind to the C-terminal domain of cellular RNA polymerase II which has been proposed to support cap snatching (Engelhardt and Fodor, 2006). NS1 was found to interact with several cellular factors involved in splicing, such as NS1-binding protein (NS1-BP), the 30kDa subunit of the cleavage and polyadenylation factor (CPSF) and the poly(A)-binding protein PAB-II (Wolff et al., 1998; Nemeroff et al., 1998; Chen et al., 1999). Besides being

important for viral transcription, these interactions contribute to host cell protein shut off.

Apart from exploiting cellular proteins to transcribe and replicate the viral genome, the virus utilises cellular proteins to induce or inhibit apoptosis and to interfere with the host cell immune system. Apoptosis and its regulation will be explained in more detail in Section 1.1.7. The innate immune response is the ”first line of defence” and very important for fighting a viral infection. Cellular receptors recognise specific pathogen-associated molecular patterns (PAMPs) such as 5’ triphosphorylated RNA, which does not exist naturally in a cell (Pichlmair et al., 2006). The cellular receptor RIG-I gets activated upon RNA binding. The CARD domain of RIG-I interacts with the CARD domain of the mitochondrial membrane protein MAVS (also known as VISA, IPS-1 and CARDIF) and triggers a signalling cascade that leads to the activation of several transcription factors such as IRF-3 and NFκB. These transcription factors are translocated to the nucleus and form an ”enhanceosome” complex on the IFN-β promoter (Figure 1.8) (Seth et al., 2005; Xu et al., 2005; Kawai et al., 2005; Meylan et al., 2005).

IFN-β is subsequently secreted from the cell and functions in an autocrine or paracrine manner by binding to the IFN-α/β-receptor on the cell surface. This triggers a JAK/STAT signalling cascade leading to the expression of IFN-stimulated genes, which create an antiviral state within the cell that limits viral replication. Influenza A viruses have evolved a number of strategies to prevent this in order to replicate efficiently. The small non-structural protein NS1 was shown to be the main IFN-antagonist. It inhibits RIG-I signalling, most likely by preventing the ubiquitination of the CARD domain of RIG-I by inhibiting the ubiquitin-ligase TRIM25 (Gack et al., 2009). Influenza viruses also act downstream of the IFN-α/β-receptor, e.g. by enhancing the expression of suppressor of cytokine signaling-3 (SOCS-3) proteins (Pauli et al., 2008). SOCS-3 proteins were shown to negatively regulate the JAK/STAT pathway by inhibition of the JAK kinase activity (Starr et al., 1997; Song and Shuai, 1998). Additionally host-cell protein shut-off by NS1 and the polymerase complex as described above also adds to counteraction of the innate immune response.

The interplay between a virus and its host determines the clinical outcome of the infection. By expressing cytokines and IFNs the host intends to inhibit viral replication, however this response may be detrimental for the host under certain circumstances. Especially high pathogenic avian H5N1

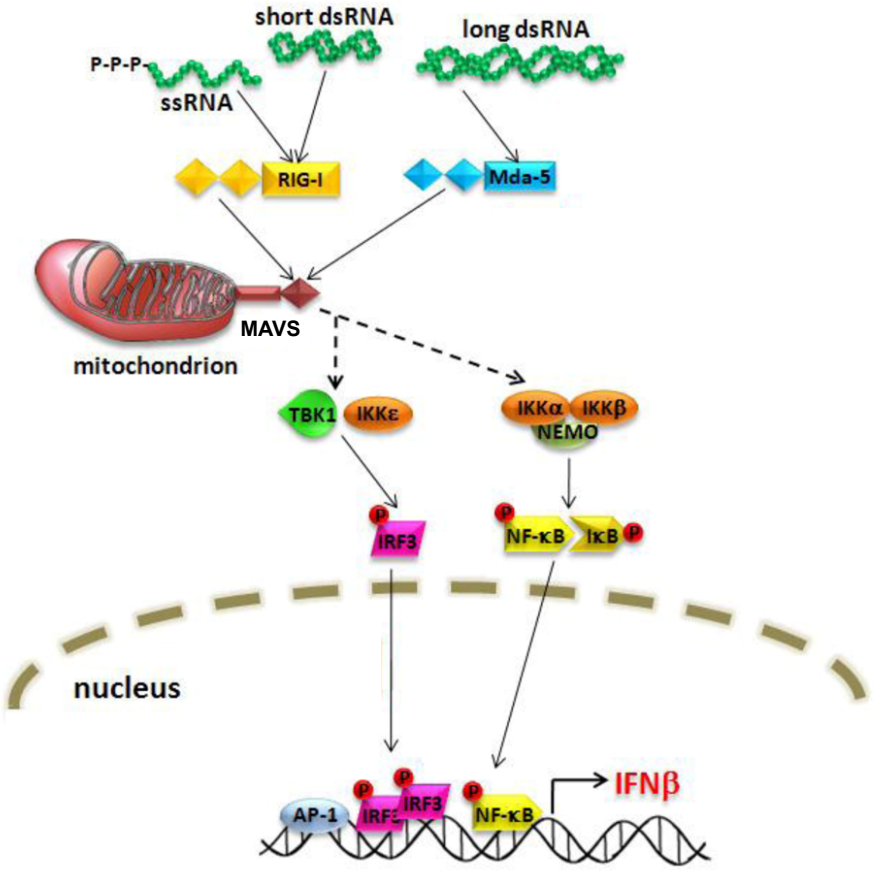

Figure 1.8: Schematic of IFN-β induction by viral RNA: Influenza A viruses induce IFN-β via RIG-I. The CARD domains of RIG-I and MAVS interact which leads to the activation of IRF-3 and NFκB. Translocation of these transcription factors to the nucleus initiates IFN-β expression. Picture adapted from Shaw (2009).

viruses were shown to induce the innate immune response in an excessive way that it becomes disadvantageous for the host (de Jong et al., 2006; Alberts et al., 2010).

Collectively it can be said that the host-virus-relation must be a well balanced one. The virus must be able to control the host for successful replication. It needs to find the right balance to infect, replicate and escape from the host cell to infect a new cell or host before the host either induces an effective immune response or the infection ends fatally before replication is completed. Interactions with host proteins are therefore indispensable and viruses in a new host need to adapt to get the right balance.

1.1.7 Apoptosis and its regulation by viral proteins

Apoptosis, also known as programmed cell death, is an extremely powerful way to remove cells without causing an inflammatory response. Apoptosis is one of the oldest first-line defences against viral infections and viruses have generated many ways during evolution to modulate the process. Apoptosis can be differentiated from necrosis by specific cellular and nuclear morphological changes (Kerr et al., 1972). Cells shrink, DNA is fragmented, apoptotic cells lose contact to their neighbouring cells, and the cell is finally broken up into small vesicles. These vesicles are removed by macrophages or neighbouring cells via phagocytosis and no immune response is induced. Apoptosis can be activated through a number of stimuli, external or internal, resulting in extrinsic or intrinsic induction both leading to the activation of several caspases (Figure 1.9). Mitochondria are thought to be the central element in the intrinsic pathways. Mitochondrial transmembrane potential is disrupted upon stimuli, which leads to the release of cytochrome C into the cytoplasm (Liu et al., 1996). The permeability transition can be mediated by a pore protein complex in the mitochondrial membrane. This permeability transition pore complex (PTPC) is a large complex with three major components, VDAC, ANT and cyclophilin D. ANT (adenine nucleotide translocator) is the most abundant protein in the inner mitochondrial membrane, whereas VDAC (voltage dependent anion channel) is the most abundant protein in the outer membrane. Upon activation, they are thought to form a non-selective pore, following a sudden increase in the inner mitochondrial permeability and an up-regulated entry of water with the result of osmotic swelling (Shoshan-Barmatz et al., 2010; Keinan et al., 2010). Several proteins in the cytoplasm and the mitochondrial membrane regulate the mitochondrial membrane potential and therefore apoptosis. These proteins belong to the so-called Bcl-2 family. Members of this family are pro- or anti-apoptotic. Pro-survival members such as Bcl-2 and Bcl-X_L stabilise the mitochondrial membrane e.g. by sequestering pro-apoptotic members (Cheng et al., 2001). Pro-apoptotic members of the Bcl-2 family (e.g. Bax, Bak) can change the permeability of the outer mitochondrial membrane either by integrating into the mitochondrial membrane and forming pores or via induction of mitochondrial permeability transition at the inner mitochondrial membrane by interacting with members of the PTPC. The idea that apoptosis is induced only by host cells to defend itself and limit viral replication was found to be imperfect as evidence

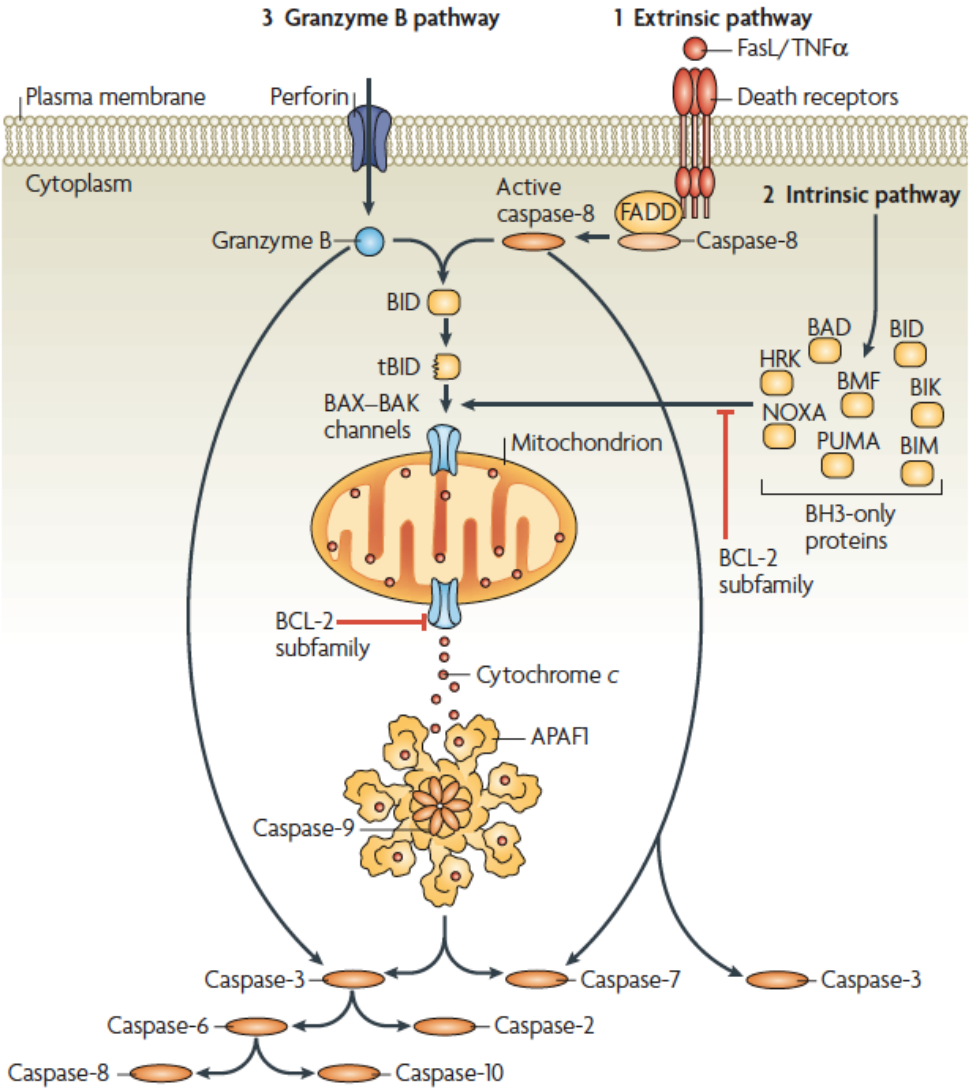

Figure 1.9: Apoptosis induction pathways: Three routes can lead to the induction of caspases that results in apoptosis. **(1)** The extrinsic pathway is activated by binding of FasL or TNF-α to a death receptor on the cell surface. This triggers a recruitment of adaptor proteins and Caspase-8 to the receptor, which leads to the activation of casapse-8. Active caspase-8 proteolytically processes and activates a number of other caspases leading to cell death. **(2)** The intrinsic pathway involves the activation of BH-3 only proteins of the Bcl-2 family. These pro-apoptotic family members are negative regulated by anti-apoptotic members of the same family. Upon activation, cleavage of BID into truncated BID (tBID) promotes cytochrome C release from mitochondria either by interacting with the PTPC or by integration of Bax/Bak into the mitochondrial membrane. Cytochrome C release activates the formation of an apoptosome in the cytoplasm (APAF-1 and Caspase-9). Crosstalk between pathway (1) and (2) is possible via Caspase-8. **(3)** The granzyme pathway is activated by delivery of granzyme into the cytoplasm through a cell surface perforin channel. Picture taken from Taylor et al. (2008).

increased for viral-induced apoptosis. Several viruses have found ways to modulate the induction of apoptosis. Inhibition of apoptosis can help viruses to prolong their replication time within the cell or to evade the immune system. Many viruses also stimulate apoptosis which may help the virus to spread or to dysregulate the host immune system by specifically inducing apoptosis in immune cells. However, this process needs to be tightly regulated in order not to kill the host cell too quickly. Often apoptosis seems to be beneficial for the pathogenicity of the virus. A large number of viruses encode proteins that modulate mitochondrial apoptosis, some of which are listed in Figure 1.10. These proteins target components of the PTPC or members of the Bcl-2 family, such as Bax, Bak or Bcl-2. They may also be able to directly integrate in the mitochondrial membrane to induce mitochondrial membrane permeabilisation (MMP).

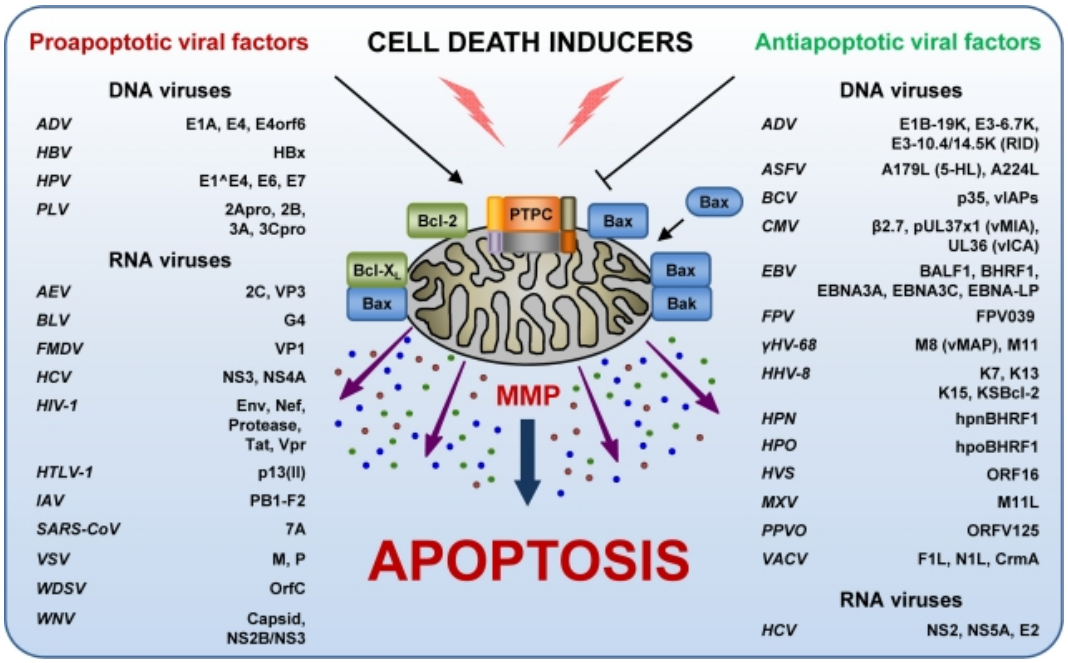

Figure 1.10: Viral peptides involved in modulating mitochondrial apoptosis: Viral proteins may be pro- or antiapoptotic modulating the mitochondrial membrane permeabilisation (MMP). This can be by acting on the permeability transition pore complex (PTPC) or via interacting with members of the Bcl-2 family. Virus names are listed in abbreviations. Picture taken from Galluzzi et al. (2008).

Hepatitis B virus protein X (HBx) was found to interact with VDAC3 to induce apoptosis, similar to HIV-1 protein Vpr, which additionally interacts with ANT. HTLV-1 encodes a small protein called p13(II), which also targets mitochondria and causes swelling and fragmentation of the mitochondria (D'agostino et al., 2005). All three proteins were shown to have an

amphipathic α-helix that is necessary for the integration in the mitochondrial membrane (Takada et al., 1999; Shirakata and Koike, 2003; Jacotot et al., 2000, 2001; D'Agostino et al., 2002). The HIV- protease was found to proteolytically activate caspase-8, which triggers apoptosis (Nie et al., 2002). Other viral proteins target members of the Bcl-2 family to induce or suppress apoptosis. Beside its interaction with VDAC and ANT, HIV-1 Vpr was also found to induce mitochondrial membrane permeabilisation in a Bax-dependent manner (Andersen et al., 2006). Especially anti-apoptotic viral proteins have sequence or conformational similarities to pro-survival members of the Bcl-2 family. This includes the adenovirus protein E1B-19K that acts similar to the cellular Bcl-2 protein and sequesters Bax and Bak (Han et al., 1996, 1998; Cuconati et al., 2002).

It is not surprising that influenza A viruses also regulate apoptosis. Induction can be either by extrinsic or intrinsic mechanisms (Lowy, 2003). Several influenza virus proteins were shown to induce cell death. Earlier studies had already revealed that induction of apoptosis relies on the replication of the virus as UV or chemically inactivated viruses did not induce apoptosis (Takizawa et al., 1993; Hinshaw et al., 1994). In infected cells, levels of the biological active form of TGF-β increase. This cytokine usually exists in an inactive form in all cells. The viral neuraminidase was shown to activate TGF-β, which induces apoptosis (Schultz-Cherry and Hinshaw, 1996). Expression of M1 from plasmids induces apoptosis, possibly by interacting with caspase-8 (Morris et al., 2002; Zhirnov et al., 2002b). Another inducer is NS1, although its role is rather controversial. Expression of NS1 was shown to induce apoptosis in different cell lines (Schultz-Cherry et al., 2001; Lam et al., 2008). On the other hand, recombinant viruses lacking NS1 were shown to be greater inducers of apoptosis, suggesting that NS1 could be anti-apoptotic. However, this may be due to its role in antagonising IFN expression (Zhirnov et al., 2002a). Beside this, an IFN-independent anti-apoptotic function was reported for NS1. NS1 was shown to bind to and activate PI3K by binding to the p85β subunit (Hale et al., 2006). PI3K is involved in a number of cellular processes such as cell proliferation and survival and the activation of PI3K by NS1 was thought to prevent apoptosis (Ehrhardt et al., 2007). More recent data using recombinant viruses that fail to induce the PI3K pathway, however, show that the activation does not affect apoptosis (Jackson et al., 2010). The second non-structural protein, PB1-F2, was shown to be pro-apoptotic,

which is described in Section 1.2.2. Overall, the induction of apoptosis by influenza A viruses is thought to be supportive for viral replication. Wurzer et al. showed that the activation of caspases-3 is essential for viral replication in that knockdown of caspase-3 led to retention of vRNPs in the nucleus (Wurzer et al., 2003). A recent study suggested a positive role of Bax in the virus replication cycle, and thereby support the findings of Wurzer et al. (McLean et al., 2009): although cells lacking Bax still underwent apoptosis, the downregulation of Bax resulted in retention of NP in the nucleus and decreased virus titres.

1.2 PB1-F2 and its reported functions within infected cells

When the gene products of influenza A viruses were first characterised, ten proteins expressed from eight negative strand RNA segments were described (Palese and Schulman, 1976; Ritchey et al., 1976; Palese et al., 1977; Inglis et al., 1979; Lamb et al., 1981). Then, about 20 years later, an additional protein was found to be expressed from segment 2 by a process called leaky ribosomal scanning. The 87-90 aa long protein was discovered during a search for unknown CD8+ T cell epitopes and was named PB1-F2 (Chen et al., 2001).

The mechanism for leaky ribosomal scanning is not an invention of influenza A viruses. It is a strategy that is also used by other viruses such as bunyaviruses, paramyxoviruses and vesicular stomatitis virus (Elliott, 1989; Bellini et al., 1985; Luk et al., 1986; Herman, 1986). Beside overlapping ORFs, viruses have evolved several other strategies to increase their coding capacity, e.g. splicing events (e.g. influenza A virus segment 7 and 8), ambisense sequences (e.g. Uukuniemi virus S segment, Rift Valley fever virus S segment), overlapping Stop-Start sequences (influenza B viruses), RNA editing (e.g. measles virus, human parainfluenza virus type 3) and the use of self-cleaving peptide (e.g. picornavirus 2A) (Inglis et al., 1979; Lamb et al., 1981; Simons et al., 1990; Giorgi et al., 1991; Horvath et al., 1990; Cattaneo et al., 1989; Galinski et al., 1992; Lloyd et al., 1986).

1.2.1 General information about PB1-F2

In 2001, the existence of a small protein ($\sim$10.5 kDa) translated from an internal +1 ORF from segment 2 was reported by Chen et al. (Chen et al., 2001). Because the protein is translated from a second ORF, it was named PB1-frame 2 (short PB1-F2). In contrast to PB1-F2, the start codon of PB1 is in a suboptimal Kozak consensus sequence (Kozak, 1986; Chen et al., 2001). Therefore, it was suggested that ribosomes which miss the first AUG continue to scan for another AUG along the mRNA until they reach one in a stronger consensus sequence further downstream (Chen et al., 2001). This process is called leaky ribosomal scanning. Sequence analysis revealed that almost all avian influenza virus strains contain a full length PB1-F2 but human H1N1 viruses isolated after 1947 and classical swine H1N1 virus isolates express a truncated version of 57 aa or 11 aa, respectively (Zell et al., 2007). The pandemic H1N1 virus from 2009 only expresses 11 aa of the PB1-F2 ORF as it contains three stop codons at position 12, 58 and 88 (Trifonov and Rabadan, 2009). PB1-F2 is not incorporated into virions, it only is present in infected cells, and the protein is expressed early in infection. About 2 hours post infection it can be detected by Western blot analysis with maximum expression at 5 hpi. The protein has a half-life of only 30 min and degradation is mediated by the proteasome (Chen et al., 2001). The intracellular localisation differs between infected cells. Independent of the cell type, it was observed that PB1-F2 localises in about half of cells to the mitochondrial membrane, whereas in other cells it stays in the nucleus and in the cytoplasm (Chen et al., 2001; Zamarin et al., 2005). The protein was shown to induce apoptosis via mitochondria in a cell-dependent manner. In contrast to epithelial cells, immune cells seem to be affected by PB1-F2 expression (Chen et al., 2001). This feature of PB1-F2 will be discussed in more detail below.

1.2.2 PB1-F2 and its pro-apoptotic function

About 55% of cells infected with A/PR/8/34 show a mitochondrial localisation of PB1-F2 (Chen et al., 2001). The mitochondrial targeting signal (MTS) is located between amino acids 65 and 87 and forms a charged amphipathic α-helix (Gibbs et al., 2003). Another prediction for the MTS is between amino acids 46 and 75 (Yamada et al., 2004). The observed differences are most likely the result of various methodologies employed by the two groups.

The sequence identified by Yamada et al. is consistent with the finding that viruses isolated from European swine had a truncated PB1-F2 of 79 aa that still localises to mitochondria (Zell et al., 2007). The MTS is similar to the sequence of a protein called p13(II) from HTLV-1. PB1-F2 was shown to interact with two mitochondrial membrane proteins, ANT3 (adenine nucleotide translocase) in the inner mitochondrial membrane and VDAC1 (voltage-dependent anion channel) in the outer mitochondrial membrane (Zamarin et al., 2005). It was suggested that this interaction is involved in the induction of apoptosis since both mitochondrial proteins are part of the permeability transition pore, which has been shown to play a role in programmed cell death (Belzacq et al., 2002; Zaid et al., 2005). Whether PB1-F2 alone is able to induce apoptosis, or if viral infection is needed, is not clear. Whereas Yamada et al. (Yamada et al., 2004) did not find efficient induction of cell death by just transfecting cells with a PB1-F2 expressing plasmid, other groups report it is an intrinsic feature of the protein and no other viral proteins are required (Chen et al., 2001; Gibbs et al., 2003). It might depend on the amount of PB1-F2 produced in transfected cells and on the cell type. PB1-F2 was shown to oligomerise and it was found to form variably sized pores in phospholipid bilayers (Chanturiya et al., 2004; Henklein et al., 2005). Oligomerisation was mapped to the α-helix in the C-terminus of the protein (Bruns et al., 2007). To what extent the interaction of PB1-F2 with ANT3 and VDAC1 is responsible for the induction of apoptosis is not known. Several hypothesis have been proposed. PB1-F2 could mediate a bridge between the two mitochondrial proteins and therefore cause mitochondrial membrane permeabilisation and cytochrome C release. Another possibility is the formation of multimeric PB1-F2 complexes which themselves could form pores and lead to cytochrome C release (Zamarin et al., 2005). Additionally, expression of PB1-F2 was shown to sensitise cells to the effect of TNF-α and DNA damage, stimuli that are known to trigger apoptosis (Zamarin et al., 2005). It is not well understood why cell death is only induced in immune cells, whereas epithelial cells are not affected, although PB1-F2 localises to mitochondria in all cell types. A different expression level of the isoforms of ANT1 and VDAC3 was suggested, but no clear evidence for this hypothesis exists (Zamarin et al., 2006). More cellular factors might be involved in this process. Possible candidates would be the pro-apoptotic proteins Bax and Bak. Bax was shown to interact with the PTPC, which is important for the

induction of apoptosis by the permeability transition pore (Marzo et al., 1998; Shimizu et al., 1999; Giorgi et al., 2002). The HIV-1 protein Vpr was shown to bind ANT and VDAC and induces apoptosis, which was shown to be a Bax-dependent process (Jacotot et al., 2000; Andersen et al., 2006).

1.2.3 Involvement of PB1-F2 in influenza A virus pathogenicity

The involvement of PB1-F2 in viral pathogenicity is not clearly understood nor defined yet. Inducing apoptosis in immune cells, e.g. in alveolar macrophages, could impair the host immune system, decrease viral clearance from lungs and therefore increase virulence (Chen et al., 2001; Zamarin et al., 2006). Beside this, PB1-F2 was also shown to help development of secondary bacterial infections caused by *Streptococcus pneumoniae*, possibly by lowering the host defence system (McAuley et al., 2007). Secondary bacterial infections are the most common but also the most severe complications of influenza A virus infections (McCullers and Rehg, 2002). The C-terminus of PB1-F2 appeared to be responsible for this effect, as mice were unaffected when only the N-terminal peptide was given (McAuley et al., 2007). Despite the fact that some strains do not seem to be affected by deletion of PB1-F2 in tissue culture (e g. A/PR/8/34), introducing PB1-F2 from the highly pathogenic strain A/Brevig Mission/1/1918 into a A/PR/8/34 background had a clear effect on plaque size, *in vitro* growth and pathogenicity in mice, suggesting that the protein can influence some functions (Zamarin et al., 2006; McAuley et al., 2007). With regards to this, one amino acid in the ORF of PB1-F2 was identified to be different compared to less pathogentic influenza A viruses, residue 66. Most strains encode an asparagine at position 66 with the exception of A/Brevig Mission/1918 and the highly pathogenic avian strains from the 1997 H5N1 group. These viruses code for serine at position 66. Exchanging just amino acid 66 (N66S) led to an increase in viral lung titres in infected mice, raised the level of cytokines and finally led to higher mortality (Conenello and Palese, 2007). To what extent PB1-F2 contributes to viral pathogenesis remains unclear. PB1-F2 of some strains might lead to an increased pathogenicity in a specific genetic background, but other viral strains might not profit from PB1-F2 expression.

1.3 Reverse genetics of negative-strand RNA viruses

1.3.1 Synthesis of non-segmented and segmented RNA viruses

In molecular virology, reverse genetics describes the generation of infectious viruses from cloned cDNA. This methodology allows the direct manipulation of the viral genome to study the relationship between virus structure, morphology and components and the pathogenicity of a virus. Beside this, reverse genetics is a powerful tool for generating vaccines.
The first RNA virus generated from cloned DNA was the bacteriophage Qβ (Taniguchi et al., 1978). Transfection of cloned DNA into *E. coli* resulted in the formation of infectious phages. In 1981, Racaniello et al. transfected mammalian cells with a plasmid containing a cDNA copy of the poliovirus genome which also led to the production of infectious virus particle (Racaniello and Baltimore, 1981). Reverse genetics systems of many other positive-strand RNA viruses, such as Sindbis virus and Semliki forest virus, followed (Rice et al., 1987; Liljeström et al., 1991). Genomes of positive-strand RNA viruses transfected into cells serve as mRNA and newly expressed viral proteins can replicate the viral genome, however transfection of cDNA was shown to be also effective (Racaniello and Baltimore, 1981). Rescue of negative-strand RNA viruses turned out to be more difficult and complex, because neither the genome nor the antigenome can serve as mRNA and the minimal infectious unit is an RNP. This means viruses have to deliver their own replication machinery including the RNA-dependent RNA polymerase. The need of the polymerase and the nucleoprotein was determined in minireplicon systems for influenza viruses, but also other negative-strand RNA viruses such as VSV and bunyavirus (Honda et al., 1988; Szewczyk et al., 1988; Pattnaik and Wertz, 1991; Dunn et al., 1995).

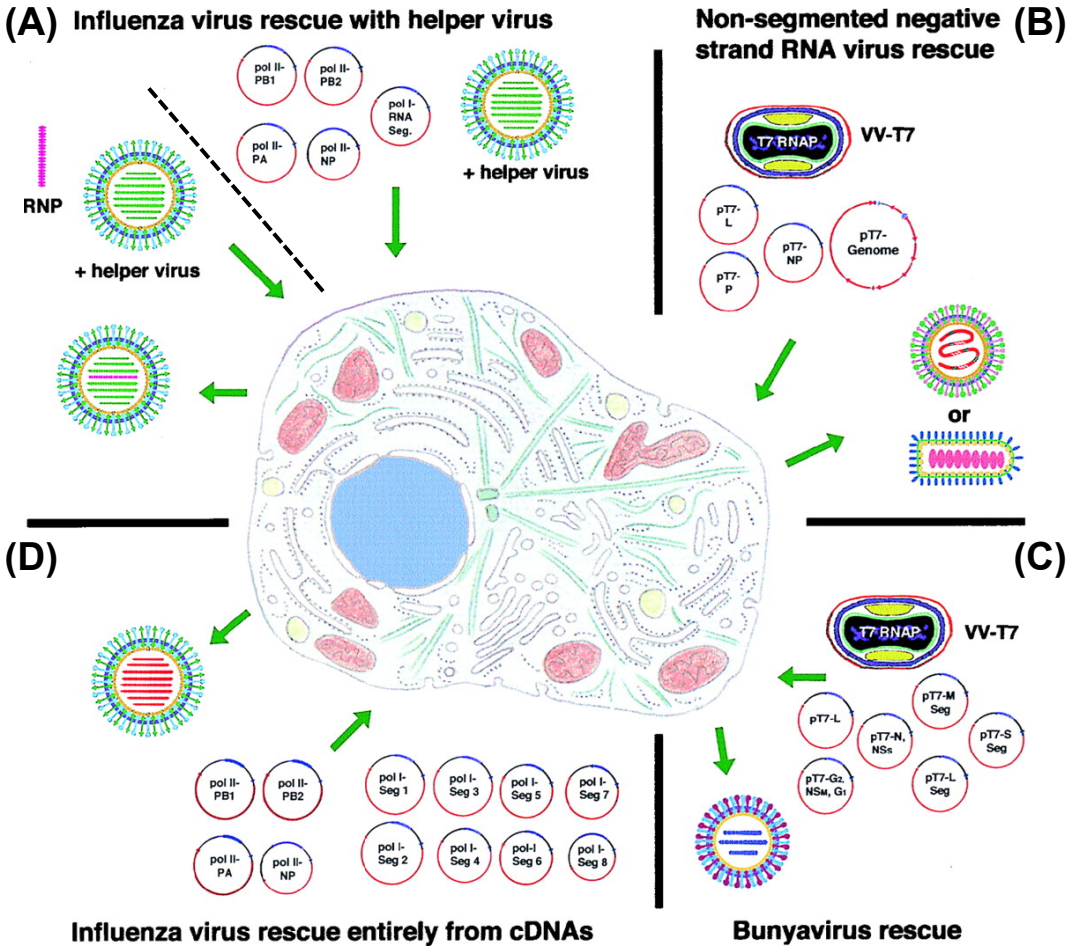

Figure 1.11: Strategies to generate negative strand RNA viruses from cDNA: **(A)** Individual replacement of segments of the influenza virus genome either by *in vitro* reconstitution or *in vivo* assembly of RNP followed by infection with a helper virus. **(B)** Rescues of non-segmented negative-strand RNA viruses was done by transfecting plasmids with the viral antigenome under a T7 promoter along with plasmids encoding the viral proteins to support RNP formation. T7 polymerase was supplied by infection with a recombinant Vaccinia viruses expressing the T7 RNAP (VV-T7) or by transfected cell lines stably expressing T7 RNAP. **(C)** The first rescue of a segmented negative-strand RNA virus was reported for Bunyamwera viruses. Transfection of plasmids encoding the three RNA segments (antigenomic sense) together with plasmids expressing the viral proteins using a T7 promoter. T7 RNAP was supplied by infection with VV-T7 or by transfected cell lines stably expressing T7 RNAP. **(D)** One method to rescue influenza A viruses is using the 12-plasmid rescue system. Eight segments coding for each RNA segment under control of the RNA polymerase I promoter along with four plasmids encoding the polymerase subunits and the nucleoprotein (under control of the pol II promoter) were transfected into a target cell. Picture adapted from Pekosz et al. (1999).

The first steps towards modifying the genome of a negative-strand RNA virus were done by Luytjes et al. (1989). cDNA in negative orientation of

chloramphenicol acetyltransferase (CAT) gene was cloned under the control of a T7 promoter and *in vitro*-synthesised virus-like RNA was transfected into cells along with purified polymerase proteins and nucleoprotein. Superinfection with a helper virus resulted in the generation of viruses carrying the CAT gene (Luytjes et al., 1989). Using the approach of Luytjes et al., the introduction of site-directed mutations into the influenza virus genome followed (Enami et al., 1990). In 1993, a T7-independent system was developed utilising cellular RNA polymerase I (pol I) removing the need to infect with recombinant vaccinia viruses or generating stably transfected cell lines (Zobel et al., 1993). The products of cellular RNA polymerase I do not have 5' or 3' modifications, which results in the synthesis of precise viral RNA segments. The hemagglutinin coding sequence or the CAT gene were cloned between a mouse polymerase I promoter sequence and mouse termination elements which resulted in the generation of vRNAs *in vitro* and *in vivo*. Primer extension analysis confirmed the precise 5' and 3' end (Zobel et al., 1993; Neumann et al., 1994). Pleschka et al. used a similar system to reconstitute viral RNPs intracellular. They transfected cells with four plasmids expressing the three polymerase subunits and the nucleoprotein under polymerase II promoter along with a plasmid coding for an RNA-like transcript under the control of the human polymerase I promoter and hepatitis delta virus genomic ribozyme (Pleschka et al., 1996). This new approach was an alternative to *in vitro* reconstitution assays which removed the need of purifying viral proteins (Figure 1.11 (A)). Intracellular generation of RNPs followed by infection with a helper virus resulted in the production of recombinant viruses (Pleschka et al., 1996). However, all the systems described above were based on helper viruses and therefore required strong selection methods to separate the recombinant and the helper virus. Selection was achieved by using temperature-sensitive helper viruses, change of host range due to the inserted mutation, trypsin-independent growth or the use of specific antibodies (Li et al., 1995; Yasuda et al., 1994; Subbarao et al., 1993a; Pleschka et al., 1996; Enami and Palese, 1991).

The first negative-strand RNA virus rescue entirely from cloned cDNA was done by Schnell et al. in 1994, who rescued rabies virus (Schnell et al., 1994). The antigenome of this non-segmented virus was cloned under the control of a T7 promoter and transfected into cells along with plasmids expressing the proteins N, L and P. Infection with a recombinant vaccinia virus expressing the T7 polymerase resulted in the formation of infectious

rabies viruses. The key to a successful approach was the use of the antigenome rather than the genome. It is believed that the genome which is in a negative orientation could hybridise with the mRNA of the co-transfected N, L and P expressing plasmids, which would strongly interfere with virus replication (Figure 1.11 (B)). A further development of the system was the use of stably transfected cell lines that constitutively express T7 polymerase (Radecke et al., 1995). In the following years, several other non-segmented negative-strand RNA viruses were rescued, such as Measles virus, Sendai virus, Ebola virus and many others (Radecke et al., 1995; Garcin et al., 1995; Volchkov et al., 2001; Neumann et al., 2002).

Two years after the rescue of rabies viruses, the successful rescue of a segmented negative-strand RNA virus was reported. Bridgen and Elliott described the rescue of the three-segmented Bunyamwera virus from cloned DNA and showed that it is possible to generate more than one vRNA artificially (Bridgen and Elliott, 1996). The viral genome was cloned into plasmids flanked by the T7 polymerase promoter and hepatitis delta virus ribozyme. Cells were transfected with these plasmids together with plasmids expressing all viral proteins. Infection with recombinant vaccinia virus provided the T7 polymerase (Figure 1.11 (C)).

The rescue of influenza viruses proved to be more difficult due to the complexity of the genome and the proteins necessary for vRNP formation. In 1999, two groups reported the generation of influenza A viruses entirely from cDNA (Neumann et al., 1999; Fodor et al., 1999). Neumann et al. cloned the cDNA of each viral segment between a human RNA polymerase I promoter and a mouse RNA polymerase I terminator (Figure 1.12(A)). These eight plasmids were transfected into 293T cells along with four plasmids expressing the viral polymerase subunits and the nucleoprotein (Neumann et al., 1999), which led to the generation of infectious influenza A viruses (Figure 1.11(D)). The approach of Fodor et al. was similar, using a hepatitis delta virus ribozyme instead of a mouse Pol I terminator sequence (Figure 1.12(B)) (Fodor et al., 1999). In the following years, several attempts were made to improve the system, mainly by reducing the numbers of plasmids required. Hoffmann et al. developed two 8-plasmid rescue systems, a bidirectional and a unidirectional approach (Figure 1.12 (C and D)). The viral cDNA was cloned between a polymerase I promoter and terminator and this Pol I cassette was flanked by a polymerase II promoter and polyadenylation signal, which allowed the synthesis of viral

RNA and mRNA from one plasmid (Hoffmann et al., 2000a; Hoffmann and Webster, 2000; Hoffmann et al., 2000b).

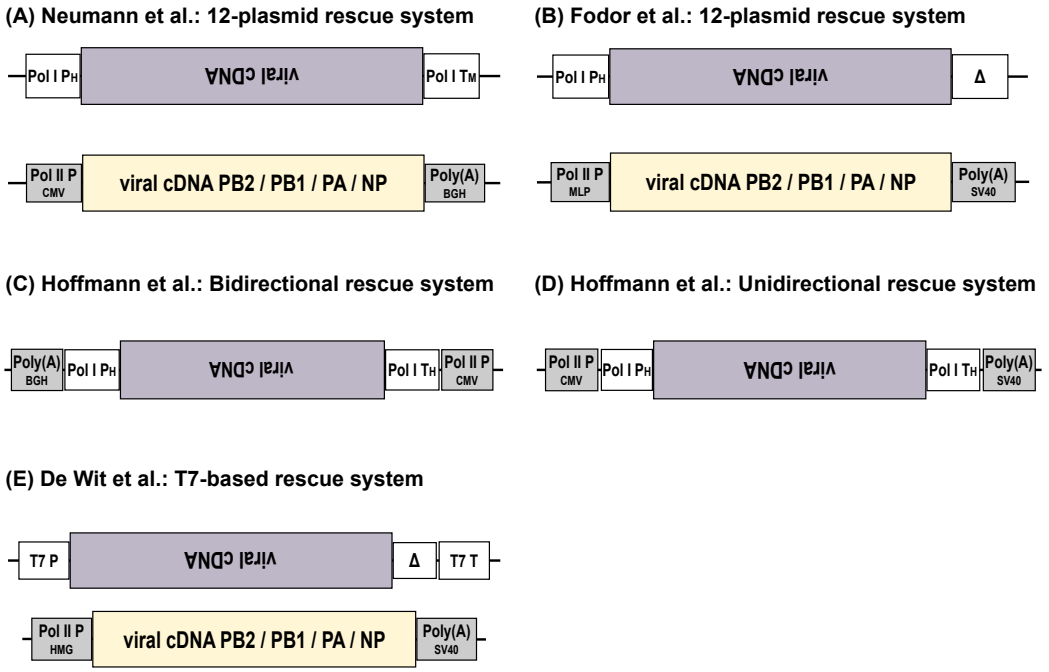

Figure 1.12: Reverse genetics systems for influenza A viruses: (A) 12-plasmid rescue system developed by Neumann et al. (1999). Eight plasmids expressing viral RNA are co-transfected with four plasmids expressing viral proteins PB2, PB1, PA and NP. **(B)** 12-plasmid rescue system developed by Fodor et al. (1999). Eight plasmids expressing viral RNA are co-transfected with four plasmids expressing viral proteins PB2, PB1, PA and NP. **(C)** Bidirectional 8-plasmid rescue system developed by Hoffmann et al. (2000a,b). Viral cDNA is inserted between the polymerase I promoter and terminator sequence flanked by polymerase II promoter and polyadenylation signal in a bidirectional orientation. **(D)** Unidirectional 8-plasmid rescue system developed by Hoffmann and Webster (2000). Viral cDNA is inserted between the polymerase I promoter and terminator sequence flanked by polymerase II promoter and polyadenylation signal in a unidirectional orientation. **(E)** T7 based rescue system developed by de Wit et al. (2007). Eight plasmids expressing the viral RNA under the control of a T7 promoter and terminator are transfected along with four plasmids expressing viral polymerase proteins and nucleoprotein. Pol I P_H=Human polymerase I promoter; Pol I T_M=mouse polymerase I terminator; Pol II P_{MLP}=Adenovirus type 2 major late promoter; Pol II P_{CMV}=Polymerase II promoter derived from cytomegalovirus; $Poly(A)_{SV40}$=simian virus 40 polyadenylation signal; $Poly(A)_{BGH}$=bovine growth hormone polyadenylation signal; Δ=hepatitis delta virus ribozyme sequences; T7 P=T7 polymerase promoter; T7 T=T7 polyermase terminator; Pol II P_{HMG}=mouse hydroxymethylglutaryl coenzyme A reductase promoter.

The position of the two promoters relative to the cDNA determined if the system was bidirectional or unidirectional, and if viral RNA produced was vRNA or cRNA, respectively. Although infectious virus could be recovered with both systems, the unidirectional system was less efficient and much lower viral titres were obtained (Hoffmann and Webster, 2000). Recently, even more compact procedures were developed for vaccine production. Cells suitable for vaccine production are not suitable for transfections with high numbers of plasmids in parallel. Neumann et al. generated a system with cDNA of either all segments cloned into one plasmid or six segments on one plasmid and the cDNA for NA and HA on a second. The plasmids were transfected with two additional plasmids that provide the polymerase subunits (combined on one plasmid) and the nucleoprotein. This reduced the number of plasmids to be transfected from 8 or 12 to only 3 or 4 plasmids (Neumann et al., 2005).

The use of RNA polymerase I promoters in influenza A virus rescues has some advantages compared to the T7-based system. Influenza A viruses replicate in the nucleus and only the RNA polymerase I is located in this compartment, whereas the T7 polymerase localises to the cytoplasm. However, the cellular polymerase I promoter shows host specificity, and the human polymerase I promoter is not functional in cells of avian or canine origin. Such rescue systems are therefore limited to specific cell types. A T7 based system was generated to rescue influenza A viruses in a variety of cells including human, canine and avian cells (Figure 1.12(E)). The system was improved by adding a nuclear localisation sequence to the T7 polymerase to support efficient transcription of influenza A virus cDNA (de Wit et al., 2007).

Beside rescue systems for the Bunyamwera virus and influenza A viruses, several other segmented negative-strand and ambisense RNA viruses have been rescued from cloned cDNA in the last decade, amongst them influenza B and C viruses, Thogoto virus, Rift Valley fever virus and recently the arenaviruses Lassa virus, lymphocytic choriomeningitis virus (LCMV) and Junin virus (JUNV) (Hoffmann et al., 2002; Crescenzo-Chaigne and van der Werf, 2007; Wagner et al., 2001; Ikegami et al., 2006; Albariño et al., 2011; Sánchez and de la Torre, 2006; Emonet et al., 2011).

1.3.2 Expression of foreign epitopes and proteins

The concept of integrating foreign epitopes or even complete genes into viral genomes seems appealing. It offers a wide range of opportunities to study the virus in more detail regarding genome size, packaging of segments or replication of the genome. It would also offer a straightforward way for drug screening. Additionally, the insertion of foreign sequences would allow the engineering of vaccines that immunise against multiple pathogens. Although the integration of foreign sequences often is not stable and insertion of large genes does not always support viral replication, some approaches have shown promise. Several non-segmented viruses e.g. VSV and Rabies virus carrying HIV-I epitopes have been tested for vaccine use (Schnell et al., 2000; Rose et al., 2001). VSV has also been used to express influenza A virus HA and NA, which protected mice from challenge with a lethal dose of influenza virus (Kretzschmar et al., 1997; Roberts et al., 1998a). However, the problem using VSV is the strong induction of an immune response against the VSV G protein, which prevents reinfection and also re-boosting of the vaccination (Rose et al., 2000).

Influenza A viruses have been also used to insert epitopes and genes into the viral genome. Chimeric hemagglutinins were engineered and studied as well as the integration of HIV-I epitopes into one of the influenza virus glycoproteins (Li et al., 1992, 1993; Muster et al., 1994, 1995). Garcia-Sastre et al. studied the use of an internal ribosomal entry site (IRES) to insert polypeptides containing amino acid sequences from the gp41 protein of HIV-1 into segment 6 of influenza A viruses (García-Sastre et al., 1994). The generation of influenza A viruses carrying bicistronic segments would also allow the insertion of full-length proteins. Segment 6 and 8 were mainly used for such attempts. In 1994, Percy et al. made a bicistronic segment 6 expressing the bacterial chloramphenicol acetyltransferase (CAT). A short self-cleaving 2A peptide from a FMDV was used to ”cleave” the two proteins during translation (Percy et al., 1994). The downside of this approach was the presence of additional amino acid residues on the upstream protein corresponding to the 2A peptide, which may interfere with the protein structure or function. However, a recombinant virus with GFP inserted upstream or downstream of NA via 2A may be a useful tool for drug screening (Li et al., 2010).

The proof that the viral promoter is not only functional when at the exterior of a viral segment opened up a path to use a duplicated promoter internally

between two ORFs (Flick and Hobom, 1999b; Machado et al., 2003, 2006). Three different proteins (GFP, VP0c and CAT) were successfully introduced and expressed from an ORF downstream of NA via duplicated 3'UTR (Chapter 5; Figure 5.10).

Segment 8 was used for the insertion of GFP or IL-2 using two different method, first the overlapping Stop-Start cassette from an influenza B virus and second an artificial caspase-cleavage site (Kittel et al., 2004, 2005). The different strategies to express foreign genes in influenza A viruses are introduced in more detail in Chapter 5.

1.4 Aims

Because of the nature of segment 2 expressing PB1-F2 from an internal overlapping ORF, the possibilities to study this protein are rather limited. Introduction of point mutations have to be chosen carefully in order not to alter the amino acid sequence of the overlapping polymerase subunit.
Several goals were defined at the beginning of the project to investigate the role of PB1-F2 on viral replication, apoptosis and virulence. To make PB1-F2 more accessible for genetic modifications, it was planned to separate the overlapping PB1-F2 ORF from the PB1 ORF:

- Deletion of PB1-F2 by inserting three point mutations (Chapter 3)
- Inserting PB1-F2 as an independent ORF into segment 2 using three different methods (Chapter 5):
  - Insertion of PB1-F2 via an overlapping Stop-Start cassette
  - Insertion of PB1-F2 using a duplicated promoter
  - Insertion of PB1-F2 using a short self-cleaving 2A peptide (FMDV)
- Insertion of PB1-F2 as an independent ORF into segment 6 and 7 using a duplicated promoter (Chapter 5)

After engineering the plasmids, viruses were rescued, the effectiveness of the constructs for PB1-F2 expression has been tested and recombinant viruses were characterised using different experiments. Investigations of the phenotypic characterisation included comparisons of plaque sizes, growth characteristics, the ability to induce apoptosis and *in vivo* replication using a mouse model.
With the discovery of N40 and the resulting consequences that deletion of PB1-F2 by mutation of its start codon had on the level of N40, aims of this project were adjusted:

- Deletion of PB1-F2 by inserting two point mutations (Chapter 3)
- Engineering of N40 and PB1-F2/N40 mutant viruses (Chapter 6)
- *in vitro* and *in vivo* characterisation of the recombinant viruses (Chapter 3 and 6)

The influence of PB1-F2 on viral polymerase activity and the ability to degrade cellular polymerase II was tested. After the discovery that the polymerase subunits PB2 and PA participate in the cellular RNAPII degradation, amino acids that are potentially involved were identified, mutated and recombinant viruses were tested for their effect (Chapter 4).

Chapter 2

MATERIALS AND METHODS

2.1 Cell lines and tissue culture

2.1.1 Cell lines used in this study

Cells that were used in this study are summarised in Table 2.1.

Name	Description
293FT	Highly transfectable clone derived from human embryonal kidney cells
A549	Adenocarcinomic human alveolar basal epithelial cell line
MDCK	Madin-Darby Canine Kidney epithelial cell line
RAW/W	Mouse leukaemic monocyte macrophage cell line
Macrophage 1 and 2	Fresh human macrophages type 1 and 2

Table 2.1: Cell lines used in this study.

MDCK cells were used for virus propagation, purification, titration, immunoblotting, measuring virus growth and in protein labelling experiments. A549 cells were also used for measuring virus growth and immunoblotting and several other assays to characterise the different influenza A virus mutants such as primer extension assays. 293FT cells were used for influenza A virus rescues as well as transfection for luciferase assays. RAW/W cells were used in a cell viability assay. Human macrophages were used in a macrophage assay.

2.1.2 Cell maintenance

Cell monolayers were maintained in 75 cm^2 (medium) or 175 cm^2 (large) culture flasks (Greiner) in DMEM (Dulbecco's modified Eagle medium; Invitrogen) and incubated at 37°C and 5% CO_2. DMEM was supplemented with 10% fetal bovine serum (FBS). Cell monolayers were passaged regularly using Trypsin/EDTA. Therefore cells were washed with PBS before adding 3 ml (medium flask) or 5 ml (large flask) of Trypsin/EDTA. Cells were incubated for up to 20 min to detach and Trypsin/EDTA solution was removed from the cells by centrifugation (1000xg, 5min). Pelleted cells were resuspended in fresh DMEM supplemented with FBS and 1/8 of the cells was transferred into a new flask.

2.1.3 Macrophage subset differentiation protocol

The mononuclear cell fraction of freshly drawn blood was used to isolate CD14+ cells by magnetic cell sorting. Cells were centrifuged at 300xg for 10 min and the supernatant was removed completely. Pellet was resuspended in 16 µl MACS buffer (PBS / 2% FCS / 2mM EDTA) per 10^7 total cells and 4 µl anti-CD14 microbeads (Miltenyi Biotec) were added and gently mixed. After 20 min incubation at 4℃ cells were washed with 5 ml MACS buffer and centrifuged at 300xg for 6 min. Cells were resuspended in 500 µl cold MACS buffer and applied onto a MACS LS column (Miltenyi Biotec), which had been rinsed with MACS buffer. Unlabelled cells (flow-through) were collected by washing the column three times with MACS buffer. After removal of the column from the magnet, they were placed in a 15 ml falcon tube. 5 ml MACS buffer were added onto the column and cells were flushed out using a plunger. CD14+ cells were washed, counted and resuspended in culture medium IMDM (R&D Systems).

CD14+ cells were cultured in 24-well plates in IMDM containing penicillin/streptomycin (PPA Laboratories, 50U/ml) and 10% heat-inactivated FCS. To generate the macrophage subset 1 or 2, cells were cultured in the presence of either GM-CSF (Peprotech) or M-CSF (R&D Systems) as seen in Table 2.2.

Macrophage subset	**Differentiation media**
Macrophage 1	IMDM supplemented with FCS and GM-CSF at final concentration of 50 U/ml
Macrophage 2	IMDM supplemented with FCS and M-CSF at final concentration of 25 ng/ml

Table 2.2: Macrophage subset and the required media.

At day 2 and day 4, fresh media containing the appropriate cytokine (GM-CSF or M-CSF) was added to the cells. Cells were ready for further experiments at day 6, when they were infected with influenza A virus (A/Udorn/72).

2.2 Virus infections

2.2.1 Viruses used in this study

Recombinant viruses used in this study are listed in Tables 2.3 to 2.6.

Name	Description
rUdo WT	recombinant wild-type IAV (A/Udorn/1972)
rWSN WT	recombinant wild-type IAV (A/WSN/33)

Table 2.3: Recombinant wild type viruses (A/Udorn/72 and A/WSN/33) used in this study. Plasmids to generate the viruses were provided by D. Jackson (University of St Andrews, UK)

Name	Description
rUdo $\triangle$AUG	recombinant Udorn virus deficient in its PB1-F2 expression; point mutations in segment 2 at position 120, 153 and 291
rWSN $\triangle$AUG	recombinant WSN virus deficient in its PB1-F2 expression; point mutations in segment 2 at position 120, 153 and 291; described previously by Zamarin et al. (2006)
rWSN F2-11	recombinant WSN virus deficient in its PB1-F2 expression; point mutations at position 153 and 291; the N-terminal 11 aa of PB1-F2 are expressed
rWSN $\triangle$N40	recombinant WSN virus deficient in its N40 expression; point mutations in segment 2 at position 142; PB1 residue 40 Met $\rightarrow$ Leu; described previously by Wise et al. (2009)
rWSN $\triangle$F2/$\triangle$N40	recombinant WSN virus deficient in PB1-F2 and N40; point mutations in segment 2 at position 144 and 291; PB1 residue 40 Met $\rightarrow$ Ile; two stop codons to delete PB1-F2 at aa 9 and 58

Table 2.4: Recombinant WSN and Udorn viruses carrying mutations in segment 2: The different viruses are deficient in the expression of PB1-F2, N40 or deficient in both ORF.

Name	Description
rWSN △AUG-StSt-F2	recombinant WSN virus carrying three point mutations to delete PB1-F2; expression of PB1-F2 from an individual ORF from segment 2 via an overlapping Stop-Start codon
rWSN △AUG-2A-F2	recombinant WSN virus carrying three point mutations to delete PB1-F2; expression of PB1-F2 from an individual ORF from segment 2 using the self-cleaving 2A peptide (FMDV)
rWSN △AUG/NA-F2	recombinant WSN virus carrying three point mutations to delete PB1-F2; expression of PB1-F2 from an individual ORF from segment 6 using a duplicated promoter
rWSN F2-11/NA-F2	recombinant WSN virus carrying two point mutations to delete PB1-F2; expression of PB1-F2 from an individual ORF from segment 6 using a duplicated promoter

Table 2.5: Recombinant influenza A viruses (A/WSN/33) carrying an individual PB1-F2 ORF in segment 2 or segment 6.

Name	Description
rWSN $PB2_{504}$	recombinant WSN virus deficient; point mutation in segment 1; PB2 residue 504 Val $\rightarrow$ Ile
rWSN PA_{550}	recombinant WSN virus deficient; point mutation in segment 3; PA residue 550 Leu $\rightarrow$ Ile
rWSN $PB2_{504}$ /PA_{550}	recombinant WSN virus deficient; point mutations in segment 1 and 3; PB2 residue 504 Val $\rightarrow$ Ile and PA residue 550 Leu $\rightarrow$ Ile

Table 2.6: Recombinant WSN viruses carrying mutations in segment 1 and 3.

2.2.2 Virus rescues

Influenza A virus rescues were done using the 12-plasmid rescue system described by Neumann et al. (1999). Eight plasmids expressing the viral RNA segments (pHH-PB2, pHH-PB1, pHH-PA, pHH-HA, pHH-NP, pHH-NA,

pHH-M, pHH-NS: 0.5 µg each) together with four plasmids expressing viral proteins for the three polymerase subunits (pcDNA-PB2 1 µg; pcDNAPB1 1 µg; pcDNA-PA 0.2 µg) and the nucleoprotein (pcDNA-NP 1 µg) were transfected into 293FT cells using FuGENE 6 transfection reagent (Roche). Plasmids were mixed with 3 µl FuGENE/1 µg DNA and 130 µl DMEM containing 3% FBS.

After an incubation time of 20 min this mixture was added dropwise to the confluent 293FT cell monolayer. Cells were incubated at 37℃ and 5% CO_2. After 20 h the transfected 293FT cells were mixed with MDCK cells and transferred to a 25cm^2 flask for incubation in 5 ml DMEM supplemented with 10% FBS. To allow propagation of the virus the supernatant was removed after 6 to 8 h and 5 ml serum-free DMEM containing 2.5 µg/ml N-acetyl trypsin (Sigma) was added to the cells. Recombinant viruses were harvested before cytopathic effect was 100%. Supernatants were centrifuged at ∼1000xg for 5 minutes and aliquoted into cryovials for storage of the virus rescue stock at -70℃ .

2.2.3 Preparation of IAV elite stocks by plaque purification

A series of 10-fold dilutions of influenza A virus rescue stocks were prepared. 6-well plates with 80% confluent MDCK cells were washed with PBS before 200 µl of the virus dilutions were added to the cells. Cells were incubated for absorption of the virus at 37℃ . After 1 hour the inoculum was removed and 2 ml of the overlay media (Table 2.7) was added to each well. After the overlay had set, plates were inverted and incubated for 3 days at 37℃ and 5% CO_2. At day three plaques were clearly visible. The agar overlaying the virus plaque was removed using a sterile pipette tip and the plug was expelled into serum-free DMEM. Serum-free DMEM including N-acetylated trypsin containing the plaque purified virus was added to MDCK cells in a 25 cm^2 flask for growing up elite stocks. Supernatants were harvested after 2 or 3 days, when cytopathic effect was 70-80%. Cell debris was removed by centrifugation (1000xg; 5 min) and virus solution was aliquoted into cryovials for storage at -70℃ .

Overlay media	**2 x DMEM**
12.5 ml 2 x DMEM	13.4 g DMEM
12.5 ml 2% Agarose	3.7 g $NaHCO_3$
2 µg/ml N-acetyl trypsin	10 mM HEPES pH 7.4
$\rightarrow$ filter sterilization	485 ml H_2O

Table 2.7: Chemical composition of the influenza A virus plaque assay overlay media.

2.2.4 Preparation of virus working stocks

To prepare working stocks of influenza A viruses, 80% confluent monolayers of MDCK cells (75cm^2 flask) were washed with PBS to remove traces of fetal bovine serum. Cells were inoculated in serum-free DMEM at an MOI of 0.001 plaque-forming units (pfu). Cells were incubated at 37℃ and 5% CO_2 and supernatants were harvested when cytopathic effect was 70-80%. Cellular debris was removed by centrifugation (1000xg, 5min) and virus working stocks were aliquoted into cryovials and stored at -70℃ . Virus titres were determined as described below (subsection 2.2.6).

2.2.5 Virus infections

Influenza A virus infections at any desired MOI were carried out in serum-free DMEM. Prior to any infection, cells were washed with PBS to remove traces of serum. 200 µl (per 6-well plate) of the virus dilution was added to the confluent cell monolayer. Cells were incubated for 1 hour at 37℃ / 5% CO_2 with gentle rocking every 15 min. Inoculum was removed and serum-free DMEM was added to the cells, with or without N-acetyl trypsin and incubated at 37℃ / 5% CO_2 for the required time.

2.2.6 Virus titration

Influenza A virus titration was carried out on MDCK cells in 6-well plates. DMEM was removed from the confluent monolayer and cells were washed with PBS to remove traces of serum. Virus stocks were serially diluted 10-fold in serum-free DMEM and 200 µl of virus dilution was added to each well before incubation at 37℃ / 5% CO_2. Plates were gently rocked every 15

min. During this time, the overlay media was prepared, using Avicel instead of Agarose. 2x DMEM (table 2.7) was mixed with 2.4% Avicel (2.4g Avicel / 100 ml H_2O; autoclaved) at a ratio of 1:1 and 2 µg/ml N-acetyl trypsin was added. After 1 hour inoculum was removed and 2 ml overlay media were added to the cells following further incubation ($\sim$ 3 days). Cells were fixed by adding PBS / 4% formaldehyde to the cells. Fixing was left for several hours. Overlay media was removed and cells were stained with crystal violet (0.1% crystal violet, 3.6% formaldehyde, 1% methanol, 20% ethanol in H_2O) or by immunostaining as described below (Section 2.2.7). Plaques were counted and virus titres were calculated as pfu/ml, taking into account the original dilutions of the viruses.

number of plaques x dilution x 5 (200 µl virus added per dish) = pfu/ml

2.2.7 Immunostaining

Fixed cells were washed with PBS and 500 µl PBN (PBS, 1% BSA, 0.02% sodium azide) was added to each well. Cells were placed on rocker for 1 hour at room temperature. PBN was removed and replaced with 500 µl primary antibody (goat antisera raised against A/Udorn/72). After incubation for 1 hour cells were washed with PBN and 500 µl secondary anti-goat IgG alkaline phosphatase (AP)-conjugated antibody was added for 1 hour. Cells were washed with PBN and incubated with 500 µl/well of alkaline phosphatase substrate (as per manufacturer's instructions; Sigma-Aldrich; FAST BCIP/NBT) until plaques were visible. To stop the reaction, cells were rinsed with water and placed to dry.

2.2.8 Virus yield assay

To determine replication of infectious virus over time, confluent MDCK cells were infected with virus dilutions at an MOI of 3 for a single replication cycle or at an MOI of 0.001 for a multi replication cycle. Infection was carried out as described above (Section 2.2.5). Inoculum was left for 1 hour to absorb and was subsequently replaced by serum-free DMEM (supplemented with 2.5 µg/ml N-acetyl trypsin for a multi replication cycle). Cells were incubated at 37℃ /5% CO_2 and supernatants were harvested at specific time points post infection. Virus titre was determined by plaque assays as described earlier (Section 2.2.6).

2.2.9 *In vivo* virulence assay

6-7 week old female BALB/c mice were inoculated intranasally with $5x10^3$ pfu virus. Each mouse was weigthed and anaesthetised for a few seconds to allow infection with one of the different virus strains. Eight or ten mice were infected with the same virus and placed into one chamber. Infection with PBS was used as a control. Mice were weighted ever day to monitor weight loss. At day four and day seven, four mice of each group were culled using CO_2. Mice were also culled if weight loss was close to 25%. Lungs were taken for virus titration. For this, 6-well-plates with confluent MDCK cells were prepared. Frozen lungs were diced and placed in a pre-chilled plastic bijoux with 1.5 ml cold serum-free DMEM. Lung tissue was homogenised using an OMNI TH homogeniser: 5 bursts at 20,000 rpm for 3 seconds and a final burst for 6 seconds were delivered. Supernatants were transferred into a fresh cryovial and centrifuged at 3000 rpm at 4℃ for 5 min. Clear supernatants were transferred into a new cryovial and stored on ice until titration. A series of 10-fold dilutions of each lung preparation was made. 6-well plates with confluent MDCK cells were washed twice with PBS before 400 µl of the virus dilutions were added to the cells. Cells were incubated for absorbtion of the virus at 37℃ and gently rocked every 10 min. After 1 hour the incoculum was removed and 2 ml of the overlay media (12.5 ml 2x DMEM, 12.5 ml 1.2% Avicel, 2 µg/ml N-acetyl trypsin) was added to each well. Plates were incubated for 3 days at 37℃ and 5% CO_2. At day 3, 2 ml of 4% formaldehyde was added to each well for fixing. Overlay was removed and cells were stained with crystal violet until plaques were clearly visible.

2.3 Plasmid DNAs

2.3.1 Plasmids used in this study

Plasmids to rescue A/WSN/33 and A/Udorn/72 were kindly provided by David Jackson (University of St Andrews, UK). These plasmids were also used as a template for mutagenesis of segment 1, 2, 3 and 6. Several other plasmids were engineered during this study to allow performance of different assays such as luciferase assay or transfections of 293FT cells.

pcDNA 3.1(+)	parental vector for protein expression used in luciferase assays, transfections and rescues; Invitrogen
pGEMT Easy / pGEMT	linear vector with T-overhangs for PCR cloning; Promega
pJC3	parental vector: pcDNA 3.1(+); GFP-2A-mCherry under CMV promoter
pcDNA-PB2, pcDNA-PB1, pcDNA-PA, pcDNA-NP	plasmids expressing the three polymerase subunits (PB2, PB1, PA) and the nucleoprotein (NP) of either A/WSN/33 or A/Udorn/72
pHH21	parental vector for rescue plasmids coding for the viral RNA (Neumann et al., 1999)
pHH-PB2, pHH-PB1, pHH-PA, pHH-HA, pHH-NP, pHH-NA, pHH-M, pHH-NS	plasmids coding for the viral RNA segments 1-8 of either A/WSN/33 or A/Udorn/72
pHH-ΔATG	parental plasmid: pHH-PB1 WSN or Udorn; PB1-F2 deleted by insertion of three point mutations ($T_{120}C$; $C_{153}G$; $G_{291}A$)
pHH-F2-11	parental plasmid pHH-ΔATG WSN; PB1-F2 deleted by two point mutations ($C_{153}G$; $G_{291}A$)
pHH-ΔATG-StSt-F2	parental plasmid: pHH-ΔATG WSN; PB1 gene connected to PB1-F2 by an overlapping Stop-Start sequence (TAATG)
pHH-ΔATG-3'UTR-F2	parental plasmid: pHH-ΔATG WSN; PB1 gene connected to PB1-F2 by via a duplicated promoter (3'UTR)
pHH-ΔATG-2A-F2	parental plasmid: pHH-ΔATG WSN; PB1 gene connected to PB1-F2 by via a FMDV self-cleavage 2A peptide

pHH-NA-F2	original plasmid pHH-NA WSN; neuraminidase gene is connected to PB1-F2 via a duplicated promoter (3'UTR)
pHH-$\triangle$N40	original plasmid: pHH-PB1 WSN; $Met_{40} \rightarrow Leu_{40}$ to delete N40
pHH-$\triangle$F2/$\triangle$N40	original plasmid: pHH-PB1 WSN; $Met_{40} \rightarrow Ile_{40}$ to delete N40; two stop codons introduced at aa 9 and 58 to disrupt PB1-F2 ORF
pcDNA-$\triangle$ATG	pcDNA3.1(+) vector with PB1-F2 deletion in PB1 (three point mutations as in pHH-$\triangle$ATG)
pcDNA-F2-11	pcDNA3.1(+) vector with WSN PB1-F2 deletion in PB1 (two point mutations as in pHH-F2-11)
pcDNA-$\triangle$N40	pcDNA3.1(+) vector expressing WSN PB1 carrying the mutation $Met_{40} \rightarrow Leu_{40}$ to delete N40
pcDNA-$\triangle$F2/$\triangle$N40	pcDNA3.1(+) vector expressing WSN PB1 with N40 and PB1-F2 deletion
pHH-Renilla	pHH-backbone carrying renilla in a negative orientation embedded in NP-UTRs
pCMV-FF	plasmid carrying the firefly gene under the control of a CMV promoter
pHH-PB2 $V_{504}I$	PB2 WSN with an aa change $Val_{504} \rightarrow Ile_{504}$
pHH-PA $L_{550}I$	PA WSN with an aa change $Leu_{504} \rightarrow Ile_{504}$

Table 2.8: List of plasmids used in this study.

2.3.2 Amplification of plasmid DNA

E. coli JM109 cells were grown in 5ml Luria-Bertani (LB) medium (10g/l bacto-tryptone, 5g/l yeast extract, 10mM NaCl, pH 7.5), or plated on solid LB medium supplemented with 1.5% (w/v) agar. Media was supplemented with ampicillin (100 µg/ml) or kanamycin (50 µg/ml) for selection.

2.3.3 Preparation and transformation of competent *E.coli*

Competent *E.coli* JM109 were obtained using the "Z-competent *E.coli* Tranformation kit" (Zymo research) according to the manufacturer's protocol.

To transform competent *E. coli* JM109, 50-100 ng DNA was added to 100 µl competent cells and spread onto LB-agar plates containing ampicillin or kanamycin. Plates were inverted and incubated at 37℃ for 12-16 hours. Single colonies were used to set up mini-cultures.

2.3.4 Preparation of plasmid DNA

For small-scale preparations of plasmid DNA, 10 ml of LB-media supplemented with ampicilin (100 µg/ml) was inoculated with a single *E.coli* colony and incubated overnight at 37℃ in a shaking incubator. DNA plasmid preparation was done either using the QIACube or manually using the QIAprep Spin Miniprep Kit (QIAGEN Ltd., UK) according to the manufacturer's protocol. DNA was eluted in 50 µl H_2O. For larger scale DNA preparations 50 ml bacterial cultures were grown overnight at 37℃ in a shaking incubator. DNA was extracted using the QIAGEN Plasmid Maxi Kit according to the manufacturer's instructions.

2.3.5 Determination of DNA concentration

Concentration of dsDNA was determined by measurement of Abs_{260} using a NanoDrop ND-1000 spectrophotometer (Thermo Scientific). Purity of the DNA sample was estimated by calculating the Abs_{260}/Abs_{280} ratio. Ratio values greater then 1.8 were considered as acceptable.

2.4 Manipulation of plasmid DNA

2.4.1 Synthetic oligonucleotides

All synthetic oligonucleotides that were used throughout this study are listed in the Tables 2.9 to 2.14.

name	**sequence 5' → 3'**	**description**
sv01	GAT CCT CCA TAC AGC CAC GGA ACA GGA ACA	T_{120}C PB1 Udo For
sv02	GTT CCT GTT CCG TGG CTG TAT GGA GGA TC	T_{120}C PB1 Udo Rev

sv03	TGG ACA CAG TGA ACA GAA CAC ATC AAT ATT	C_{153}G PB1 Udo For
sv86	GGA ACA GGA TAC ACC ATG GAC ACA GTG AAC AGA ACA C	C_{153}G PB1 Udo Rev
sv05	ACA AAC AGA CTG TGT CCT AGA AGC AAT GGC	G_{291}A PB1 Udo For
sv06	GCC ATT GCT TCT AGG ACA CAG TCT GTT TGT	G_{291}A PB1 Udo Rev
sv09	ACC CTC CTT ACA GCC ACG GGA CAG GAA CAG	T_{120}C PB1 WSN For
sv10	CTG TTC CTG TCC CGT GGC TGT AAG GAG GGT	T_{120}C PB1 WSN Rev
sv11	GAT ACA CCA TGG ATA CTG TGA ACA GGA CAC	C_{153}G PB1 WSN For
sv12	GTG TCC TGT TCA CAG TAT CCA TGG TGT ATC	C_{153}G PB1 WSN Rev
sv13	CAA ACA GAT TGT GTA TTA GAA GCA ATG GCC	G_{291}A PB1 WSN For
sv14	GGC CAT TGC TTC TAA TAC ACA ATC TGT TTG	G_{291}A PB1 WSN Rev

Table 2.9: List of synthetic oligonucleotides used to delete PB1-F2 in A/Udorn/72 and A/WSN/33.

name	**sequence 5' $\rightarrow$ 3'**	**description**
sv07	CAG ACG GCA AAA ATC TAG AAT TTA GCT TGT	PB1 *Xba*I site For
sv08	ACA AGC TAA ATT CTA GAT TTT TGC CGT CTG	PB1 *Xba*I site Rev
sv26	CTT GCG GGA GAC GTC GAG TCC AAC CCC GGG CCC ATG GGA CAG GAA CAG GAT AC	2A-PB1-F2 For 1 WSN
sv22	GTG ATG CGA TCT AGA CAG CTG TTG AAT TTT GAC CTT CTT AAG CTT GCG GGA GAC GTC GAG T	2A-PB1-F2 For 2

sv27	GCG CTC ATC TAG AGT AGA AAC AAG GCA TTT TTT CAT GAA GGA CAA GCT AAA TTC ACT ATT TTT GCC GT	PB1-F2 Rev 1 WSN
sv28	CAC TAT TTT TGC CGT CTG AGC TCT TCA ATG GTG GAA CAG ATC TTC AGC TTG TCC ACT CGT GTT TGC	PB1-F2 Rev 2 WSN
sv32	CAG ACG GCA AAA ATA ATG CAT TTA GCT TGT	PB1 *Nsi*I For
sv33	ACA AGC TAA ATG CAT TAT TTT TGC CGT CTG	PB1 *Nsi*I Rev
sv34	ATC CTC CAT ATG CAT CAG GAA CAG GAT AC	PB1-F2 *Nsi*I For
sv40	GGC TGA CAT GCA TGT AGA AAC AAG GCA TTT TTT CAT GAA GGA CAA GCT AAA TTC ACT ATT TTT GCC GT	PB1-F2 *Nsi*I Rev 1 WSN
sv38	AGA CGG CAA AAA TAA TGG GAC AGG AAC AG	TAATG For WSN
sv39	CTG TTC CTG TCC CAT TAT TTT TGC CGT CT	TAATG Rev WSN
sv65	CGG CAA AAA TAG TGA ATC TAG ATT GTC C	*Xba*I 3'UTR For WSN
sv66	GGA CAA TCT AGA TTC ACT ATT TTT GCC G	*Xba*I 3'UTR Rev WSN
sv103	GAT GTC AGT CTC GAG ATG GGA CAG GAA CAG GAT AC	*Xho*I-PB1-F2 For
sv104	ACT GAC ATC GCT AGC TCA GCT TGT CCA CTC GTG	*Nhe*I-PB1-F2 Rev
sv105	GAT GTC AGT CTC GAG ATG GTG AGC AAG GGC GAG GA	*Xho*I-mCherry For
sv106	ACT GAC ATC GCT AGC TTA TTT GTA CAA TTC ATC CAT GCC GC	*Nhe*I-mCherry Rev

sv117	CGT CTC AGG GAG CGA AAG CAG GAG TTT AAA TG	*Bsm*BI-NA For
sv118	CTC GAG TTA AAC TCC TGC TTT CG CTG AAT TCC TAC TTG TCA ATG GTG AAC GG	NA-*Xho*I Rev
sv119	TGG TGA ACG GCA ACT CAG CAC CGT CTG GCC AGC TAG CCT CGA GTT AAA CTC CTG CTT TCG CT	adds 3'UTR to NA Rev 1
sv120	GTC TCC TAT TAG TAG AAA CAA GGA GTT TTT TGA ACA AAC TAC TTG TCA ATG GTG AAC GGC AAC TCA G	adds 3'UTR to NA Rev 2
sv121	GGT TCC AAA GGT GAC GTT TTT GTC	removes *Bsm*BI from NA For
sv122	GAC AAA AAC GTC ACC TTT GGA ACC	removes *Bsm*BI from NA Rev
sv115	CGT CTC AGG GAG CAA AAG CAG GTA GAT ATT G	*Bsm*BI-M For
sv100	CTC GAG CTT TCA ATA TCT ACC TGC TTT TGC TGA ATT CTT ACT CCA GCT CTA TGT TGA C	adds *Xho*I to M Rev
sv101	AGC TCT ATG TTG ACA AAA TGA CCA TCG TCA ACA TCG CTA GCC TCG AGC TTT CAA TAT CTA CC	adds 3'UTR to M Rev
sv102	TTA TTG GAG ACG AGT AGA AAC AAG GTA GTT TTT TAC TCC AGC TCT ATG TTG ACA AAA TGA CC	adds Mend and 5'UTR Rev
sv116	CGT CTC CTA TTA GTA GAA ACA AGG TAG	*Bsm*BI-M Rev

sv129	ACC CTC CTT ACA GCC ATG GGA CAG GAA CAG	C_{120}T PB1 WSN For
sv130	CTG TTC CTG TCC CAT GGC TGT AAG GAG GGT	C_{120}T PB1 WSN Rev

Table 2.10: List of synthetic oligonucleotides used to insert PB1-F2 into segment 2 (A/WSN/33) or segment 6 (A/WSN/33).

name	**sequence 5' → 3'**	**description**
sv19	GAG TAC TGG TCG ACC TCC GAA GTT G	to sequence pHH For 1
sv78	GAC ACT TTC GGA CAT CTG G	to sequence pHH For 2
sv29	GTA TAT CTT TCG CTC CGA GTC GGC	to sequence pHH Rev 1
sv79	CAG GTG TCC GTG TCC GTG TC	to sequence pHH Rev 2
sv20	CAG TCT GGA CTT CCA GTT GG	PB1 internal Udorn For
sv21	GAT TGC CAG TTG GAG GCA ATG	PB1 internal WSN For
sv30	GTC TTC CCT GAT AGT CCT CAT CC	PB1 internal Udorn Rev
sv31	CAT AAA CGC CCC TGG TAA TCC TC	PB1 internal WSN Rev
sv52	GGA TGT CAA TCC GAC TTT AC	RT-PCR PB1 WSN For
sv45	GCA TCT TTG GTC ATT GTG TTC	RT-PCR PB1 WSN Rev

Table 2.11: List of synthetic oligonucleotides used for sequencing or RT-PCRs.

name	**sequence 5' → 3'**	**description**
sv172	GAAC AGG ATA CAC CTT GGA TAC TGT CAA CAG	$Met_{40} \rightarrow Leu_{40}$ PB1 WSN For
sv173	CTG TTG ACA GTA TCC AAG GTG TAT CCT GTT C	$Met_{40} \rightarrow Leu_{40}$ PB1 WSN Rev
sv174	GAA CAG GAT ACA CCA TAG ATA CTG TCA ACA G	$Met_{40} \rightarrow Ile_{40}$ PB1; PB1-F2 aa 9→ Stop WSN For
sv175	CTG TTG ACA GTA TCT ATG GTG TAT CCT GTT C	$Met_{40} \rightarrow Ile_{40}$ PB1; PB1-F2 aa 9→ Stop WSN Rev

Table 2.12: List of synthetic oligonucleotides used to delete N40.

name	sequence 5' → 3'	description
sv87	CTA GTG CAA AGC TTA TGG ATG TCA ATC CGA CTT TAC	*Hind*III-PB1 For WSN
sv88	GCA TCA CGA AGC TTC TAT TTT TGC CGT CTG AG CTC TTC	*Hind*III-PB1 Rev WSN
sv89	CTA GTG CAA AGC TTA TGG GAC AGG AAA GGA TAC	*Hind*III-PB1-F2 For WSN
sv90	CTA GTG CAA AGC TTT CAG CTT GTC CAC TCG TG	*Hind*III-PB1-F2 Rev WSN
sv91	CTA GTG CAG ATA TCA TGG ATC CAA ACA CTG TGT C	*Eco*RV-NS1 For
sv92	CTA GTG CAG ATA TCT CAA ACT TCT GAC CTA ATT G	*Eco*RV-NS1 Rev
sv93	ATG GGA GGA GAC GAG CAA AAG CAG GGT AGA TAA TCA CTC ACA GAG TGA CAT CGA AAT CAT GAC TTC GAA AGT TTA	to insert Renilla-NP(UTRs) into pHH WSN For
sv94	TTA TTG GAG ACG AGT AGA AAC AAG GGT ATT TTT CTT TAT TGT TCA TTT TTG AGA ACT CGC T	to insert Renilla-NP(UTRs) into pHH WSN Rev

Table 2.13: List of synthetic oligonucleotides used to prepare plasmids for the luciferase assay and transfections of 293FT cells.

name	sequence 5' → 3'	description
sv181	CGT TTT TTG AGA ATT AGG GAC CAA CGT GGG	PB2 $Val_{504} \rightarrow Ile_{504}$ WSN For
sv182	CCC ACG TTG GTC CCT AAT TCT CAA AAA ACG	PB2 $Val_{504} \rightarrow Ile_{504}$ WSN Rev
sv183	GGA GAT ATG CTT ATA AGA AGT GCC	PA $Leu_{550} \rightarrow Ile_{550}$ WSN For
sv184	GGC ACT TCT TAT AAG CAT ATC TCC	PA $Leu_{550} \rightarrow Ile_{550}$ WSN Rev

Table 2.14: List of synthetic oligonucleotides used for site-directed mutagenesis in order to study cellular polymerase II degradation.

2.4.2 Amplification of DNA by PCR

PCR was done using the proofreading polymerase KOD hot start polymerase or the GoTaq DNA polymerase. PCR reactions were set up according to the manufacturer's instructions in 0.5 ml thin-walled tubes using a thermo cycler.

Standard reaction using KOD hot start polymerase (Merck) (50 µl):

10x Buffer	5 µl
dNTPs (10mM each)	5 µl
25 mM Mg_2SO_4	2.5 µl
template (10-50 ng)	X µl
forward oligo (20 µM)	1.25 µl
reverse oligo (20 µM)	1.25 µl
KOD polymerase (1U/µl)	1 µl
dH_2O (fill up to 50 µl)	Y µl

PCR programme for KOD hot start polymerase:

Polymerase activation	95℃	2 min	
Denaturation	95℃	30 sec	18 - 40 cycles
Annealing	adjust to primers	30 sec	
Elongation	70℃	30 sec/kb	
Final extension	70℃	10 min	
Soak	10℃	∞	

Standard reaction using GoTaq DNA polymerase (Promega) (50 µl):

5x green or colorless Buffer	10 µl
dNTPs (10mM each)	1 µl
template (10-50 ng)	X µl
forward oligo (20 µM)	1.25 µl
reverse oligo (20 µM)	1.25 µl
GoTaq polymerase (5U/µl)	0.25 µl
dH_2O (fill up to 50 µl)	Y µl

PCR programme for GoTaq DNA polymerase:

Polymerase activation	95℃	2 min	
Denaturation	95℃	30 sec	25 - 35 cycles
Annealing	adjust to primers	30 sec	
Elongation	72℃	1 min/kb	
Final extension	72℃	10 min	
Soak	10℃	∞	

2.4.3 QuikChange site-directed mutagenesis

To introduce point mutations into influenza viral segments, QuikChange site-directed mutagenesis was used. Therefore, two complementary oligonucleotide primers carrying the desired mutation were used in a PCR reaction. KOD hot start polymerase (Merck) was used as DNA polymerase. Before transformation of the plasmids, the mix was treated with *Dpn*I to digest parental methylated plasmids. Newly synthesised plasmid are not methylated and therefore not targeted by *Dpn*I. DNA was transformed into *E.coli* JM109 cells. After amplification and preparation of plasmid DNA (as described in Section 2.3.4), the nucleotide sequences were determined to ensure the insertion of the point mutation.

Standard QuikChange reaction using KOD hot start polymerase (50 µl):

10x Buffer	5 µl
dNTPs (10mM each)	5 µl
25 mM Mg_2SO_4	2.5 µl
template (10-50 ng)	X µl
forward oligo (20 µM)	1.25 µl
reverse oligo (20 µM)	1.25 µl
KOD polymerase (1U/µl)	1 µl
dH_2O (fill up to 50 µl)	Y µl

PCR programme for QuikChange site-directed mutagenesis:

Polymerase activation	95℃	2 min	
Denaturation	95℃	30 sec	
Annealing	adjust to primer	1 min	18 - 20 cycles
Elongation	70℃	30 sec/kb	
Final extension	70℃	10 min	
Soak	10℃	∞	

2.4.4 A-overhang PCR and T/A cloning

For sequencing or cloning purposes, DNA fragments had to be cloned into pGEM-T or pGEM-T Easy vector (Promega). To add a single adenine to a blunt end PCR fragment, reaction was set up as followed:

10x Taq DNA polymerase Buffer	5 µl
dATP (5mM)	5 µl
vector DNA (PCR)	50 µl
Taq DNA polymerase (0.5U/µl)	1 µl

Incubate for 15 min at 72℃

Subsequently 1-2 µl of the DNA fragments were cloned into pGEM-T or pGEM-T Easy vectors according to the manufacturer's instructions.

2.4.5 Restriction endonuclease digestion of DNA

Restriction digests were done in 20 µl reactions according to the protocols of the respective enzymes. Enzymes were used from different companies, such as Fermentas, New England Biolabs and Promega. A standard reaction contained 2 µl 10x reaction buffer, 1 µl BSA, 1 unit enzyme /µg DNA. dH_2O was added to obtain a final volume of 20 µl. The reaction was incubated at room temperature, 30℃ , 37℃ or 55℃ according to the manufacturer's protocol.

2.4.6 Agarose Gel electrophoresis

Separation of DNA fragments was carried out in a horizontal electrophoresis containment using 1% (w/v) agarose - TAE solutions with 4 µg/ml ethidium bromide. Gels were covered with 1x TAE buffer and samples containing

loading dye were added into the wells before applying 100V for 30-60 min. Gels were analysed using an ultra-violet transilluminator.

2.4.7 Extraction of DNA from agarose gels

PCR products or endonuclease digestion reactions were separated on an agarose gel as described above (Section 2.4.6). DNA fragments of interest were excised from the gel using a scalpel. Extraction of DNA was carried out using the SV Gel and PCR purification kit (Promega) by following the manufacturer's instructions. Products were diluted in water.

2.4.8 Dephosphorylation of DNA and DNA ligation

Digested DNA fragments with sticky or blunt ends were combined using the Rapid DNA Ligation Kit (Roche). To prevent self-ligation of linearised vectors with overlapping sticky ends, DNA was dephosphorylated before DNA ligation using the Rapid DNA Dephos & Ligation Kit (Roche) according to the manufacturer's protocol. Ligated DNA was transformed into *E.coli* JM109 competent cells and plated on LB-Agar plates containing ampicillin or kanamycin.

Dephosphorylation (20 µl):

10x rAPid Alkaline Phosphatase Buffer	2 µl
rAPid Alkaline Phosphatase (1U/µl)	1 µl
vector DNA (up to 1 µg)	X µl
H_2O (fill up to 20 µl)	Y µl

Incubation for 10 - 30 min at 37°C and inactivation for 2 min at 75°C .

DNA ligation (20 µl):	
5x DNA Dilution Buffer	2 µl
vector DNA (50 ng)	X µl
insert DNA (150 ng)	Y µl
H_2O	fill up to 10 µl
Mix thoroughly	
Add:	
2x T4 DNA Ligation Buffer	10 µl
T4 DNA Ligase (5U/µl)	1 µl
Mix thoroughly	
Incubate for 5 min at room temperature	

2.5 Manipulation of RNA

2.5.1 Total cellular RNA extraction

To obtain viral RNA, confluent MDCK or A549 cells were infected with different virus strains at an MOI of 1 or 3 and incubated o/n. Viral RNA was extracted from infected cells using the RNeasy Mini Kit (Qiagen) following the manufacturer's instructions.

2.5.2 Determination of RNA concentration

Concentration of RNA was determined by measurement of Abs_{260} using a NanoDrop ND-1000 spectrophotometer (Thermo Scientific). Purity of the RNA sample was estimated by calculating the Abs_{260}/Abs_{280} ratio. Ratio values $\sim$ 2.0 were considered as acceptable.

2.5.3 RNA reverse transcription

Generation of complementary DNA (cDNA) and further amplification was done in a two-step-reaction using the Moloney Murine Leukemia Virus (M-MLV) Reverse Transcriptase (Promega) for the cDNA synthesis and the GoTaq DNA polymerase (Promega) for further amplification.

1. cDNA synthesis (50 µl):

RNA	3 µl
forward oligo (20 µM))	1 µl
H_2O	11 µl

Incubate 5 min at 72°C and 5 min on ice

Add 35 µl RT-PCR mix:

dNTPs (10mM each)	1 µl
5x M-MLV buffer	10 µl
M-MLV (reverse transcriptase) (200U/µl)	1 µl
H_2O	23 µl

Incubate 90 min at 42°C

2. PCR (50 µl):

cDNA	5 µl
forward oligo (20 µM))	1 µl
reverse oligo (20 µM)	1 µl
H_2O	3 µl
5xGoTaq Buffer	10 µl
dNTPs (10mM each)	1 µl
GoTaq polymerase (5U/µl)	0.25 µl
H_2O	28.75 µl

PCR programme for GoTaq DNA polymerase as described in Section 2.4.2.

2.5.4 Primer extension assay

For primer extension analysis, primers were labelled using [γ- ^{32}P]ATP. All primers are listed in Table 2.15. Reactions were set up as followed:

Primer labelling (49 µl):

primer (10 mM)	0.5 µl
10x T4 PNK buffer	5 µl
[γ-^{32}P]ATP	1 µl
H_2O	41.5 µl

Incubate 5 min at 70°C

Add:

T4 PNK (10 U/µl)	1 µl

Label for 30 min at 37℃
Denature for 20 min at 65℃
cool on ice

name	sequence 5' → 3'	description
PB2-2198	TGCTAATTGGGCAAGGAGAC	vRNA segment 1
182-PB2	GCCATCATCCATTTCATCCT	mRNA/cRNA segment 1
NA-1280	TGGACTAGTGGGAGCATCAT	vRNA segment 6
160-NA	TCCAGTATGGTTTTGATTTCCG	mRNA/cRNA segment 6
NS-734	TGATTGAAGAAGTGAGACACAG	vRNA segment 8
226-NS	CGCTCCACTATTTGCTTTCC	mRNA/cRNA segment 8
5SrRNA	TCCCAGGCGGTCTCCCATCC	5SrRNA

Table 2.15: List of synthetic oligonucleotides used for Reverse transcription in Primer extension analysis. Sequences taken from the dissertation by Philip Kerry.

To label a DNA ladder, a plasmid was digested with multicutter enzyme and DNA fragments were cleaned using the SV Gel and PCR purification kit (Promega). 5 µl of this digested DNA mix was used for labelling as described above. Labelled primers and DNA ladder were purified using microspin column G-25 (Fisher/GEHealthcare) as described on manufacturer's instructions. For primer extension analysis, 2.5 µg RNA were mixed with labelled primers in a final volume of 5 µl. After incubation at 90℃ for 5 min, RNA-primer mix was cooled on ice before the transcription reaction mix was added (as described below).

Add 5 µl of 2x transcription reaction mix:

dNTPs (10mM)	1 µl
5x M-MLV buffer	10 µl
M-MLV Reverse Transcriptase (200U/µl)	1 µl
H_2O	13 µl

Incubate at 42℃ for 2 h

8 µl formamide loading buffer (95% formamide, 20mM EDTA, bromophenol blue, xylene cyanol-FF) were added to the reaction mix and incubated at 95℃ for 3 min. After cooling the mixture on ice and a short centrifugation,

samples were separated on a 6 %- polyacrylamide gel containing 6M Urea (Geneflow SequaGel 6). Before detecting signals by autoradiography, gels were dried using a geldryer at 80 ℃ for 2.5 h. Quantification was done by a Fujifilm FLA-5000 fluorescent image analyzer and data were analysed using the ImageGauge software (Quant mode). Therefore, intensity was measured within a specified region by enclosing the desired band with a rectangle. Same size of rectangles were used for all bands and background intensity was subtracted from the measured values (Figure 2.1). For primer extension, intensities of vRNA, cRNA, mRNA and 5S rRNA were determined and expression levels of all viral RNA species were quantified and normalised against cellular 5S rRNA levels. Calculated ratios of viral RNA species of rWSN WT were set to 100 %.

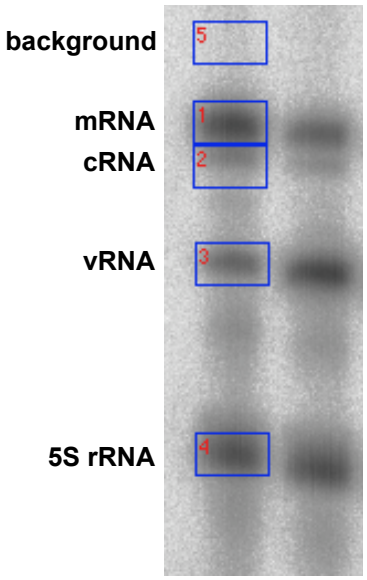

Figure 2.1: Quantification using ImageGauge software: Desired regions were enclosed by rectangular boxes of the same size. Background intensity was subtracted from the other intensities and expression levels of RNA species were normalised against 5S rRNA.

2.6 Protein analysis

2.6.1 SDS polyacrylamide gel electrophoresis

Cell lysates were prepared by adding 100 - 300 µl loading buffer (120 mM Tris; 4% SDS; 0.1% bromphenol blue; 20% glycerol, 10% 2-mercaptoethanol). Samples were treated with Benzonase (Novagen) or sonicated to reduce viscosity. Proteins were separated through 4-12% NuPAGE polyacrylamide gradient gels (Invitrogen), 8%, 12.5%

or 15% Bis-Tris polyacrylamide gels (as described below) or 16% Tricine-SDS-PAGE (as described in Schägger (2006)).

Bis-Tris polyacrylamide Gels were prepared as followed:

	Resolving Gel		
	8%	**12.5%**	**15%**
30% Acrylamide/BIS	3.2 ml	5 ml	6 ml
RGB	3 ml	3 ml	3 ml
H_2O	5.8 ml	4 ml	3 ml
10 % APS	100 µl	100 µl	100 µl
TEMED	10 µl	10 µl	10 µl

	Stacking Gel
30% Acrylamide/BIS	1.0 ml
SGB	1.5 ml
H_2O	3.5 ml
10 % APS	55 µl
TEMED	10 µl

	Resolving Gel Buffer (RGB) / 1l	**Stacking Gel Buffer (SGB) / 1l**
TRIS	181.5 g	59.0 g
SDS	4.0 g	4.0 g
pH	8.9	6.7

Tricine-SDS-PAGE were prepared as followed:

	Resolving Gel 16%	**Sample Gel 4%**
30% Acrylamide/BIS	13.2 ml	1.5 ml
3x Gel buffer	10 ml	3 ml
H_2O	6.8 ml	7.5 ml
10 % APS	100 µl	90 µl
TEMED	10 µl	9 µl

	3x Gel buffer	10x Anode buffer	10x Cathode buffer
TRIS	3.0 M	1.0 M	1.0 M
Tricine	-	-	1.0 M
HCl	1.0 M	0.225 M	-
SDS	0.3%	-	1.0%
pH	8.45	8.9	$\sim$ 8.25

MOPS or MES buffers were used for Bis-Tris gels and Gradient gels depending on the aspired separation of proteins. For Tricine-SDS-PAGE, 1 x Anode buffer was added as the lower electrophoresis buffer, 1 x Cathode buffer was used as the upper electrophoresis buffer.

2.6.2 Immunoblotting

Polypeptides were separated by electrophoresis as described above (Section 2.6.1) before transferring to nitrocellulose membrane (Hybond-C Extra, GE Healthcare) using the Trans-Blot SD semi-dry electrophoretic transfer cell (BIORAD) according to the manufacturer's instructions. After transfer, membranes were incubated for 2 h in PBS supplemented with 5% (w/v) skimmed milk powder and 0.1% (v/v) Tween 20 (blocking buffer) and incubated 2 h to overnight with primary antibody, diluted in blocking buffer according to the manufacturer's instructions. Membranes were washed with blocking buffer multiple times before incubation with horseradish peroxidase (HRP) - conjugated secondary antibody for 1 or 2 h. Membranes were washed again multiple times with blocking buffer before proteins were detected using the SuperSignal West Pico Chemiluminescent substrate (Thermo Scientific) according to the manufacturer's recommendations. The membrane was exposed to Kodak X-Omat film.
Accumulation of proteins was measured with the luminescence image analyzer (Fujifilm LAS 4000) and data were analysed using the ImageGauge software (Quant mode). Therefore, intensity was measured within a specified region by enclosing the desired area with a rectangle. Same size of rectangles were used for all bands and background intensity was subtracted from the measured values. Intensities for each protein was determined and normalised against α-tubulin.

2.6.3 Antibodies

Antibodies were used in immunoblotting and immunostaining. Primary and secondary antibodies used in this study are listed below in Tab 2.16.

Target protein	Manufacturer
PB1-F2 (PR8) polyclonal	A kind gift from D. Mitzner (ViroLogik GmbH, Erlangen, Germany)
PB1 V19 (aa 50-370 PR8) polyclonal	A kind gift from Paul Digard (University of Cambridge, UK)
PB1 (vC-19) polyclonal	Santa Cruz Biotechnology, Inc.
α-tubulin	Sigma
RNA Polymerase II H5 monoclonal	Covance
RNA Polymerase II 8WG16 monoclonal	Covance
α-Udorn polyclonal	A kind gift from D. Jackson (University of St Andrews, UK)
DsRed polyclonal	Clontech Laboratories, Inc.
Anti-Mouse-HRP	Sigma
Anti-Rabbit-HRP	Cell Signalling
Anti-Sheep-HRP	Abcam
Anti-Goat-AP	Santa Cruz Biotechnology, Inc.

Table 2.16: Antibodies used in this study.

2.6.4 Metabolic [^{35}S] methionine radio-isotopic labelling of proteins

Confluent MDCK cell monolayers (6-well plate) were infected with influenza A virus at an MOI of 3 as described previously (Section 2.2.5). At the desired time points, culture media was removed and cells were washed with PBS. To starve the cells, 1 ml of methionine-free medium was added. After 30 min, medium was replaced with methionine-free medium supplemented with 30 µCi/ml [^{35}S] methionine. Cells were incubated at 37℃ for 1 h before adding 300 µl loading buffer for further analysis via SDS polyacrylamide gel electrophoresis (Section 2.6.1).

2.7 Miscellaneous assays

2.7.1 Luciferase assay

The Dual-Luciferase Reporter Assay System (Promega) was used. 24-well plates with confluent 293FT cells were transfected with different amounts of plasmids (Table 2.17). Total concentration of plasmids was kept equal by adding different amounts of pcDNA3.1(+) vector. Transfections were done using the FuGene 6 reagent (Roche) according to the manufacturer's protocol. Measurements were done after an incubation time of 24 h according to the manufacturer's instructions. Firefly was used as a transfection control. Measured values were normalised against wild type (pcDNA-PB1) firefly values and percentage for each transfection mix was calculated relative to cells transfected with pcDNA-PB1.

Plasmid	**amount (ng):**
pcDNA-PB2	50
pcDNA-PB1	50
pcDNA-PA	12.5
pcDNA-NP	50
pcDNA-PB1 or different PB1-F2 and N40 mutants	50
pcDNA-PB1-F2	50
pcDNA-N40	50
pHH-Renilla	20
pCMV-FF	20
pcDNA-3.1(+)	add up to total amount of 450

Table 2.17: Plasmids used for luciferase assays: A total amount of 450 ng was transfected into 293FT cells.

2.7.2 Cell viability assay

WST-1 (Roche) was used as a substrate to measure cell viability. 96-well plates with confluent MDCK, A549 or RAW/W cells were infected with different virus strains at an MOI of 30. 100 µl of the infection mix was added to the cells and left at 37℃ for 1 h. Inoculum was removed and serum-free DMEM was added. After 8 h incubation at 37℃ DMEM was replaced with

colorless DMEM containing 5 µl/well WST-1. Cells were further incubated until significant color had developed. Measurement was done using an ELISA microplate reader at 450 nm (690 nm reference wavelength). The assay was done in triplicates and results were averaged.

2.7.3 Flow cytometry

Cells were washed with PBS without Ca^{2+} / Mg^{2+}. 250 µl ice cold EDTA was added to detach the cells. After 20 min incubation on ice, cells were harvested into FACS tubes and washed with PBS containing Ca^{2+} / Mg^{2+}.
To assess apoptosis (AxV^+ / PI^-) and necrosis (AxV^+ / PI^+) cells were stained with FITC-conjugated annexin (Roche: AnxA5-FITC) in binding buffer (HBSS containing 2 mM $CaCl_2$) for 15 min on ice. Propidium iodide (Sigma, 3 µg/ml) was added 1 min before analysis of the sample. Data were measured using the FL1 and FL2 detectors on a FACSCalibur flow cytometer (BD Biosciences). Data were analysed using the CELLQUEST software and FlowJo software (Tree Star).

2.7.4 Hematoxylin and eosin stain

To prepare the lungs for H&E staining, they were incubated in 70% ethanol for 1 hour followed by incubation in 100% ethanol for 1 hour (2x). Lungs were immersed in an ethanol:chloroform mixture (50:50) for 2 hours, before incubation in chloroform for 1 hour (2x). Lungs were finally placed 3 times in a low melting point paraffin wax bath for 1 hour each. After sectioning, sections were deparaffinized in xylene twice for 10 min each. To rehydrate the sections, they were immersed in a series of graded ethanol to water. Sections were stained in Harris Haematoxylin (Sigma HHS32) for 10 min and washed in water, before they were differentiated in 1% acid alcohol for 30 sec. Blueing was done using Scott's Tap Water Substitute. Sections were washed for 10 min in water and then stained in 0.5% aqueous Eosin (Eosin Yellowish) for 2 min. Sections were dehydrated in 95% ethanol and cleared with xylene. Sections were mounted on glass slides using DPX (BDH 360294H).

Chapter 3

A NEW WAY TO DELETE PB1-F2

Aims of Chapter 3

PB1-F2 knockout viruses have been reported previously. However, these were based on a strategy that also influenced the expression level of an additional protein encoded by segment 2. To overcome this problem, a new way to delete PB1-F2 was developed. The two versions of PB1-F2 knockout viruses were engineered using site-directed mutagenesis and the rescued recombinant viruses were analysed and compared using different *in vitro* and *in vivo* studies.

3.1 Introduction

3.1.1 Previous work on PB1-F2

When PB1-F2 was first discovered in 2001, it was suggested that the protein may be involved in the induction of apoptosis in immune cells (Chen et al., 2001). In the following years several other functions were associated with PB1-F2. Because the protein was not only found in the mitochondria of infected cells but also in the cytoplasm and the nucleus, the question arose whether another function exists besides the induction of apoptosis. Consequently, an interaction of PB1-F2 and the polymerase subunit PB1 was observed (Mazur et al., 2008). Deletion of PB1-F2 was shown to decrease viral polymerase activity, however, this effect was only detected for some virus strains (Mazur et al., 2008; McAuley et al., 2010b; Chen et al., 2010).

The induction of apoptosis and the upregulation of viral RNP activity are thought to have some influence on virulence (Zamarin et al., 2006; Mazur et al., 2008). Additionally, a connection between PB1-F2 expression and the levels of cytokines and chemokines was suggested, with the focus on one particular amino acid. PB1-F2 with a serine at position 66 was reported to increase virulence and inhibit the innate immune response at early time points in infection (Conenello et al., 2007, 2011). Most of these findings were based on the behaviour of mutant viruses in cells and mice.

In order to delete PB1-F2, two or three point mutations were inserted into segment 2 to abolish its expression. Most strategies had in common the mutation of the start codon of PB1-F2 and the creation of one or two stop codons further downstream.

In 2009 a third protein expressed from segment 2 was discovered. Since it is an N-terminally truncated version of the polymerase subunit PB1 lacking the first 39 amino acids, it was named N40 (Wise et al., 2009). The two internal proteins from segment 2 are translated by leaky ribosomal scanning and reinitiation (Wise et al., 2011). Alterations of start codons within the N-terminus therefore were thought to have consequences on the expression level of downstream proteins. This became noticeable when PB1-F2 deletion strains were tested to monitor the expression level of N40. Deletion of the PB1-F2 start codon resulted in an increased expression level of N40 (Wise et al., 2009). Other strategies to abolish PB1-F2 were based on insertion of a stop codon after amino acid 8 (Chen et al., 2001). This

mutation led to a change in the PB1 ORF: amino acid 40 was changed from a methionine to an isoleucine, which coincidentally also abolished N40 expression. In both cases no PB1-F2 was expressed, but both strategies had consequences on the expression level of N40 (Figure 3.1), which makes it difficult or even impossible to support some of the conclusions drawn in previous publications as they can not be clearly associated to PB1-F2.

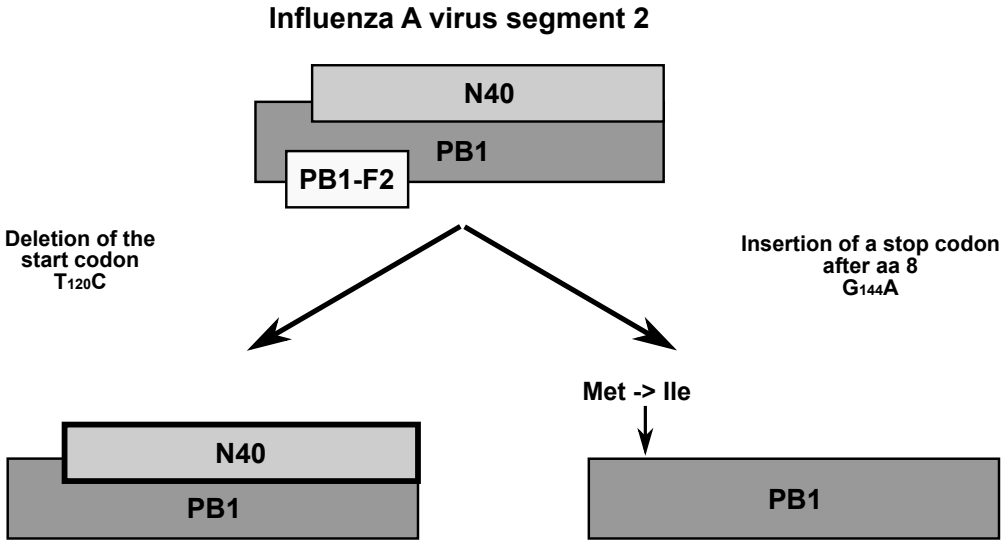

Figure 3.1: Overview of the strategies to delete PB1-F2 in different publications and their effect on PB1 and N40. The strategy on the left hand side shows the deletion of PB1-F2 by removing the start codon. This led to an increase in the expression level of N40. The second used strategy to delete PB1-F2 introduces a stop codon into PB1-F2 ORF after aa 8, but this mutation also has an effect on the PB1 ORF. A methionine is changed to an isoleucine which abolishes the expression of N40.

To address this problem, two different strategies were chosen to abrogate PB1-F2 expression (Figure 3.2). As discussed in more detail in Section 3.2, the first PB1-F2 deletion version was adopted from previously published work, where three point mutations were introduced with the disadvantage of increasing the expression level of N40 (Zamarin et al., 2006). The second strategy involved introducing two stop codons and no change to the PB1-F2 start codon was made. Using this approach the expression level of N40 should remain unaffected.

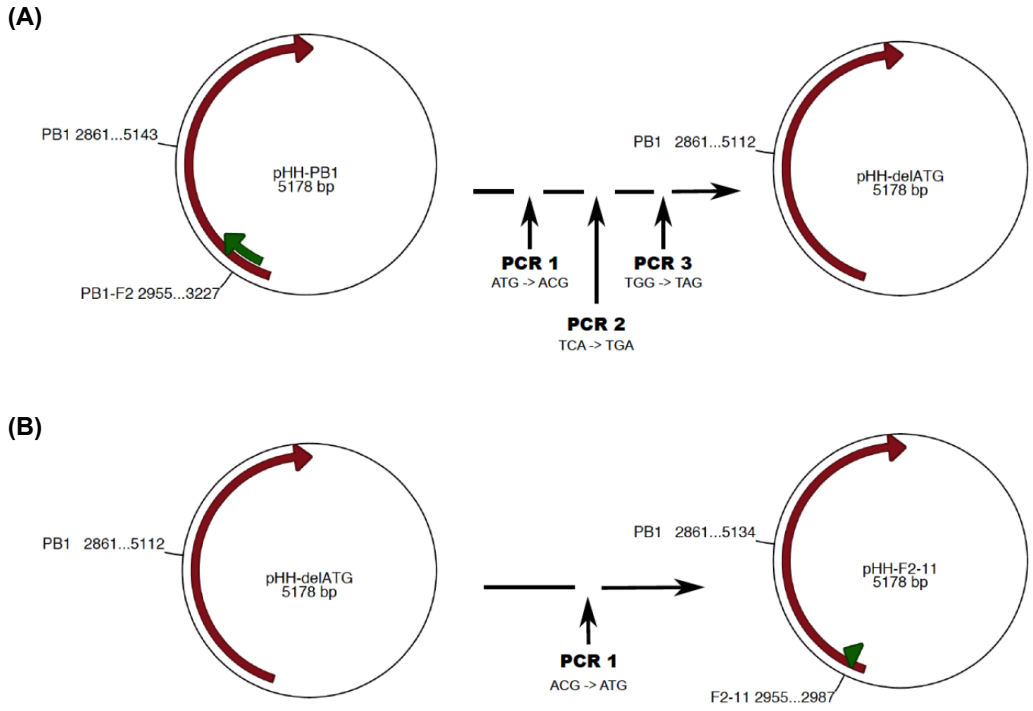

Figure 3.2: Overview of the strategies used to delete PB1-F2. (A) Three point mutations were inserted into the plasmid pHH-PB1 via site directed mutagenesis in order to delete PB1-F2. The first point mutation deleted the start codon of PB1-F2, the two mutations downstream inserted stop codons to abolish translation of the C-terminal end of PB1-F2. All mutations were silent with respect to the PB1 ORF. The obtained plasmid was termed pHH-ΔATG. **(B)** The plasmid pHH-ΔATG was used as a template to reinsert the start codon of PB1-F2 to maintain the wild type expression level of N40. The resulting plasmid was named pHH-F2-11. Translation of PB1-F2 will stop at amino acid 12, where the first stop codon was inserted.

3.2 Two ways to prevent PB1-F2 expression

3.2.1 Deletion of PB1-F2 by inserting three point mutations

Three point mutations were inserted in order to fully delete PB1-F2 as described previously (Zamarin et al., 2006). Knockout of the protein was planned for two virus strains, the H1N1 mouse adapted strain A/WSN/33 and the human strain A/Udorn/1972 (H3N2). Three consecutive PCRs were performed with primers containing one mutation each (Table 3.1). The first mutation changed the start codon from AUG to ACG (T120C), the second and third mutation (C153G and G291A) introduced two stop codons further

downstream (Figure 3.2). Introducing two stop codons was shown to be necessary in order to prevent the expression of the C-terminal domain of PB1-F2 from a downstream start codon (Zamarin et al., 2006). The C-terminus is thought to be the main inducer of apoptosis as it carries the mitochondrial targeting signal. The introduced point mutations did not alter the amino acid sequence of PB1 and N40.

Mutation	Forward primer	Reverse primer	Annealing temperature
Udorn			
T120C	sv01	sv02	60℃
C153G	sv03	sv86	61℃
G291A	sv05	sv06	61℃
WSN			
T120C	sv09	sv10	60℃
C153G	sv11	sv12	62℃
G291A	sv13	sv14	61℃

Table 3.1: Oligonucleotide primers used to delete PB1-F2 in A/WSN/33 and A/Udorn/1972. Primer Sequences are listed in Table 2.9 in Chapter 2.

PCR-mediated site-directed mutagenesis was performed using the proofreading polymerase KOD hot start. Because the three mutation sites were far from each other, three separate and sequential PCRs had to be done using specific oligonucleotide primers carrying the desired mutations. PCRs were performed according to the manufacturer's protocol; the annealing temperature for each primer pair and elongation times were adjusted empirically. Conditions for each PCR are summarised in Tables 3.1 and 3.2.

PCR products were gel purified and treated with the restriction enzyme *Dpn*I to digest the parental DNA. Plasmids were transformed into competent *E.coli* cells for further amplification. Several colonies were scanned by restriction enzyme analysis using the enzyme *Nhe*I before they were used in a subsequent PCR or before their nucleotide sequence was determined (Figure 3.3). The correct plasmid with three integrated mutations was termed pHH-$\triangle$ATG.

Step	Temperature	Time	# of cycles
Polymerase activation	95℃	2 min	1
Denaturation	95℃	30 sec	20
Annealing	adjust to primers	30 sec	
Elongation	70℃	2.5 min	
Final extension	70℃	10 min	1
Hold	10℃	∞	

Table 3.2: Cycling conditions for site-directed mutagenesis using KOD Hot Start Polymerase. The Annealing temperature varied between the PCR reactions depending on the primers used. Annealing temperatures are listed in Table 3.1.

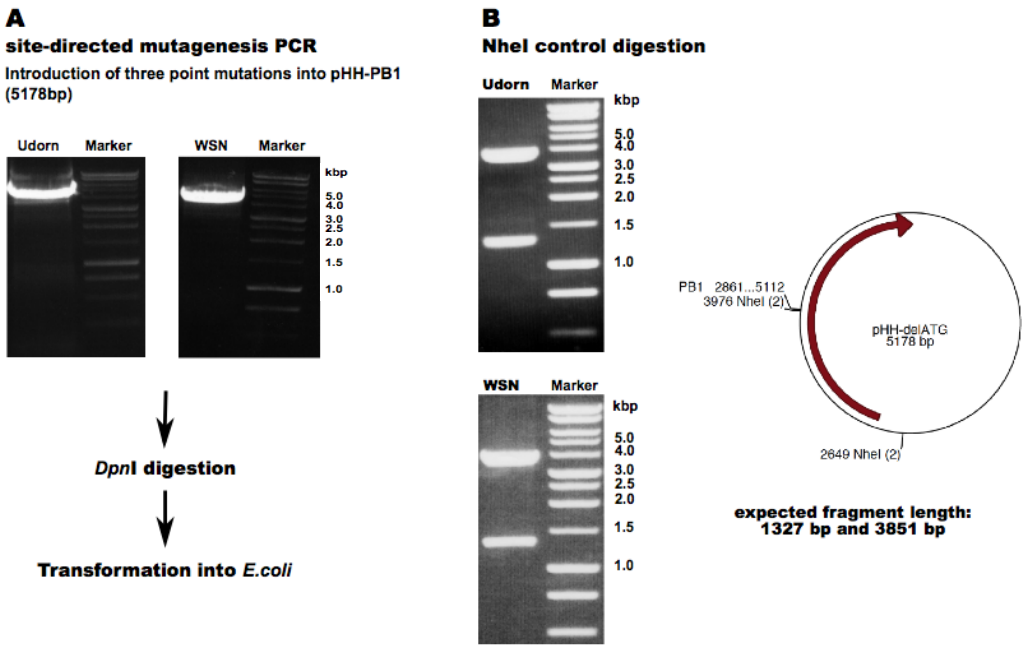

Figure 3.3: Deletion of PB1-F2 by introducing three point mutations into segment 2. (A) Site-directed mutagenesis PCR was used to introduce three mutations into the plasmid pHH-PB1. PCR products were electrophoresed through a 1% agarose gel and visualized on a UV transilluminator. DNA was recovered from the gel followed by a *Dpn*I digest and amplification in *E.coli*. **(B)** Obtained plasmids were digested using the enzyme *Nhe*I and electrophoresed through a 1% agarose gel. The obtained fragments showed the expected length of 1327 and 3851 bp. Marker: Promega 1kb DNA ladder.

3.2.2 Deletion of PB1-F2 by inserting two point mutations

Due to the interdependency of PB1, PB1-F2 and N40 expression, removal of the PB1-F2 start codon led to an increase in the expression level of

N40 (Wise et al., 2009). Other approaches to delete PB1-F2 involved the insertion of a stop codon after amino acid 8 which led to the abolition of N40 expression (Chen et al., 2001; Zamarin et al., 2006). To overcome this problem and to keep N40 protein levels comparable to that of WT, the start codon of PB1-F2 was regenerated and deletion of PB1-F2 was obtained by two stop codons further downstream with the first stop codon after aa 11 (Figure 3.2 B).
Site-directed mutagenesis was performed using PCR to regenerate the start codon into the sequence. The previously described plasmid pHH-△ATG carrying all three mutations was used as a template. Instead of starting with the WT segment 2 and inserting two point mutations by subsequent PCR reactions this approach was chosen to keep the number of PCRs, and therefore the possibility of introducing errors to a minimum as the plasmid pHH-△ATG was already sequenced. The oligonucleotide primers used for this reaction and the conditions for the PCR are listed in Table 3.3. The correct plasmid, named pHH-F2-11, was verified by nucleotide sequencing to ensure the correct insertion of the mutations. The plasmid pHH-F2-11 was only created for the H1N1 strain A/WSN/33.

Mutation	Forward primer	Reverse primer	Annealing temperature
Start-F2	sv129	sv130	66℃

Table 3.3: Oligonucleotide primers used to regenerate the start codon into pHH-△ATG to create pHH-F2-11. Primer Sequences are listed in Table 2.9 in Chapter 2.

3.3 Rescue and characterisation of the PB1-F2 deletion viruses

3.3.1 Rescue of the PB1-F2 deletion viruses

Viruses were rescued using the 12-plasmid rescue system described by Neumann et al. (1999). Eight plasmids contained the cDNA to express viral RNA corresponding to each segment of either influenza A virus A/WSN/33 or A/Udorn/1972 (pHH-PB2, pHH-PB1, pHH-PA, pHH-HA, pHH-NP, pHH-NA, pHH-M and pHH-NS). Viral sequences in the negative-sense orientation were flanked by the human polymerase

I promoter and a murine polymerase I terminator. RNA polymerase I transcribes cellular genes into ribosomal RNA (rRNA) and does not introduce 5' and 3' modifications to the RNA like 5' cap or poly(A) structures. The use of this approach allowed the generation of specific viral RNA segments indistinguishable from authentic viral RNAs. To ensure the formation of ribonucleoproteins within the cell, four additional plasmids expressing the three polymerase subunits and the nucleoprotein were also transfected (pcDNA-PB2, pcDNA-PB1, pcDNA-PA and pcDNA-NP). These four genes were in the positive orientation and under the control of a polymerase II promoter to allow immediate expression of the viral proteins (Figure 3.4). Virus rescues were carried out for the WT and the deletion mutants $\triangle$AUG and F2-11 (rUdo WT, rUdo $\triangle$AUG, rWSN WT, rWSN $\triangle$AUG and rWSN F2-11). Transfection lacking the cDNA for segment 5 (pHH-NP) was always used as a negative control for virus rescues. Transfections were done in human embryonic kidney cells (293FT). After 24h, 293FT cells were co-cultivated with MDCK cells in a small tissue culture flask in the presence of trypsin. MDCK cells support efficient replication of influenza A viruses, whereas 293FT cells do not. Supernatant was harvested when cytopathic effect (CPE) was 80-100%.

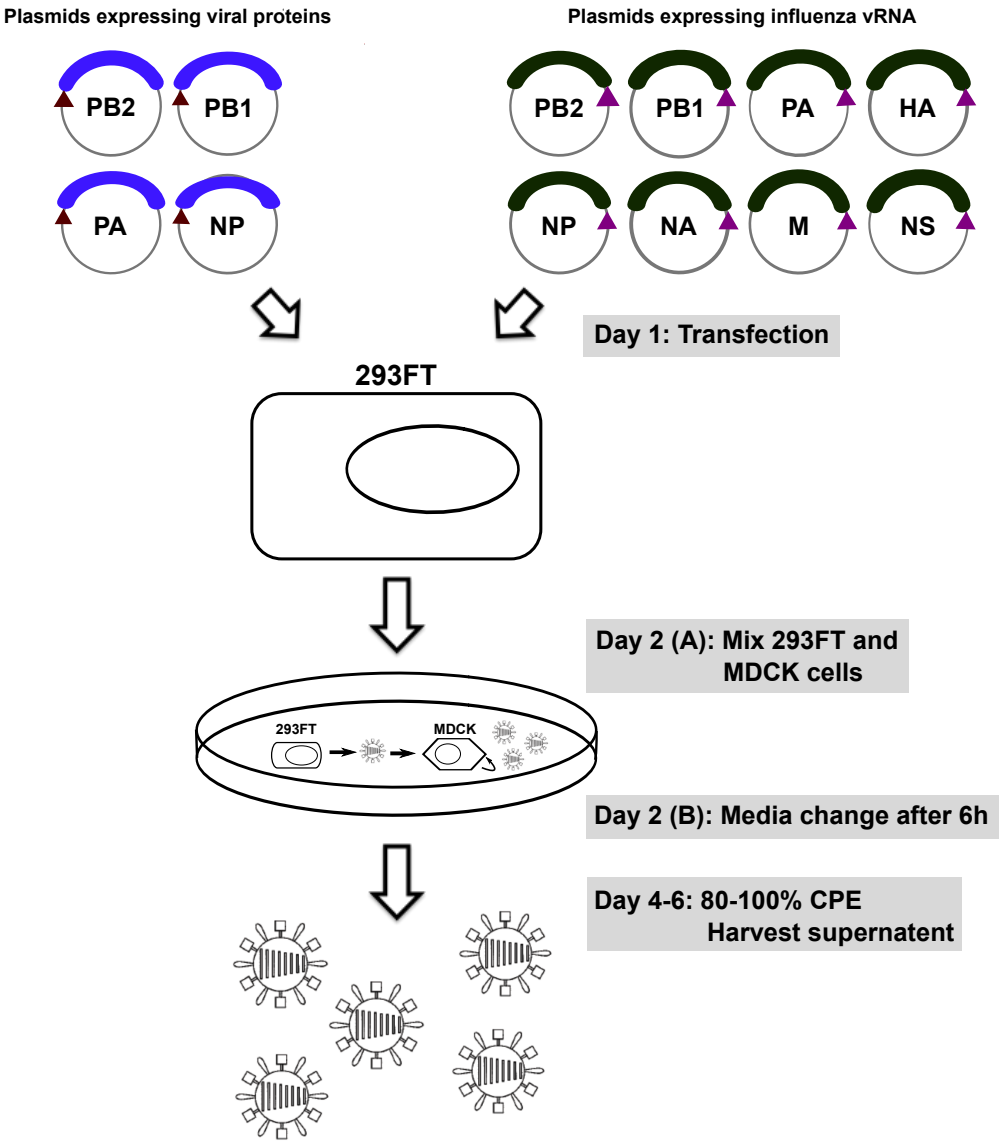

Figure 3.4: Influenza A virus rescue using a 12-plasmid rescue system: A total of 12 plasmids were transfected into 293FT cells. 8 plasmids expressing the vRNA for each segment. Additionally 4 plasmids were transfeted expressing the viral polymerase proteins and the nucleoprotein. On day 2 the 293FT cells were mixed with MDCK cells to ensure virus propagation. Media was changed to DMEM containing trypsin 6 hours later. When CPE is 80-100% supernatant was harvested.

To monitor segment 2 and the inserted mutations, RNA was isolated from the supernatant of infected MDCK cells and used in an RT-PCR reaction in order to sequence the obtained PCR product. Results for all three A/WSN/33 viruses are shown in Figure 3.5 with nucleotides of interest indicated by green and red boxes. Viruses that contained the expected mutations were used for further experiments.

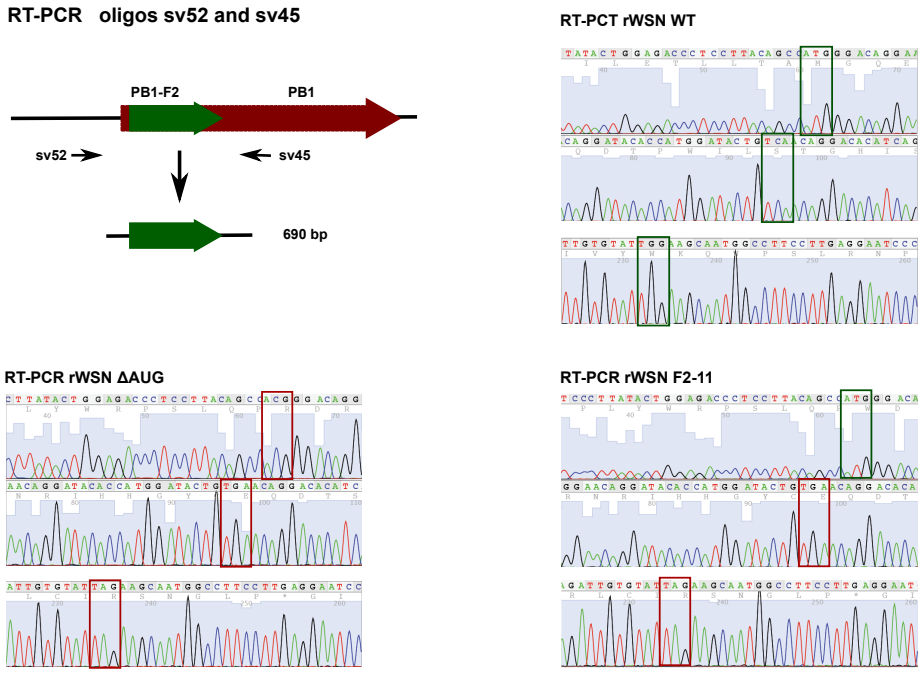

Figure 3.5: Sequencing data from RT-PCR reactions to verify the inserted mutations in rWSN ΔAUG and rWSN F2-11. RNA of MDCK cells - infected with either rWSN WT, rWSN ΔAUG or rWSN F2-11 viruses - was isolated and used in an RT-PCR reaction to amplify the beginning of segment 2. The obtained PCR products were sequenced for examination of inserted mutations. The green boxes indicate original sequences and red boxes show nucleotide sequences changed by site-directed mutagenesis.

The presence or absence of the PB1-F2 protein in infected cells was determined by Western blot analysis. MDCK cells were infected with the different viruses at an MOI of 3 and incubated for 8 h. Proteins were separated by different acrylamide gels - 16% Tricine-SDS-PAGE or 4-12% Gradient Bis-Tris gels, depending on the protein to be examined (Figure 3.6). As seen in Figure 3.6 (A), PB1-F2 was only expressed in cells infected with rWSN WT viruses whereas PB1-F2 was absent in cells infected with either of the PB1-F2 deletion viruses. Infection was monitored by

detecting the polymerase subunit PB1. A protein of slightly smaller weight corresponding to N40 was easily seen in cells infected with rWSN ∆AUG, but a similar band was poorly detected in rWSN WT and rWSN F2-11 infected cells. The increased expression level of N40 in cells infected with rWSN ∆AUG is most likely caused by the deleted start codon of PB1-F2 as described previously (Wise et al., 2009). Differences in the expression levels were quantified by measuring the chemiluminescence as can be seen in Figure 3.7. Similar expression levels of PB1 were observed for all three recombinant viruses, whereas cells infected with recombinant ∆AUG showed a strong increase in N40 expression. α-tubulin was used as a cellular loading control.

Figure 3.6 (B) shows the Western blot for the rUdorn WT and the ∆AUG mutant. Antibodies used to detect PB1 and PB1-F2 were raised against proteins from the H1N1 strain A/PR8/34. Unfortunately the antibody for PB1-F2 did not cross react with the Udorn protein in Western blots. Most likely this is due to the low sequence similarity between PB1-F2 from A/PR8/34 and A/Udorn/72, as seen in Figure 3.6 (D), whereas PR8 is much closer related to WSN (Figure 3.6 (C)). Because the N40 level was markedly increased in cells infected with rUdo ∆AUG compared to WT, it could only be speculated that PB1-F2 was successfully deleted. Although the antibody used to detect PB1 and N40 was also raised against the PR8 protein, it detected both WSN and Udorn proteins as the amino acid sequence similarity of residues 50-370 is about 96% (data not shown).

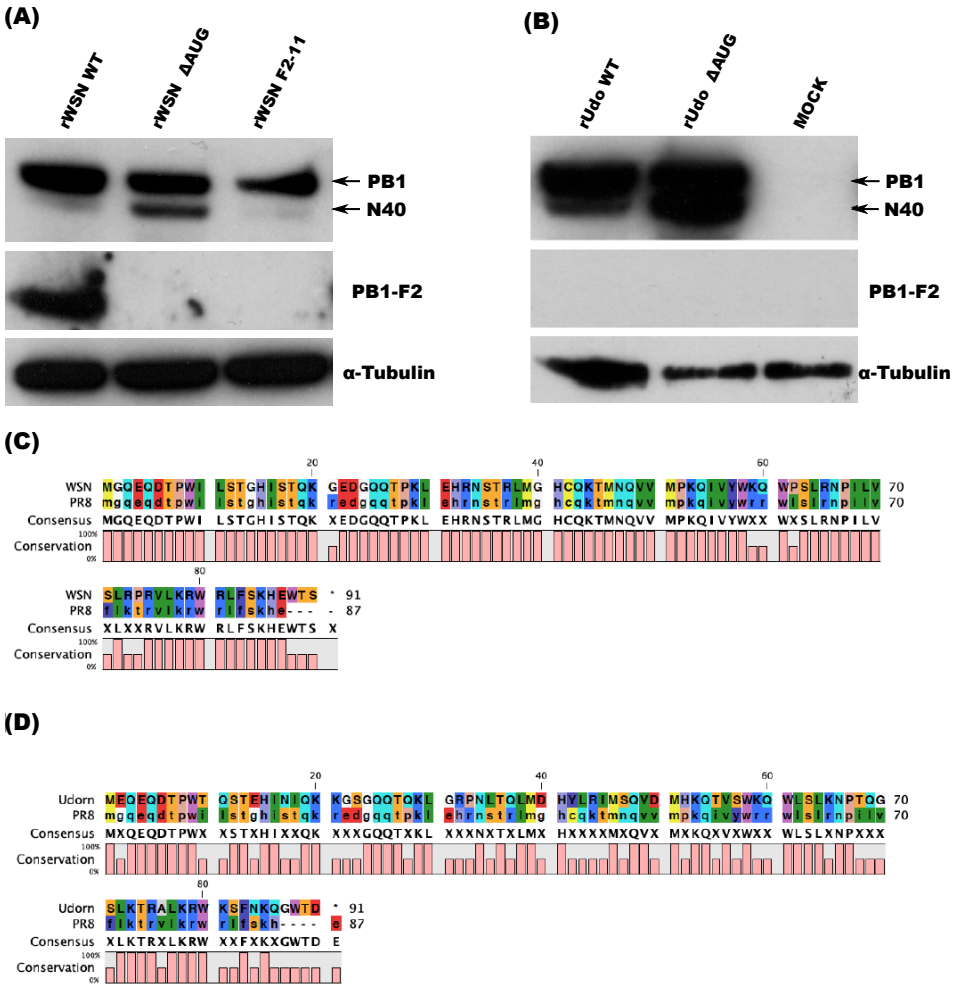

Figure 3.6: Western blot to confirm deletion of PB1-F2 in cells infected with **(A)** WSN and **(B)** Udorn PB1-F2 deletion viruses. 4 - 12% gradient Bis-Tris gels were used for PB1 and N40 detection, whereas 16% Tricine-SDS-PAGE was used for WB to detect the small hydrophobic protein PB1-F2. α-tubulin was used as an internal loading control. **(C and D)** Sequence alignment for PB1-F2 protein sequences. **(C)** A/PR8/34 versus A/WSN/33; **(D)** A/PR8/34 versus A/Udorn/72.

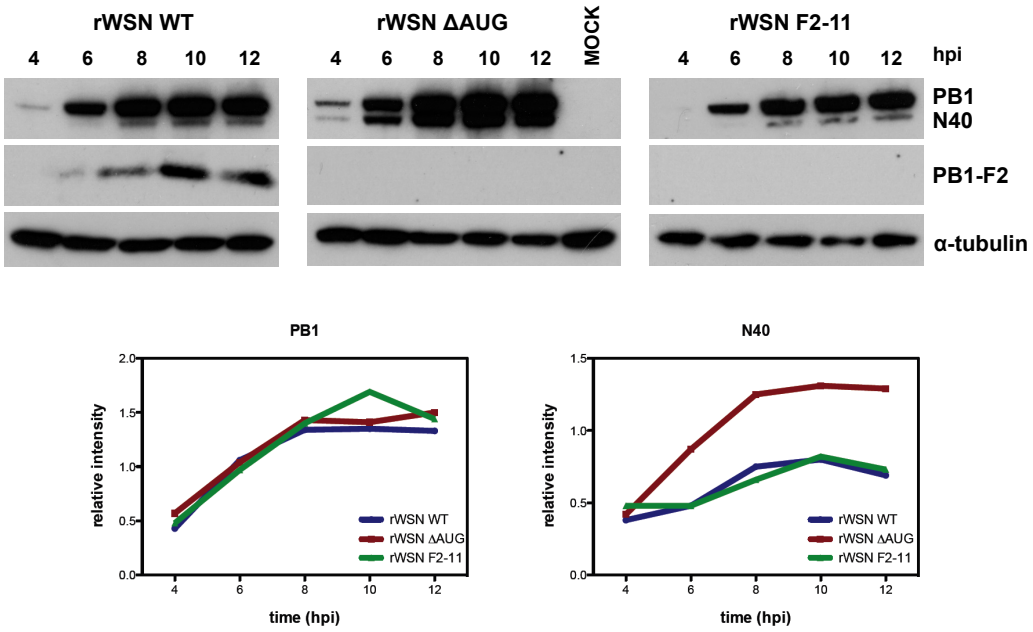

Figure 3.7: Analysis of expression levels of PB1 and N40: MDCK cells were infected at an MOI of 3 with rWSN WT, rWSN ΔAUG or rWSN F2-11 and cell lysates were collected at indicated time points. Proteins were separated using a 4-12% gradient Bis-Tris gel or 16% Tricine-SDS-PAGE and analysed by Western blot for indicated proteins. Expression levels of PB1 and N40 were quantified and normalized against α-tubulin.

3.3.2 The two deletant viruses show differences in their plaque phenotype

Plaque assays are widely used to measure the virus titre in a sample stock, but they can also be a first indication on viral fitness and viral replication. Adding a solid or semi-solid overlay onto infected cells prevents the virus from spreading through the media indiscriminately. Plaques represent an area of destroyed and dead cells. Therefore the size of the plaque can indicate possible attenuation.

Plaques were identified either indirect by staining cells using crystal-violet or by direct immunostaining of virus infected cells. The diameters of several plaques for each virus mutant were measured and compared (Figure 3.8 and 3.9). Previously, WSN viruses not expressing PB1-F2 were shown to possess a small plaque phenotype compared to WT (Mazur et al., 2008). This result could be confirmed for ΔAUG viruses. rWSN ΔAUG produced

significantly smaller plaques in MDCK cells, with a plaque diameter reduced by ∼30% (*Student's t-test* P=0.0009). Plaque size by rUdo △AUG was also reduced, however this reduction was only about 22% and not significant (*Student's t-test* P=0.0643). When comparing the plaques produced by the second PB1-F2 deletion strain rWSN F2-11, plaque size appeared similar to those measured for WT (Figure 3.8). No difference in size compared to WT was observed at 24 hpi or 3 days post infection. As both PB1-F2 mutant viruses are deficient for their PB1-F2 expression, this can only be explained by their different expression level for N40.

3.3.3 Effects of the loss of PB1-F2 on viral growth

To further evaluate the phenotypes of the different viruses, viral growth curves were determined in cultured cells for single-step and multi-step infection conditions. For the single-step growth curve, monolayers of MDCK cells were infected with the different recombinant viruses at an MOI of 3 in the absence of trypsin. After an incubation time of 2, 4, 6, 8, 10 and 12 h, virus in the supernatant was titrated by plaque assay. For the multi-step growth curve, MDCK cells were infected at an MOI of 0.001 and incubated in the presence of trypsin for 48 hours. At indicated time points, supernatants were harvested and titrated as described in Section 2.2.6.
Under multi-step growth condition the virus yield of rWSN △AUG was ∼ 100 times lower than rWSN WT virus. On the other hand the rWSN F2-11 virus grew similarly to the recombinant WT virus (Figure 3.10(A)). A different result was observed in a single-step cycle (Figure 3.10(B)): whereas rWSN F2-11 was comparable to WT, rWSN △AUG showed an increased growth.
Unlike the growth characteristics of rWSN △AUG, rUdo △AUG showed a similar growth behaviour to WT virus, both in single-step and multi-step cycles (Figure 3.11).

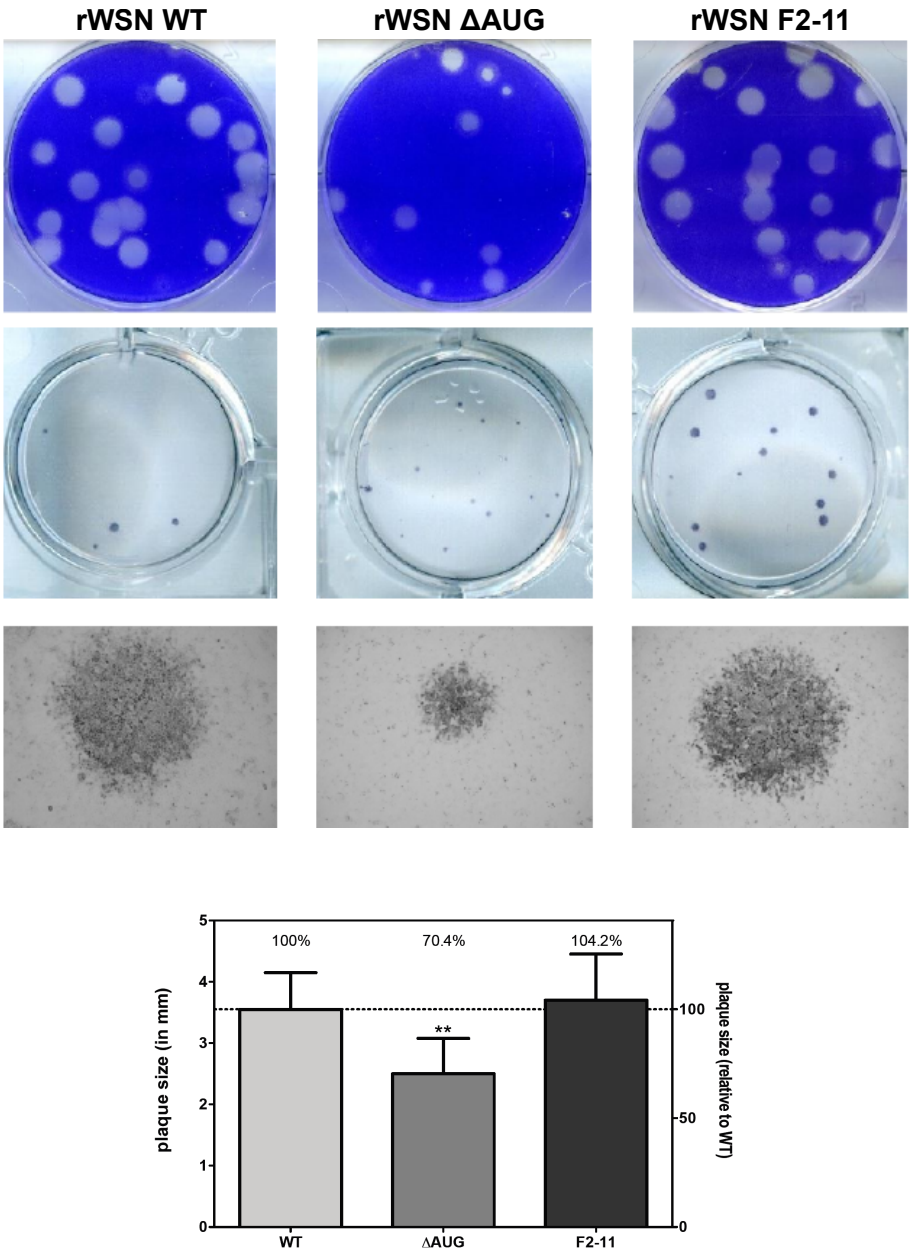

Figure 3.8: Plaque phenotype by recombinant WSN viruses lacking PB1-F2 expression: MDCK cells were infected with recombinant viruses. Cells were overlayed with 1.2% Avicel-DMEM and incubated for 3 days (top panel) or 24 h (middle and lower panel) at 37℃ . Mean values for ∼30 plaques/recombinant virus (3 dpi) are plotted and error bars represent the SEM. Differences in plaque sizes are significant between rWSN WT and rWSN ΔAUG virus ($P<0.01$) but not between rWSN WT and rWSN F2-11 virus.

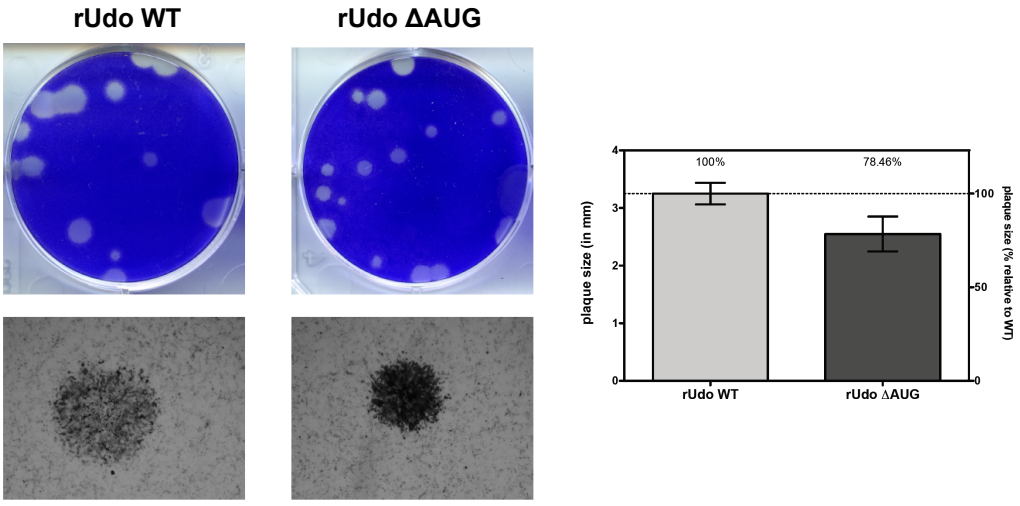

Figure 3.9: Plaque phenotype by recombinant Udorn viruses lacking PB1-F2 expression. MDCK cells were infected with recombinant viruses. Cells were overlayed with 1.2% Avicel-DMEM supplemented with N-acetyl trypsin and incubated for 3 days (top panel) or 24 h (lower panel) at 37℃ . Mean values for ∼30 plaques/recombinant virus (3 dpi) are plotted and error bars represent the SEM.

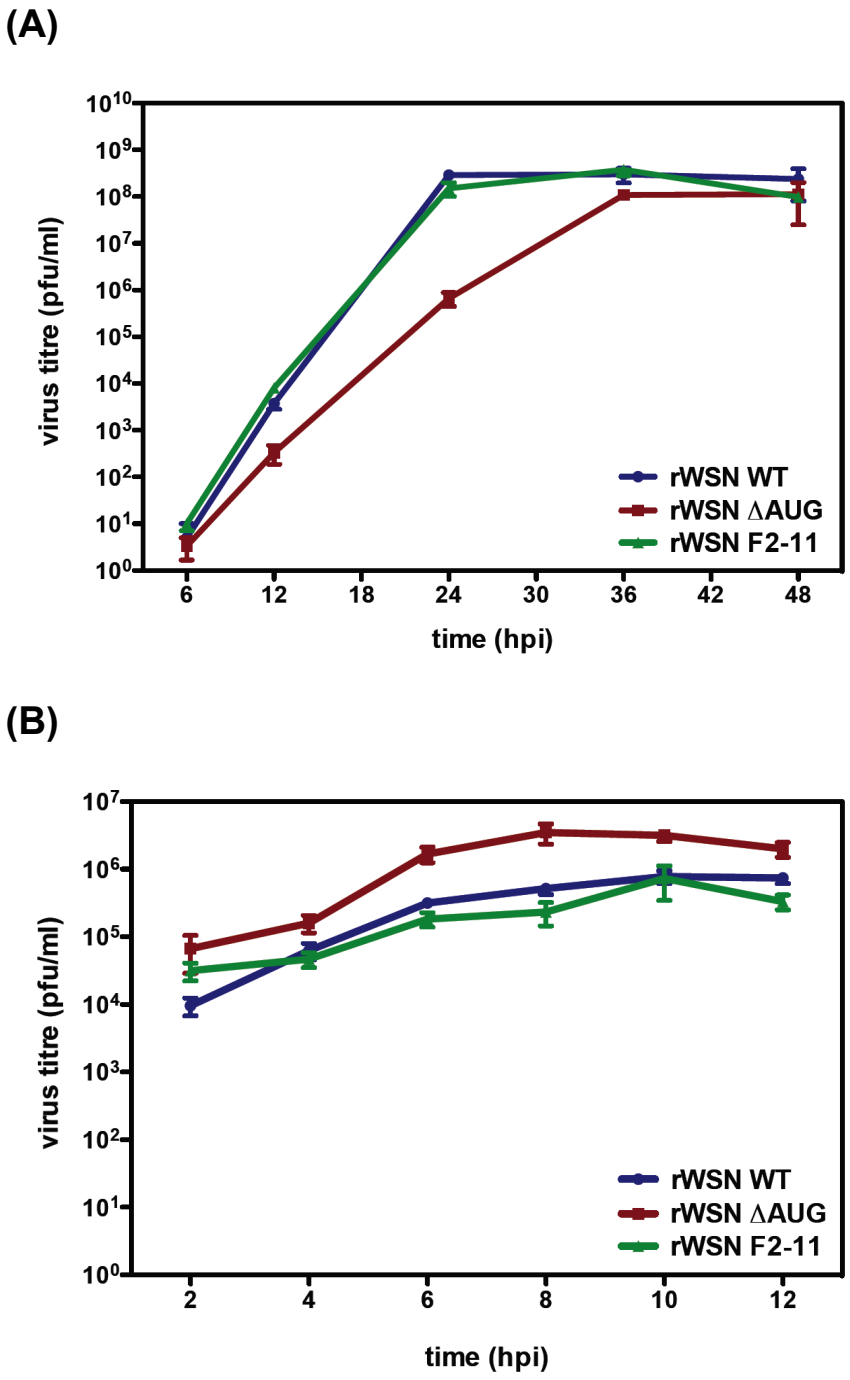

Figure 3.10: WSN virus growth: Triplicate MDCK monolayers were infected with the recombinant WSN viruses WT, ΔAUG and F2-11 at an **(A)** MOI of 0.001 for multi-step growth curve and **(B)** MOI 3 for single-step growth curve. For multi-step growth curve, media was supplemented with N-acetyl trypsin. Supernatants were harvested at indicated time points post infection and virus titres were determined by plaque assay. Error bars represent the SEM of each set of triplicates.

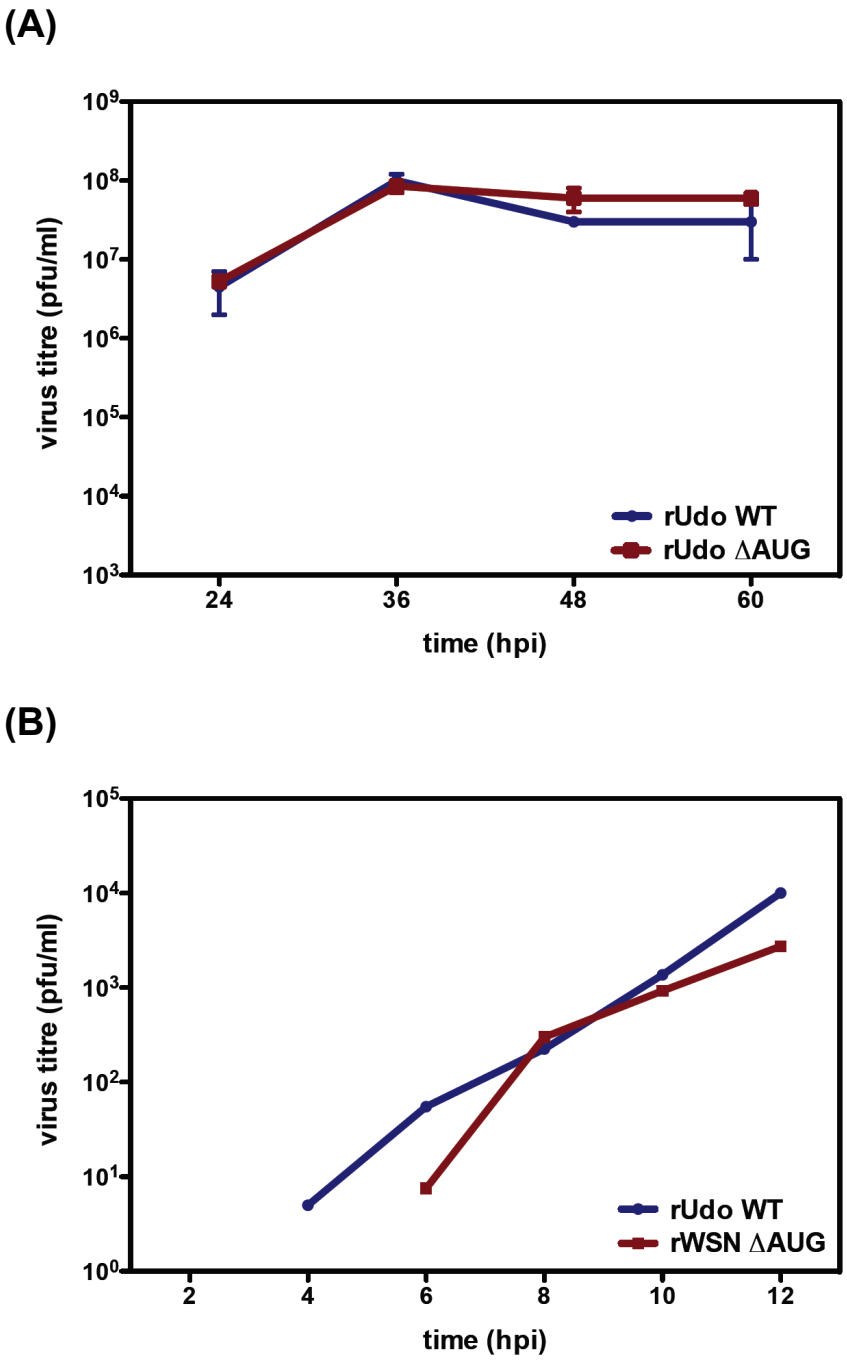

Figure 3.11: Udorn virus growth: Triplicate MDCK monolayers were infected with the recombinant Udorn viruses WT and ΔAUG at **(A)** an MOI of 0.001 for multi-step growth curve and **(B)** MOI 3 for single-step growth curve. Media was supplemented with N-acetyl trypsin. Supernatants were harvested at indicated time points post infection and virus titres was measured by plaque assay.

3.3.4 △AUG viruses are attenuated in their ability to induce apoptosis *in vitro*

PB1-F2 was shown previously to be involved in the induction of apoptosis, specifically in immune cells (Chen et al., 2001; Zamarin et al., 2005). By creating knockout mutants, the induction of apoptosis in immune cells was reduced significantly (Chen et al., 2001). Later, this function was shown to be specific for only a number of strains (Chen et al., 2010; McAuley et al., 2010a). It was not known if PB1-F2 from the A/WSN/33 strain is involved in the induction of apoptosis. To test this, a mouse macrophage cell line (RAW/W) was infected with rWSN WT and 8 hours later cells were tested for cell viability (Figure 3.12) using a commercially available cell viability assay. In comparison to mock infected cells, RAW/W cells treated with rWSN WT were less viable (-25%), assuming that cells died from apoptosis or necrosis due to the viral infection.

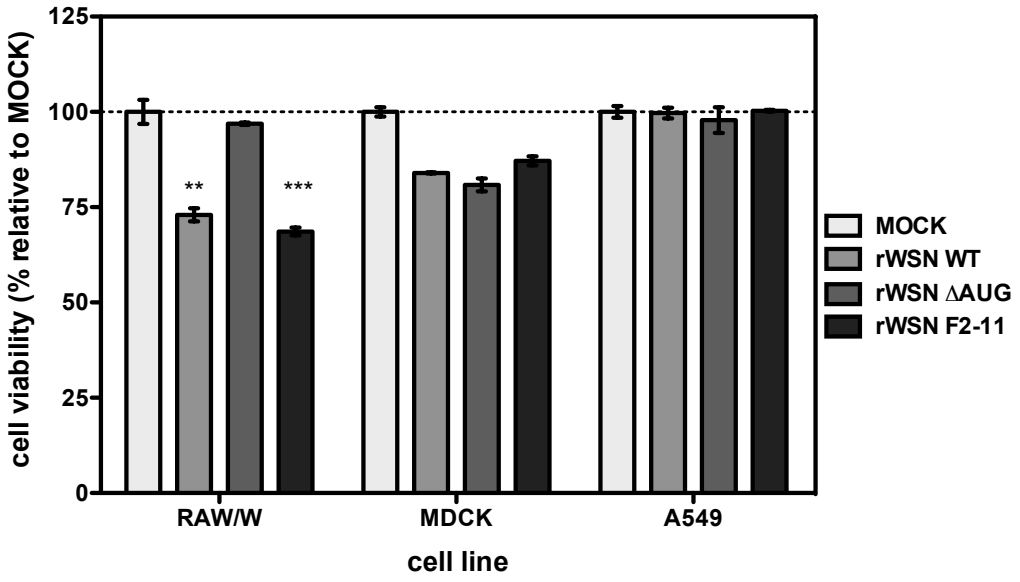

Figure 3.12: Cell viability assay: Monolayers of MDCK, A549 and RAW/W cells in 96-well plates were infected with either rWSN WT, rWSN △AUG or rWSN F2-11 at an MOI of 30 and tested for their viability after 8 h according to the manufacturers protocol. PBS was used as a control. Mean values ± SEM are plotted. **, $P<0.01$; ***, $P<0.001$.

To examine the role of WSN virus PB1-F2 in apoptosis, both WSN viruses with PB1-F2 deletions were analysed. As seen in Figure 3.12, only one of the deletant viruses was attenuated (rWSN △AUG), whereas rWSN

F2-11 showed a similar reduction as rWSN WT in the number of viable cells after infection. In MDCK cells, all viruses showed a similar loss of viability. These cells are known to be a permissive cell line for influenza A virus replication and were previously shown not to be targeted by PB1-F2 apoptosis (Chen et al., 2001). The loss of cell viability could be therefore connected to apoptosis due to NS1 expression and viral replication. A549 cells on the other hand are a cell line that does not support viral replication to the same extent as MDCK cells, reflected by the results in the cell viability assay.

To test the difference in apoptosis induction in immune cells by the more human relevant strain A/Udorn/72, human macrophages were separated from fresh blood. By adding different cytokines to the growth media, macrophages were divided into classical macrophages (Mφ1) or alternative macrophages (Mφ2) (Verreck et al., 2004). Infection was done using rUdo WT and rUdo $\triangle$AUG at different MOI (0.1, 1 and 5) and cells were collected at indicted time points (Figure 3.13). Levels of apoptosis were measured by staining cells with FITC-conjugated AnnexinV and propidium iodide (PI) followed by flow cytometry. Uninfected cells and cells infected with UV-treated influenza viruses were used as controls. As can be seen in Figure 3.13 (A), levels of apoptosis were similar for both macrophage subsets and at all virus MOI, suggesting that the 6 hpi time point was too early. At the later time point (20 hpi), an increase in apoptosis was observed (Figure 3.13 (B)). Several common features were noticed for both macrophage subsets: (1) Induction of apoptosis depended on viral replication as cells treated with UV-inactivated viruses did not show an increase in apoptosis compared to uninfected cells. (2) Induction of apoptosis was dose-dependent. With increasing MOI, levels of apoptosis also increased. (3) Viruses deficient in PB1-F2 (rUdo $\triangle$AUG) induced apoptosis in macrophages less efficiently. Differences were also observed between the two subsets of macrophages. Mφ2 seemed to be more susceptible to infection as an increase in apoptosis was already noticed at MOI 0.01. At higher MOIs, only small differences were observed between Mφ1 and Mφ2 infected with rUdo WT. However, PB1-F2 deletion viruses induced apoptosis in Mφ1 only at the highest MOI, whereas at this MOI the difference between rUdo WT and rUdo $\triangle$AUG infected cells almost disappeared.

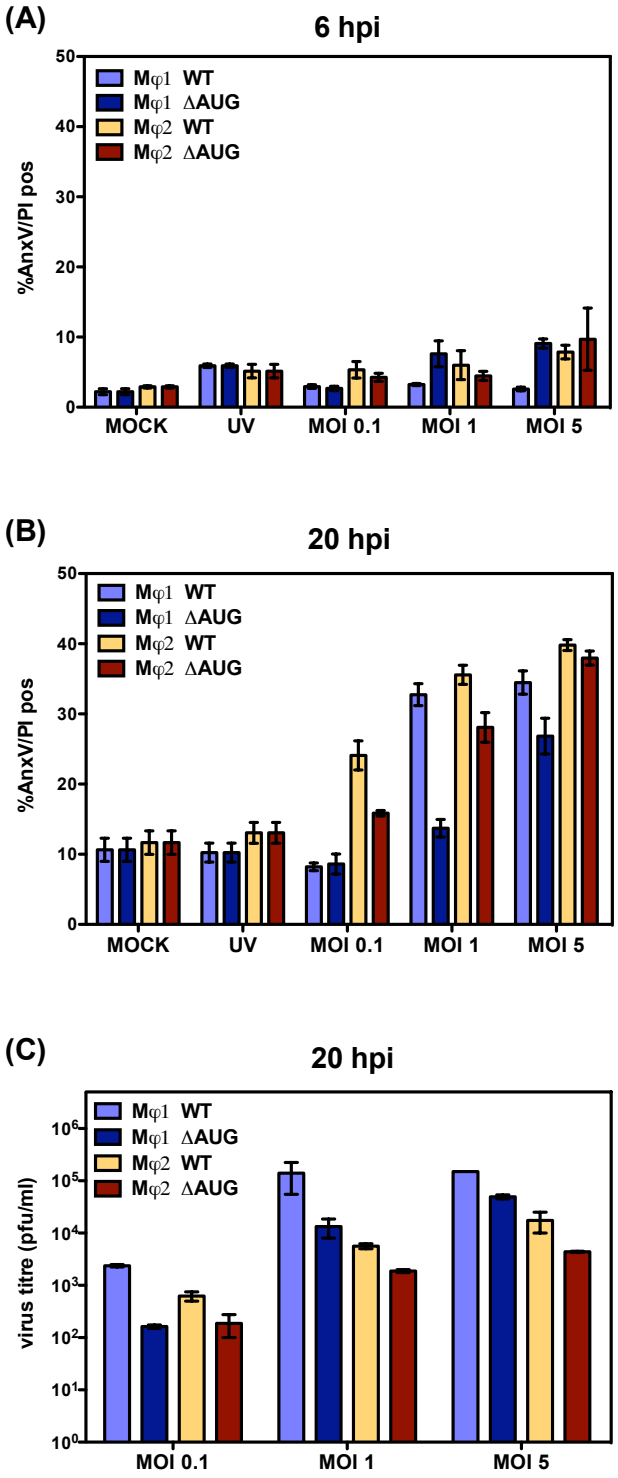

Figure 3.13: Macrophage assay: Human macrophages were divided into subsets by specific cytokines and infected with A/Udorn/72 WT or ΔAUG at indicated MOI. UV-treated influenza virus or MOCK infected cell served as control. **(A)** 6 hpi or **(B)** 20 hpi, cells were analysed by flow cytometry for apoptotic markers. **(C)** At 20 hpi, supernatant of infected cells was used for virus titration by plaque assay. Mean values ± SEM of triplicate measurements are plotted. This experiment was done in collaboration with M. Hoeve; University of Edinburgh.

Viral titres were measured by plaque assays at 20 hpi. An opposite effect was observed. Mφ1 were more susceptible for influenza A virus infection, however rUdo WT viruses replicated better in both subsets. The decrease in replication of rUdo $\triangle$AUG could also be the cause of a less efficient induction of apoptosis.

3.3.5 Effects of PB1-F2 deletion on virulence in mice

PB1-F2 was the subject of several *in vivo* experiments to investigate its influence on viral replication and pathogenicity. Previous reports showed an enhancing effect of PB1-F2 on virulence for some virus strains and an influence of one particular amino acid (aa 66) on viral pathogenicity (Zamarin et al., 2006; Conenello et al., 2007, 2011). For A/WSN/33 it was reported that the loss of PB1-F2 increased the survival rate and lowered weight loss and viral lung titres in infected mice (Zamarin et al., 2006). However this work was done using chimeric viruses or viruses with the deleted start codon for PB1-F2, which also alters the expression level of N40. To test whether the difference was due to PB1-F2 or N40, 6-7 week-old female BALB/c mice were infected with the two distinct mutant viruses as well as the WT virus. Inoculation was done intranasally using 5 x 10^3 pfu. Each group consisted of 8-10 mice, and weight was measured daily. Four mice per group were culled at day 4 to measure virus titre in the lungs. The remaining mice were culled on day 7 or when weight loss reached a critical point of -25%. Lung titres were measured for each group by plaque assay.

Figure 3.14(A) shows the weight loss of mice infected with rWSN WT, rWSN $\triangle$AUG or rWSN F2-11. PBS treated mice served as a control group, where no weight loss was observed. As expected, mice infected with the WT virus started to lose weight from day 2. Several clinical signs were observed such as staring coat and increased respiratory effort. The same symptoms and a similar weight loss were observed for mice infected with rWSN F2-11 viruses. However, mice infected with rWSN $\triangle$AUG viruses did not show any symptoms and no weight loss was measured. Viral titres for all groups were determined. Lungs of PBS infected mice were, as expected, negative for virus detection (data not shown). As seen in Figure 3.14(B), viral titres for rWSN WT and rWSN F2-11 were similar at both tested time points. Lung titres for rWSN $\triangle$AUG infected mice however were significantly reduced (* $P<0.05$; ** $P<0.01$). It is not known if viral titres were reduced throughout

the infection, as viral titres might have peaked earlier or later in infection and therefore remained undiscovered.

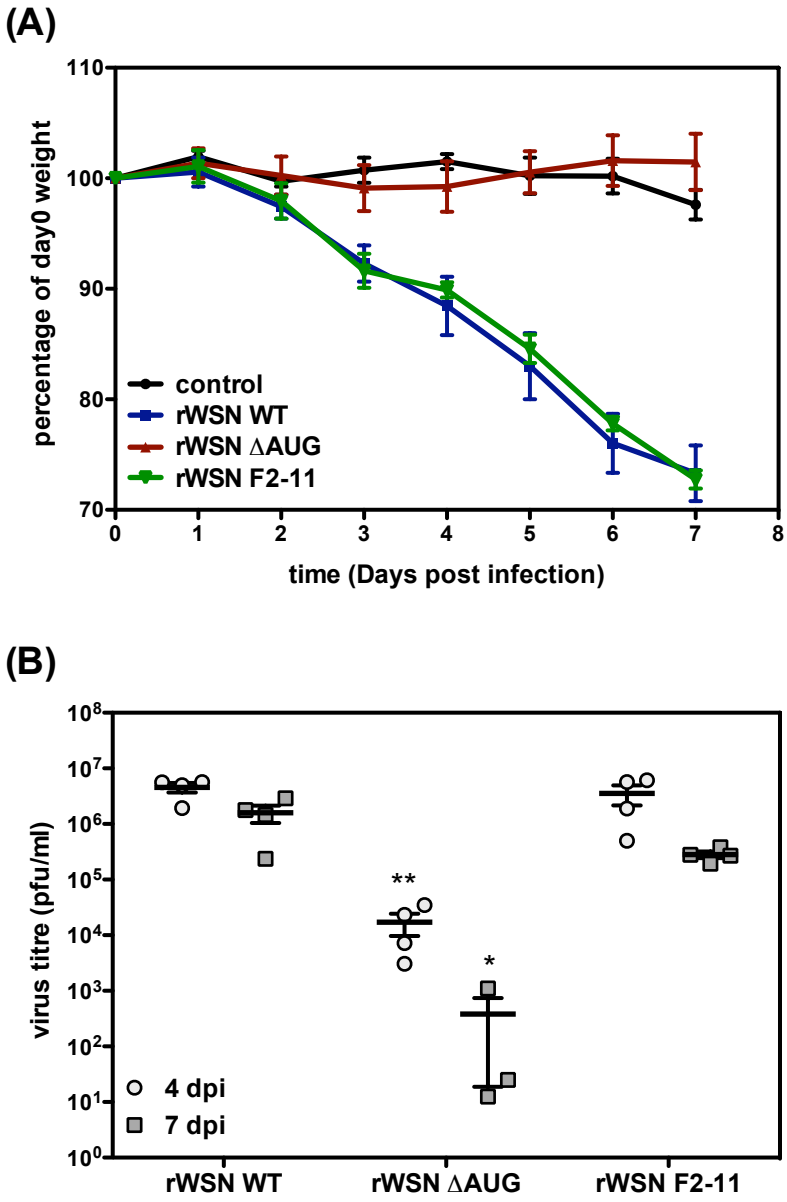

Figure 3.14: Virulence of the recombinant WSN viruses WT, ΔAUG and F2-11 in mice: Groups of 8 female BALB/c mice were infected with the recombinant WSN viruses WT, ΔAUG and F2-11 with $5x10^3$ pfu. **(A)** Weight loss was measured every day over a period of 7 days. Day 0 was set as 100% for each group. **(B)** At day 4 and day 7, 4 mice of each group were culled and lung virus titres were determined by plaque assay. Mean values ±SEM are plotted. * $P<0.05$; ** $P<0.01$. Mouse infections were done in collaberation with B. Dutia and her lab at the University of Edinburgh.

Two mice per group were used for lung histology at day 7 pi (Figure 3.15). WT and F2-11 infected mice showed very similar signs of infection including infiltrations of immune cells into interstitial regions and alveoli. Areas of necrosis were detected in terminal airways, which contained cellular debris. This reflects the symptoms of the mice such as increased respiratory effort. However, mice infected with rWSN $\triangle$AUG showed partial acute haemorrhage into alveoli. This was however restricted to small areas of the lung and terminal airways seemed to be unaffected. Almost no neutrophiles and macrophages were detected in the interstitial regions and alveoli. This could explain the missing clinical signs, as gas exchange in alveoli may be largely unaffected. The lack of infiltrated immune cells could be evidence for less production of cytokines caused by these viruses. As for the virus titre, comparing different time points will be required to understand pathology of these viruses better. It is not known if the observed phenotypes would be observed throughout the experiment or if virus pathology by $\triangle$AUG is delayed and therefore different to what is seen in WT and F2-11 infected mice.

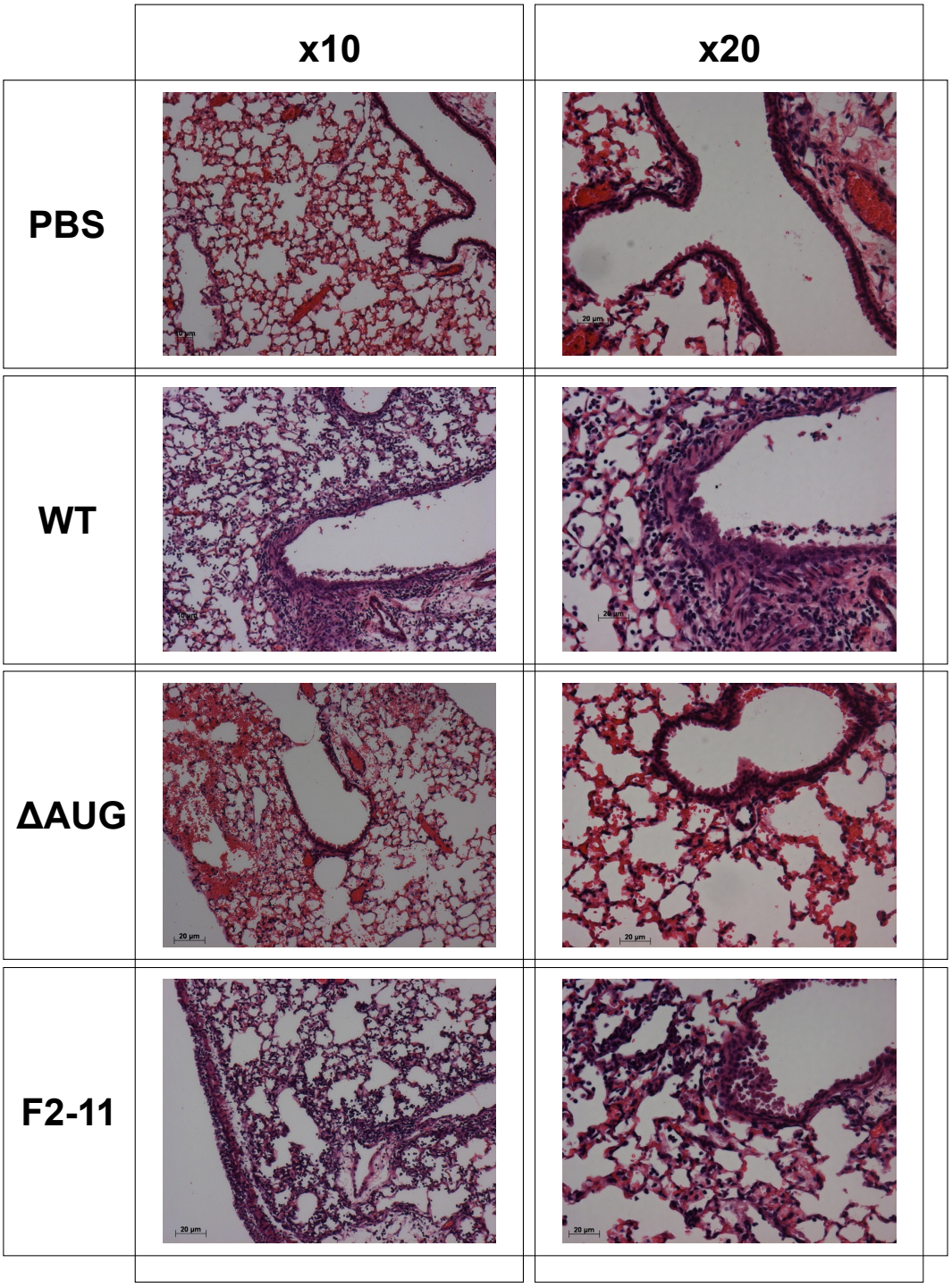

Figure 3.15: Histological section of lungs from BALB/c mice infected with WT WSN or PB1-F2 deletion viruses: Mice were infected intranasally with 5x10^3 pfu of the panel of recombinant WSN viruses - WT, ΔAUG and F2-11. PBS served as a negative control. At day 7 p.i. lung sections were stained with Hematoxylin & Eosin. Mice infected with WT and F2-11 viruses showed significant increased numbers of neutrophils in the alveoli as well as necrosis of the bronchus epithelial wall. Mice infected with ΔAUG viruses on the other hand showed signs of acute hemorrhage, but less cellular infiltration. Bronchus epithelial wall remained mainly intact. This work was done with the help of Jill McVee, University of St Andrews.

3.4 Discussion

The aim of this Chapter was the analysis and comparison of two PB1-F2 deletion strains. Previous work on PB1-F2 used deletion viruses including a deleted start codon to abolish PB1-F2 expression (Zamarin et al., 2006). When this project was started, we decided to introduce the same mutations into PB1-F2. However, in 2009, a third protein (N40), translated from the very same mRNA, was described and it was shown that removal of the PB1-F2 start codon influenced the downstream protein expression level (Wise et al., 2009). Therefore we decided to create the second PB1-F2 deletion mutant to compare phenotypes and, if possible, dissect effects caused by PB1-F2 or N40. This second method abolished PB1-F2 translation after amino acid 11. A similar mutation is present in recent pandemic H1N1 viruses from 2009 (Ramakrishnan et al., 2009). In previous reports, PB1-F2 was shown to be involved in the induction of apoptosis in a cell-type dependent manner (Chen et al., 2001; Zamarin et al., 2006). However, these findings were mainly based on the analysis of only one virus strain - A/PR8/34. Comparison of several other influenza A virus strains showed that the induction of apoptosis is a strain specific feature (McAuley et al., 2010a). It was suggested that an ILV motif (amino acids 68-70) in the C-terminus is involved, because it is present in A/PR8/34, but absent in most other virus strains which do not induce apoptosis. Amino acid sequence alignments showed that this motif is also present in PB1-F2 of the closely related strain A/WSN/33 (Figure 3.6). Indeed, apoptosis was induced in mouse macrophages by rWSN WT viruses, however the loss of PB1-F2 alone did not show any alteration of this ability. RAW cells infected with rWSN F2-11 also underwent apoptosis to the same extent as WT (Figure 3.12). It seems likely that induction of apoptosis is not the main function of PB1-F2 but it may be an accessory feature of some individual strains to counteract the immune response and gain virulence. Similar observations were made in the human macrophage experiments (Figure 3.13). Both subsets of human macrophages infected with A/Udorn/72 underwent apoptosis in a dose-dependent manner, although levels of apoptosis were reduced in cells infected with rUdo $\triangle$AUG virus. However, to draw a firm conclusion, the experiment should be repeated including a virus deficient for PB1-F2 but expressing normal N40 levels. Additionally, it should be noted that viruses with an increased N40 expression level in a

PB1-F2 deficient background showed reduced viral growth (Figure 3.13). Consistent with the findings on plaque phenotype, rWSN △AUG viruses showed an attenuation in viral growth when cells were infected with a low MOI (Figure 3.8; 3.10 (A)). However, when cell monolayers were infected with a high MOI, this attenuation was no longer observed (Figure 3.10 (B)). It could be hypothesised that high levels of N40 have a negative impact on counteracting the immune system. In this case, no differences would be expected at infection with a high multiplicity when every cell in a dish is infected, but would be disadvantageous in infections with a low MOI. One possibility to test this hypothesis would be to measure viral growth in immune incompetent cells. It was noted that single-step growth curves did not follow a typical exponential curve (Figure 3.10(B)). It is known that infections at high MOI can support production of defective interfering particles (DIs). Although DIs usually arise after serial passages, single mutations may be sufficient to induce the production of DIs at high multiplicity infection (Odagiri and Tobita, 1990; Odagiri et al., 1994). In the reported case, viruses also grew normally in multi-step growth curves. Viruses in the present study were plaque purified and only passaged once to grow up viral stocks to use for further investigations. However, it can not be ruled out that (1) these stocks acquired single mutations or (2) rescue plasmids already carried a mutation, which supported the formation of DIs. This mutation would be subsequently present in all viruses rescued. Alternatively, the experimental designs and conditions may be suboptimal and lower MOI (MOI 1) could be used to reduce formation of defective interfering particles.

Animal models are critical for influenza research. The most commonly used model systems are mice, hamsters, ferrets and non-human primates. Although mice are not naturally infected by influenza viruses, they have a lot of advantages because they are easy to handle, small and have a known genetic background that can also be modified. Mouse adapted virus strains made it possible to infect mice and to study effects on pathogenicity or immune response. Different inbred mouse strains were shown to have different susceptibility and both the host and virus genetic background influence the outcome of an infection (Srivastava et al., 2009; Boon et al., 2009; Blazejewska et al., 2011). In this study, BALB/c mice were used to test the effect of PB1-F2 deletions on viral pathogenicity. As described previously, deletion of PB1-F2 (△AUG) caused an attenuation in these mice (Zamarin et al., 2006). These results were confirmed in

the present study. No weight loss was observed in mice infected with rWSN ΔAUG. However, WT and F2-11 virus-infected mice rapidly lost weight and developed symptoms (Figure 3.14). Lung virus titres confirmed the attenuation of rWSN ΔAUG viruses. However, it requires further investigations whether an increased N40 protein level caused decreased titre in the lung and if this decrease was present throughout the infection cycle. Viral titres may reach those of WT infected mice, but at a different time point. Also, other viral strains and the effect of PB1-F2 deletions in combination with varying N40 levels should be tested to better understand the role of PB1-F2 in pathogenicity.

The reasons for an attenuation of overexpressed N40 in a PB1-F2 deficient background are still unknown. N40 lacks the N-terminal 39 amino acids of PB1, but most of the interaction sites with viral and cellular proteins are probably still available. A number of interaction partners for PB1 have been described, although the sites within the protein remain unidentified for many of them. The NFκB pathway was shown to be important for an infection of influenza A viruses (Nimmerjahn et al., 2004). Induction of IKK leads to the activation and translocation of NFκB into the nucleus, where it regulates the expression of more than 150 genes such as cytokines and pro-apoptotic genes (Pahl, 1999). A search for host cell interacting partners revealed a number of viral proteins interacting with members of this pathway, including HA, M1 and NP, but also the polymerase subunits (Flory et al., 2000; Shapira et al., 2009). The expression of single influenza virus proteins was sufficient to induce this pathway (Flory et al., 2000). NFκB activation also results through RIG-I activation as part of the host cell immune response (Figure 1.8). RIG-I is activated by binding to 5' triphosphorylated RNA and the CARD domain of RIG-I subsequently interacts with the CARD domain of MAVS. This protein is an mitochondrial membrane protein that activates IKKα/β and IKKγ which leads to the activation of NFκB and IRF-3. Recently, an interaction of PB1-F2 and MAVS was described (Varga et al., 2011). The authors found a suppression of IFN-β expression due to PB1-F2. This suppression was even enhanced if PB1-F2 carried a serine at position 66. Surprisingly, an opposite effect was seen in epithelial cells infected with the PB1-F2-deficient virus overexpressing N40 (ΔAUG) (Goffic et al., 2010; Varga et al., 2011). The conflicting results may be an effect of increased level of N40 in the experiments carried out with the ΔAUG virus. A hypothesised model of MAVS signalling and the influence of PB1-F2 is

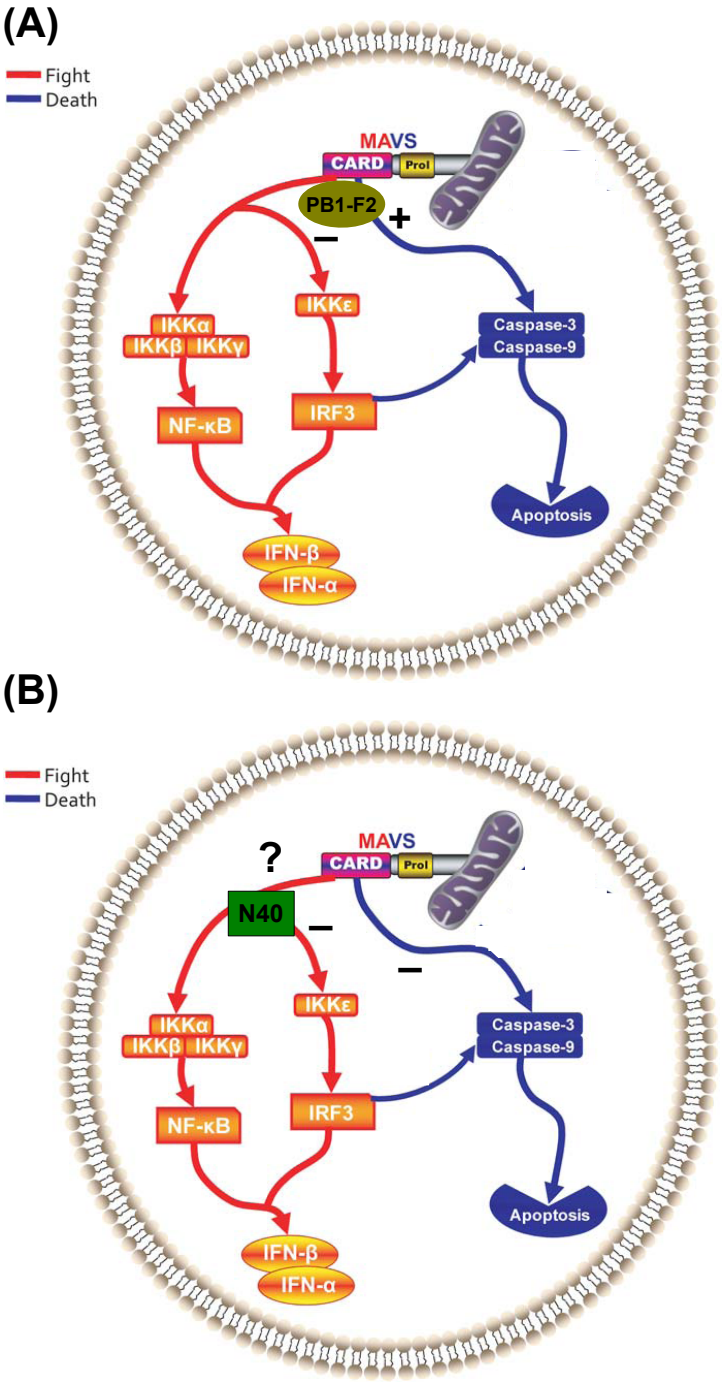

Figure 3.16: Model of the effect the Influenza A virus has on the MAVS signalling : (A) A dual mechanism was reported for MAVS proteins, inducing apoptosis or activating NFκB leading to the expression of IFN-β. PB1-F2 was also found to be involved in both events, however PB1-F2 suppresses the induction of IFN-β upon interaction with MAVS. **(B)** In cells infected with a virus deficient for PB1-F2 but overexpressing N40, a lack of apoptosis in immune cells was reported as well as a decrease in IFN-β expression. Latter may be due to the higher levels of N40. The picture was adapted from (Lei et al., 2009).

shown in Figure 3.16. Beside IFN-induction, MAVS proteins were also shown to be involved in the regulation of apoptosis (Lei et al., 2009). Interestingly, it was shown that MAVS regulate apoptosis by suppressing the mitochondrial membrane protein VDAC1, which is also an interaction partner of PB1-F2 (Xu et al., 2010; Zamarin et al., 2005).

The question arises whether the PB1-F2 ORF is in place to regulate the expression levels of the downstream N40. When Zell et al. analysed the sequences available in databases, they only found 5 strains out of $>$2200 that did not have a start codon for PB1-F2 (Zell et al., 2007). About 87% do encode an ORF $>$78 amino acids, however human H1N1 strains after 1950 in particular possess a truncated PB1-F2. Classical swine viruses have a stop codon introduced after amino acid 11. The recently emerged pandemic H1N1 (2009) carries a segment 2 that originates from swine influenza strains and only has a truncated PB1-F2 ORF with stop codons at amino acid 12, 58 and 88. Efforts were made to introduce PB1-F2 into these 2009 pandemic strain in order to determine any possible effects of the full-length protein on viral pathogenicity. The viruses did not significantly benefit of the presence of the protein (Hai et al., 2010). Therefore, if and to what extent, PB1-F2 and N40 are important remains unknown. To date, data are partly controversial whether PB1-F2 increases viral pathogenicity or not. But it has become more evident that PB1-F2 functions in a highly strain and cell type specific manner and an overall conclusion might be difficult. What can be said from the findings made in this Chapter is that the design of mutants is critically important and some of the published results made with PB1-F2 deletion viruses may need to be reconsidered.

3.5 Summary of Chapter 3

Two PB1-F2 deletion viruses were engineered (overview in Table 3.4).

Virus	Mutation	Protein levels	Phenotype
△AUG	T120C	PB1: WT	small plaques
	C153C	PB1-F2: null	attenuation *in vitro*
	G291A	N40: overexpression	attenuation *in vivo*
F2-11	C153G	PB1: WT	WT phenotype
	G291A	PB1-F2: null	
		N40: WT	

Table 3.4: Summary Chapter 3: Introduced mutations into PB1 abolished PB1-F2 ORF. Whereas the PB1 level appears unaffected for both strains, △AUG viruses overexpress N40. This led to a major attenuation both *in vitro* and *in vivo.*

The removal of the start codon of PB1-F2 had a dramatic effect on the virus both *in vitro* and *in vivo*. The only difference between △AUG viruses and F2-11 is the altered level of N40, which seems to have detrimental effects on plaque size, growth and especially on virulence. This findings are important as many previous studies to determine the function of PB1-F2 are based on the deletion of the PB1-F2 ORF by removing the start codon. Here it was shown that N40 needs to be taken into consideration when designing PB1-F2 mutants.

Chapter 4

CELLULAR POLYMERASE II DEGRADATION

Aims of Chapter 4

The viral RNA dependent RNA polymerase was reported to bind to the largest subunit of cellular RNA polymerase II (Engelhardt et al., 2005). This interaction resulted in degradation of the hypophosphorylated form of the cellular polymerase. Two single point mutations within the viral polymerase subunits were tested for their influence on degradation and host cell protein shut-off.

The first mutation was located in the polymerase subunit PB2 (V504I), a second mutation was introduced in the polymerase subunit PA (L550I). The effects of the individual single point mutations were analysed as well as the effect of a double mutation.

4.1 Interaction of the influenza A virus RdRp and cellular RNA polymerase II and the consequences of this interaction

Cellular mRNA synthesis is performed by a multiprotein complex called RNA polymerase II (RNAP II). The carboxy-terminal domain (CTD) of the largest subunit plays a major role during the transcription cycle. It contains over 50 repeats of a heptapeptide YSPTSPS, which are differentially phosphorylated during the transcription process (Figure 4.1). Upon phosphorylation of serine-5 residues, the RNAPII initiates transcription. Following further phosphorylation at serine-2 residues, transcription proceeds into elongation (Komarnitsky et al., 2000). Coupled with these different phosphorylation stages are varying affinities for transcription factors and factors involved in 5' and 3' end processing of pre-mRNAs (Schroeder et al., 2000; Komarnitsky et al., 2000; Kim et al., 1997; McCracken et al., 1997).

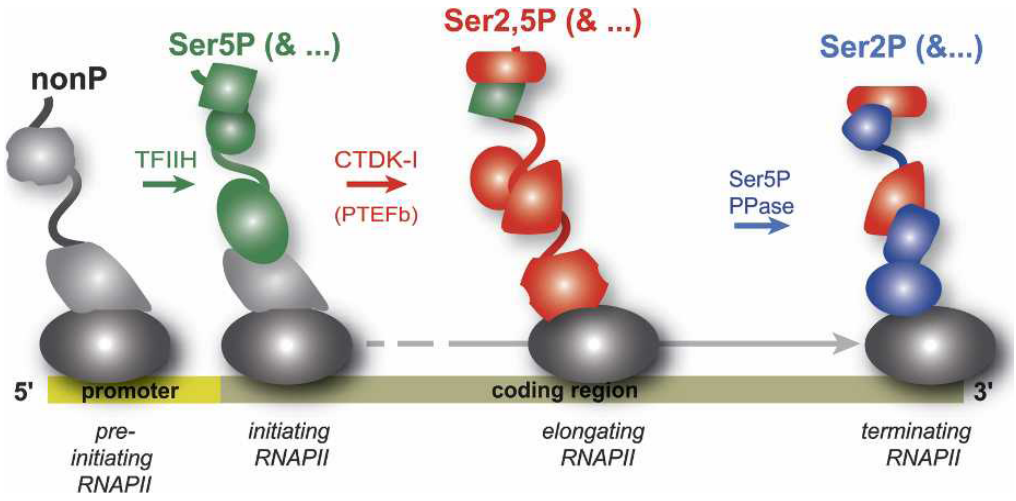

Figure 4.1: Differential phosphorylation of the CTD of cellular RNAPII: The hypophosphorylated form of the CTD gets phosphorylated at serine-5 residues which initiates transcription. Proceeding into elongation is realised by serine-2 phosphorylation. Taken from Phatnani and Greenleaf (2006).

Although influenza A viruses encode their own RNA-dependent RNA polymerase (RdRp), it was assumed for a long time that viral replication depends on a functional cellular RNA polymerase II. Two events in the viral life cycle are thought to be coupled to cellular transcription:
(1) Viral transcription depends on the availability of 5' cap structures of

cellular mRNAs (Bouloy et al., 1978; Plotch et al., 1981).
(2) Influenza A virus segments 7 and 8 produce spliced mRNAs, and splicing is performed by the cellular splicing machinery (Inglis et al., 1979; Lamb et al., 1981).
Viral RdRp was found to interact with the largest subunit of cellular RNAPII (Engelhardt et al., 2005). More specifically, this interaction was shown to be between the viral polymerase trimer and the C-terminal domain (CTD). None of the polymerase subunits alone nor one of the dimers were able to bind to and degrade the RNAPII. Interaction was confirmed between the RdRp and the CTD in its hyperphosphoryated form, more specifically with the Serine-5-phosphorylated form (Engelhardt et al., 2005). It is believed that this provides the viral polymerase with 5' capped pre-mRNAs that are needed to initiate viral transcription. However, following interaction, the largest subunit of the RNAPII in its hypophosphorylated form was shown to be degraded (Rodriguez et al., 2007).
When this project was started, the involvement of the individual viral polymerase segments was not known. Hence, the impact of PB1-F2 was determined by evaluating the degradation of RNAPII in rWSN WT or rWSN $\triangle$AUG infected cells. Specific antibodies were used to differentiate between the different phosphorylated forms of the CTD (Table 4.1).

Antibody	**Epitope**	**Recognition**
8WG16	Non-phosphorylated	Non-phosphorylated repeats
H5	Ser2-P	Ser-2P, Ser5-P, Ser2-P + Ser5-P

Table 4.1: Anti-CTD monoclonal antibodies recognising specific epitopes depending on their phosphorylation state. (Jones et al., 2004; Rodriguez et al., 2007)

Confluent monolayers of MDCK cells were infected with one of the two viruses and cells were lysed at the indicated time points. Results of the western blot analysis are shown in Figure 4.2. Consistent with previous reports (Rodriguez et al., 2007), a decrease in the accumulation of the hypophosphorylated RNAPII in rWSN WT infected cells was observed from 6 hpi onwards. In contrast, no decrease was observed in the accumulation level of Serine-2-phosphorylated RNAPII, detected by the antibody H5. The degradation correlated with the onset of viral protein synthesis. No difference was observed in cells infected with the rWSN $\triangle$AUG virus, suggesting that PB1-F2 and N40 are not involved in the process.

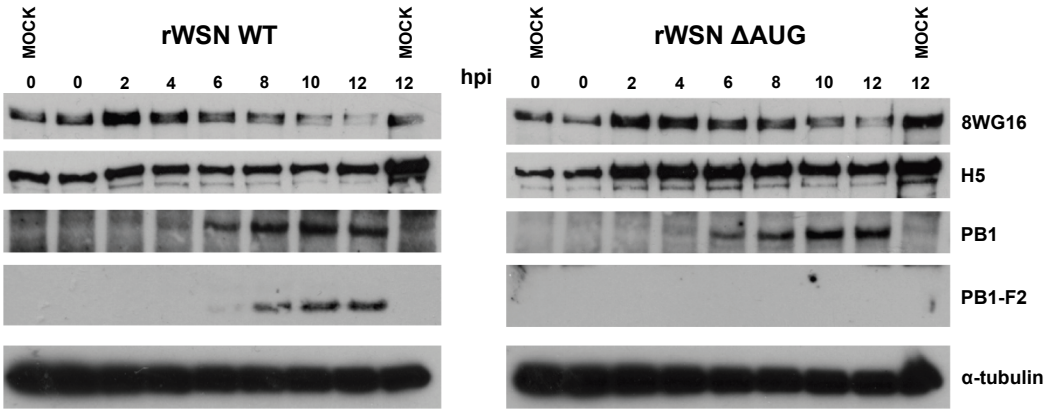

Figure 4.2: Degradation of cellular polymerase II did not depend on PB1-F2: Confluent monolayers of MDCK cells were infected with rWSN WT, rWSN ΔAUG or Mock infected at an MOI of 3 and cells were lysed at the indicated time points. 8% Bis-Tris gels were used to detect the cellular polymerase using the antibodies 8WG16 and H5. 4 - 12% gradient Bis-Tris gels were used for PB1 detection, whereas 16% Tricine-SDS-PAGE was used to detect the small hydrophobic protein PB1-F2. α-tubulin was used as an internal loading control.

More recently the involvement of PB2 and PA were suggested, when comparing low-virulence (lvPR8) and high-virulence (hvPR8) strains of A/PR/8/34 for their ability to degrade the largest subunit of RNAPII (Rodriguez et al., 2009). It was shown that the degradation was restricted to non-attenuated viral strains, because the lvPR8 and a cold-adapted strain (A/Ann Arbor/6/60) were found not to degrade the cellular polymerase. When comparing recombinant viruses, segment 1 and 3 gene products were identified to contribute to the degradation whereas segment 2 did not have an influence.

It is not fully understood how the interaction between cellular RNAPII and viral RdRp is maintained. A recent study suggested the kinase cyclinT1/CDK9 to function as a mediator between the CTD and the viral polymerase complex (Zhang et al., 2010a). CDK9 was shown to bind to all three polymerase subunits, PB2, PB1 and PA, and the interaction promoted viral transcription. Cyclin T1/CDK9 phosphorylates serine-2 residues in the CTD of the large subunit (Marshall et al., 1996). Previously, binding was especially suggested between RdRp and the Ser-5P form of the CTD (Engelhardt et al., 2005), but phosphorylation of serine-5 residues is performed by a different kinase (TFIIH). If the viral polymerase complex binds directly to the CTD with Serine-5-phosphorylation or if this interaction is also mediated by an adaptor protein is unknown.

4.2 Mutations in the polymerase subunit PB2 and PA involved in degradation of cellular polymerase II

It was shown by Rodriguez et al., that the hvPR8 strain induced degradation of cellular RNAPII, whereas the lvPR8 variant had no influence (Rodriguez et al., 2009). Segment 1 and 3 gene products were identified as the key components for the differences, although only three amino acids in PB2 and two residues in PA differed between the two variants (Grimm et al., 2007). A/WSN/33 is a closely related strain also inducing RNAPII degradation. To determine whether any of the above mentioned amino acids were involved in degradation, recombinant WSN viruses were engineered to analyse the influence of the residues individually. First, mutation sites were chosen. Therefore, an alignment was performed for segment 1 and 3, comparing the amino acid sequence of both PR8 variants and WSN (Figures 4.3 and 4.4). Two residues - one in each segment - were identified to be identical in hvPR8 and WSN, but differed from lvPR8. The remaining three different residues were either different in all three viruses or WSN shared the sequence with lvPR8 (Table 4.2). Amino acid 504 in PB2 and 550 in PA were mutated to isoleucine in order to change the sequence of WSN to the sequence found in the lvPR8 variant. Oligo nucleotide sequences are listed in Table 2.14. Mutations were introduced by PCR-mediated site-directed mutagenesis (Section 2.4.3).

	Amino acid		
Viral protein	**lvPR8**	**hvPR8**	**A/WSN/33**
PB2 aa105	Ile	Met	Val
PB2 aa456	Asn	Asp	Asn
PB2 aa504	Ile	Val	**Val**
PA aa193	Gln	His	Gln
PA aa550	Ile	Leu	**Leu**

Table 4.2: Comparison of residues that differed between lvPR8, hvPR8 and WSN: The two residues that were mutated in WSN are shown in bold.

PB2

```
A/lvPR8/34_H1N1_      MERIKELRNLMSQSRTREILTKTTVDHMAIIKKYTSGRQEKNPALRMKWMMAMKYPITAD 60
A/hvPR8/34_H1N1_      MERIKELRNLMSQSRTREILTKTTVDHMAIIKKYTSGRQEKNPALRMKWMMAMKYPITAD 60
A/WSN/1933_H1N1_      MERIKELRNLMSQSRTREILTKTTVDHMAIIKKYTSGRQEKNPALRMKWMMAMKYPITAD 60
                      ************************************************************

A/lvPR8/34_H1N1_      KRITEMIPERNEQGQTLWSKMNDAGSDRVMVSPLAVTWWNRNGPITNTVHYPKIYKTYFE 120
A/hvPR8/34_H1N1_      KRITEMIPERNEQGQTLWSKMNDAGSDRVMVSPLAVTWWNRNGPMTNTVHYPKIYKTYFE 120
A/WSN/1933_H1N1_      KRITEMIPERNEQGQTLWSKMNDAGSDRVMVSPLAVTWWNRNGPVTSTVHYPKIYKTYFE 120
                      ********************************************:*.************

A/lvPR8/34_H1N1_      RVERLKHGTFGPVHFRNQVKIRRRVDINPGHADLSAKEAQDVIMEVVFPNEVGARILTSE 180
A/hvPR8/34_H1N1_      RVERLKHGTFGPVHFRNQVKIRRRVDINPGHADLSAKEAQDVIMEVVFPNEVGARILTSE 180
A/WSN/1933_H1N1_      KVERLKHGTFGPVHFRNQVKIRRRVDINPGHADLSAKEAQDVIMEVVFPNEVGARILTSE 180
                      :************************************************************

A/lvPR8/34_H1N1_      SQLTITKEKKEELQDCKISPLMVAYMLERELVRKTRFLPVAGGTSSVYIEVLHLTQGTCW 240
A/hvPR8/34_H1N1_      SQLTITKEKKEELQDCKISPLMVAYMLERELVRKTRFLPVAGGTSSVYIEVLHLTQGTCW 240
A/WSN/1933_H1N1_      SQLTTTKEKKEELQGCKISPLMVAYMLERELVRKTRFLPVAGGTSSVYIEVLHLTQGTCW 240
                      **** *********.********************************************

A/lvPR8/34_H1N1_      EQMYTPGGEVRNDDVDQSLIIAARNIVRRAAVSADPLASLLEMCHSTQIGGIRMVDILRQ 300
A/hvPR8/34_H1N1_      EQMYTPGGEVRNDDVDQSLIIAARNIVRRAAVSADPLASLLEMCHSTQIGGIRMVDILRQ 300
A/WSN/1933_H1N1_      EQMYTPGGEARNDDVDQSLIIAARNIVRRATVSADPLASLLEMCHSTQIGGVRMVNILRQ 300
                      *********.*******************:*******************:***:****

A/lvPR8/34_H1N1_      NPTEEQAVDICKAAMGLRISSSFSFGGFTFKRTSGSSVKREEEVLTGNLQTLKIRVHEGY 360
A/hvPR8/34_H1N1_      NPTEEQAVDICKAAMGLRISSSFSFGGFTFKRTSGSSVKREEEVLTGNLQTLKIRVHEGY 360
A/WSN/1933_H1N1_      NPTEEQAVDICKAAMGLRISSSFSFGGFTFKRTSGSSVKREEEVLTGNLQTLKIRVHEGY 360
                      ************************************************************

A/lvPR8/34_H1N1_      EEFTMVGRRATAILRKATRRLIQLIVSGRDEQSIAEAIIVAMVFSQEDCMIKAVRGDLNF 420
A/hvPR8/34_H1N1_      EEFTMVGRRATAILRKATRRLIQLIVSGRDEQSIAEAIIVAMVFSQEDCMIKAVRGDLNF 420
A/WSN/1933_H1N1_      EEFTMVGRRATAILRKATRRLIQLIVSGRDEQSIAEAIIVAMVFSQEDCMIKAVRGDLNF 420
                      ************************************************************

A/lvPR8/34_H1N1_      VNRANQRLNPMHQLLRHFQKDAKVLFQNWGVEPIDNVMGMIGILPDMTPSIEMSMRGVRI 480
A/hvPR8/34_H1N1_      VNRANQRLNPMHQLLRHFQKDAKVLFQNWGVEPIDDVMGMIGILPDMTPSIEMSMRGVRI 480
A/WSN/1933_H1N1_      VNRANQRLNPMHQLLRHFQKDAKVLFQNWGIESIDNVMGMIGILPDMTPSTEMSMRGVRI 480
                      ******************************:*.**:************** *********

A/lvPR8/34_H1N1_      SKMGVDEYSSTERVVVSIDRFLRIRDQRGNVLLSPEEVSETQGTEKLTITYSSSMMWEIN 540
A/hvPR8/34_H1N1_      SKMGVDEYSSTERVVVSIDRFLRVRDQRGNVLLSPEEVSETQGTEKLTITYSSSMMWEIN 540
A/WSN/1933_H1N1_      SKMGVDEYSSAEKIVVSIDRFLRVRDQRGNVLLSPEEVSETQGTEKLTITYSSSMMWEIN 540
                      **********:*::*********:************************************

A/lvPR8/34_H1N1_      GPESVLVNTYQWIIRNWETVKIQWSQNPTMLYNKMEFEPFQSLVPKAIRGQYSGFVRTLF 600
A/hvPR8/34_H1N1_      GPESVLVNTYQWIIRNWETVKIQWSQNPTMLYNKMEFEPFQSLVPKAIRGQYSGFVRTLF 600
A/WSN/1933_H1N1_      GPESVLVNTYQWIIRNWETVKIQWSQNPTMLYNKMEFEPFQSLVPKAVRGQYSGFVRTLF 600
                      ********************************************:*************

A/lvPR8/34_H1N1_      QQMRDVLGTFDTAQIIKLLPFAAAPPKQSRMQFSSFTVNVRGSGMRILVRGNSPVFNYNK 660
A/hvPR8/34_H1N1_      QQMRDVLGTFDTAQIIKLLPFAAAPPKQSRMQFSSFTVNVRGSGMRILVRGNSPVFNYNK 660
A/WSN/1933_H1N1_      QQMRDVLGTFDTAQIIKLLPFAAAPPKQSGMQFSSLTINVRGSGMRILVRGNSPVFNYNK 660
                      **************************** ***** *:*:**********************

A/lvPR8/34_H1N1_      ATKRLTVLGKDAGTLTEDPDEGTAGVESAVLRGFLILGKEDRRYGPALSINELSNLAKGE 720
A/hvPR8/34_H1N1_      ATKRLTVLGKDAGTLTEDPDEGTAGVESAVLRGFLILGKEDRRYGPALSINELSNLAKGE 720
A/WSN/1933_H1N1_      TTKRLTVLGKDAGPLTEDPDEGTAGVESAVLRGFLILGKEDRRYGPALSINELSNLAKGE 720
                      :************.************************************************

A/lvPR8/34_H1N1_      KANVLIGQGDVVLVMKRKRDSSILTDSQTATKRIRMAIN 759
A/hvPR8/34_H1N1_      KANVLIGQGDVVLVMKRKRDSSILTDSQTATKRIRMAIN 759
A/WSN/1933_H1N1_      KANVLIGQGDVVLVMKRKRNSSILTDSQTATKRIRMAIN 759
                      ******************:*******************
```

Figure 4.3: Alignment of polymerase subunit PB2. Two A/PR8/34 variants and A/WSN/33 were compared for their amino acid sequence of the polymerase subunit PB2. The high virulent (hv) PR8 strain was shown to be more potent in the degradation of cellular polymerase than the low virulent (lv) PR8 variant. A/WSN/33 is known to degrade cellular polymerase. One amino acid (highlighted in dark red) differed between hvPR8 and lvPR8, but not between hvPR8 and A/WSN/33 and was therefore chosen for site-directed mutagenesis. Amino acids in light red show sites that differed between all three strains or between hvPR8 and WSN and were therefore not chosen for site-directed mutagenesis.

PA

```
A/lvPR8/34_H1N1_      MEDFVRQCFNPMIVELAEKTMKEYGEDLKIETNKFAAICTHLEVCFMYSDFHFINEQGES 60
A/hvPR8/34_H1N1_      MEDFVRQCFNPMIVELAEKTMKEYGEDLKIETNKFAAICTHLEVCFMYSDFHFINEQGES 60
A/WSN/1933_H1N1_      MEDFVRQCFNPMIVELAEKAMKEYGEDLKIETNKFAAICTHLEVCFMYSDFHFIDEQGES 60
                      ******************:**********************************:*****

A/lvPR8/34_H1N1_      IIVELGDPNALLKHRFEIIEGRDRTMAWTVVNSICNTTGAEKPKFLPDLYDYKENRFIEI 120
A/hvPR8/34_H1N1_      IIVELGDPNALLKHRFEIIEGRDRTMAWTVVNSICNTTGAEKPKFLPDLYDYKENRFIEI 120
A/WSN/1933_H1N1_      IVVELGDPNALLKHRFEIIEGRDRTIAWTVINSICNTTGAEKPKFLPDLYDYKKNRFIEI 120
                      *:**********************:****:**********************:******

A/lvPR8/34_H1N1_      GVTRREVHIYYLEKANKIKSEKTHIHIFSFTGEEMATKADYTLDEESRARIKTRLFTIRQ 180
A/hvPR8/34_H1N1_      GVTRREVHIYYLEKANKIKSEKTHIHIFSFTGEEMATKADYTLDEESRARIKTRLFTIRQ 180
A/WSN/1933_H1N1_      GVTRREVHIYYLEKANKIKSEKTHIHIFSFTGEEMATKADYTLDEESRARIKTRLFTIRQ 180
                      ************************************************************

A/lvPR8/34_H1N1_      EMASRGLWDSFRQSERGEETIEERFEITGTMRKLADQSLPPNFSSLENFRAYVDGFEPNG 240
A/hvPR8/34_H1N1_      EMASRGLWDSFRHSERGEETIEERFEITGTMRKLADQSLPPNFSSLENFRAYVDGFEPNG 240
A/WSN/1933_H1N1_      EMASRGLWDSFRQSERGEETIEERFEITGTMRKLADQSLPPNFSSLENFRAYVDGFEPNG 240
                      ***********:************************************************

A/lvPR8/34_H1N1_      YIEGKLSQMSKEVNARIEPFLKTTPRPLRLPNGPPCSQRSKFLLMDALKLSIEDPSHEGE 300
A/hvPR8/34_H1N1_      YIEGKLSQMSKEVNARIEPFLKTTPRPLRLPNGPPCSQRSKFLLMDALKLSIEDPSHEGE 300
A/WSN/1933_H1N1_      YIEGKLSQMSKEVNARIEPFLKSTPRPLRLPDGPPCSQRSKFLLMDALKLSIEDPSHEGE 300
                      **********************:********:****************************

A/lvPR8/34_H1N1_      GIPLYDAIKCMRTFFGWKEPNVVKPHEKGINPNYLLSWKQVLAELQDIENEEKIPKTKNM 360
A/hvPR8/34_H1N1_      GIPLYDAIKCMRTFFGWKEPNVVKPHEKGINPNYLLSWKQVLAELQDIENEEKIPKTKNM 360
A/WSN/1933_H1N1_      GIPLYDAIKCMRTFFGWKEPNVVKPHEKGINPNYLLSWKQVLAELQDIENEEKIPRTKNM 360
                      ************************************************************:****

A/lvPR8/34_H1N1_      KKTSQLKWALGENMAPEKVDFDDCKDVGDLKQYDSDEPELRSLASWIQNEFNKACELTDS 420
A/hvPR8/34_H1N1_      KKTSQLKWALGENMAPEKVDFDDCKDVGDLKQYDSDEPELRSLASWIQNEFNKACELTDS 420
A/WSN/1933_H1N1_      KKTSQLKWALGENMAPEKVDFDDCKDVGDLKQYDSDEPELRSLASWIQNEFNKACELTDS 420
                      ************************************************************

A/lvPR8/34_H1N1_      SWIELDEIGEDVAPIEHIASMRRNYFTSEVSHCRATEYIMKGVYINTALLNASCAAMDDF 480
A/hvPR8/34_H1N1_      SWIELDEIGEDVAPIEHIASMRRNYFTSEVSHCRATEYIMKGVYINTALLNASCAAMDDF 480
A/WSN/1933_H1N1_      SWIELDEIGEDAAPIEHIASMRRNYFTAEVSHCRATEYIMKGVYINTALLNASCAAMDDF 480
                      **********.***************:********************************

A/lvPR8/34_H1N1_      QLIPMISKCRTKEGRRKTNLYGFIIKGRSHLRNDTDVVNFVSMEFSLTDPRLEPHKWEKY 540
A/hvPR8/34_H1N1_      QLIPMISKCRTKEGRRKTNLYGFIIKGRSHLRNDTDVVNFVSMEFSLTDPRLEPHKWEKY 540
A/WSN/1933_H1N1_      QLIPMISKCRTKEGRRKTNLYGFIIKGRSHLRNDTDVVNFVSMEFSLTDPRLEPHKWEKY 540
                      ************************************************************

A/lvPR8/34_H1N1_      CVLEIGDMLTRSAIGQVSRPMFLYVRTNGTSKIKMKWGMEMRRCLLQSLQQIESMIEAES 600
A/hvPR8/34_H1N1_      CVLEIGDMLLRSAIGQVSRPMFLYVRTNGTSKIKMKWGMEMRRCLLQSLQQIESMIEAES 600
A/WSN/1933_H1N1_      CVLEVGDMLLRSAIGHVSRPMFLYVRTNGTSKIKMKWGMEMRRCLLQSLQQIESMIEAES 600
                      ****:****:*****:******************************************

A/lvPR8/34_H1N1_      SVKEKDMTKEFFENKSETWPIGESPKGVEESSIGKVCRTLLAKSVFNSLYASPQLEGFSA 660
A/hvPR8/34_H1N1_      SVKEKDMTKEFFENKSETWPIGESPKGVEESSIGKVCRTLLAKSVFNSLYASPQLEGFSA 660
A/WSN/1933_H1N1_      SVKEKDMTKEFFENKSETWPVGESPKGVEEGSIGKVCRTLLAKSVFNSLYASPQLEGFSA 660
                      ******************:*********.****************************

A/lvPR8/34_H1N1_      ESRKLLLIVQALRDNLEPGTFDLGGLYEAIEECLINDPWVLLNASWFNSFLTHALS 716
A/hvPR8/34_H1N1_      ESRKLLLIVQALRDNLEPGTFDLGGLYEAIEECLINDPWVLLNASWFNSFLTHALS 716
A/WSN/1933_H1N1_      ESRKLLLIVQALRDNLEPGTFDLGGLYEAIEECLINDPWVLLNASWFNSFLTHALR 716
                      ******************************************************
```

Figure 4.4: Alignment of polymerase subunit PA. Two A/PR8/34 variants and A/WSN/33 were compared for their amino acid sequence of the polymerase subunit PA. The high virulent (hv) PR8 strain was shown to be more potent in the degradation of cellular polymerase than the low virulent (lv) PR8 variant. A/WSN/33 is known to degrade cellular polymerase. One amino acid (highlighted in the red box) differed between hvPR8 and lvPR8, but not between hvPR8 and A/WSN/33 and was therefore chosen for site-directed mutagenesis. The amino acid in light red shows the site that differed between hvPR8 and WSN and was therefore not chosen for site-directed mutagenesis.

4.3 Rescue and characterisation of the mutant viruses

Two viruses carrying individual mutations in segment 1 (PB2 $\rightarrow$ V504I) and 3 (PA $\rightarrow$ L550I) were engineered as well as a virus carrying both mutations. Virus rescues were done using the 12-plasmid rescue system, which is described in more detail in Section 2.2.2. Viruses were plaque purified and the nucleotide sequence of the appropriate segment was determined before they were used in further experiments. Viral replication was shown to be coupled to cellular transcription and the influence of the inserted mutations on this association was tested. As a first indicator for the efficiency of viral replication, plaque assays were performed and plaque sizes were measured and compared. Confluent MDCK cells were infected with serial dilutions of the three mutant viruses as well as the WT virus. Cells were covered with 1.2% Avicel-DMEM and incubated for three days. As shown in Figure 4.5, no differences were observed regarding plaque size.

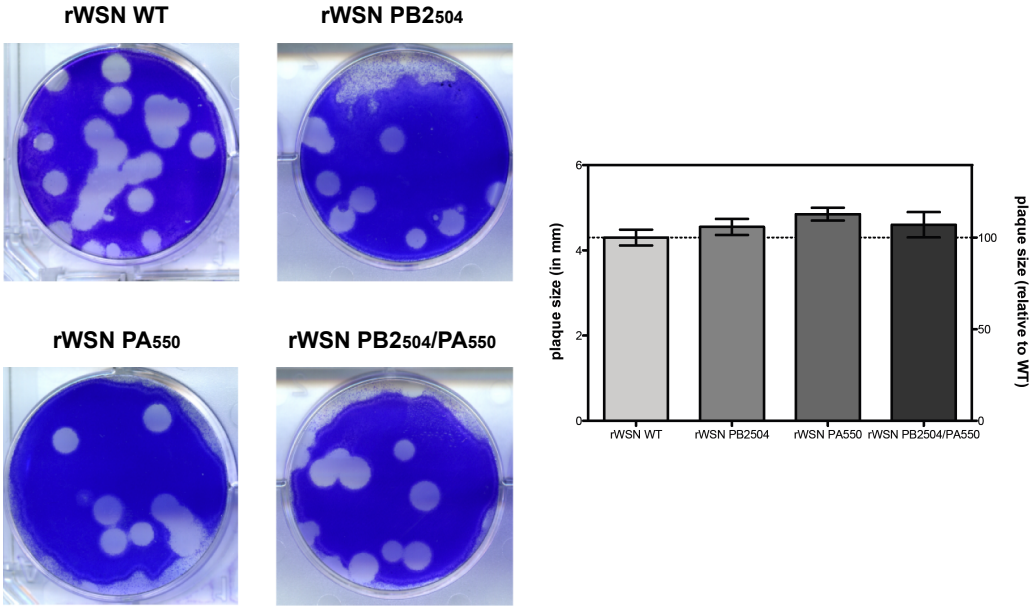

Figure 4.5: Plaque phenotype of the three polymerase II degradation mutants. Confluent MDCK cells were infected with serial dilutions of rWSN WT, rWSN $PB2_{504}$, rWSN PA_{550} or rWSN $PB2_{504}/PA_{550}$. Cells were covered with 1.2% Avicel-DMEM and incubated at 37 ℃ for three days. Cells were fixed with formaldehyde and stained for plaques using crystal violet. Mean values for $\sim$30 plaques/recombinant virus are plotted and error bars represent the SEM.

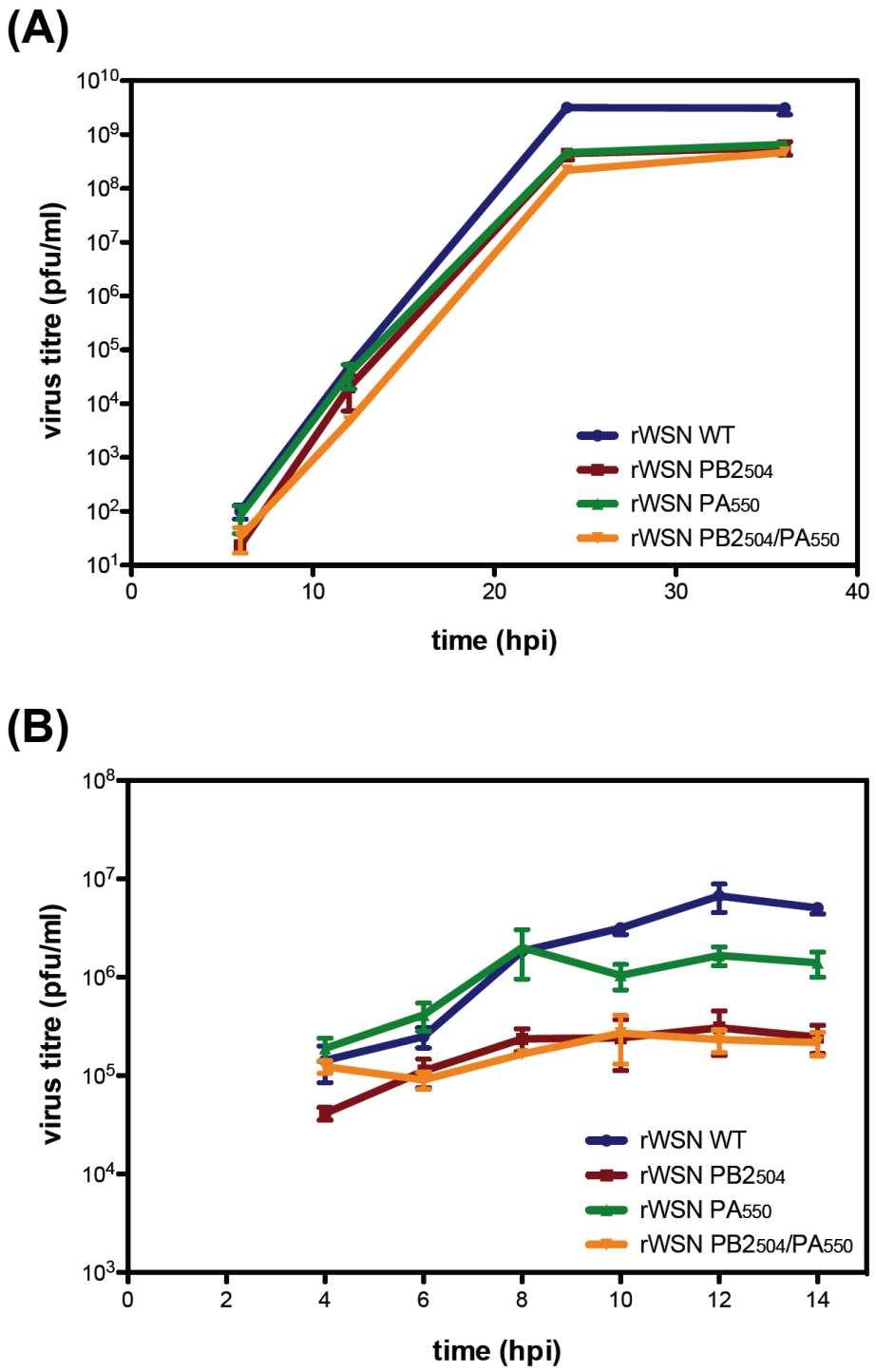

Figure 4.6: Growth of the three polymerase mutant viruses: Triplicate MDCK monolayers were infected with the recombinant WSN viruses WT, $PB2_{504}$, PA_{550} or $PB2_{504}/PA_{550}$ at an **(A)** MOI of 0.001 and **(B)** MOI 3. For multi-step growth conditions, media was supplemented with N-acetyl trypsin. Supernatants were harvested at the indicated time points post infection and virus titres were determined by plaque assay. Error bars represent the SEM of each set of triplicates.

To assess viral replication under multi-step and single-step growth conditions, confluent MDCK cells were infected with MOI of 0.001 or MOI of 3, respectively. At the indicated time points, supernatants were harvested and viral growth was determined by plaque assay. As can be seen in Figure 4.6, all three recombinant viruses were attenuated under both conditions. However, major differences were observed in the single-step growth curve (Figure 4.6 (B)). Viruses carrying the mutation in segment 1 (rWSN $PB2_{504}$ and rWSN $PB2_{504}/PA_{550}$) were markedly attenuated compared to WT virus. The virus with a single-point mutation in segment 3 showed an intermediate phenotype.

4.4 Degradation of cellular RNA polymerase II

To determine the influence of the two residues on the degradation of cellular RNAPII, confluent A549 cells were infected with the WSN viruses carrying single point mutations in segment 1 or 3, or with the double mutant, at an MOI of 3. At indicated time points, cells were lysed and the amount of cellular RNAPII was compared to that in WT infected cells (Figure 4.7 (A)). Accumulation of RNAPII was measured by chemiluminescence. As can be seen in Figure 4.7 (B), no difference was observed regarding the hypophosphorylated form of the cellular RNAPII, which decreased similarly in all virus-infected cells. The Ser2-P form detected by antibody H5 was not degraded (Figure 4.7 (C)). Virus growth was determined by measuring the synthesis of the viral protein NS1 and by measuring the viral titre. Although NS1 accumulated to similar levels in all virus infected cells (Figure 4.7 (D)), lower viral titres were observed in cells infected with viruses carrying a point mutation in PB2 and / or PA (Figure 4.7 (E)). However, this decrease was not due to a defect in the degradation of the cellular polymerase II.

Degradation of RNAPII was thought to have an influence on host cell protein shut off. The three mutant viruses carrying mutations in the polymerase subunits PB2 or PA were therefore analysed for their ability to shut off host cell protein synthesis. Confluent MDCK cells were infected with rWSN WT, rWSN $PB2_{504}$, rWSN PA_{550} or rWSN $PB2_{504}/PA_{550}$ at an MOI of 3 or mock infected. At the indicated time points, proteins were labelled with [^{35}S] methionine (Figure 4.8). All viruses produced efficient levels of viral proteins and host cell protein synthesis was shut-off by all mutant viruses to a similar degree compared to WT virus (Figure 4.8(A and B)).

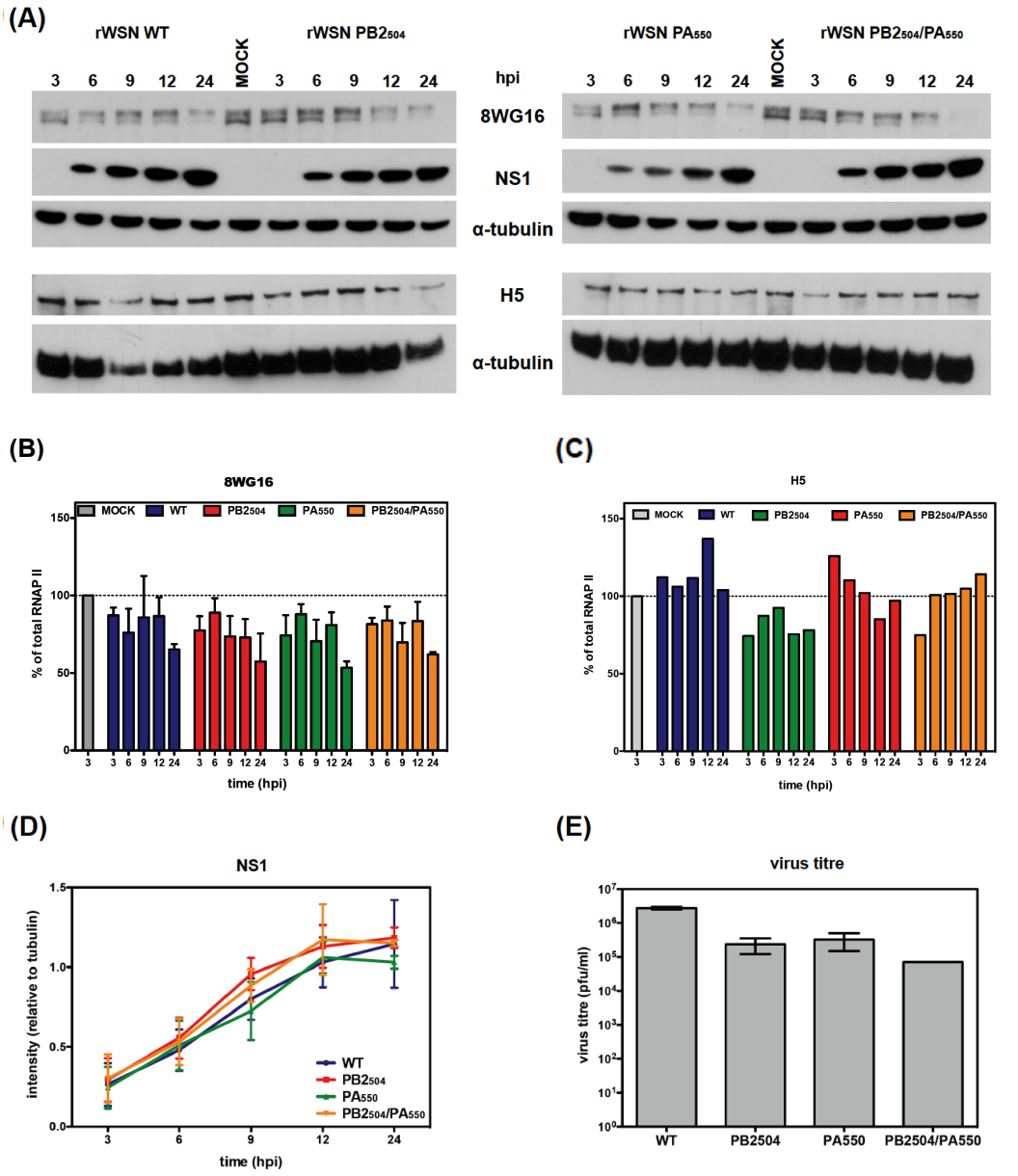

Figure 4.7: Degradation of cellular polymerase II . Confluent monolayers of A549 cells were infected with rWSN WT, rWSN $PB2_{504}$, rWSN PA_{550} or rWSN $PB2_{504}/PA_{550}$ at an MOI of 3 or Mock infected and cells were lysed at the indicated time points. **(A)** 8% Bis-Tris gels were used to detect the cellular polymerase using the antibodies 8WG16 and H5. 4 - 12% gradient Bis-Tris gels were used to detect NS1. α-tubulin was used as an internal loading control. **(B)** Analysis of the accumulation of the hypophosphorylated form of the cellular RNAPII. Mean values of three independent experiments are plotted. Error bars represent the SEM. **(C)** Analysis of the accumulation of the Ser2-P form of the cellular RNAPII. **(D)** Analysis of the accumulation of NS1. Mean values of three independent experiments are plotted and error bars represent the SEM. **(E)** At 24 hpi, supernatants were harvested and viral titres were determined by plaque assay.

Synthesis of the viral proteins was determined by measuring the accumulation of NP and NS1/M1. The latter two proteins did not separate efficiently on a 4-12% Gradient Bis-Tris gel to measure them individually. When viral protein synthesis was quantified, slight differences were observed. Early in infection, NS1/M1 and NP were produced to similar levels or even at higher levels in cells infected with the polymerase mutant viruses. However, later in infection *de novo* synthesis seemed to drop, and less viral proteins were made, which could explain the attenuation seen in viral growth (Figure 4.8 (C and D)).

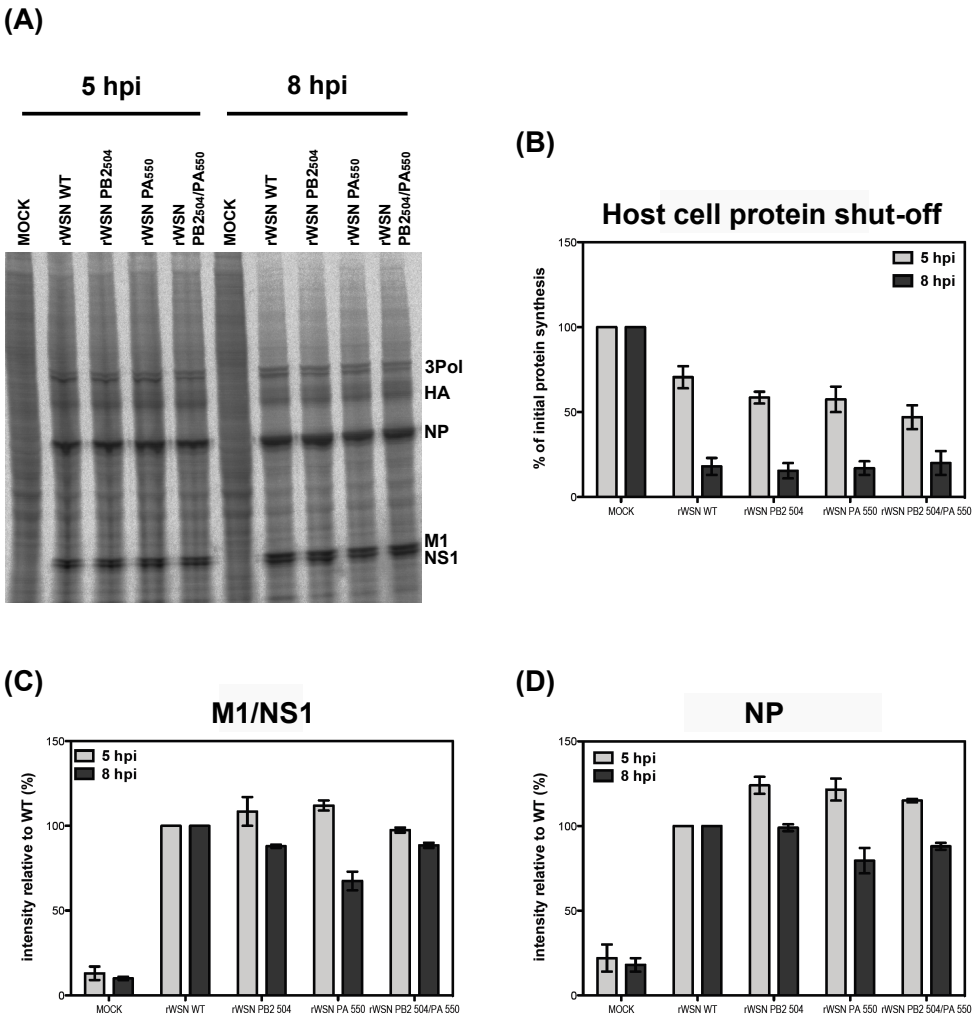

Figure 4.8: Host cell protein shut-off and *de novo* synthesis of viral proteins by polymerases mutant viruses: MDCK cells were infected with the panel of viruses at an MOI of 3. Proteins were labelled with [^{35}S] methionine. **(A)** Cells were lysed at 5 or 8 hpi and proteins were separated using a 4-12% gradient Bis-Tris gel. **(B)** Host cell protein shut-off was quantified. **(C and D)** *De novo* synthesis of viral proteins M1/NS1 and NP were quantified.

4.5 Discussion

The aim of this work was the identification of amino acids in viral polymerase proteins that are critical for the degradation of cellular RNA polymerase II. Previous work showed that two variants of the influenza A virus strain PR8 differed in their ability to induce degradation of the CTD of RNAPII. Segment 1 and 3 gene products were identified to be involved in the process (Rodriguez et al., 2009). Two amino acids were determined by sequence alignments that differed between WSN and lvPR8 but were identical between WSN and hvPR8 (Figure 4.3, 4.4). These two sites were changed by site-directed mutagenesis and three mutant viruses were rescued: two viruses with a single point mutation either in segment 1 or 3 and one double mutant virus. Although the mutant viruses showed defects in viral growth (Figure 4.6), they did not show major differences in the degradation of the cellular RNA polymerase II (Figure 4.7) or in shutting off host cell protein synthesis (Figure 4.8). However, *de novo* synthesis of viral proteins was impaired later in infection.

The degradation of the cellular RNA polymerase II was in the center of several recent studies. However, findings varied regarding the phosphorylation state that was targeted for degradation (Rodriguez et al., 2007; Vreede et al., 2009). Whereas Rodriguez et al. only found that the hypophosphorylated CTD was degraded, Vreede et al. also observed a decrease of the phosphorylated forms of the RNAPII. However, this latter finding was only seen in virus infected cells, but was absent in cells transfected with plasmids that expressed the viral polymerase subunits. This strongly suggests the involvement of other viral proteins in the process. A recent report described an interaction between the viral RdRp and the cyclin T1/CDK9 (Zhang et al., 2010a). Cyclin T1/CDK9 is a kinase responsible for the phosphorylation of Serine 2-residues in the CTD and it was shown to serve as an adaptor between the RdRp and the cellular RNAPII. If and to what extent this interaction is involved in degradation of the phosphorylated form of RNAPII is not known. The authors only reported degradation of the non-phosphorylated RNAPII. If binding of the RdRp to the CTD in its non-phosphorylated or Ser5-P forms is mediated directly, or via an adaptor protein, could not be answered by their study (Zhang et al., 2010a).

Here, I only observed degradation of the hypophoshorylated form of the CTD as shown by Rodriguez et al. and Zhang et al. (Rodriguez et al.,

2007; Zhang et al., 2010a). It can be excluded that the differences seen by Vreede et al. were due to virus strain specificities as all the mentioned studies analysed A/WSN/33 (Rodriguez et al., 2007; Vreede et al., 2009; Zhang et al., 2010a). However, the cause of the variations remain unknown. The observation that the RdRp binds to the hyperphosphorylated CTD, but degrades the non-phosphorylated RNAPII, needs further investigations to understand the process in more detail.

A study by Rolling et al. demonstrated that the amino acids 504 in PB2 and 550 in PA contribute to viral polymerase activity in A/PR/8/34 (Rolling et al., 2009). Isoleucine→valine ($PB2_{504}$) and isoleucine→leucine (PA_{550}) increased polymerase activity, and led to enhanced virulence in mice. Similarly, when changing the two residues in WSN to residues that are present in the lvPR8 variant, the virus was less efficient in replication as seen by the reduced viral titres. However, degradation of cellular RNA polymerase II was not affected. Previously other sites in the viral polymerase subunits were identified to contribute to the RNAPII degradation. One residue within the polymerase subunit PA (T157A) was reported to delay polymerase II degradation (Rodriguez et al., 2007). This particular amino acid is identical in WSN, hvPR8 and lvPR8 and was therefore not chosen in this experiment (Figure 4.4). However, it makes it likely that additional residues are involved in the process of degradation and a combination of several amino acids may be important. Therefore changing one or two residues in A/WSN/33 might not have the desired effect and further studies are needed to understand the mechanism and to identify amino acids that are involved.

Degradation of cellular RNAPII is believed to add to the observed host cell protein shut-off. This is a very powerful but also rigorous way for the virus to prevent antiviral responses. Influenza A viruses have developed a number of strategies that act in combination. Beside degrading cellular RNA polymerase II, the non-structural protein NS1 in particular was found to interfere with the expression of host cell proteins. For instance, the protein was shown to interact with CPSF30, which leads to a general inhibition of 3' end processing of cellular pre-mRNA (Nemeroff et al., 1998). Also, NS1 is involved in inhibition of the nuclear export of cellular mRNA (Fortes et al., 1994). Because several mechanisms add to host cell shut-off, small differences may be difficult to observe as they would be covered by other strategies. One possible way to look at slight differences in host protein

shut-off induced by degradation of RNAPII would, therefore, be the use of an NS1 free system that could be realised by the use of an NS1-deletion virus.

Taken together, the changes in viral replication observed by the described recombinant viruses with mutations in PB2 and PA are likely due to an altered polymerase activity rather than the loss of the ability to degrade the cellular RNAPII. This attenuation may be caused by altered affinities of the viral polymerase complex for cellular or viral interaction partners, which led to the observed decrease in viral growth. The identification of amino acids involved in the degradation of the RNAPII is likely to be more complex. The process of degradation combines the requirement of correct trimerisation of the viral polymerase subunits and binding to the CTD either directly or via adaptor proteins which may be even different depending on the phosphorylation state of the CTD.

4.6 Summary Chapter 4

Three viruses carrying changes in segment 1 and 3 were engineered (summarised in Table 4.3). The viruses with a single-point mutation and the virus with a double mutation were analysed for their ability to degrade the cellular RNAPII and to induce host cell protein shut-off.

Virus	**Mutation**	**Degradation of RNAPII**	**Phenotype**
rWSN $PB2_{504}$	V504I	+	reduced levels of viral proteins growth attenuation
rWSN PA_{550}	L550I	+	reduced levels of viral proteins growth attenuation
rWSN $PB2_{504}/PA_{550}$	PB2: V504I PA: L550I	+	reduced levels of viral proteins growth attenuation

Table 4.3: Summary chapter 4: Mutations that were introduced into segment 1 and 3 to identify residues involved in the cellular polymerase II degradation.

The tested amino acid changes caused a growth attenuation and the levels of *de novo* synthesised proteins were changed. However, this attenuation was not due to a defect in the ability to degrade the hypophosphorylated form of the CTD.

Chapter 5

GENERATION OF VIRUSES EXPRESSING PB1-F2 AS A SEPARATE ORF

Aims of Chapter 5

In order to freely study PB1-F2, it was planned to separate the PB1-F2 ORF from the PB1 ORF. This would allow the introduction of mutations and deletions, without affecting the polymerase subunit PB1. Several strategies were designed and tested for their expression of PB1-F2.
Insertion into segment 2 was done by three different strategies: the use of an overlapping Stop-Start codon, the use of the self-cleaving 2A peptide and the insertion of an internal viral promoter. Insertion into segment 6 and 7 was only done using the internal viral promoter.
It should be noted that the existence of N40 was not known when PB1-F2 was first separated from its original ORF and expressed in segment 2 as an individual gene.

5.1 Introduction

Insertion of foreign epitopes or even foreign genes into a viral genome has become a powerful strategy to study virus replication in general, as well as to design vaccines and therapeutics. Genome manipulation technologies and reverse genetic systems are now available for many DNA and RNA viruses (for a general overview see Section 1.3). A favoured method is the engineering of a bicistronic gene and the rescue of infectious viruses expressing the gene of interest. Often viral translation strategies are exploited to secure the expression of the foreign gene. These strategies include internal ribosomal entry sites (IRES), internal promoters, short self-cleaving peptides or overlapping Stop-Start sequences (García-Sastre et al., 1994; Flick and Hobom, 1999b; Machado et al., 2003; Percy et al., 1994; Kittel et al., 2005).

For the present study, three of these strategies were used in order to introduce PB1-F2 into the viral genome as an individual gene. The separation of the two ORFs was necessary to allow the study of PB1-F2 in more detail, as insertion of mutations would be restricted in the original sequence context. Every point mutation would have to be carefully chosen in order not to change the PB1 amino acid sequence. Therefore, the PB1 and PB1-F2 coding sequences were separated. First, segment 2 was chosen for the insertion. It was hypothesised that expression of the two genes from the same segment would be closer to the natural infection situation as PB1 and PB1-F2 are both originally translated from segment 2. In addition, PB1 and PB1-F2 have been shown to interact (Mazur et al., 2008) and therefore expression at the same time and place within the cell may be important. However, it is not known if, and to what extent, this is essential. Three strategies were used for the insertion of PB1-F2 downstream of PB1: (1) via an internal promoter; (2) by using the short self-cleaving 2A peptide derived from foot-and-mouth disease virus; and (3) by introducing an overlapping **UAA**UG Stop-Start codon.
It was published before that insertion of a foreign gene into segment 6 using an internal promoter was successful and the expression of the foreign gene was stable over several passages. Therefore this strategy was also chosen (Machado et al., 2003, 2006). All the mentioned strategies and the cloning of the bicistronic segments are explained in more detail in the sections below.

5.2 Strategies to express PB1-F2 separately in segment 2

5.2.1 Inserting PB1-F2 via an overlapping Stop-Start codon

Viruses have developed a number of strategies to initiate translation from one messenger RNA. One of these strategies is termination-reinitiation by an overlapping Stop-Start codon. The stop codon is in close proximity to the downstream or even upstream start codon and this can lead to a coupled termination-reinitiation process. It is known that this process also controls the amount of the downstream product as the second ORF is translated at low frequency (5-10%) (Child et al., 1999). In eukaryotic systems, upstream ORFs are short ($<$13 codons) and they do not code for a full length protein. However, they may downregulate the expression level of the second protein (Kozak, 2001). Termination-reinitiation in viruses is different as the upstream ORF can be much longer, often encoding a full-length functional protein. This was first described for influenza B virus segment 7 (Horvath et al., 1990). A pentanucleotide sequence **UAA**UG regulates the translation of the matrix protein 1 (M1) and the ion channel protein BM2. The overlapping Stop-Start strategy was later also described for several other virus families including *Caliciviridae* and *Paramyxoviridae* (Figure 5.1) (Meyers, 2003, 2007; Ahmadian et al., 2000; Gould and Easton, 2005). The positions of the stop and start codons vary in different viruses.

The insertion of a foreign gene into influenza A virus segment 8 using the overlapping Stop-Start mechanism was previously shown to be successful (Kittel et al., 2005). GFP or the human interleukin gene IL-2 were inserted downstream of NS1. The virus was shown to be stable over at least 5 passages in its ability to express the foreign gene and was therefore chosen as one strategy. A bicistronic segment 2 was engineered carrying the **UAA**UG Stop-Start pentanucleotide between PB1 and PB1-F2. First, PB1-F2 expression in its original position was deleted by inserting three point mutations as described in Section 3.2.1. This construct was used as a template for inserting the PB1-F2 ORF downstream of PB1. Two subsequent PCR reactions were performed to add the overlapping Stop-Start pentanucleotide upstream of PB1-F2 as well as inserting 40 nt of the 5'end of PB1 downstream of PB1-F2 (Figure 5.2). This was shown to

a) ***Caliciviridae - Lagovirus and Vesivirus***

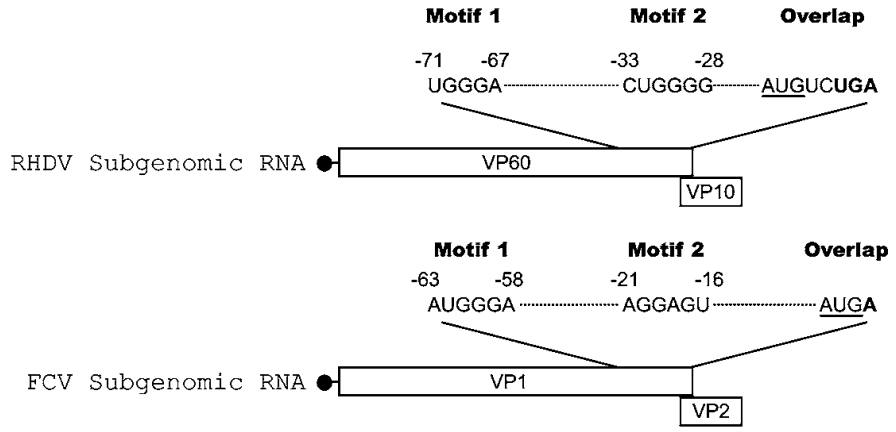

b) ***Orthomyxoviridae - Influenzavirus B***

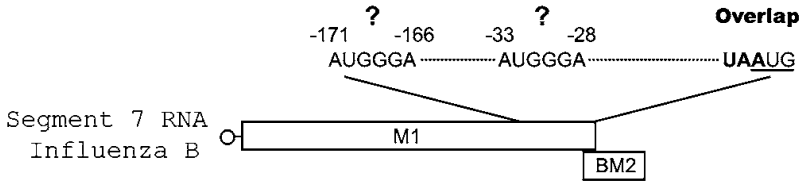

c) ***Paramyxoviridae - Pneumovirus (RSV, PVM) and Metapneumovirus (APV)***

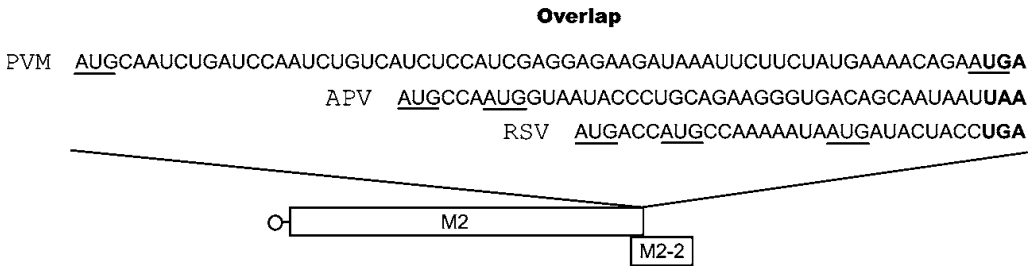

Figure 5.1: Termination-reinitiation strategies: Overlaps showing the Stop-Start cassette. They vary between the different viruses. Upstream motifs have been shown to be important for the reinitiation event. Taken from (Powell et al., 2008b).

be important for efficient packaging of the segment into viral particles (Liang et al., 2005). Oligo sv34 containing the **UAA**UG pentamer sequence and the two reverse oligos sv28 and sv40 including 40 nt of the PB1-sequence were used for the PCR reactions. *Nsi*I was chosen as restriction enzyme and sites were included in the newly created PB1-F2 construct. This site was also introduced into pHH-$\triangle$ATG by site-directed mutagenesis using oligo primers sv32 and sv33 (Figure 5.2 PCR 1-3). All primer sequences are listed in Table 2.10. PCRs were done using the KOD hot start polymerase. Following restriction enzyme digestion with *Nsi*I, the StSt-PB1-F2 construct and pHH-$\triangle$ATG were fused. The *Nsi*I site between PB1 and PB1-F2 was removed from the plasmid in a final PCR reaction (Figure 5.2). The obtained plasmid was termed pHH-$\triangle$ATG-StSt-F2. After amplification in *E.coli*, plasmids were screened by restriction enzyme digestion and promising plasmids were sequenced to ensure correct insertion of the insert into pHH-$\triangle$ATG.

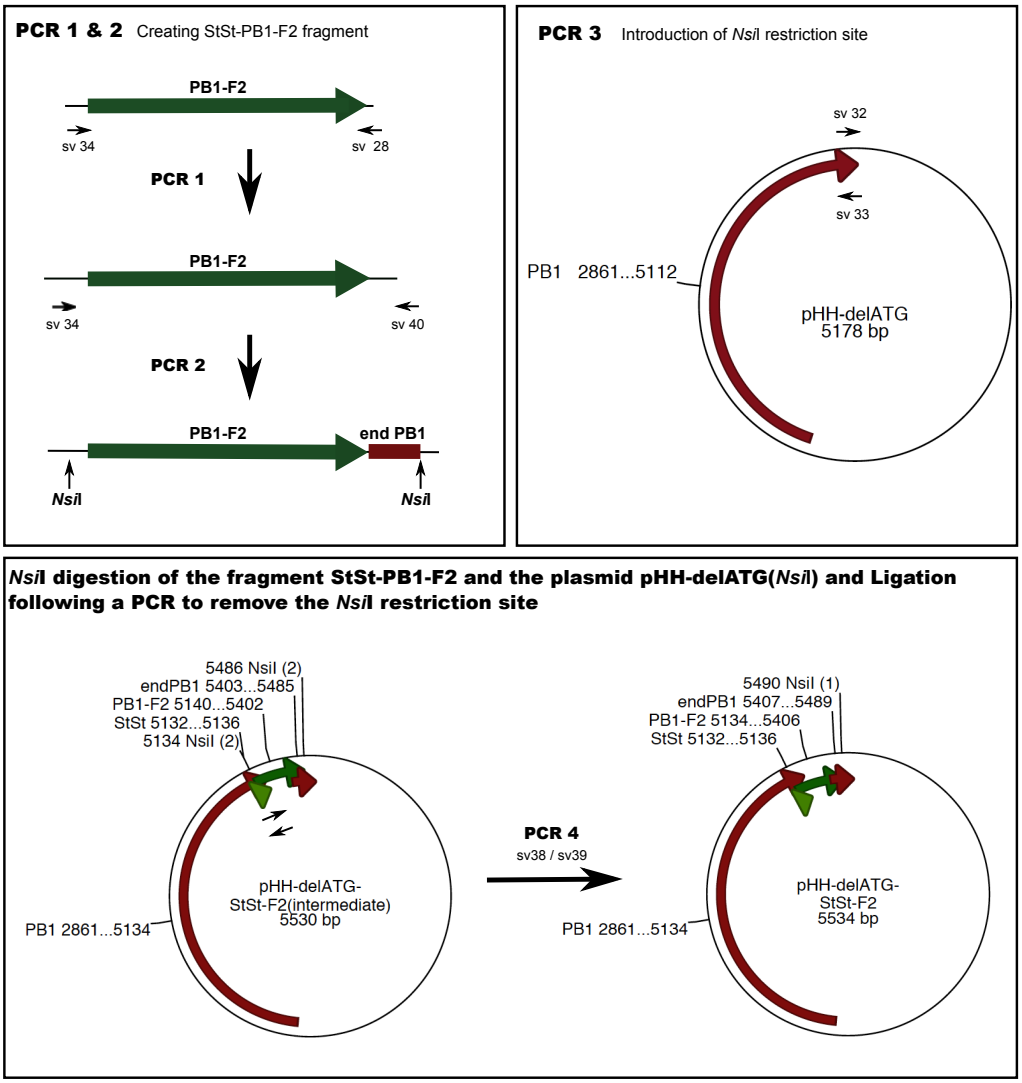

Figure 5.2: Schematic overview of the cloning of pHH-ΔATG-StSt-PB1-F2: Two separate PCRs (PCR 1 and 2) were performed to create the fragment StSt-PB1-F2. This fragment has an *Nsi*I restriction site near both ends. Downstream of PB1-F2, 40 nt of the PB1 gene were inserted to ensure correct packaging of the modified segment into viral particles. To prepare the plasmid pHH-ΔATG for inserting the StSt-PB1-F2 fragment, an *Nsi*I restriction site was created via site directed mutagenesis PCR (PCR 3). *Nsi*I digestion of pHH-ΔATG(*Nsi*I) and the fragment StSt-PB1-F2 following ligation led to the plasmid pHH-ΔATG-StSt-F2. Removal of the *Nsi*I sites via site directed mutagenesis changed the second codon of PB1-F2 back into the original sequence (PCR 4). The developed final plasmid pHH-ΔATG-StSt-F2 was used to rescue viruses carrying PB1-F2 on segment 2 as an individual gene.

5.2.2 The usage of the short self-cleaving 2A peptide

The self-cleaving 2A peptide derives from the foot-and-mouth disease virus (Ryan et al., 1991). This (+) sense RNA virus belongs to the *Picornaviridae* family and the genome serves as an mRNA in infected cells. After, but also during translation, the polyprotein is cleaved into individual proteins by viral proteases. One of these 'proteases' is the short 2A sequence (Ryan et al., 1991). Cleavage occurs at the C-terminus of 2A between a glycine and a proline residue, by a process described as ribosomal skipping (Donnelly et al., 2001). It was shown that 2A can be used to cleave the artificial polyprotein CAT-2A-GUS (Ryan and Drew, 1994). Percy et al. adapted this strategy and used it to express CAT from segment 6 in influenza A viruses (Percy et al., 1994). Whereas this strategy was successful and viruses were stable when passaged in MDCK cells, an attempt to insert GFP downstream of a truncated NS1 gene using the 2A peptide was not (Lu et al., 2004). Recently, a new attempt was made to insert GFP into the viral genome by introducing the gene into segment 6 upstream or downstream of NA (Li et al., 2010). The 2A autocleavage sequence was inserted between NA and GFP. Addition of the N-terminus including the transmembrane domain of NA fused to GFP made it possible to incorporate GFP into viral particle, which may be a useful tool to study antiviral therapeutics.

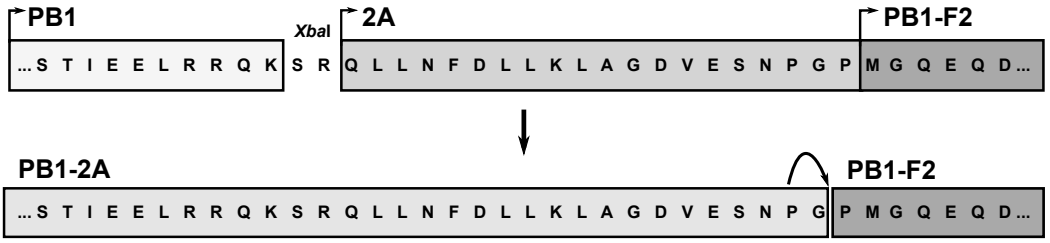

Figure 5.3: Sequence of the FMDV self-cleaving 2A peptide: PB1-F2 was fused to PB1 via a FMDV self-cleaving 2A peptide. A *Xba*I restriction enzyme site was introduced downstream of PB1 to insert the 2A-PB1F2 construct. 2A cleavage occurs at its own C-terminus between a glycine and a proline. As a consequence, PB1 has a C-terminal extension of 21 aa after cleavage and PB1-F2 carries a proline at its N-terminus.

Here, I used the FMDV 2A sequence to express PB1-F2 from segment 2 as an individual ORF (Figure 5.3). PB1 and PB1-F2 were fused together via 2A, creating one single ORF; 22 amino acids were inserted in total. This

also included an *Xba*I restriction enzyme site between PB1 and 2A. During translation, 2A is thought to cleave at its own C-terminus between a glycine and proline residue. As a consequence, the released PB1 protein has an addition of 21 amino acids at its C-terminus, and PB1-F2 carries a proline at its N-terminus (Figure 5.3).

Cloning was done in several steps as summarised in Figure 5.4. PB1-F2 was amplified in two PCR reactions, in which the 2A sequence was added upstream of PB1-F2 and 40 nt of the 5'end of PB1 were added downstream of PB1-F2. This was shown to be necessary for efficient packaging of the segment into viral particles (Liang et al., 2005). *Xba*I restriction enzyme sites were used to insert the 2A-PB1-F2 construct into pHH-$\triangle$ATG. To do this, an *Xba*I restriction enzyme site was introduced into the plasmid by site directed mutagenesis PCR (PCR 3). Thereby, the stop codon was removed from PB1 to create one long open reading frame that which will be "cleaved" by the 2A peptide during translation. Following ligation of 2A-PB1-F2 and pHH-$\triangle$ATG, the obtained plasmid was further amplified in *E. coli*. All PCRs were done using a KOD hot start polymerase according to the protocol described in Section 2.4.2. A list of all primer sequences can be found in Table 2.10. The plasmid obtained was named pHH-$\triangle$ATG-2A-F2 and sequenced to ensure to correct insertion of the fragment 2A-PB1-F2.

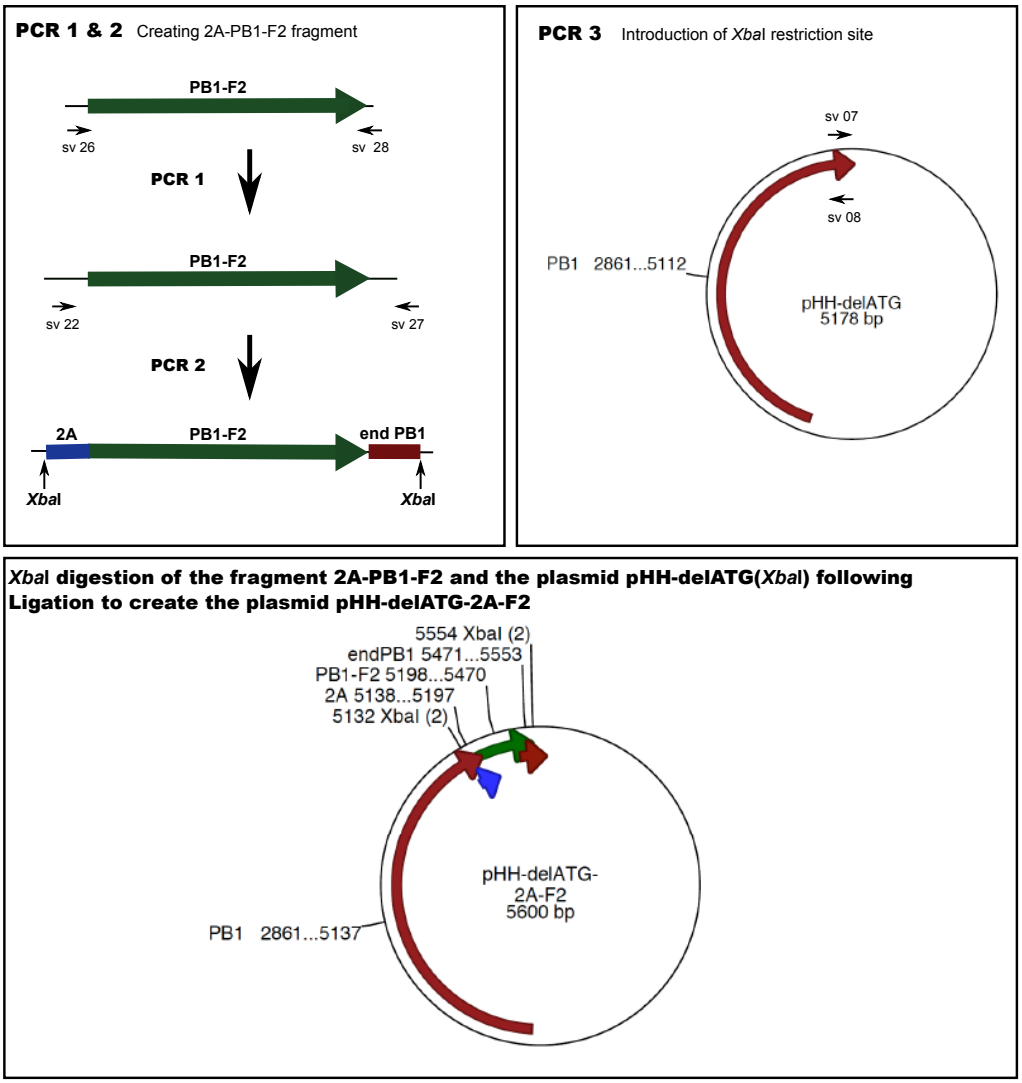

Figure 5.4: Schematic overview of the cloning of pHH-ΔATG-2A-F2: Two seperate PCRs (PCR 1 and 2) were performed to create the fragment 2A-PB1-F2. This fragment has *Xba*I restriction enzyme sites near both ends. Downstream of PB1-F2, 40 nt of the PB1 gene were inserted in order to ensure correct packaging of the segment into viral particles. To prepare the plasmid for inserting the 2A-PB1-F2 fragment, an *Xba*I restriction site was created via site directed mutagenesis PCR (PCR 3). This PCR also removed the stop codon of PB1. *Xba*I digestion of the plasmid pHH-ΔATG(*Xba*I) and the fragment 2A-PB1-F2 following ligation led to the final plasmid pHH-ΔATG-2A-F2 which was used to rescue viruses carrying PB1-F2 on segment 2 as an individual ORF.

5.2.3 Use of an internal promoter

The demonstration that internal promoters are functional allowed a new strategy for engineering bicistronic segments (Flick and Hobom, 1999b). The 3' and 5' UTRs of each segment are highly conserved and serve as viral promoters for vRNA, cRNA and mRNA synthesis. They interact with each other to form a panhandle or corkscrew structure which is necessary for transcription and replication of the viral genome (Hsu et al., 1987; Flick et al., 1996). The insertion of a duplicated 3'UTR between two foreign genes showed that both 3'UTRs can interact with the 5'UTR (Flick and Hobom, 1999b). This approach was used by Machado et al. to insert foreign genes into segment 6 of A/WSN/33 (Machado et al., 2003). The insertion of CAT was shown to be stable upon several passages. However, viral growth and plaque size were restricted. An optimised strategy was published in 2006, where 42 nt of the native neuraminidase ORF were added to the 5'UTR. This helped efficient replication and packaging of the bicistronic segment (Machado et al., 2006).

PB1-F2 with a 3'UTR upstream and 40 nt of the PB1-end coding sequence was synthesised by the company GenScript. *Xba*I restriction enzyme sites flanked the construct. This site was chosen to insert the PB1-F2 fragment into the plasmid pHH-$\triangle$ATG. Before fusion of PB1-F2 and pHH-$\triangle$ATG was possible, an *Xba*I restriction enzyme site also had to be inserted into the plasmid pHH-$\triangle$ATG by site directed mutagenesis PCR (Figure 5.5 PCR 1). Following ligation, the *Xba*I site between PB1 and the internal promoter was removed by site-directed mutagenesis PCR (Figure 5.5). All primer sequences are listed in Table 2.10. PCR reactions were done using the KOD hot start polymerase (see Section 2.4.2). The plasmid obtained was sequenced and named pHH-$\triangle$ATG-3'UTR-F2.

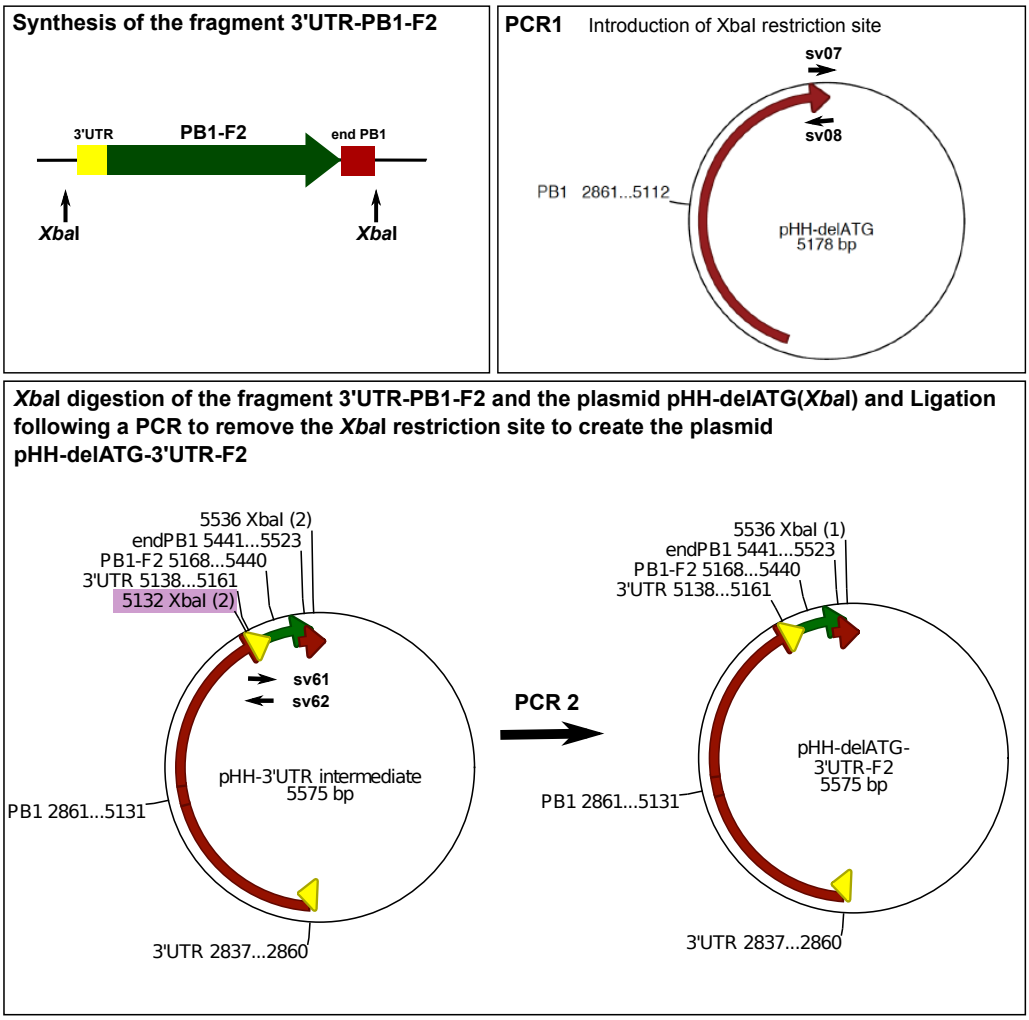

Figure 5.5: Schematic overview of the cloning of pHH-ΔATG-3'UTR-F2: The fragment 3'UTR-PB1-F2 was synthesised by the company GenScript. Beside *Xba*I restriction sites on both ends, the fragment also holds 40 nt of the 5'end of the PB1 gene downstream of the PB1-F2 ORF for packaging of the segment into virus particles. To insert the fragment into pHH-ΔATG, an *Xba*I restriction enzyme site was introduced via site directed mutagenesis PCR (PCR 1). After *Xba*I digestion of the plasmid pHH-ΔATG(*Xba*I) and the fragment, both were combined to create the plasmid pHH-ΔATG-3'UTR-F2. The *Xba*I site was removed from the intermediate plasmid in a subsequent PCR by site directed mutagenesis (PCR 2).

5.3 Rescue and characterisation of viruses carrying PB1-F2 as an independent ORF in segment 2

5.3.1 Rescue of viruses with a bicistronic segment 2

Virus rescues were done as before using the 12-plasmid rescue system (see Section 2.2.2 and 3.3.1). The plasmid encoding WT segment 2 (pHH-PB1) was individually exchanged with either of the plasmids containing PB1-F2 in a separate ORF (pHH-$\triangle$ATG-StSt-F2; pHH-$\triangle$ATG-2A-F2; pHH-$\triangle$ATG-3'UTR-F2). Rescue supernatants were used for plaque assay and single plaques were picked to grow up viral stocks.
Viruses with an overlapping Stop-Start cassette and the self-cleaving 2A peptide were successfully rescued. However, the rescues using pHH-$\triangle$ATG-3'UTR-F2 did not show any CPE after several days and no plaques were observed following plaque assay. Therefore, only rWSN $\triangle$AUG-StSt-F2 and rWSN $\triangle$AUG-2A-F2 were available for further characterisation. To ensure the correctness of the viral stocks, MDCK cells were infected at an MOI of 3 and RNA was isolated and used in an RT-PCR reaction in order to sequence the obtained PCR product. Two parts of segment 2 were amplified and sequenced: (1) the original PB1-F2 location to ensure the inserted mutations to delete PB1-F2 were still in place, and (2) the junction of PB1 and PB1-F2.

5.3.2 Characterisation of viruses with a bicistronic segment 2

Expression of both proteins from the biscistronic segment was determined by western blot analysis. MDCK cells were infected with the different viruses at an MOI of 3 and at 8 hpi, cells were lysed and proteins were separated by SDS-PAGE. As can be seen in Figure 5.6(A), viral proteins NS1 and PB1 are expressed in all infected cells to similar quantities. As expected, N40 was overexpressed in cells infected with the bicistronic segment 2 viruses, as they carry a deletion of the start codon to abolish PB1-F2 in the original ORF ($\triangle$AUG). This mutation caused an up-regulation of N40 as shown in Chapter 3. It was also tested if PB1-F2 can be expressed from the additional ORF (Figure 5.6(B)). Unfortunately only WT infected cells showed expression of

PB1-F2. However, it is possible that the level of expressed PB1-F2 from the individual ORF was low and therefore below the detection limit.

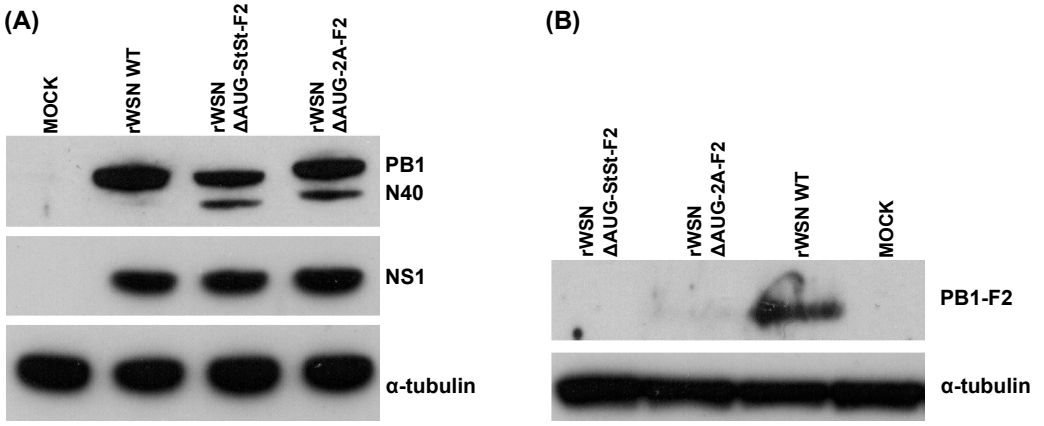

Figure 5.6: Western blot analysis of viruses with a bicistronic segment 2: MDCK cells were infected with a panel of recombinant viruses and viral protein expression was determined 8 hpi. **(A)** 4 - 12% Bis-Tris gradient Bis-Tris gels were used to detect PB1, N40 and NS1. **(B)** 16% Tricine-SDS-PAGE was used to detect PB1-F2. α-tubulin was used as an internal loading control.

Monolayers of MDCK cells were infected with serial dilutions of the virus and 1 or 3 dpi tested for their ability to form plaques (Figure 5.7). All viruses were capable of inducing CPE in immuno-competent cells. However, striking differences were observed regarding plaque size. Recombinant viruses with an overlapping Stop-Start cassette were $\sim$ 22% smaller on day 3 compared to WT plaques. rWSN $\triangle$AUG-2A-F2 viruses showed a reduction of 40% in plaque size. The differences between WT and mutant virus plaque size were significant, when analysed by *Student's t-test* (* $P<0.05$; *** $P<0.001$).

To further investigate the characteristics of the recombinant viruses carrying PB1-F2 as an individual ORF in segment 2, the growth properties were analysed. MDCK cells were infected with the different viruses at either low or high MOI (0.001 or 3, respectively) for multi-step or single-step growth curve. At indicated time points, supernatants were harvested and viral growth was measured by plaque assay. As can be seen in Figure 5.8, viruses with an extended genome length grew to lower titres under both conditions. In agreement with plaque sizes, rWSN $\triangle$AUG-StSt-F2 was less attenuated than rWSN $\triangle$AUG-2A-F2. Viruses with the self-cleaving 2A peptide grew more slowly especially early in infection.

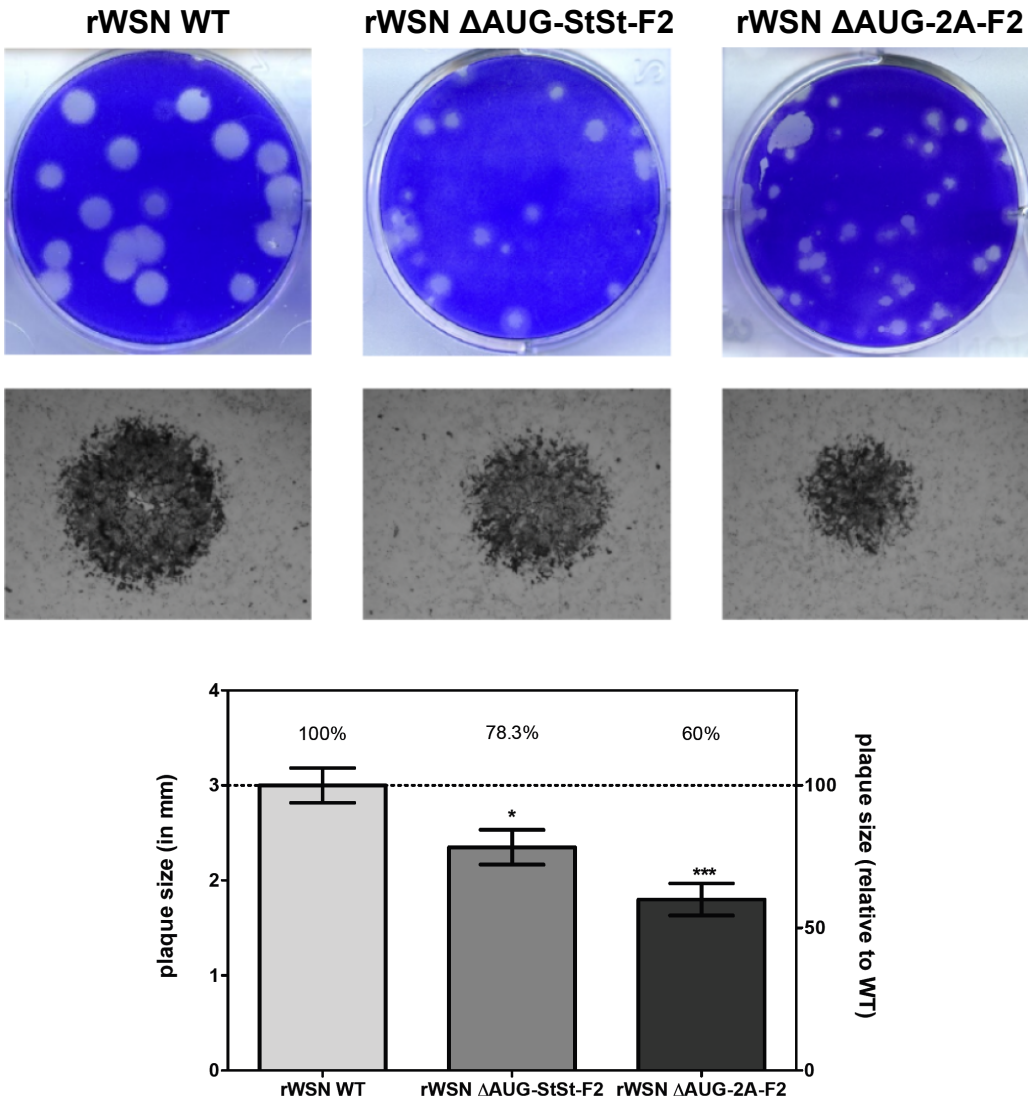

Figure 5.7: Plaque Assay of viruses with a bicistronic segment 2: Confluent monolayers of MDCK cells were infected with recombinant viruses. Cells were overlayed with 1.2% Avicel-DMEM and incubated for 3 days (top panel) or 24 h (bottom panel) at 37℃ . Mean values for ∼30 plaques/recombinant virus (3 dpi) are plotted and error bars represent the SEM. Differences in plaque sizes are significant between rWSN WT and rWSN ΔAUG-StSt-F2 or rWSN ΔAUG-2A-F2 virus (*Student's t-test*: * $P<0.05$; *** $P<0.001$).

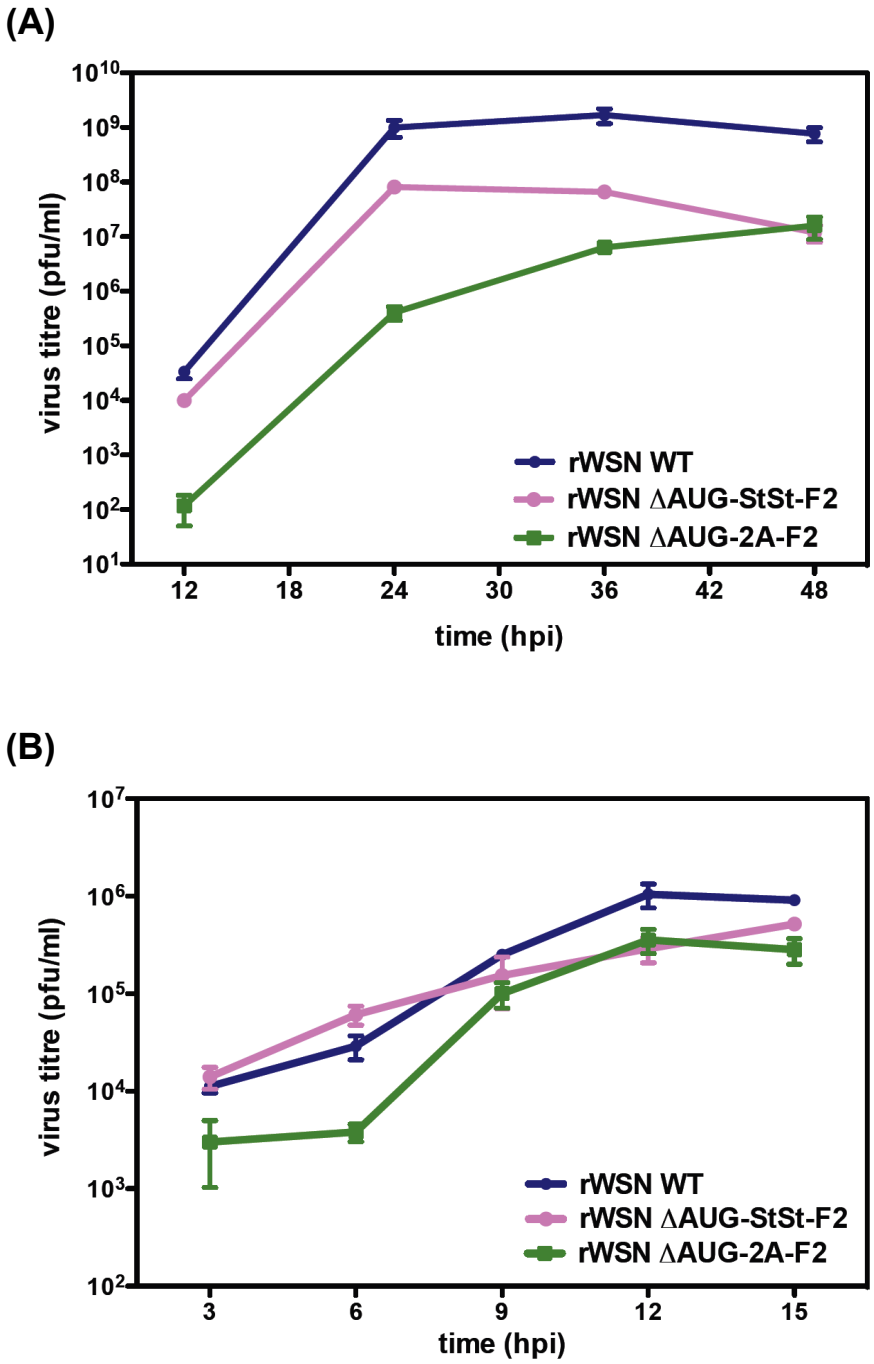

Figure 5.8: Growth of viruses with a bicistronic segment 2: Triplicate MDCK monolayers were infected with the recombinant WSN viruses WT, ΔAUG-StSt-F2 and ΔAUG-2A-F2 at an **(A)** MOI of 0.001 for multi-step growth curve and **(B)** MOI 3 for single-step growth curve. For multi-step growth curve, media was supplemented with N-acetyl trypsin. Supernatants were harvested at the indicated time points post infection and virus titres were determined by plaque assay. Error bars represent the SEM of each set of triplicates.

One reported function of PB1-F2 was the induction of apoptosis specifically in immune cells. As shown in Chapter 3 (Figure 3.12), recombinant viruses lacking the PB1-F2 ORF (△AUG) were attenuated in their ability to reduce cell viability in a mouse macrophage cell line (RAW/W). Although no expression of PB1-F2 was detected by western blotting, an attempt was made to test if the reinsertion of PB1-F2 into the viral genome had any effect. Monolayers of MDCK cells and RAW/W cells in 96 well plates were infected with the recombinant viruses at an MOI of 30 and cell viability was measured 8 h later using a commercially available assay. As shown in Figure 5.9, MDCK cells show a similar reduction in cell viability for all viruses. These cells were not targeted for apoptosis by PB1-F2. A different pattern was observed for infected RAW/W cells. rWSN WT viruses reduced cell viability, but no difference was observed between rWSN △AUG, rWSN △AUG-StSt-F2 and rWSN △AUG-2A-F2 viruses.

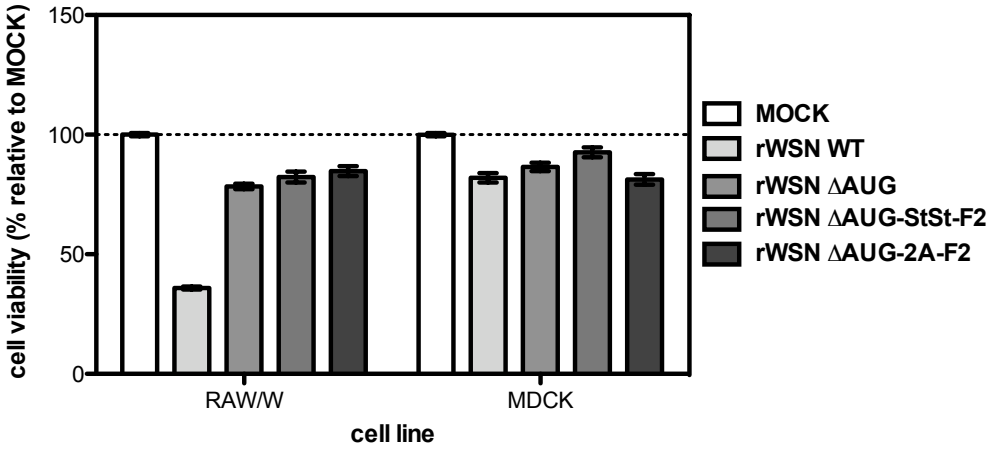

Figure 5.9: Induction of apoptosis by viruses with a bicistronic segment 2: Triplicate monolayers of MDCK and RAW/W cells in 96-well plates were infected with the panel of viruses at an MOI of 30 and tested for their viability after 8 h. PBS was used as a control. Mean values ± SEM are plotted.

Various possibilities could explain the observed phenotypes: (1) PB1-F2 is not expressed from a bicistronic segment 2; (2) the expression level of PB1-F2 is too low; (3) PB1-F2 itself is not responsible for the attenuation; or (4) the extended genome length counteracts any impact of PB1-F2.
To insert mutations into PB1-F2 and study the effects of these changes, it is an absolute requirement to restore the phenotype of WT viruses compared to deletion viruses. However, no PB1-F2 was detected and phenotypes

were still comparable to rWSN △AUG virus. Introduction of PB1-F2 into segment 2 therefore may not be ideal. Additionally, when these constructs were made, N40 had not yet been identified and all viruses were made in the △AUG background.

5.4 Strategies to express PB1-F2 separately in segment 6 and segment 7

5.4.1 Insertion of PB1-F2 into segment 6 via duplicated 3'UTR sequence

No PB1-F2 was detected in cells infected with viruses carrying a bicistronic segment 2. Therefore a different strategy was evaluated. Insertion of foreign genes into segment 6 has been reported previously (Machado et al., 2003, 2006). Different ORFs were successfully introduced downstream of NA (Figure 5.10). To insert VP01, CAT or GFP into segment 6, the 3'UTR was duplicated and inserted as an internal promoter between NA and the gene of interest. The foreign gene itself was inserted via a multiple cloning site. 70 nucleotides containing the end of the neuraminidase gene and the 5'UTR were added

the inserted gene to ensure the correct packaging and functionality of the segment (Figure 5.10).

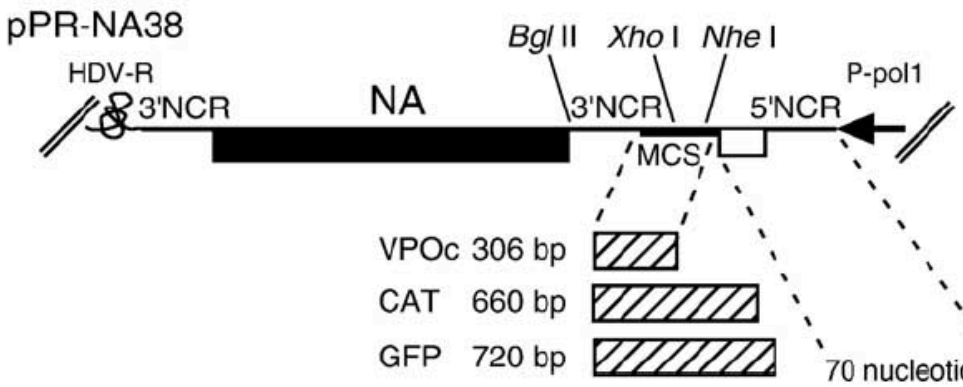

Figure 5.10: Schematic structure of bicistronic segment 6: VP0c, CAT or GFP was inserted between *Xho*I and *Nhe*I. Downstream of the internal promoter and the second ORF is an extended 5' region containing the last 42 nt of NA and the 5'UTR. Taken from Machado et al. (2006).

The strategy of Machado et al. was used as a model for the insertion of PB1-F2 downstream of NA and M2 in segment 6 and 7, respectively. As proof of principle to show functionality of the construct, mCherry was inserted instead of PB1-F2. Figure 5.11 shows the cloning strategy for inserting PB1-F2 or mCherry into segment 6. First, an internal *Bsm*BI restriction site was removed by an overlap PCR. At the same time, the internal promoter and the multi-cloning site were added downstream of NA. Before the construct was ligated into pGEMT Easy, 42 nt of the end of the NA ORF plus the 5'UTR were added (Figure 5.11(A)). In parallel, restriction enzyme sites *Xho*I and *Nhe*I were added upstream and downstream of PB1-F2 or mCherry by PCR (Figure 5.11(B)). pGEMT Easy-NA and the insert were fused together and subsequently inserted into pHH21 via *Bsm*BI sites (Figure 5.11(C)). All primer sequences are listed in Chapter 2 in Table 2.10. PCRs were done using the KOD hot start polymerase according to the protocol described in Section 2.4.2.

5.4.2 Insertion of PB1-F2 into segment 7 via duplicated 3'UTR

Similar to segment 6, segment 7 was prepared for the insertion of PB1-F2 or mCherry. As can be seen in Figure 5.12(A), 4 sequential PCR reactions were performed to introduce the internal promoter, the multiple cloning site and 42 nt of the end of the ORF of M2. The construct was flanked by *Bsm*BI restriction enzyme sites and it was inserted into pGEMT Easy. PB1-F2 or mCherry were prepared as described above for the insertion into segment 6. After ligation of pGEMT Easy-M and the insert, the bicistronic segment 7 was inserted via *Bsm*BI into pHH21 (Figure 5.12(C)). All primer sequences are listed in Table 2.10. PCRs were done using the KOD hot start polymerase according to the protocol described in Section 2.4.2.

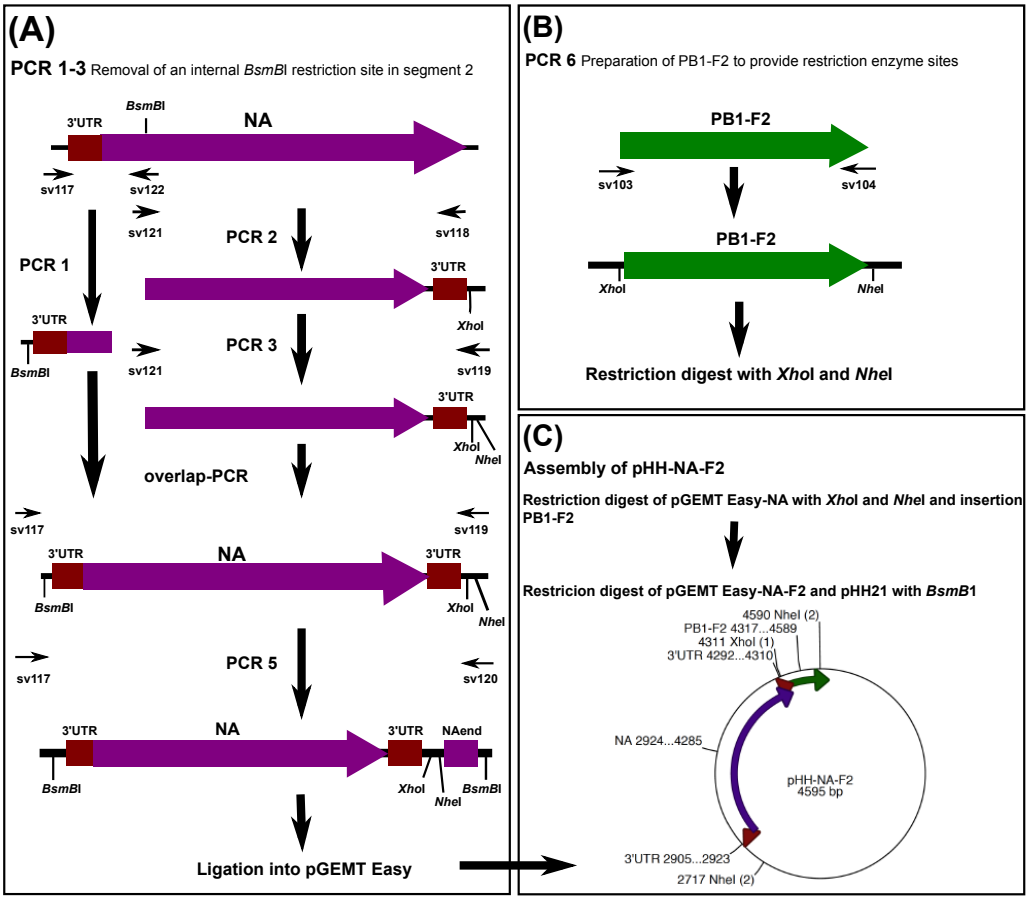

Figure 5.11: Schematic overview of the engineering of pHH-NA-3'UTR-F2: (A) Several PCR reactions were performed to insert the internal promoter, a multiple cloning site and 42 nt of NA downstream of NA. At the same time, an internal *Bsm*BI restriction site was removed from NA. The construct was finally inserted into pGEMT Easy. **(B)** PB1-F2 was amplified and restriction enzyme sites were introduced upstream and downstream of the ORF to allow insertion into segment 6. As an alternative to PB1-F2, mCherry was amplified. **(C)** PB1-F2 was inserted via *Xho*I and *Nhe*I into pGEMT Easy-NA. The bicistronic segment 6 was finally inserted into pHH21 via *Bsm*BI restriction sites.

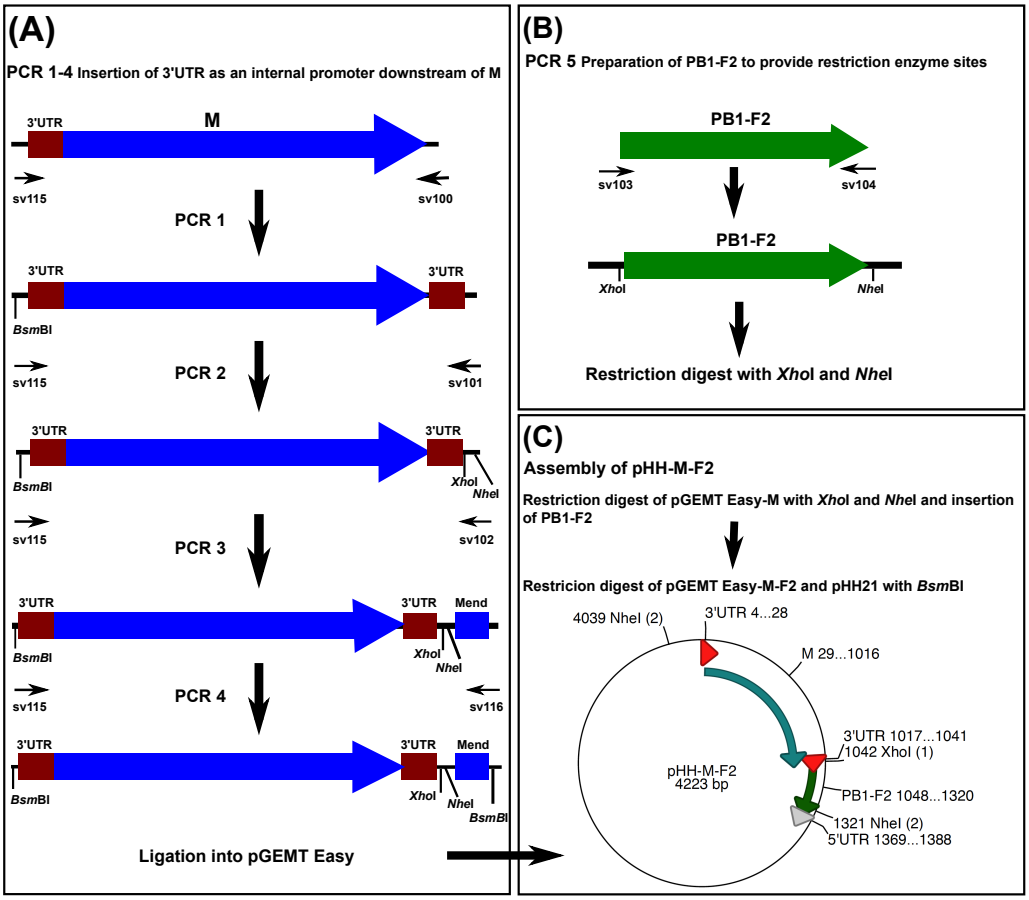

Figure 5.12: Schematic overview of the engineering of pHH-M-3'UTR-F2: (A) Several PCR reactions were performed to insert the internal promoter, a multiple cloning site and 42 nt of M downstream of M. The construct was finally inserted into pGEMT Easy. **(B)** PB1-F2 was amplified and restriction enzyme sites were introduced upstream and downstream of the ORF to allow insertion into segment 7. Additional to PB1-F2, mCherry was amplified. **(C)** PB1-F2 was inserted via *Xho*I and *Nhe*I into pGEMT Easy-M. The bicistronic segment 7 was finally inserted into pHH21 via *Bsm*BI restriction sites.

5.5 Virus rescue and characterisation of the viruses with an internal promoter

5.5.1 mCherry and PB1-F2 expression from biscistronic segments 6 and 7

To determine if the constructs were functional, a mini-genome assay was performed. Four plasmids expressing the polymerase subunits and the nucleoprotein were transfected into 293FT cells together with plasmids expressing viral RNA for bicistronic segment 6 or 7. As shown in Figure 5.13, mCherry was expressed successfully from segment 7, whereas no expression of mCherry was observed from segment 6. Plasmid pJC3, that expresses GFP-2A-mCherry under the control of a CMV promoter, served as a positive control and western blot analysis confirmed expression of mCherry from segment 7.

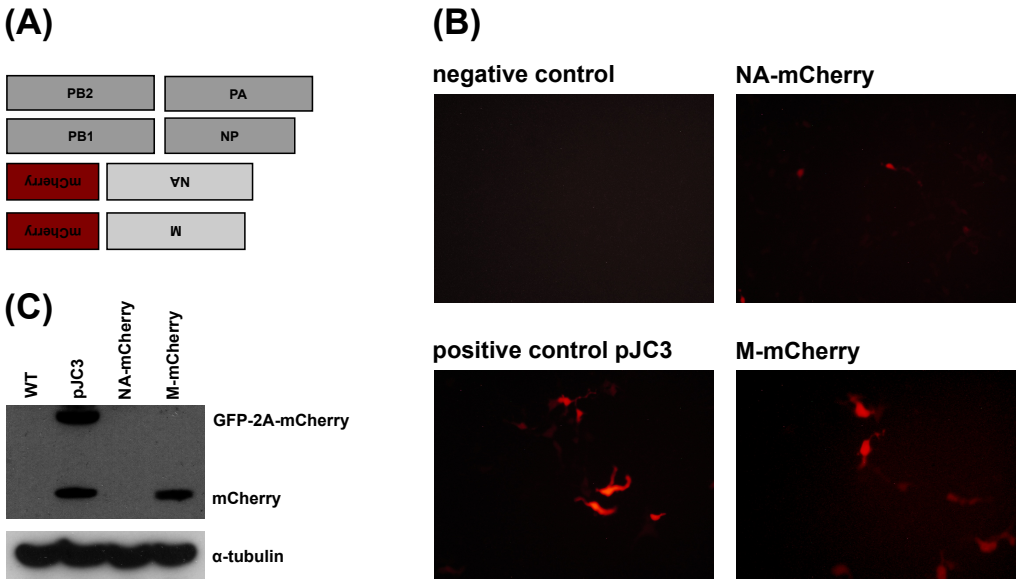

Figure 5.13: Expression of mCherry and PB1-F2 from bicistronic segment 6 and 7: (A) Transfection of four plasmids expressing the polymerase subunits and the bisistronic segment 6 or 7 into 293FT cells. **(B)** M-Cherry expression was determined by immunofluorescence of the transfected 293FT cells. No bisistronic segment was transfected as a negative control. pJC3 was used as a positive control, which expressed GFP-2A-mCherry under a CMV promoter. **(C)** Western blot analysis to confirm expression of mCherry.

virus	segment 2	bicistronic segment
rWSN △AUG/NA-F2	△AUG	NA-F2
rWSN F2-11/NA-F2	F2-11	NA-F2
rWSN NA-mCherry	WT	NA-mCherry
rWSN △AUG/M-F2	△AUG	M-F2
rWSN M-mCherry	WT	M-mCherry

Table 5.1: Viruses rescued with bicistronic segments 6 or 7

Although the bicistronic segment 6 was negative for the expression of mCherry in the minigenome assay, all bicistronic segments were used to rescue recombinant viruses. Rescues were performed using the 12-plasmid rescue system described in Sections 2.2.2 and 3.3.1. Table 5.1 shows the plasmid combinations used to rescue viruses expressing mCherry or PB1-F2 from segment 6 and 7. All viruses could be rescued, however no mCherry expression was observed in cells infected with rWSN NA-mCherry or rWSN M-mCherry viruses (data not shown).
Different recombinant virus versions were rescued carrying PB1-F2 in segment 6 or 7 (Table 5.1). The PB1-F2 ORF in its original position was always deleted by either three or two mutations (△AUG or F2-11, respectively). To determine expression of PB1-F2 from segment 6 and segment 7, MDCK cells were infected with recombinant viruses rWSN △AUG/NA-F2, rWSN F2-11/NA-F2 or rWSN △AUG/M-F2 at an MOI of 3 and cell lysates were analysed 8h later by western blotting. As shown in Figure 5.14, only viruses with a bicistronic segment 6 expressed PB1-F2. No PB1-F2 was detected in cells infected with rWSN △AUG/M-F2. Compared to WT infected cells, PB1-F2 was produced at much higher levels in cells infected with NA-F2 viruses. As seen before, the level of N40 was much higher in cells infected with viruses that have a △AUG mutation.

5.5.2 Phenotypic characterisation of viruses with a bicistronic segment 6

Viruses with the bicistronic segment 7 did not show any expression of PB1-F2, therefore only recombinant viruses with segment 6-F2 were used

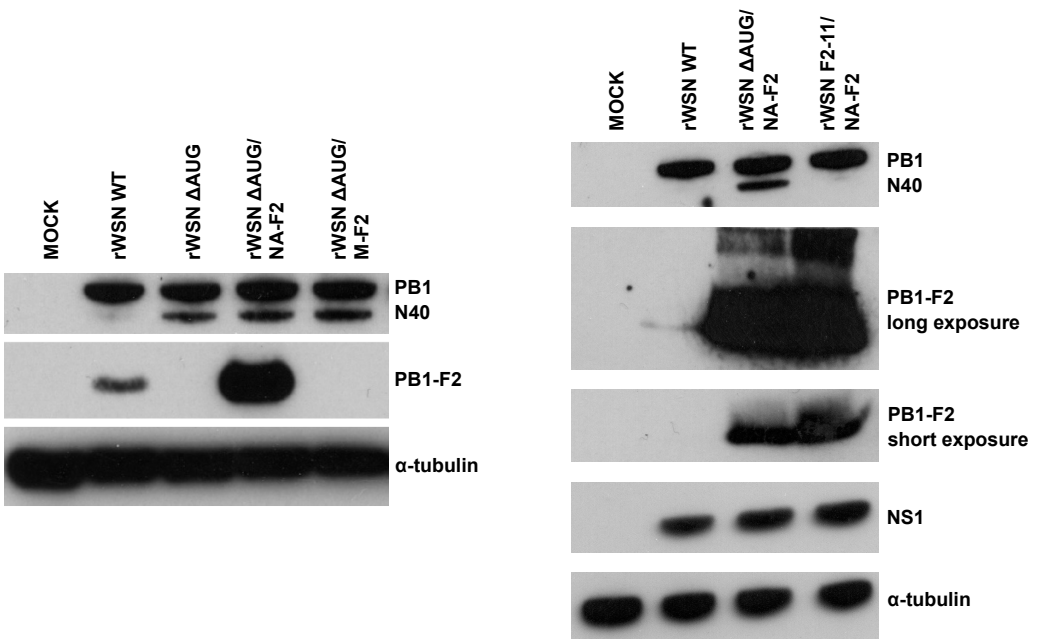

Figure 5.14: Expression of PB1-F2 from bicistronic segment 6 and 7: MDCK cells were infected with a panel of recombinant viruses and at 8 hpi, viral protein expression was determined. 4 - 12% gradient Bis-Tris gels were used to detect PB1, N40, NS1 and α-tubulin. 16% Tricine-SDS-PAGE was used to detect PB1-F2. Because PB1-F2 is overexpressed in cells infected with viruses carrying a bicistronic segment 6, short and long exposures of the blot are shown.

for further analyses. Confluent monolayers of MDCK cells were infected with serial dilutions of NA-F2 viruses and overlayed with 1.2% Avicel-DMEM. Incubation for 24 or 72 h was followed by fixing and staining either of the cell monolayers with crystal violet or immunostaining of virus infected cells using anti-Udorn antibodies (Figure 5.15). The plaque sizes were different to those of WT observed at 24 or 72 hpi and measurement of the diameter of several plaques (3 dpi) showed that viruses with a bicistronic segment 6 had a significant reduction in plaque size by $\sim$40 % (*Students t-test*: P $<$ 0.0005).

Although PB1-F2 was overexpressed from segment 6, no increase in plaque size compared to rWSN $\triangle$AUG was observed. Furthermore, plaque size of viruses with two point mutations in segment 2 (rWSN F2-11/NA-F2) was also reduced, whereas rWSN F2-11 viruses had a plaque phenotype comparable to WT viruses. Confluent MDCK cells were infected with bicistronic viruses at an MOI of 0.001 and cell supernatants were taken for virus growth analysis. As can be seen in Figure 5.16, viruses containing a

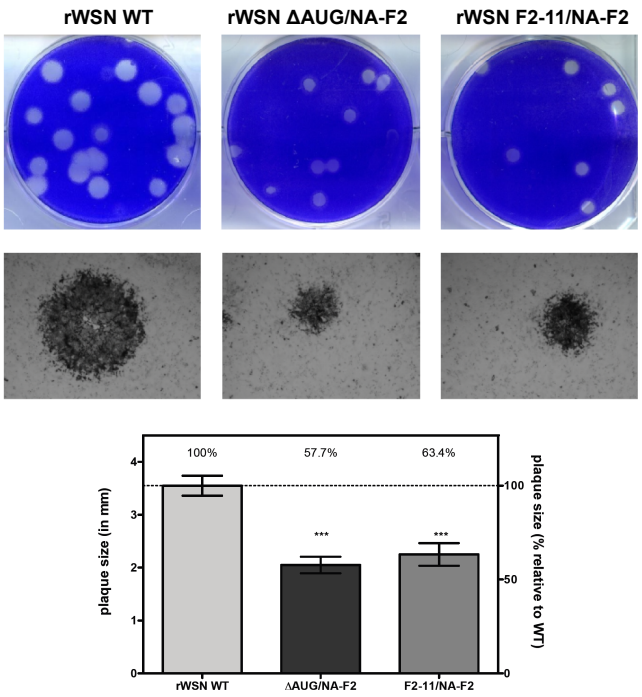

Figure 5.15: Plaque assay of viruses with a bicistronic segment 6: Confluent monolayers of MDCK cells were infected with the panel of recombinant viruses. Cells were overlayed with 1.2% Avicel-DMEM and incubated at 37℃ for 3 days (top panel) or 24 h (bottom panel). Mean values for ∼30 plaques/recombinant virus (3 dpi) are plotted and error bars represent the SEM. Differences in plaque sizes are significant between rWSN WT and rWSN ΔAUG/NA-F2 or rWSN F2-11/NA-F2 virus (*** $P<0.001$)

bicistronic segment in combination with segment 2 -ΔAUG were attenuated by about 100-fold compared to WT viruses. Viruses with segment 2-F2-11 grew similar to WT viruses. This phenotype had already been seen for viruses with PB1-F2 deletions (Figure 3.10(A)).

5.5.3 Bicistronic segment 6 and the consequences on virulence

It was suggested that PB1-F2 is involved in the virulence of influenza A viruses (Zamarin et al., 2006; McAuley et al., 2007). Viruses not expressing PB1-F2 were shown to be attenuated, but only if the start codon of PB1-F2 was removed (Chapter 3). Viruses with a bicistronic segment 6 were shown to overexpress PB1-F2 compared to WT viruses. These viruses were used to test any effect PB1-F2 may have *in vivo*. Female BALB/c mice, 6-7 weeks old, were infected with the different viruses or with PBS as negative control; 8 mice per group were inoculated intranasally with $5x10^3$ pfu. The weight of each mouse was observed daily. On day 4 and day 7, 4 mice per group were culled and lungs were used to measure the virus lung titre.

As can be seen in Figure 5.17(A), both bicistronic viruses did not cause any weight loss in infected mice. No difference was observed compared to

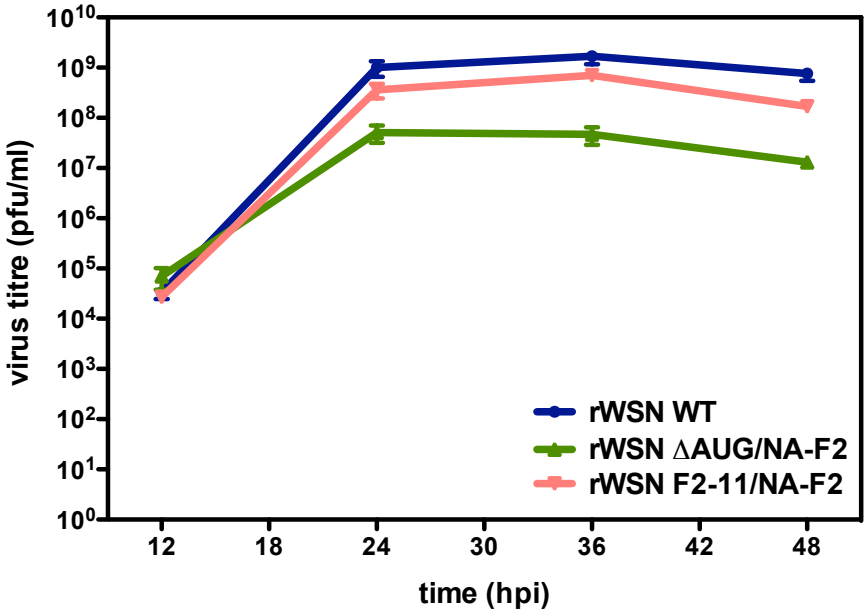

Figure 5.16: Growth of viruses with a bicistronic segment 6: Triplicate MDCK monolayers were infected with the recombinant WSN viruses WT, ΔAUG/NA-F2 and F2-11/NA-F2 at an MOI of 0.001 for multi-step growth curve. Media was supplemented with N-acetyl trypsin. Supernatant was harvested at indicated time points post infection and virus titres were determined by plaque assay. Error bars represent the SEM of each set of triplicates.

PBS infected mice. WT infected mice on the other hand lost weight rapidly. Virus titres in lungs of mice infected with WT viruses were up to 10^7 pfu/ml on day 4 and only decreased to $\sim 10^6$ pfu/ml on day 7. Mice infected with the NA-F2 viruses had a 100-1000-fold difference in virus lung titres on day 4. On day 7, almost no virus was detectable and the titre of 2 or 3 mice infected with rWSN ΔAUG/NA-F2 and rWSN F2-11/NA-F2 was below the detection limit (Figure 5.17(B)). It seems that these viruses were not able to efficiently replicate in a host under the pressure of the immune system. As seen for growth curves in MDCK cells before, rWSN F2-11/NA-F2 viruses grew slightly better in lungs of infected mice than rWSN ΔAUG/NA-F2 viruses, however both recombinant viruses were almost cleared from lungs of infected mice by day 7.

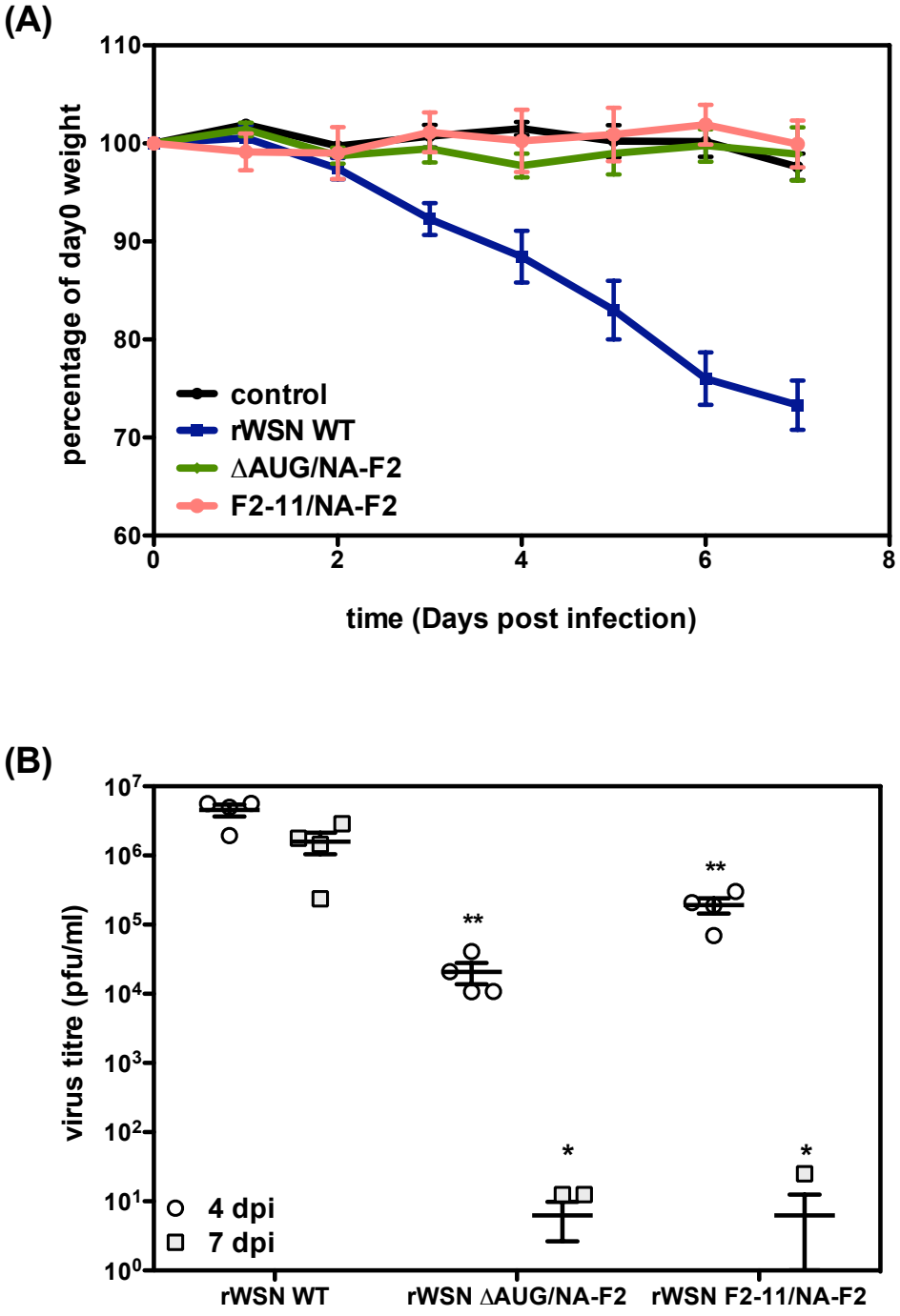

Figure 5.17: Weight and virus lung titres of mice infected with bicistronic segment 6 viruses: Groups of 8 female BALB/c mice were infected with the recombinant WSN viruses WT, ΔAUG/NA-F2 and F2-11/NA-F2 with $5x10^3$ pfu. **(A)** Weight loss was measured every day over a period of 7 days. Day 0 was set as 100% for each group. **(B)** At day 4 and day 7, 4 mice of each group were culled and lung virus titres were determined by plaque assay. Mean values ±SEM are plotted. *Student's t-test*: * $P<0.05$; ** $P<0.01$. Mouse infections were done in collaberation with B. Dutia and her lab at the University of Edinburgh.

5.6 Stability of bicistronic segments over 10 passages

Genetic stability of the bicistronic segments is critical for the functional analysis of the inserted ORF and the foreign gene may be lost over time (Kittel et al., 2004; Lu et al., 2004). However, previous work showed that it is possible to stably insert a foreign ORF into segment 6 of the viral genome (Percy et al., 1994; Machado et al., 2003, 2006). The arrangement of the chimeric segment was thereby important for the stability.

The four bicistronic viruses encoding PB1-F2 as a separate ORF were passaged 10 times in MDCK cells at low MOI. Besides western blot analysis to detect PB1-F2 expression and analysis of the plaque phenotype, segment 2 or 6 RNA was amplified in an RT-PCR reaction to determine the stability of the segment.

Figure 5.18 shows the plaque phenotype of all viruses at passages 1, 5 and 10. Recombinant viruses with an additional ORF gave smaller plaques than WT at passage 1. However, at passage 10 all viruses, except rWSN $\triangle$AUG-2A-F2, had increased their plaque size significantly (Figure 5.18). This suggests that the viruses may have accumulated mutations that helped to replicate the bicistronic segment or the additional ORF was removed from the viral genome.

To test this, MDCK cells were infected with the panel of recombinant viruses and cell lysates were analysed for the expression of PB1-F2 and NS1 by Western blotting (Figure 5.19). As shown by detection of NS1, viruses were propagated efficiently until passage 10. One exception was the recombinant virus $\triangle$AUG-2A-F2 where no viral proteins could be measured at passage 10. The reason for this is unknown, as plaques were obtained using the supernatant of the same passage. As before, no PB1-F2 was detected in cells infected with viruses with a bicistronic segment 2. Therefore, no conclusion could be made as to whether PB1-F2 still existed as a separate ORF.

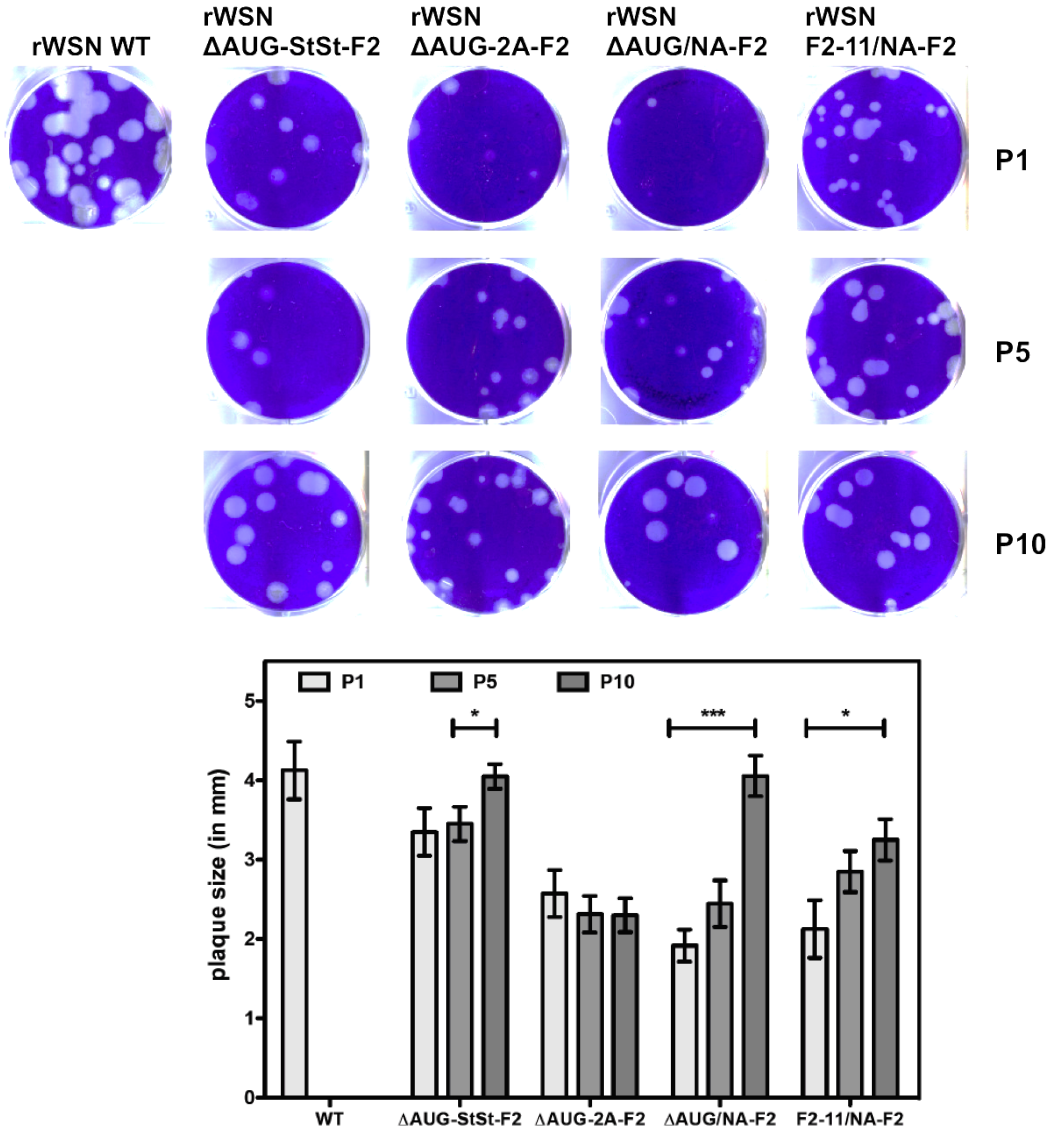

Figure 5.18: Plaque phenotype of viruses with bicistronic segments after serial passages: MDCK cells were infected with a serial dilution of the recombinant viruses. Passage 1 is shown on the top, passage 5 in the middle, passage 10 at the bottom. Mean values for ∼20 plaques per virus and passage number (3 dpi) are plotted and error bars represent the SEM. *Student's t-test*: * $P<0.05$; *** $P<0.001$

For viruses with a bicistronic segment 6, high levels of PB1-F2 were observed at a low passage number. However, the level of PB1-F2 decreased by passage 5 and at passage 10 almost no PB1-F2 was detected in cells infected with rWSN F2-11/NA-F2 viruses. Cells infected with rWSN ∆AUG/NA-F2 viruses showed a different pattern for passage 10. Two bands were observed, one at the expected size of PB1-F2, but also a smaller band. This may be due to the loss or the deletion of part of the ORF (Figure 5.19).

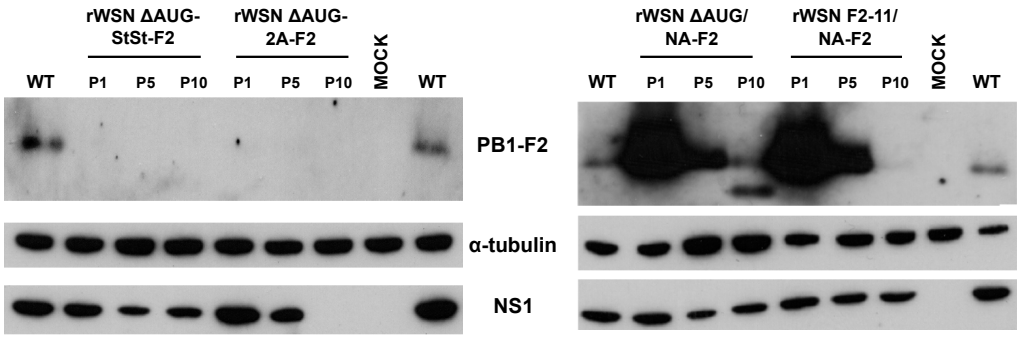

Figure 5.19: Western blot analysis of viruses with bicistronic segments after serial passage: MDCK cells were infected with a panel of recombinant viruses and at 8 hpi viral protein expression was determined. 4 - 12% gradient Bis-Tris gels were used to detect NS1 and α-tubulin. 16% Tricine-SDS-PAGE was used to detect PB1-F2.

The observed phenotypes suggested that the PB1-F2 ORF was removed from the bicistronic segments. To evaluate this, MDCK cells were infected with the panel of viruses derived from the different passages. Total RNA was extracted from cells and used in an RT-PCR reaction to amplify segment 2 or 6 (Figure 5.20). Oligonucleotides used for the PCRs were designed to anneal within PB1 or NA and the corresponding 5'UTR. Viruses with a full-length bicistronic segment 2 were expected to give products of 488 nt or 552 nt (StSt-F2 or 2A-F2, respectively). WT segment 2 was expected to give a product of only 175 nt. Figure 5.20(A) shows the result of the RT-PCR reaction for biscistronic segment 2 viruses. Viruses with an overlapping Stop-Start codon seem to lose PB1-F2 after several passages. RT-PCR products of RNA extracted from viruses at passage 2 had the expected size of 488 nt, by passage 5, two bands were observed. The shorter band corresponds to the size of WT segment 2. At passage 10, only the WT band remained. On the other hand, rWSN ∆AUG-2A-F2 virus seemed to

be stable up to passage 10 in MDCK cells. All bands were extracted from the gel and the nucleotide sequence was determined.

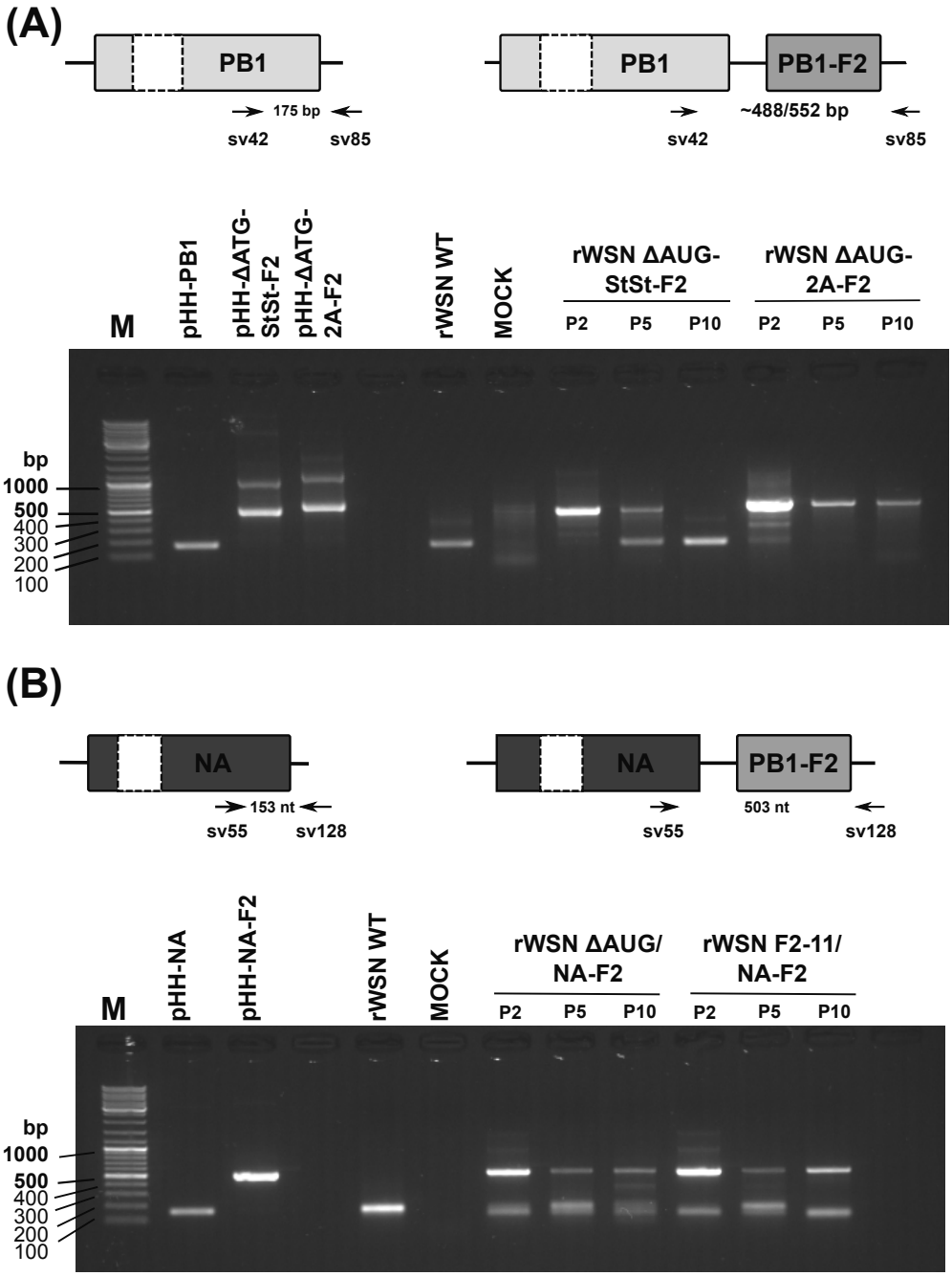

Figure 5.20: RT-PCR analysis of viruses with bicistronic segments after serial passages: The stability of **(A)** a bicistronic segment 2 and **(B)** a bicistronic segment 6 was analysed by RT-PCR using oligonucleotides binding at the end of PB1 or NA and within the 5'UTR. Expected product size are shown in the graphics. Products were extracted from the 1% agarose gel and sequenced.

This confirmed the loss of the PB1-F2 ORF in rWSN △AUG-StSt-F2 virus. It was also confirmed that rWSN △AUG-2A-F2 virus was stable up to passage 10. All bicistronic segment 6 carrying viruses show a pattern that would suggest a partial loss of the downstream ORF (Figure 5.20(B)). The large band with an approximate size of 500 bp matches the expected size of the bicistronic segment and the lower band is about the size of the WT segment. Both bands were extracted from the agarose gel and their nucleotide sequence was determined. As expected, the upper band represents a bicistronic segment 6. However, the smaller band did not align with any part of segment 6 or PB1-F2 but it was found to be a non-specific product corresponding to segment 3. A thin intermediate size product was also found for rWSN△AUG/NA-F2 at passage 10, which may be a degradation product of PB1-F2. Although this PCR product was not sequenced, it would explain the finding observed in the western blot analysis (Figure 5.19). In summary, it seems that RNA segments with an internal promoter are stable until at least passage 5, but a fraction may partially lose the downstream ORF after that.

5.7 Discussion

The aim of this Chapter was the engineering of a virus that expressed PB1-F2 from an independent ORF. This detachment from the PB1 ORF would make PB1-F2 accessible for inserting mutations or deletions. Also, PB1-F2 could be tagged by short sequences (e.g. V5 epitope tag), because the applications of the available antibody were limited. This would allow the study of its localisation within the cell by immunofluorescence in the context of a viral infection or the search for interacting partners by immunoprecipitations.

Three segments with different options were tested for expressing PB1-F2 or mCherry (overview in Table 5.2). However, only PB1-F2 expression from segment 6 was efficient.

A variety of potential reasons why the expression of mCherry from segment 6 and 7 and PB1-F2 from segment 2 and 7 was not successful will be discussed.

Until now, only insertions of foreign genes into segment 6 and 8 have been reported. Here, I inserted PB1-F2 into segment 2, which is one of the largest segments in the viral genome. This was chosen because of the supposed advantage the expression of PB1-F2 from its original segment may have had. Strategies tested were: (1) an internal promoter, (2) an overlapping Stop-Start cassette, and (3) a short self-cleaving 2A peptide that derived from foot-and-mouth disease virus. Although viruses with a 2A sequence and the Stop-Start cassette could be rescued, none of the recombinant viruses expressed PB1-F2.

Termination-reinitiation is naturally used by influenza B viruses. Recently, it was shown that the success of reinitiation depends on the sequence directly upstream the Stop-Start-cassette. This sequence is now known as TURBS (termination upstream ribosome binding site) (Powell et al., 2008a, 2011). The combination of two facts may be the reason why expression from this segment was not successful: (1) naturally only $\sim$10% of the ribosomes reinitiate at the downstream start codon and therefore the expression level of PB1-F2 may be too low for detection, and (2) the upstream sequence of PB1 does not contain TURBS. Additionally, this bicistronic segment was not stable and PB1-F2 sequence was lost gradually following passage in MDCK cells.

Although PB1-F2 ORF was stably inserted into segment 2 using the FMDV

(1) △AUG: Segment 2 with three point mutations		
Bicistronic segment	**Virus**	**Strategy**
segment 2 △AUG-F2	rWSN △AUG-StSt-F2	overlapping StopStart
segment 2 △AUG-F2	rWSN △AUG-2A-F2	self-cleaving 2A peptide
segment 6 NA-F2	rWSN △AUG/NA-F2	internal promoter
segment 7 M-F2	rWSN △AUG/M-F2	internal promoter
(2) F2-11: Segment 2 with two point mutations		
Bicistronic segment	**Virus**	**Strategy**
segment 6 NA-F2	rWSN F2-11/NA-F2	internal promoter
(3) WT: Segment 2 without mutations		
Bicistronic segment	**Virus**	**Strategy**
segment 6 NA-mCherry	rWSN NA-mCherry	internal promoter
segment 7 M-mCherry	rWSN M-mCherry	internal promoter

Table 5.2: Summary of viruses rescued with a bicistronic segment: PB1-F2 or mCherry were inserted into segment 2, 6 or 7 and rescued in combination with segment 2 with or without mutations to knock-out PB1-F2.

2A peptide, no PB1-F2 protein was detected in infected cells. The efficiency of the cleavage of artificial proteins was previously reported to be ∼80% (Ryan and Drew, 1994). However, the immediate sequence upstream of 2A was shown to have some importance in the efficiency of cleavage (Donnelly et al., 1997). Also, 2A and '2A-like' sequences form an α-helix which may be important for the ribosomal skipping process (Donnelly et al., 1997, 2001). The secondary structure of the nascent PB1 may interfere with the correct formation of the secondary structure of 2A and therefore with the cleavage. The amounts of PB1-F2 produced may also be very low and below the detection limit because of the severe attenuation of the virus, especially at early times in infection. The antibody used to detect PB1-F2 often resulted in high background in western blot analysis, and long exposure times to detect small amounts of proteins were challenging. Previously, the insertion of a CAT gene upstream of segment 6 with the use of 2A was shown to be successful, however, the attempt to engineer a bicistronic segment 8

containing GFP was not (Percy et al., 1994; Lu et al., 2004). This suggests that the segment as well as the inserted gene may be important for the success of this strategy.

It was suggested that the genome size may limit the application of inserting foreign genes into the influenza A virus genome (García-Sastre et al., 1994; Machado et al., 2003). Insertion of PB1-F2 downstream PB1 via 2A increased the segment size to over 2700 nt. Regardless, the virus appeared very flexible and the bicistronic segment was packed into virus particles and viruses stably maintained the segment.

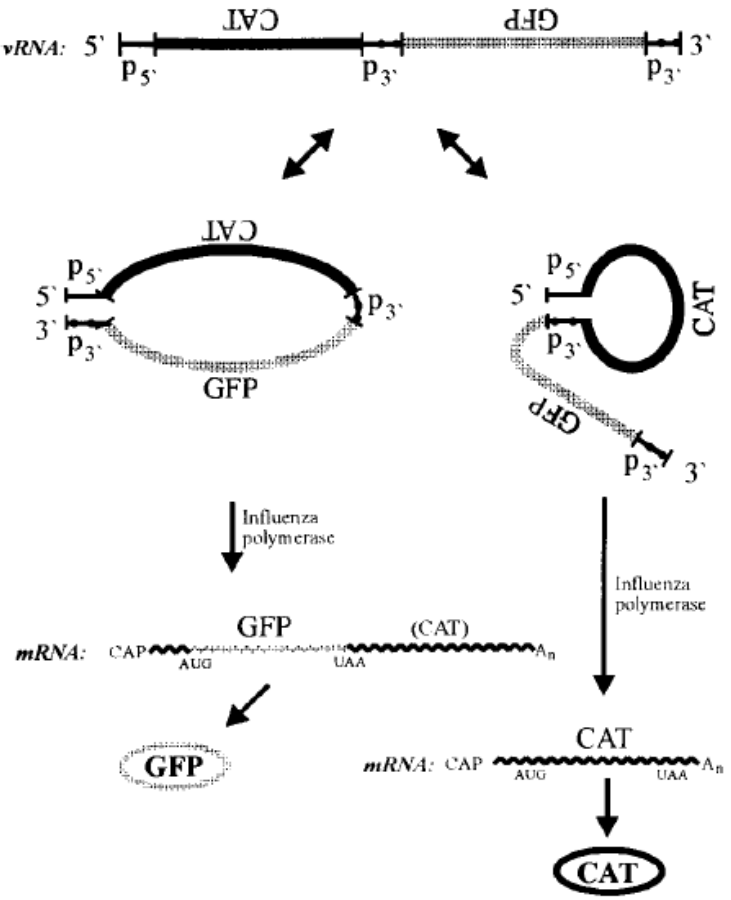

Figure 5.21: Replication and transcription of bicistronic segments: Scheme of replication and transcription of a bicistronic segment carrying GFP and CAT joint by an internal promoter. The 5'UTR can interact with the outer 3'UTR and transcription leads to the formation of a bicistronic mRNA and GFP expression (left). Interaction of the 5'UTR with the internal promoter results in the transcription and replication of a monocistronic RNA and the expression of CAT (right). Taken from Flick and Hobom, 1999.

Another approach that was chosen to insert PB1-F2 into the viral genome

was the use of an internal promoter in segment 2 or segment 6. Whereas a bicistronic segment 2 carrying an internal promoter could not be rescued, a bicistronic segment 6 was successful and PB1-F2 was expressed in high quantities. Expression levels even exceeded WT levels. One reason for this may be a different activity of the segment 6 promoter. PB1-F2 was inserted downstream of the original ORF, so that the second ORF would be maintained during replication. It was shown by Flick et al. that internal promoters result in the formation of subgenomic RNAs expressing the downstream gene (Figure 5.21) (Flick and Hobom, 1999b; Machado et al., 2006). This would subsequently lead to the loss of the upstream gene if this was not essential for the virus. A short subgenomic segment, only encoding PB1-F2, is likely to be generated in infected cells, which could be also included as a ninth segment into viral particles. It also could compete with the full-length bicistronic segment, which would, if selected instead of the long bicistronic segment, lead to the formation of defective interfering (DI) particles (Figure 5.21). Additionally, it was reported that the expression levels of neuraminidase were lower compared to WT infected cells (Machado et al., 2003).

The plaque sizes of rWSN $\triangle$AUG/NA-F2 and rWSN F2-11/NA-F2 were smaller compared to WT viruses, which can be explained by the points discussed above. However, plaque size increased after several passages. Although the insertion of a foreign gene into segment 6 was previously shown to be stable up to passage 6, PB1-F2 may be partially removed from segment 6 after passage 5. This would explain the increase in plaque size after several passages as well as the appearance of a short PB1-F2 fragment detected in Western blot analysis. The attempt to insert a foreign gene into segment 7 was not successful. Although mCherry expression was observed in a minigenome assay, the rescued viruses did not express the fluorescent protein. The insertion of a gene downstream of M2 may interfere with the splicing of M1 mRNA. A different reason was discussed by Machado et al. (Machado et al., 2003, 2006). The authors suggested that the high GC content of GFP may inhibit viral replication. A similar GC content of over 60% was calculated for mCherry, whereas the WSN genome only has a GC content of $\sim$ 42%.

The initial approach to study PB1-F2 by separating the ORFs and insert PB1-F2 downstream of PB1 was made before N40 was discovered. It was hypothesised at the time that any attenuation caused by PB1-F2 may be

restored by inserting PB1-F2 and expressing it from an independent ORF. This would allow the characterisation of the protein and its role in the viral life cycle. However, it was shown in Chapter 3, that the loss of PB1-F2 alone is not responsible for the attenuation of PB1-F2 knockout viruses. In fact, it was shown to be due to an overexpression of N40 in a PB1-F2 deletion background. Additionally, no real advantage of viruses expressing PB1-F2 from segment 6 was observed, independent of the strategy used to delete PB1-F2 in segment 2. Nevertheless, the separation of the two ORF can be a useful tool to study the role of PB1-F2. PB1-F2 stable integrated in the influenza A virus genome could help to identify motifs for interaction partners or important amino acids for virulence and PB1-F2 could be tagged with a short peptide (FLAG-tag, V5-tag). A combined strategy of the methods discussed in this Chapter may be a possible approach by inserting PB1-F2 downstream of NA via a 2A peptide. Regarding the disadvantages of 2A, alternative methods may be examined, such as the use of a caspase recognition site (CRS). This artificial site is only nine amino acids long and the introduction was genetically stably over several passages (Kittel et al., 2004). Cellular caspases are thought to recognise the sites and cleave the polyprotein into the individual proteins posttranslationally. This would minimise the amino acids remaining at the C- or N-terminus of the cleaved proteins.

5.8 Summary of Chapter 5

PB1-F2 was inserted as an independent ORF into the influenza A virus genome. The following strategies were used and verified for their success:

(1) Insertion into Segment 2		
Virus	**Phenotype**	**Stability**
rWSN △AUG-StSt-F2	no PB1-F2 expression attenuated in growth small Plaque size fitness increase after P5	PB1-F2 lost after passage 5
rWSN △AUG-2A-F2	no PB1-F2 expression attenuated in growth small Plaque size	stable up to passage 10
rWSN △AUG-3'UTR-F2	not possible to rescue	
(2) Insertion into Segment 6		
Virus	**Phenotype**	**Stability**
rWSN △AUG/NA-F2	PB1-F2 overexpression attenuated in growth small Plaque size attenuation *in vivo* fitness increase after P5	PB1-F2 lost partially before P10
rWSN F2-11/NA-F2	PB1-F2 overexpression attenuated in growth small Plaque size attenuation *in vivo* fitness increase after P5	PB1-F2 lost partially before P10
(3) Insertion into Segment 7		
Virus	**Phenotype**	**Stability**
rWSN △AUG/M-F2	no PB1-F2 expression	not tested

Chapter 6

N40 AND PB1-F2 KNOCKOUT AND THE INFLUENCE ON VIRAL REPLICATION

Aims of Chapter 6

Overexpression of N40 caused an attenuation of viral replication *in vitro* and *in vivo*. For a better understanding of segment 2 gene products, N40 deletion viruses were engineered and rescued in the context of either PB1-F2 expression or PB1-F2 knockout.

The deletion of N40 was achieved by a single point mutation which changed amino acid 40 within the PB1 ORF from methionine to leucine (△**N40**).

Deletion of N40 and PB1-F2 was obtained by introducing two point mutations (△**F2**/△**N40**). The first mutation led to an amino acid change within the PB1 ORF at residue 40 (M40I) which removed the N40 start codon. Simultaneously, a stop codon was introduced into the PB1-F2 ORF. Additionally a second stop codon was introduced into the PB1-F2 sequence further downstream which had no effect on the amino acid sequence of PB1.

The influence of these segment 2 mutant viruses with different expression levels of PB1-F2 and/or N40 on viral replication was analysed.

6.1 Introduction on N40

In 2009, a 12th influenza A virus protein was described (Wise et al., 2009). Translation occurs from the same mRNA as the polymerase subunit PB1 and PB1-F2. The protein, called N40, is a shorter version of PB1 lacking the N-terminal 39 amino acids. As a consequence, N40 cannot interact with the polymerase subunit PA, however the ability to bind PB2 remains (Wise et al., 2009). Other PB1 binding partners are also likely to retain their ability to interact with N40. Figure 6.1 shows a diagram of the 5' end of segment 2 of A/WSN/33. Five AUGs are present in this region with different Kozak consensus sequences, but only ORF 1, 4 and 5 encode a full length protein. A strong consensus sequences was defined as **gccRccAUGG** with a purine at position -3 and guanine at position +4 (Kozak, 1986), however only ORF 4 and 5 fulfil this condition. Ribosomes are thought to bind to the 5' cap of mRNAs and scan along the mRNA until they reach the first suitable AUG to start translation. Because of the poor sequence context of AUG1, translation is likely to bypass this first AUG codon.

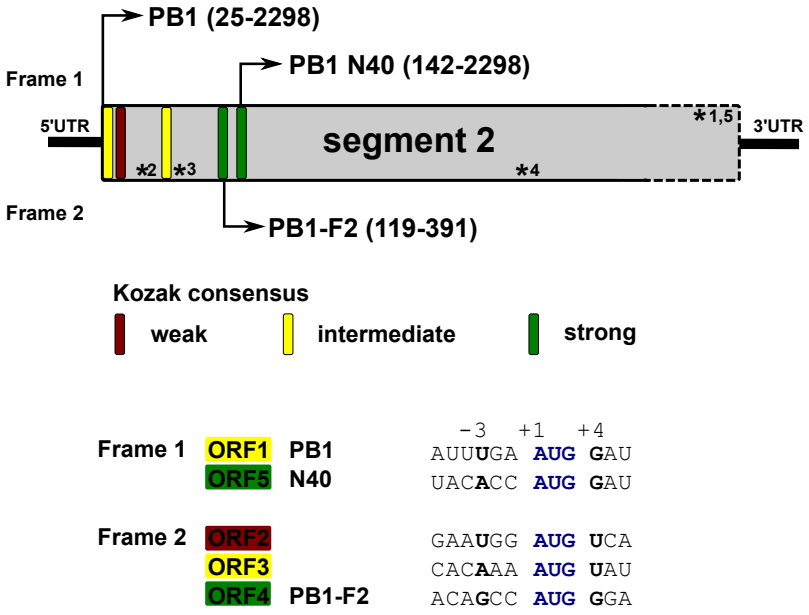

Figure 6.1: Analysis of the sequence context of the AUGs in segment 2 of A/WSN/33: Five AUG codons are present in the 5' end of segment 2. AUG1 initiates translation of PB1, AUG4 starts PB1-F2 and AUG5 N40. The short second and third ORFs do not encode a protein. Stop codons of the corresponding ORFs are shown within the graphic (*1-5). The Kozak consensus sequences of all 5 AUGs are listed and shown in different colors according to their strength. Modified from Wise et al. (2009).

The function of N40 is not known, but because most viral strains contain the ORF, it was suggested that N40 is of some importance. Wise et al. reported that expression of N40 is not essential for the viral life cycle. However, deletion of N40 in combination with an intact PB1-F2 ORF delayed viral replication of influenza A virus strain A/PR/8/34 *in vitro*. Although viral polymerase activity was increased in this context, these viruses showed a small plaque phenotype and a delay in a single-cycle growth curve (Wise et al., 2009).
Overexpression of N40 in combination with the deletion of PB1-F2 had a dramatic effect on virulence of A/WSN/33. Therefore, the impact of the loss of N40 for this virus strain was analysed. In addition to the N40 mutant, a double mutant was engineered lacking both PB1-F2 and N40 ORFs.

6.2 Deletion of N40 and deletion of N40 in combination with a PB1-F2 knockout

6.2.1 Constructing the plasmids with N40 deletions

Two N40 deletion viruses were engineered using oligonucleotide primers listed in Table 6.1. The first mutation resulted in the deletion of N40, but the PB1-F2 ORF was left unaffected (Figure 6.2(1)). A point mutation within the start codon abolished N40 expression and led to an amino acid change from methionine to leucine in the PB1 ORF. The second mutant virus was designed in such a way that besides N40, PB1-F2 was also knocked out (Figure 6.2(2)). To achieve this, methionine was changed into isoleucine within the PB1 ORF and PB1-F2 expression was terminated after amino acid 8. To fully abolish PB1-F2 expression, a second point mutation was introduced into segment 2 further downstream. This was previously shown to be necessary due to translation of the C-terminus from one of the internal AUG codons (Section 3.2.1 and Zamarin et al., 2006). Mutations were introduced by PCR-mediated site-directed mutagenesis (Section 2.4.3) and primer sequences are listed in Table 2.9 and 2.12. The obtained plasmids were named pHH-$\triangle$N40 and pHH-$\triangle$F2/$\triangle$N40 and were amplified in *E.coli* and sequenced before further use in virus rescues.

Mutation	Forward primer	Reverse primer
△N40		
A142T	sv172	sv173
△F2/△N40		
G144A	sv174	sv175
G291A	sv13	sv14

Table 6.1: Oligonucleotide primers used to delete N40 in A/WSN/33. Primer Sequences are listed in Table 2.9 and 2.12 in Chapter 2.

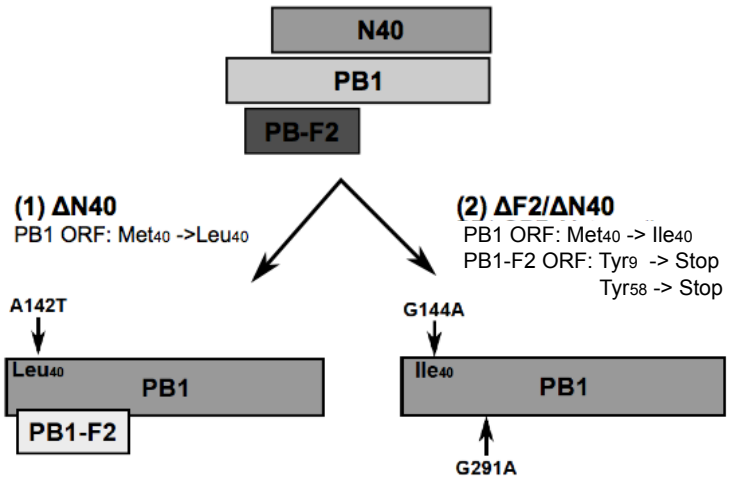

Figure 6.2: Strategy to delete N40: A/WSN/33 segment 2 encodes three polyproteins - the polymerase subunit PB1, PB1-F2 and an N-terminally truncated version of PB1 called N40. Deletion viruses were engineered by deleting the start codon of N40. **(1)** △N40: The start codon was mutated to a leucine. This mutation did not have an effect on the PB1-F2 ORF, but changed residue 40 in PB1 to a leucine. **(2)** △F2/△N40: Insertion of a point mutation led to the deletion of PB1-F2 and N40. Changing the start codon of N40 into isoleucine also introduced a stop codon into the PB1-F2 ORF at amino acid 9. Additionally, a second point mutation was introduced to abolish the expression of the C-terminus of PB1-F2 (Zamarin et al., 2006).

6.2.2 Rescue of viruses deficient for N40

Viruses were rescued using the 12-plasmid rescue system as described in Section 2.2.2 and 3.3.1. The plasmid for the expression of the vRNA of segment 2 (pHH-PB1) was exchanged by either of the N40 deletion plasmids pHH-$\triangle$N40 or pHH-$\triangle$F2/$\triangle$N40. Recombinant viruses were plaque purified and following RT-PCR, the nucleotide sequence of segment 2 was determined.

Expression of viral proteins from segment 2 was monitored by western blot analysis. Confluent monolayers of MDCK cells were infected with the panel of viruses at an MOI of 3 and cells were lysed 8 h later. Results of the western blot are shown in Figure 6.3.

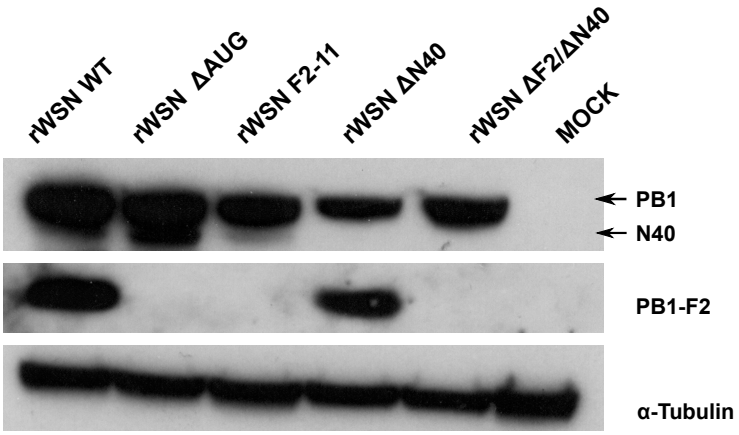

Figure 6.3: Detection of viral protein expression in cells infected with segment 2 deletion viruses: MDCK cells were infected with a panel of recombinant viruses and viral protein expression was determined 8 hpi. 4 - 12% gradient Bis-Tris gels were used to detect PB1 and N40. 16% Tricine-SDS-PAGE was used to detect PB1-F2. Detection of α-tubulin served as an internal loading control.

As expected, no N40 was detected in cells infected with either of the N40 deletion viruses rWSN $\triangle$N40 or rWSN $\triangle$F2/ $\triangle$N40. However, cells infected with the WT virus or the PB1-F2 deletion viruses $\triangle$AUG and F2-11 expressed N40, with the highest expression level noticed in cells infected with rWSN $\triangle$AUG viruses.

Expression of PB1-F2 was also monitored and as expected it was only detected in cells infected with either the WT virus or rWSN$\triangle$N40, but not in cells infected with a PB1-F2 deletion virus or the PB1-F2/N40 double mutant virus (Figure 6.3).

6.3 *In vitro* characterisation of the N40 mutant viruses

To determine any possible effect the loss of N40 may have had on virus replication, its plaque phenotype was analysed. Confluent monolayers of MDCK cells were infected with the two N40 deletion viruses. Cells were overlayed with a mixture of Avicel and DMEM supplemented with N-acetyl trypsin. At 24 or 72 hpi, cells were fixed and stained either with crystal violet or by immunostaining and plaque size was compared to those of WT infected cells. As can be seen in Figure 6.4, plaques seemed slightly smaller 24 hpi, however no difference was observed in plaque size at day 3 post infection.

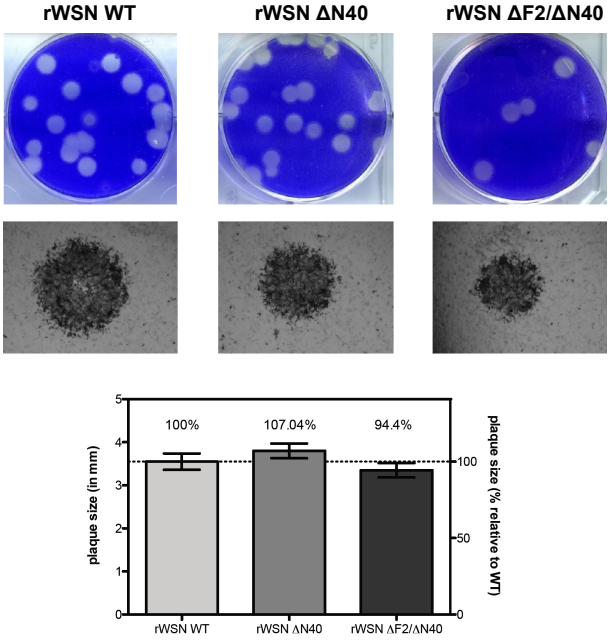

Figure 6.4: Plaque phenotype of viruses with a N40 deletion: Confluent monolayers of MDCK cells were infected with recombinant viruses. Cells were overlayed with 1.2% Avicel-DMEM and incubated at 37℃ for 3 days (top panel) or 24 h (bottom panel). Mean values ± SEM for ∼30 plaques/recombinant virus (3 dpi) are plotted.

To evaluate this further, viral growth was determined under multi-step conditions or single-step conditions. Confluent MDCK cells were infected with low or high MOI (0.001 or 3, respectively) and supernatants were collected at the indicated time points to measure viral growth. Beside MDCK cells, viral growth in a multi-step cycle was also determined in A549 cells (Figure 6.5(B)). As shown in Figure 6.5, the loss of N40 had a minor effect on viral replication in MDCK cells; in A549 cells no difference in growth was observed. This finding was independent of PB1-F2 expression and the results were in line with the observed plaque phenotype.

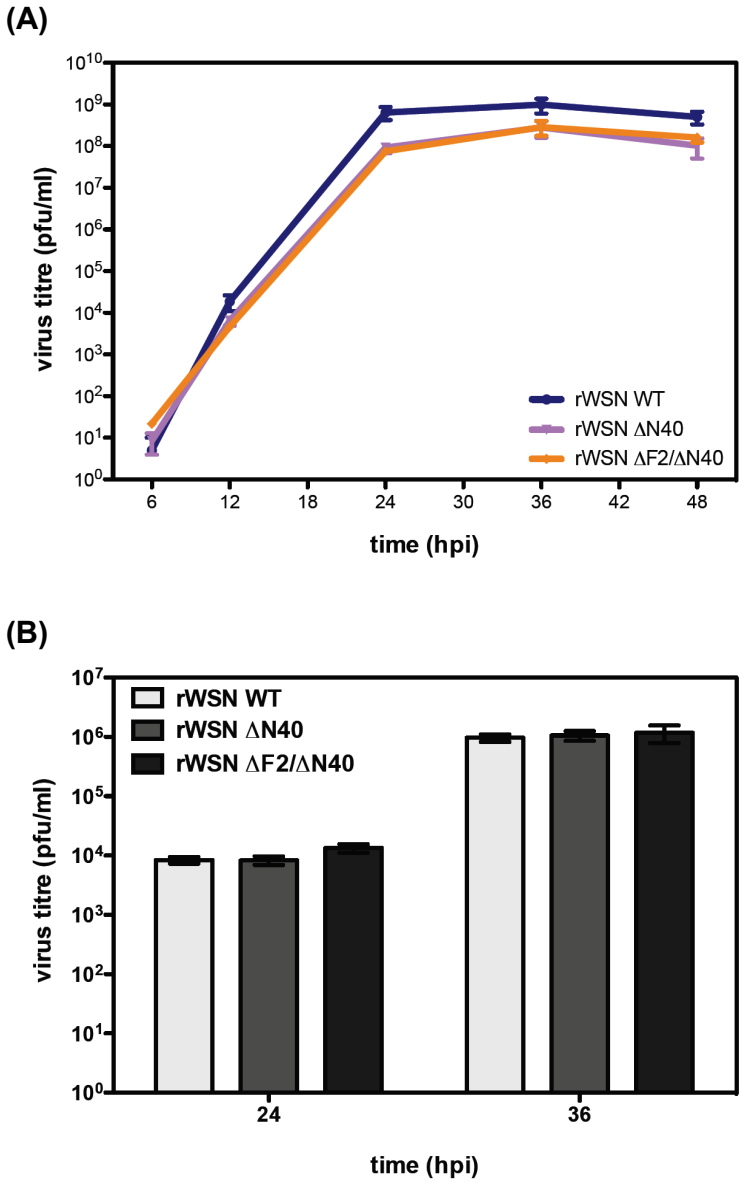

Figure 6.5: Multi-step growth curve of viruses with a N40 deletion: Triplicate MDCK cell **(A)** or A549 cell **(B)** monolayers were infected with the recombinant WSN viruses WT, ΔN40 and ΔF2/ΔN40 at an MOI of 0.001. Media was supplemented with N-acetyl trypsin. Supernatants were harvested at the indicated time points post infection and virus titres were determined by plaque assay. Mean values ±SEM of each set of triplicates are plotted.

Wise et al. reported that viral growth in a multi-step cycle was unaffected by the loss of N40, similar to the results seen in this study. However they found a delay of viral growth under single cycle conditions (Wise et al., 2009). To evaluate this for the influenza A virus strain A/WSN/33, confluent monolayers of MDCK cells were infected with either the WT or one of the

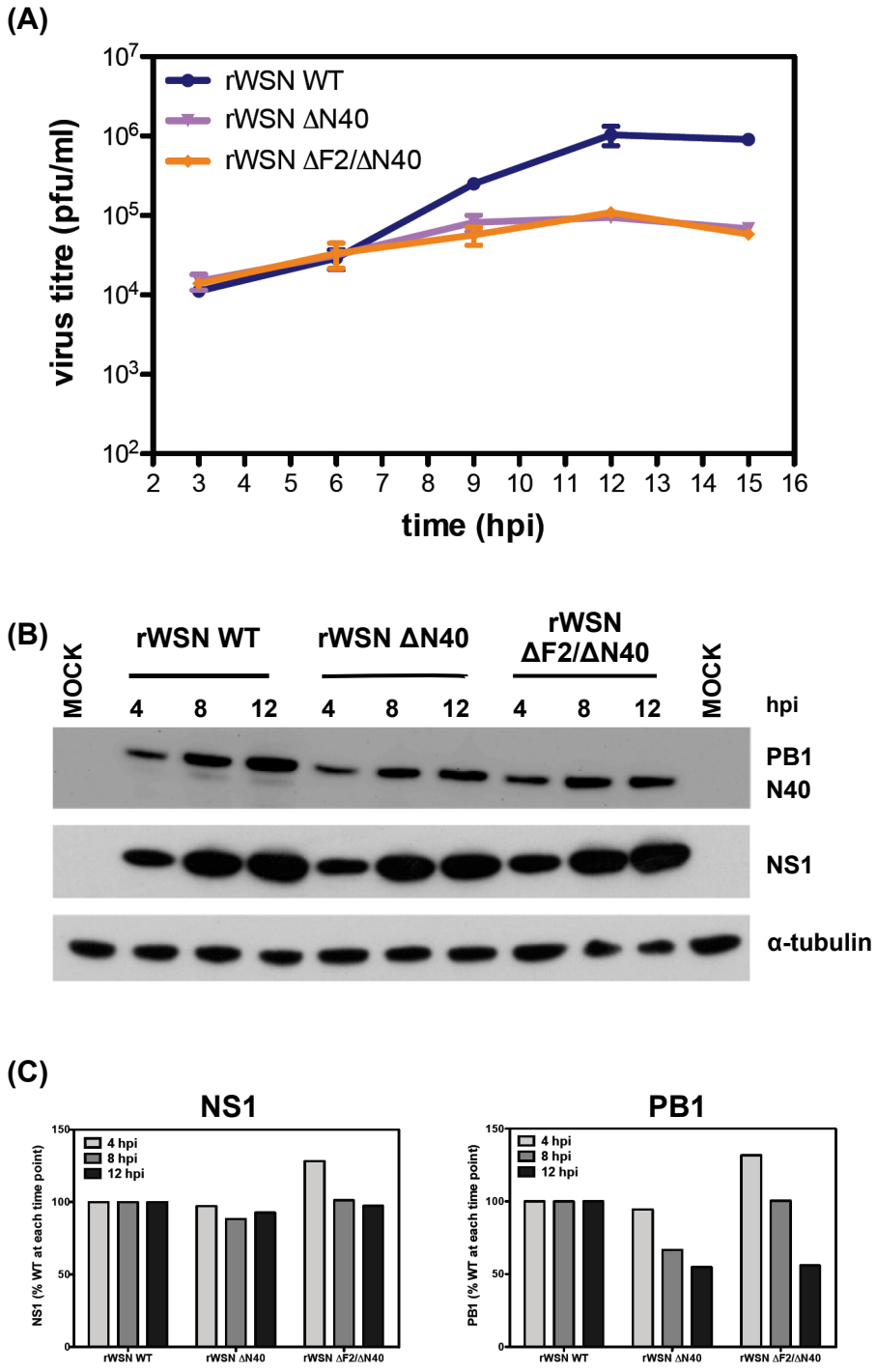

Figure 6.6: Single-step growth curve of viruses with a N40 deletion: (A) Triplicate MDCK cell monolayers were infected with the recombinant WSN viruses WT, ΔN40 and ΔF2/ΔN40 at an MOI of 3. Supernatant was harvested at indicated time points post infection and virus titres were determined by plaque assay. Mean values ±SEM of each set of triplicates are plotted. **(B)** Synthesis of viral protein was analysed by Western blot at indicated time points. 4 - 12% gradient Bis-Tris gels were used to detect PB1, N40 and NS1. α-tubulin was used as an internal loading control. **(C)** Quantification of the accumulation of NS1 and PB1.

mutant viruses at an MOI of 3 and supernatants were harvested at the indicated time points (Figure 6.6 (A)). Both N40 deficient viruses were attenuated under these conditions. Following this, viral protein synthesis was determined by western blot analysis. Although accumulation of NS1 was similar in cells infected with either virus, PB1 expression levels were decreased at later time points in cells infected with N40 deficient viruses compared to cells infected with the WT virus (Figure 6.6 (B and C)).

Based on the results described in Chapter 3 and the results in this Chapter, a mixed infection assay was used to further evaluate possible effects of N40 and PB1-F2 on viral growth. When cells were infected at a high MOI, viruses overexpressing N40 in a PB1-F2 deficient background ($\triangle$AUG) showed similar growth to WT viruses. On the other hand, viruses deficient for N40 showed an attenuated phenotype. The opposite result was found when infecting at a low MOI: $\triangle$AUG viruses were attenuated, viruses deficient for N40 showed a similar growth phenotype to WT virus. The potential of the presence of high levels of N40 in combination with the availability of PB1-F2 in the same cell was examined by infecting MDCK cells with both viruses simultaneously at an MOI of 3. Viral infections follow a Poisson distribution and $\sim$80% of cells are expected to be infected with more than one virus particle at an MOI of 3 (Knipe et al., 2001). Cells were also infected with either of the two viruses at an MOI of 3 or 6 and with WT virus (MOI 6). The results are shown in Figure 6.7. As described before, cells overexpressing N40 showed a small plaque phenotype, whereas the plaque size of $\triangle$N40 viruses was comparable to WT viruses. Infection of cells with a mixture of $\triangle$AUG and $\triangle$N40 viruses caused a mixed plaque phenotype, although the majority of plaques were similar to those seen for WT and $\triangle$N40 viruses (Figure 6.7(A)).

All viral infections gave rise to high levels of released virus and viral proteins were detected at all time points examined (Figure 6.7(B and C)). Whereas PB1-F2 was absent in cells infected with $\triangle$AUG viruses and N40 was absent in cells infected with $\triangle$N40 viruses, PB1-F2 and N40 were detected in cells infected with a mixture of rWSN $\triangle$AUG and rWSN $\triangle$N40.

Regarding viral growth, findings could be summarised as follows:

(1) Under conditions of high MOI, $\triangle$AUG viruses grew similar or even better then WT viruses, whereas $\triangle$N40 viruses showed an attenuation.

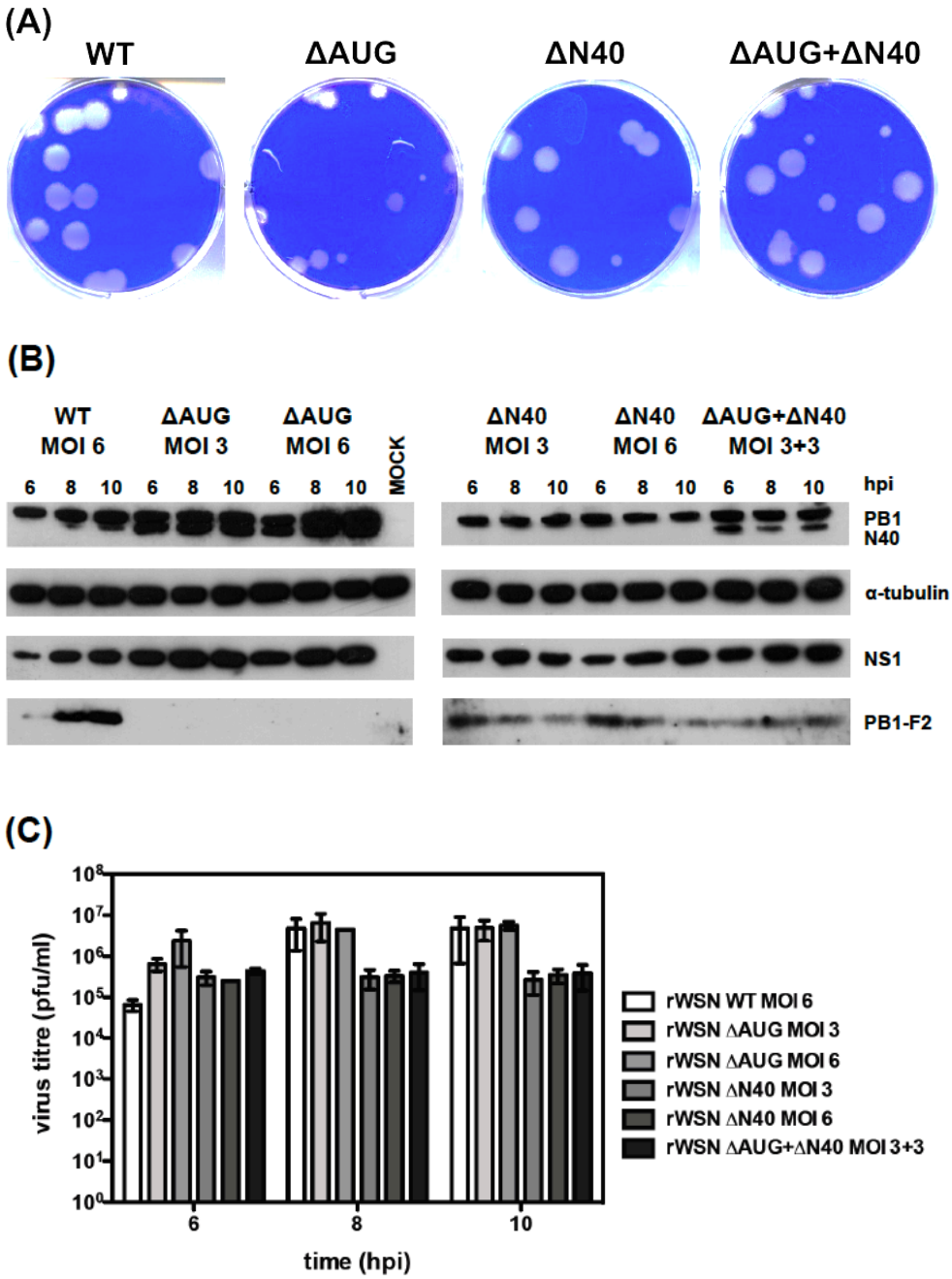

Figure 6.7: Comparison of *in vitro* phenotypes of WT, ΔAUG, ΔN40 and mixed infections: Triplicates of MDCK cell monolayers were infected with rWSN WT, rWSN ΔAUG, rWSN ΔN40 or a mixture of ΔAUG and ΔN40. **(A)** Supernatants were harvested at 8 hpi and plaque phenotype was determined. **(B)** At the indicated time points, cells were lysed and accumulation of viral proteins was determined by western blot analysis. 4-12% gradient Bis-Tris gels were used to detect PB1, N40 and NS1. 16% Tricine-SDS-PAGE was used to detect PB1-F2. α-tubulin was used as an internal loading control. **(C)** Supernatants were harvested at the indicated time points and viral growth was measured by plaque assay. Mean values $\pm$SEM of each set of triplicates are plotted.

(2) Only minor differences were observed comparing infections with MOI of 3 and MOI of 6. The differences in the percentage of infected cells for both MOI are thought to be small, as MOI of 3 led to 95%, MOI of 6 to about 99%, infected cells (Knipe et al., 2001).
(3) Viral growth in a mixed infection was more similar to growth seen for $\triangle$N40 virus rather than $\triangle$AUG virus infections.

6.4 Effect of loss of N40 on virulence in mice

Although previous reports linked the attenuated virulence in mice to the loss of PB1-F2, it is more likely that this attenuation was caused by a loss of PB1-F2 in combination with overexpression of N40 (Chapter 3: Section 3.3.5).
To determine the virulence of viruses deficient for N40, female BALB/c mice were infected intranasally with rWSN $\triangle$N40 or rWSN $\triangle$F2/$\triangle$N40 and compared to WT virus infections. Body weight was measured daily and four mice per group were culled at day 4 or day 7 in order to evaluate the viral lung titres. As can be seen in Figure 6.8(A), mice infected with rWSN $\triangle$N40 viruses lost weight similar to WT infected mice, whereas mice infected with rWSN $\triangle$F2/$\triangle$N40 viruses lost weight more slowly. At day 6 pi, these mice seemed to start gaining weight, which may be a sign for recovery. All infected mice showed symptoms of infection such as staring coat and increased respiratory effort. However, rWSN $\triangle$F2/$\triangle$N40 infected mice only started to show these symptoms after day 6, whereas WT and rWSN $\triangle$N40 virus infected mice showed symptoms as early as 4 dpi. Viral titres in the lungs measured at day 4 post infection were similar for all three viruses, but differences were observed at the later time point. Lung titres of mice infected with rWSN WT and rWSN $\triangle$N40 viruses were reduced by $\sim$ 10-fold compared to day 4 pi, however, PB1-F2/N40 double mutant viruses were reduced by almost 1000-fold at this time point (Figure 6.8(B)). These data correlate with the weight loss and the observed clinical signs.

At day 7 pi, lungs from two mice per group were taken for histology. Whereas lungs of mock-infected mice (PBS) had healthy lungs, all lungs of virus infected mice exhibited similar signs of infection. Immune cells were found in the interstitial region and within alveoli. Bronchus walls showed evidences of necrosis as the terminal airways contained cellular debris (Figure 6.9).

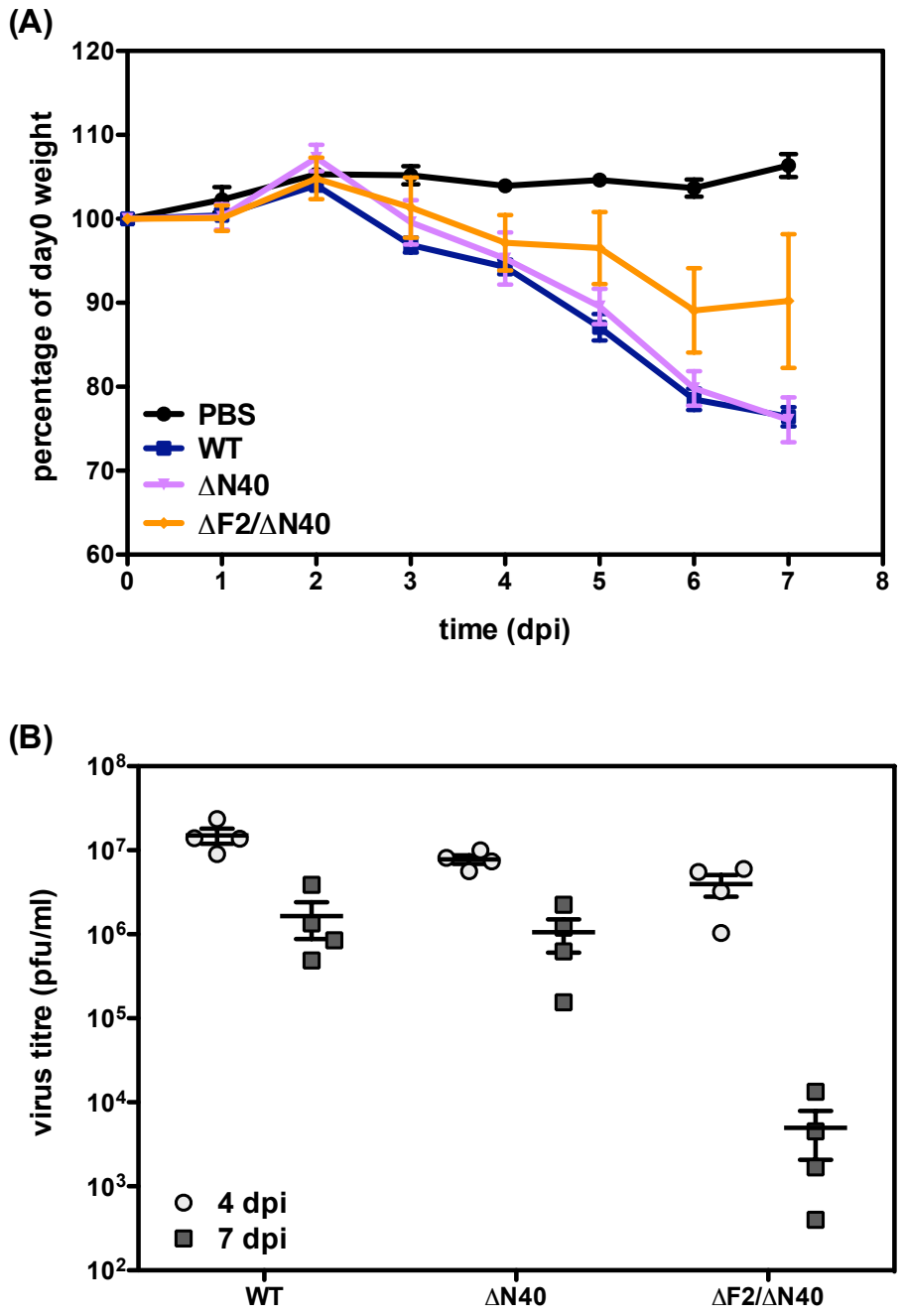

Figure 6.8: Virulence of the recombinant WSN viruses WT, ΔN40 and ΔF2/ΔN40 in mice: Groups of 8 female BALB/c mice were infected with the recombinant WSN viruses WT, ΔN40 andΔF2/ΔN40 with 5x10^3 pfu. **(A)** Weight loss was measured every day over a period of 7 days. Day 0 was set as 100% for each group. **(B)** At day 4 and day 7, 4 mice of each group were culled and lung virus titres were determined by plaque assay. Mean values ±SEM are plotted. Mouse infections were done in collaberation with B. Dutia and her lab at the University of Edinburgh.

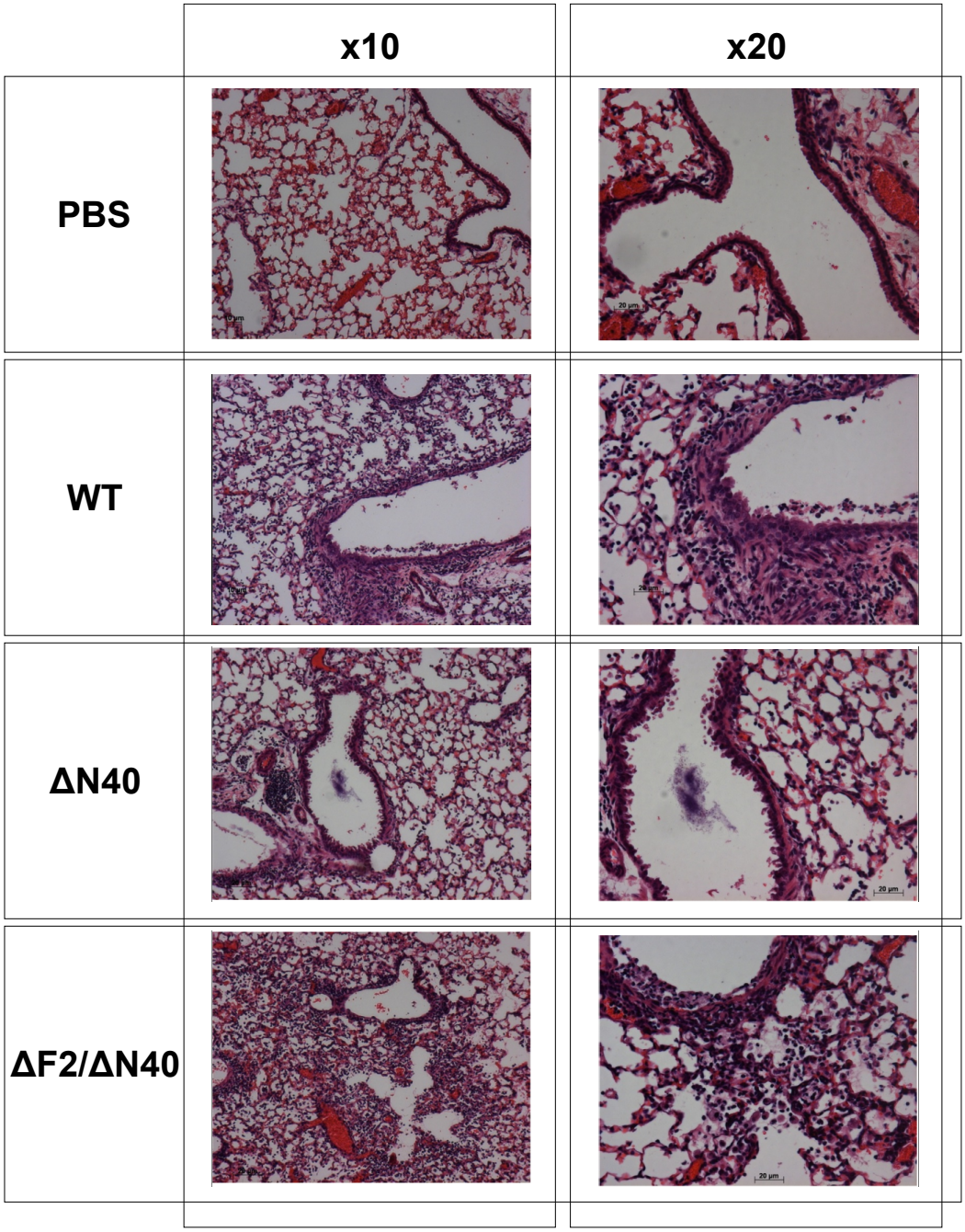

Figure 6.9: Histological section of lungs from BALB/c mice infected with WT WSN, ΔN40 and ΔF2/ΔN40 viruses: Mice were infected intranasally with $5x10^3$ pfu of the panel of recombinant WSN viruses - WT, ΔN40 and ΔF2/ΔN40. PBS served as a negative control. At day 7 pi lung sections were stained with Hematoxylin & Eosin. All virus infected mice showed markedly increased numbers of neutrophils in the alveoli as well as necrosis of the bronchus epithelial wall. This work was done with the help of Jill McVee, University of St Andrews.

To exclude the possibility that the viruses have acquired mutations that altered the expression level of PB1-F2 or N40, viral RNA of samples obtained at day 7 pi was isolated and the nucleotide sequence of segment 2 was determined. All mutations introduced by PCR-mediated site-directed mutagenesis were still in place (data not shown).

6.5 Effects of loss of PB1-F2 and N40 on viral gene expression and replication

6.5.1 *De novo* synthesis of viral proteins

The differences in the accumulation of PB1 in cells infected with viruses deficient for N40 observed by western blot analysis (Figure 6.6 (C)) were further analysed. MDCK cells were infected with PB1-F2 and N40 knockout viruses as well as the WT virus at an MOI of 3 and at the desired time points proteins were labelled with [^{35}S] methionine in order to determine the *de novo* synthesis of viral proteins. At the same time, the efficiency of host protein shut-off caused by influenza virus infections was monitored.
As can be seen in Figure 6.10 (A), all viruses efficiently produced viral proteins at all time points measured. No difference was observed for the shut-off of host cell protein synthesis. However, when quantifying protein synthesis using a Fluorescent Image Analyzer, some differences were noticed (Figure 6.10 (B)). Similar to the results in the western blot analysis (Figure 6.6 (C)), less synthesis of viral polymerase subunits (3 Pol) was observed for viruses deficient in their N40 expression. On the other hand, an increased synthesis of the three polymerase subunits was seen in cells infected with rWSN $\triangle$AUG compared to WT virus infected cells. A similar increase was noticed for the synthesis of NP in rWSN $\triangle$AUG infected cells. NS1 and M1 synthesis was overall equal for all viruses.

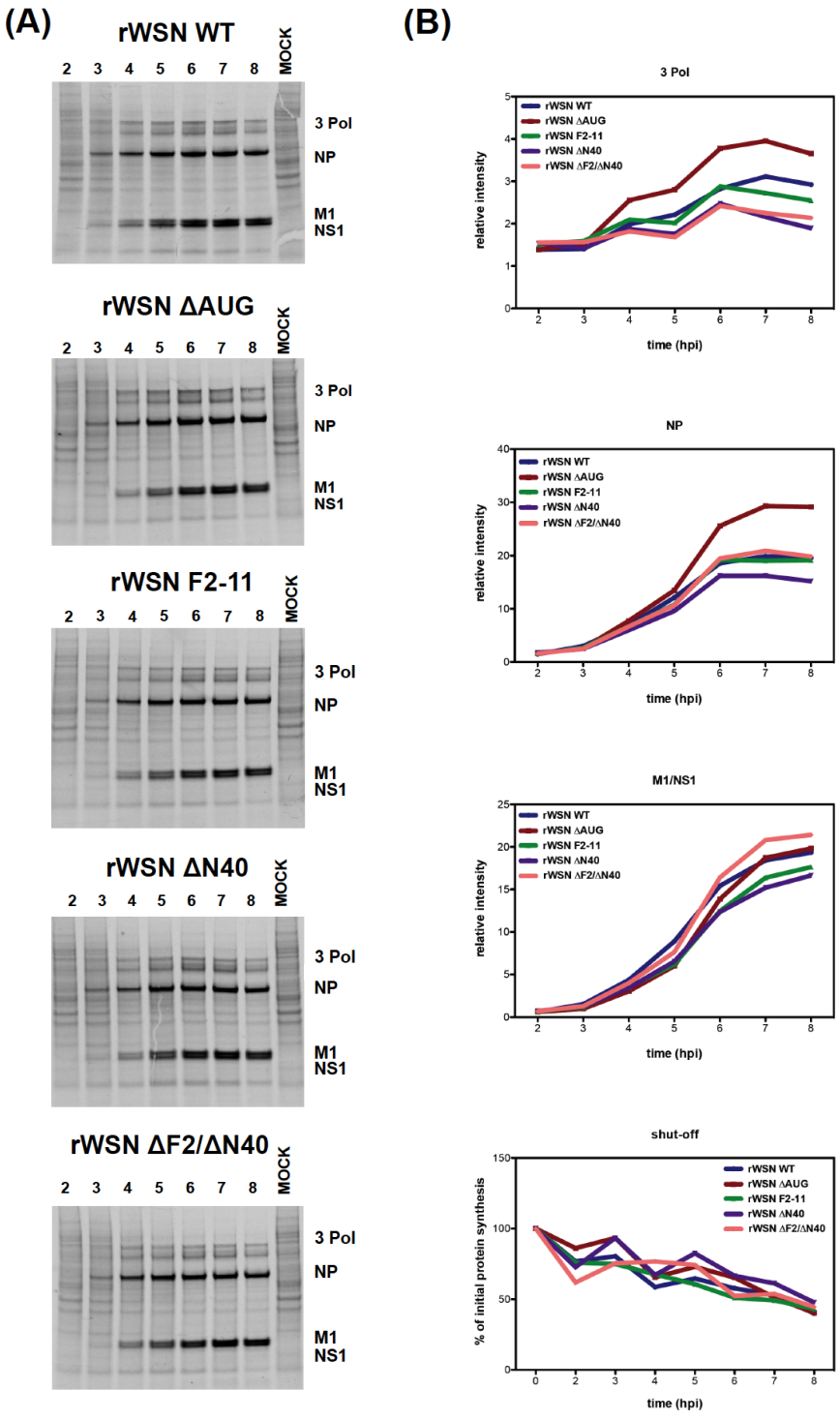

Figure 6.10: *De novo* synthesis and accumulation of viral proteins: MDCK cells were infected with the panel of viruses at an MOI of 3. Before adding methionine-free medium supplemented with 30 Ci/ml [^{35}S] methionine to the cells, cells were starved for methionine using methionine-free medium for 30 min. *De novo* synthesis of viral proteins, polymerase subunits (3 Pol), NP and M1/NS1, as well as host cell shut-off were quantified.

6.5.2 Influence of segment 2 gene products on polymerase activity

To determine whether the differences in viral protein synthesis had an influence on viral replication, the activity of the viral polymerase was tested in a mini-genome assay. Cells were cotransfected with plasmids expressing PB2, PA, NP and either PB1 WT or one of the PB1-F2 and N40 mutants. A plasmid encoding the vRNA for a virus-like Renilla luciferase was also transfected along with a transfection control plasmid expressing firefly luciferase under a CMV promoter. The Renilla luciferase was expressed efficiently and its activity was normalised and values were set to 100% for WT. This activity was compared to PB1-mutants deficient in PB1-F2 and / or N40 expression.

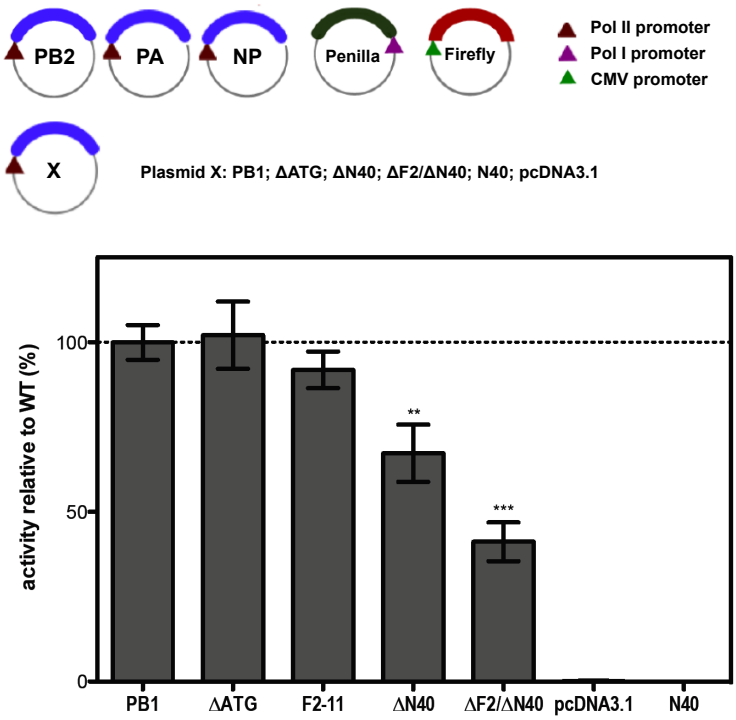

Figure 6.11: Effects of PB1-F2 and N40 on polymerase activity: Triplicates of 293FT cells were transfected with plasmids expressing PB2, PA and NP together with PB1 WT or one of the mutants deficient in PB1-F2 or N40. Activity was measured using a luciferase dual reporter assay (Promega). Values were normalised to transfection efficiency and expressed as activity compared to WT PB1. Mean values $\pm$SEM of three independent experiments are plotted. Asterisks indicate significant differences (*Student's t-test*: ** $P < 0.05$; *** $P < 0.001$).

The results are shown in Figure 6.11. The loss of PB1-F2 did not change the polymerase activity as long as N40 was still present. However, the loss of N40 led to a decrease in polymerase activity, which was enhanced by the loss of PB1-F2 (*Student's t-test*: $\triangle$N40 P=0.0059; $\triangle$F2/$\triangle$N40 P$<$0.0001). N40 was not able to replace PB1 in this system and only background Renilla activity was measured, similar to the empty vector pcDNA3.1. It should be noted that viruses knocked out for N40 have an amino acid change in the polymerase subunit PB1 and it can not be ruled out that the reduced polymerase activity is due to this mutation.

To evaluate the effect of PB1-F2 and N40 on these systems, plasmids expressing either protein were added to the transfection mixture. As shown in Figure 6.12, addition of PB1-F2, N40 or PB1-F2 and N40 to PB1, $\triangle$AUG or F2-11 did not alter the Renilla luciferase activity. A slight increase was seen when N40 was added to $\triangle$N40. Although this increase was not significant (*Student's t-test*: P=0.175), additional N40 may be counteracting the effects of the $\triangle$N40. If N40 or PB1-F2 was supplemented to $\triangle$F2/$\triangle$N40, only a small increase was noted. However, a significant change was observed when PB1-F2 and N40 were present and Renilla luciferase activity almost reached WT levels (Figure 6.12).

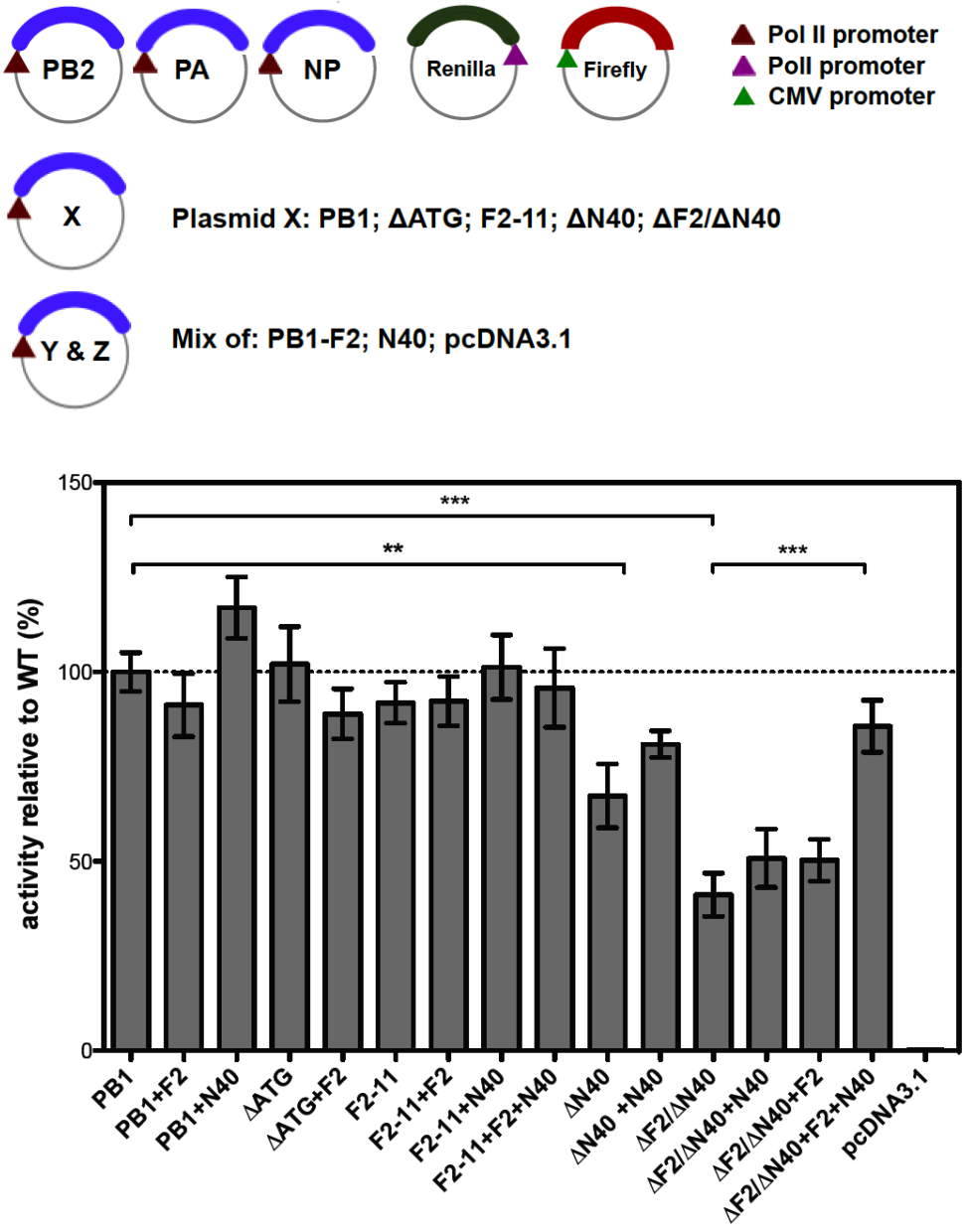

Figure 6.12: Effects of PB1-F2 and N40 on polymerase activity: Triplicate monolayers of 293FT cells were transfected with plasmids expressing PB2, PA and NP together with PB1 WT or one of the mutants deficient in PB1-F2 or N40. Additionally PB1-F2 and N40 were transfected as indicated. Activity was measured using a luciferase dual reporter assay (Promega). Values were normalised to transfection efficiency and expressed as activity compared to WT PB1. Mean values ±SEM of three independent experiments are plotted. Asterisks indicate significant differences (*Student's t-test*: ** $P < 0.05$; *** $P < 0.001$).

6.5.3 Effects of PB1-F2 and N40 on viral RNA accumulation

Overall, the loss of PB1-F2 alone did not affect viral polymerase activity, but the loss of N40 had a significant effect, which was enhanced by the loss of PB1-F2. Although rWSN △N40 and rWSN △F2/△N40 showed an attenuation in viral growth in a single-step cycle, they grew normally in a multi-step cycle and no decrease in plaque size was observed. To understand the results seen in a mini-genome assay better and to dissect the influence of segment 2 gene products on transcription and replication, primer extension assays were performed. A549 cells were infected with the different viruses and RNA was extracted at 3, 6 or 8 hpi. [γ-^{32}P]-ATP labelled primers specific for RNA segments 1, 6 or 8 were used to monitor viral mRNA, cRNA or vRNA synthesis in a Primer extension reaction. The synthesis of cellular 5S rRNA was used as internal control. Primer sequences are listed in Table 2.15 and a protocol of primer extensions is described in section 2.5.4. Products were separated on a 6% polyacrylamide/6M urea gel and detected by autoradiography. Expression levels of all RNA species at 8 hpi were quantified and normalised against 5S rRNA. Levels of RNA species of rWSN WT at each time point were set to 100%. As a comparison of the relative amounts of replication and transcription, the ratio between mRNA and cRNA (or vRNA for segment 8) was calculated. The results of the primer extension assays for segments 1, 6 and 8 are shown in Figures 6.13, 6.14 and 6.15, respectively.

All three viral RNA species and the cellular 5S rRNA were detected in the primer extension assay for segments 1 and 6. The levels of cRNA for segment 8, however, were very low, possibly due to difficulties with the available primer. Therefore, only mRNA and vRNA levels were quantified for segment 8. Other than for segments 1 and 6, the ratio of mRNA to vRNA was calculated for segment 8 to compare transcription to replication. Overall, the three tested segments showed similar results and some generalisation could be made.

(1) All viruses accumulated viral RNAs over time.

(2) Although the amounts of RNA species of the mutant viruses varied from WT virus, the ratios between the different RNA species for one segment remained similar.

(3) An exception was the △AUG virus. Accumulation of vRNA and cRNA were remarkably increased compared to mRNA levels. This led to a shift

towards replication in rWSN △AUG infected cells, as seen by the calculated ratios mRNA:c/vRNA.
However, none of these differences resulted in a change in viral titer (Figure 6.16).

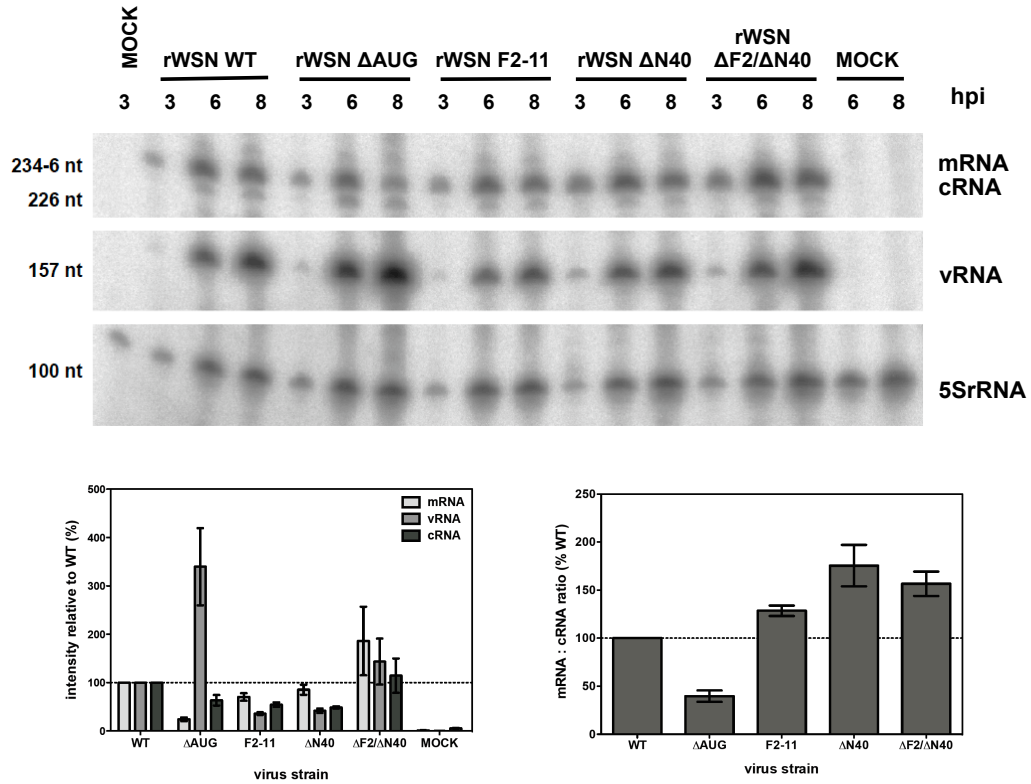

Figure 6.13: Primer extension assay segment 1: A549 cells were infected with the panel of viruses at an MOI of 3 and total RNA was extracted 3, 6 or 8 hpi. Accumulation of mRNA, cRNA, vRNA of segment 1 and cellular 5S rRNA was detected by primer extension. Products were separated on a 6% polyacrylamide/6M urea gel and detected by autoradiography. Quantification of the accumulation of mRNA, cRNA and vRNA at 8 hpi is shown. Values were normalised against cellular 5S rRNA and expressed as percentage ±SEM of WT activity. Results are based on three independent experiments. Ratios of quantified levels of mRNA and cRNA are shown. Error bars represent standard deviation of the mean (±SEM) based on three independent experiments.

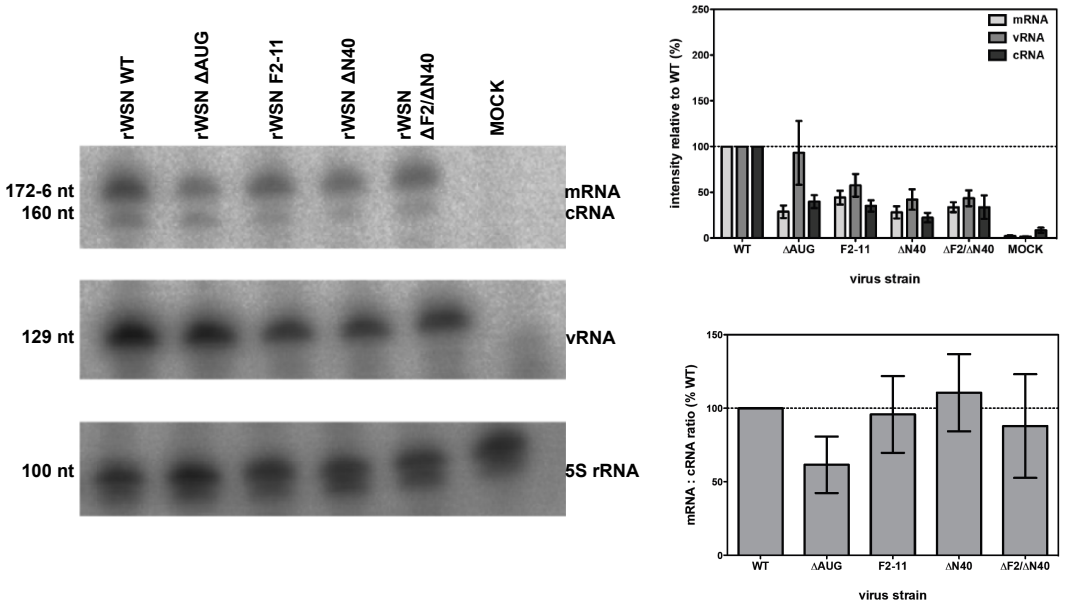

Figure 6.14: Primer extension assay segment 6: A549 cells were infected with the panel of viruses at an MOI of 3 and total RNA was extracted 8 hpi. Accumulation of mRNA, cRNA, vRNA of segment 6 and cellular 5S rRNA was detected by primer extension. Products were separated on a 6% polyacrylamide/6M urea gel and detected by autoradiography. Quantification of the accumulation of mRNA, cRNA and vRNA is shown. Values were normalised against cellular 5S rRNA and expressed as percentage $\pm$SEM of WT activity. Results are based on three independent experiments. Ratios of quantified levels of mRNA and cRNA are shown. Error bars represent standard deviation of the mean ($\pm$SEM) based on three independent experiments.

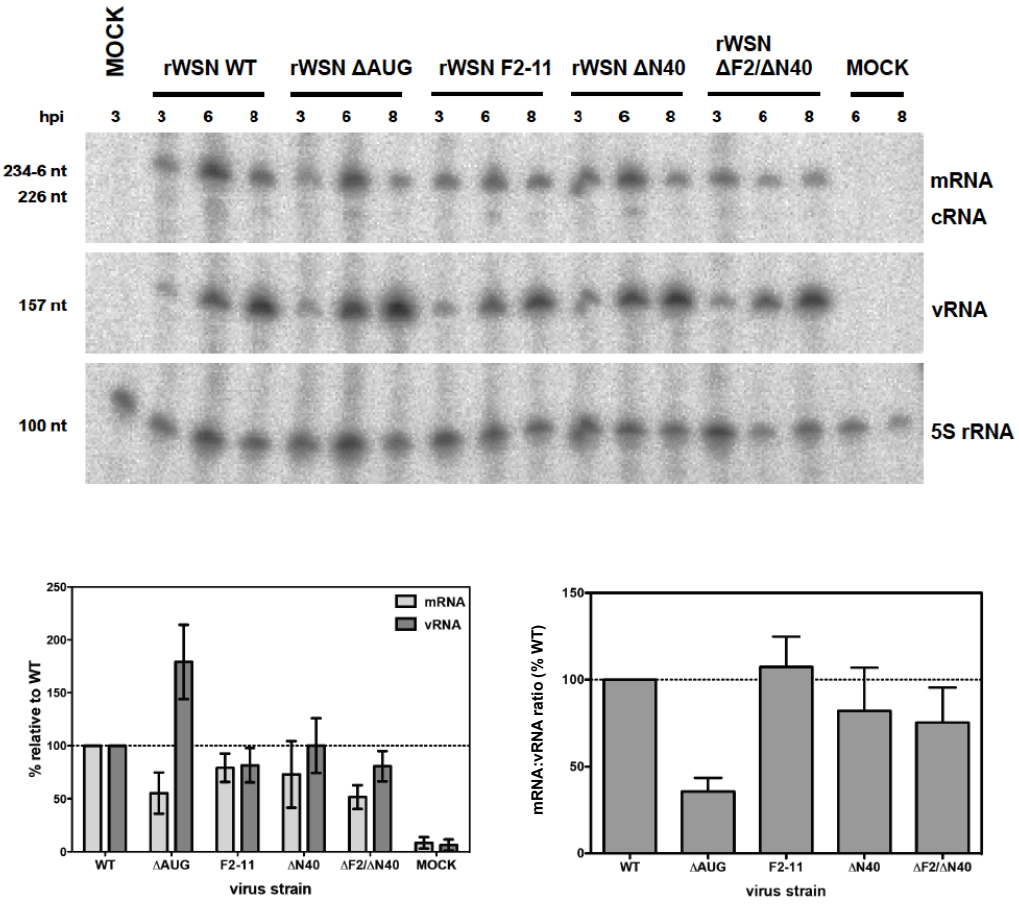

Figure 6.15: Primer extension assay segment 8: A549 cells were infected with the panel of viruses at an MOI of 3 and total RNA was extracted 3, 6 or 8 hpi. Accumulation of mRNA, cRNA, vRNA of NS1 and cellular 5S rRNA was detected by primer extension. Products were separated on a 6% polyacrylamide/6M urea gel and detected by autoradiography. Quantification of the accumulation of mRNA and vRNA at 8 hpi is shown. Values were normalised against cellular 5S rRNA and expressed as percentage ±SEM of WT activity. Results are based on three independent experiments. Ratios of quantified levels of mRNA and vRNA are shown. Error bars represent standard deviation of the mean (±SEM) based on three independent experiments.

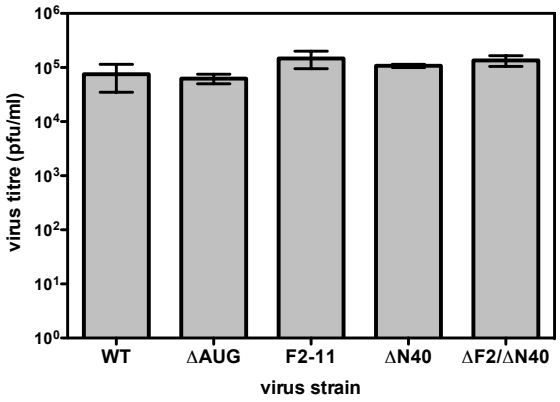

Figure 6.16: Viral titres of primer extension assay: A549 cells were infected with the panel of viruses at an MOI of 3. At 8 hpi, supernatants were harvested and viral titres were analysed by plaque assay. Results are based on three independent experiments. Error bars represent standard deviation of the mean ($\pm$SEM) based on three independent experiments.

6.6 Discussion

This chapter focussed on the influence of N40 and PB1-F2 on viral replication and transcription. Additional to the PB1-F2 mutant viruses described in Chapter 3 two more viruses were engineered, one lacking the N40 ORF, and the second mutant lacking PB1-F2 and N40 (rWSN $\triangle$N40 and rWSN $\triangle$F2/$\triangle$N40). Whereas a virus overexpressing N40 showed attenuation *in vitro* and *in vivo*, the loss of N40 did not have a great effect and viruses had a WT plaque phenotype and replicated normally in MDCK and A549 cells in a multi-step cycle (Figure 6.4, 6.5). However, when infecting at a high multiplicity, the loss of N40 had some disadvantageous effect on viral replication (Figure 6.6). Whether the loss of N40 itself or the altered level of PB1 expression was responsible for this is not known: the decrease in PB1 synthesis at later stages in infection was observed by western blot analysis (Figure 6.6(C)) and when examining synthesis of viral proteins by metabolic labelling (Figure 6.10). Opposite to the decreased levels of PB1 in N40 deficient cells, an increased level of the viral polymerase was found in cells infected with rWSN $\triangle$AUG viruses. However, it should be noted, that the three viral polymerase subunits could not be quantified separately in the metabolic labelling experiment due to their similar size. Therefore, the observed differences could be due to changes of either of the polymerase subunits. Additionally, the effect could also be caused by the enhanced presence or absence of N40 itself (Figure 6.10).

Expression of PB1-F2 and N40 may be explained by leaky ribosomal scanning, however the change in PB1 synthesis following the deletion of a downstream start codon is more difficult to understand. Digard's laboratory described previously an interdependency of the expression of all three segment 2 gene products that goes beyond leaky scanning (Wise et al., 2009). In this regard, the expression of the C-terminus of PB1-F2 was also suggested in previous studies (Figure 6.17(A)) (Zamarin et al., 2006). This would require bypassing six AUG codons including three in a strong sequence context. An observation made in western blot analysis using PB1 antibodies enhanced the discussion about an unusual expression mode for segment 2 (Figure 6.17(B)). Shorter products were detected, which may be degradation products of PB1. In this case it could be speculated that the presence or absence of N40 altered the stability of PB1. A second hypothesis would be that these products are expressed by an unknown

mechanism from AUG codons 10 or 11. Changes of the upstream AUG codons could alter their expression level. However, the expression level seemed to be independent from the number of upstream AUG codons. rWSN ΔAUG, rWSN ΔN40 and rWSN ΔF2/ΔN40 have one less AUG codon compared to WT and F2-11 viruses, but they differ in the appearance of these smaller products. When AUG4 was removed, more small downstream products were observed, whereas loss of AUG5 led to a reduction in the appearance of these downstream products.

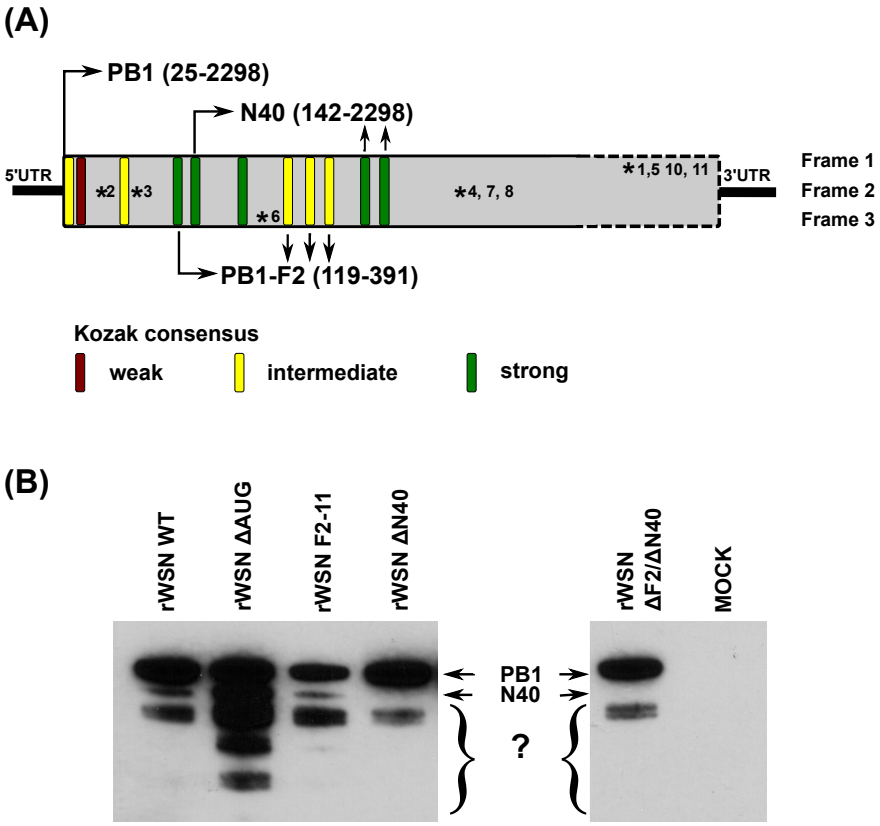

Figure 6.17: Extended analysis of the 5' end of segment 2 of A/WSN/33: (A) 11 AUG codons are present in the 5' end of segment 2. AUG1 initiates translation of PB1, AUG4 starts PB1-F2 and AUG5 N40. The short second, third and 6th ORFs do not encode a protein. AUG codons 7-9 are in frame 2 and were previously reported to express the C-terminus of PB1-F2 (Zamarin et al., 2006). AUG10 and 11 are within frame 1 and in a strong Kozak consensus context. Stop codons of the corresponding ORFs are shown within the graphic (*1-11). The Kozak consensus sequences of all AUGs are shown in different colors according to their strength. **(B)** Western blot analysis of segment 2 gene products. Additionally to the described products PB1 and N40, slightly smaller products could be found expressed from segment 2 and detected by the PB1 antibody.

How could such an hypothesis be explained? Ribosomes are thought to bind to capped 5'UTRs and start their scanning process until the first AUG is found to initiate translation (Kozak, 1999). However, many viruses have evolved mechanisms to overcome restrictions of genome size constraints by having polycistronic mRNAs. Expression of the individual genes is assured by different mechanisms, such as leaky ribosomal scanning, ribosomal shunting, use of internal ribosomal entry sites (IRES) or translation termination-reinitiation. Segment 2 of influenza A viruses code for up to three proteins in overlapping reading frames and the process by which they are expressed is at least partially by leaky ribosomal scanning (Chen et al., 2001; Wise et al., 2009). Hence, it would be unusual if AUG codons 10 or 11 are used to initiate translation by leaky scanning, because the ribosome would need to bypass several other AUGs, some in strong Kozak consensus sequences. However, several complex initiation strategies have been described for other viruses. The human papillomavirus type 16 encodes the two oncogenes E6 and E7 in one mRNA and the expression of E7 was shown to be due to an extreme process of leaky scanning bypassing up to 13 AUGs (Stacey et al., 2000). Another example was found for avian reoviruses. The three overlapping ORF from segment 1 were translated by leaky scanning and ribosomal shunting (Racine and Duncan, 2010). Just recently, a possible mechanism for the translation of influenza A virus segment 2 gene products was suggested (Wise et al., 2011). The short ORFs, between the ORFs for PB1 and PB1-F2, could have a regulatory function, with the main regulator being the short ORF2 translated from AUG3. This ORF was shown to suppress the expression of PB1-F2, but promote the expression of N40 by skipping AUG4 and directing ribosomes to AUG5 (Wise et al., 2011).

The function of N40 and even PB1-F2 are still under examination and many aspects are still unknown. One of these aspects may be a different role in human and avian cells. Leaky scanning processes were shown to be modulated by temperature (Liu et al., 1997). In this system, the first AUG was preferred at high temperatures, whereas at low temperatures the third AUG was favoured. Because humans and avian species differ in their normal temperatures, one could speculate about different expression levels of PB1, PB1-F2 and N40. If the amounts of the three proteins produced is important for viral pathogenicity in a particular host system, this could be a way of balancing the synthesis of segment 2 gene products.

Viral proteins interact with the cellular transcription and translation machinery as well as with cellular factors to down-regulate immune responses or induce apoptosis. Several viral and host cell proteins have been reported to interact with PB1. Among the viral proteins are the polymerase subunits PB2 and PA, the nucleoprotein, PB1-F2 and it was also suggested that PB1 interacts with itself. Cellular interaction partners are Hsp90, Hsp70, Ebp1 and RanBP5 (Naito et al., 2007; Mayer et al., 2007; Honda et al., 2007; Deng et al., 2006a). N40 may compete with PB1 for binding to some or all of of these proteins and in cells infected with rWSN $\triangle$AUG viruses, which overexpress N40, this competition may be disadvantageous for the virus. On the other hand, viruses deficient for N40 also showed some growth attenuation. Not all of the above mentioned proteins enhance viral replication. Hsp70 and Ebp1 were shown to interfere with viral growth (Honda et al., 2007; Li et al., 2011) and N40 may help to quench some of these effects by binding to these proteins rather than PB1. All of these interactions may have a hierarchy in timing or importance and the benefits of one or the other interaction remains unknown.

N40 itself could also have a function in the virus life cycle by modulating the viral polymerase activity. Results of the mini-genome assay would support this idea, as cells infected with plasmids deficient for N40 had a decreased polymerase activity (Figure 6.11 and 6.12). Primer extension assays showed a shift towards replication in cells infected with viruses overexpressing N40. Two options can be discussed:

(1) N40 helps to modulate the polymerase function and promotes replicase rather than transcriptase functions of PB1, or

(2) the shift is only a consequence of the increased levels of polymerase subunits and nucleoproteins observed in the protein labelling experiment.

The shift from transcription to replication is not fully understood yet. Several hypothesis have been suggested (Figure 6.18). Jorba et al. proposed a model in which the RNP-bound polymerase complex is responsible for transcription, whereas newly synthesised soluble polymerase complexes replicate the viral genome (Figure 6.18(A)) (Jorba et al., 2009). Other strategies suggest the involvement of small viral RNAs that derive from the 5' end of each segment (Figure 6.18(B)) (Perez et al., 2010; Scull and Rice, 2010). To what extent N40 may be involved in these processes is not known, but because N40 is proposed to bind several viral and host cell proteins it may have some influence. Another model for the switch from transcription

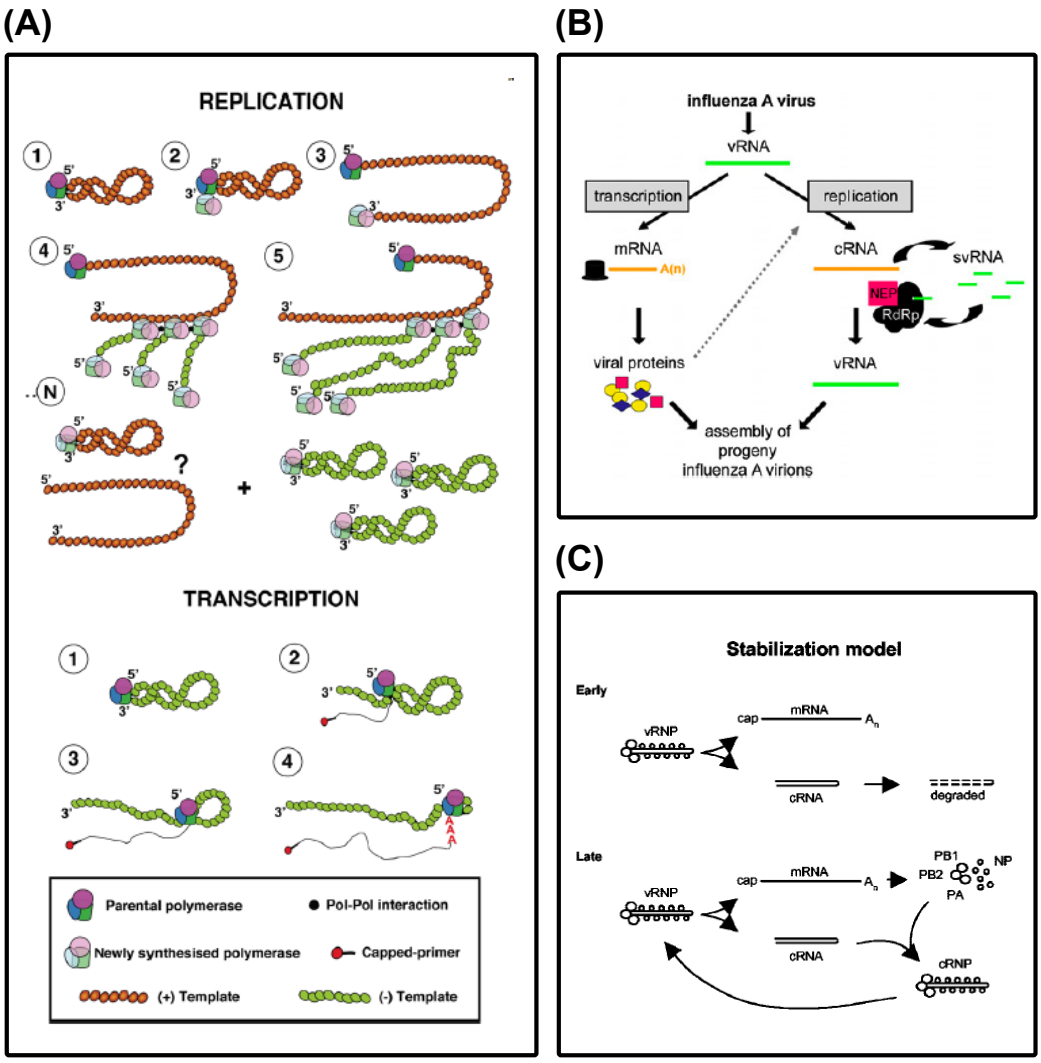

Figure 6.18: Summary of predicted models for the switch between transcription and replication: (A) Replication takes place by newly synthesised polymerase complexes coloured in semi-solid colouring. Transcription is fulfilled by the parental polymerase complex shown in solid colours. Picture taken from Jorba et al. (2009). **(B)** Synthesis of viral proteins and small viral RNAs is followed by replication. Taken from Scull and Rice (2010). **(C)** The stabilisation model was described by Vreede et al. (2004). Transcription and replication take place at the same time, but cRNA will be degraded until stabilised by newly synthesised NP and polymerase complexes.

to replication was suggested by Vreede et al. (Figure 6.18(C)) (Vreede et al., 2004). The authors proposed that both transcription and replication take place at the same time in infected cells. However at early times the replication intermediates are unstable and are likely degraded. Only later in infection, when appropriate amounts of nucleoprotein and polymerase

subunits are present, these RNA species are stabilised and replication occurs. This hypothesis would be in line with the increased levels of NP and polymerase subunits in cells infected with rWSN $\triangle$AUG viruses. Therefore, increased levels of cRNA and vRNA detected by primer extension assays may be due to higher degree of stabilisation of these RNA species. Support for this is provided by findings from Olsen et al., who suggested that high levels of viral polymerase promote replication (Olson et al., 2010).
The loss of N40 and PB1-F2 caused an attenuation to a higher degree than the loss of N40 alone (Figures 6.8 and 6.11). Replication deficits resulted in an intermediate phenotype of virulence in mice and virus was cleared more effectively from the lungs of infected mice. As seen in this Chapter and Chapter 3, the loss of either of the two proteins alone was not disadvantageous to the virus, however the alteration of both, PB1-F2 and N40, was. Efforts were made to restore the WT phenotype by infecting cells with a mixture of two viruses ($\triangle$AUG and $\triangle$N40). Ideally, cells would get co-infected with both viruses so that PB1-F2 and high levels of N40 were present in the same cell. However, the results were similar to those seen for infections with rWSN $\triangle$N40 viruses. Although infections with MOI of 3 should result in more than one virus particle in $\sim$ 80% of cells, an estimation of how many cells were infected with one particle of each of the two mutant viruses cannot be made. Alternatively, the combination of high levels of N40 and PB1-F2 does not have any advantage for the virus. To which degree each of the proteins plays a role remains unknown. The dynamics of expression of PB1, PB1-F2 and N40 and their localisation within the cell may be of some importance and may not exist in cells infected with a mix of rWSN $\triangle$AUG and rWSN $\triangle$N40.

Several differences were observed comparing the phenotypes of viruses carrying N40 deletion between the closely related strains A/WSN/33 and A/PR/8/34. Both plaque size and polymerase activity in a mini-genome assay varied. Although similar outcomes were expected due to the relatedness of the two virus strains, it should be noted that even different results for similar experiments using A/PR/8/34 were reported. For PB1-F2 deficient viruses overexpressing N40, plaques were reported to be smaller, similar or even bigger compared to WT viruses. A different influence on replication was also found (Wise et al., 2009; Mazur et al., 2008; McAuley et al., 2010b). Diverse variants of A/PR/8/34 have been shown to exist in laboratories around the world. These variants range from low virulence to

high virulence (Grimm et al., 2007; Blazejewska et al., 2011; Heynisch et al., 2010). If variants within one virus strain can cause different results, it may not be surprising that differences between two virus strains were observed. It has been suggested that a combination of changes in PB1-F2, PB2 and NS1 contribute to viral pathogenicity (Ozawa et al., 2011). It becomes more and more evident that influenza A viruses and their interactions with different hosts are very complex and studying one particular mutation may only shed light on one specific aspect.

Further studies will be necessary to define the roles of PB1-F2 and N40 in human or avian cells. A host-specific role is equally conceivable as a complex cooperation of all three segment 2 products.

6.7 Summary of Chapter 6

Additional to the segment 2 mutant viruses described in Chapter 3, two new viruses were engineered lacking the N40 ORF or PB1-F2 and N40 ORFs, respectively. A summary of the observed phenotypes is shown in Table 6.2.

Virus	Mutation	Protein levels	Phenotype
ΔN40	A142T	PB1: reduced PB1-F2: WT N40: null	normal plaque size WT phenotype *in vivo* Growth: attenuation (high MOI)
ΔF2/ΔN40	G144A G291A	PB1: reduced PB1-F2: null N40: null	normal plaque size attenuation *in vivo* Growth: attenuation (high MOI)

Table 6.2: Summary chapter 6

Viruses described in Chapter 3 and 6 were used to determine the influence of PB1, PB1-F2 and N40 on viral transcription and replication.
(1) Loss of N40 led to reduced polymerase activity, whereas the overexpression of N40 or the loss of PB1-F2 alone had no effect.
(2) Deletion of PB1-F2 (ΔAUG) or N40 resulted in changes in the expression level of PB1.
(3) Overexpression of N40 in a PB1-F2 deficient background caused a shift from transcription towards replication.

Taken together, PB1-F2 and N40 are likely to play some role in the influenza A virus life cycle, however the effects may also depend on other viral and cellular proteins. Regulation of expression of segment 2 gene products seems to be a complex process and further studies will be necessary to fully understand the interaction of these factors.

Chapter 7

CONCLUSIONS

7.1 Final remarks

When this project was started, the aim was to separate the PB1-F2 ORF from the underlying PB1 ORF. The idea was to delete PB1-F2 in its original position and insert it downstream of PB1 via three different methods. Deletion of PB1-F2 was done using a method described by Zamarin et al., introducing three point mutations including the removal of the start codon (Zamarin et al., 2006). The initial attempt to insert PB1-F2 into segment 2 did not result in a successful expression of PB1-F2. The second attempt was the insertion of the gene downstream of NA, which was more successful and the protein was expressed in high quantities. However, viruses were still attenuated, which made a mutational analysis of PB1-F2 difficult. Additionally the insertion into segment 6 via a duplicated promoter was not stable. Although not useful to study single aspects of PB1-F2 by introducing point mutations or deletions, the strategy provides a possible starting point for future evaluations. Antibodies against PB1-F2 were difficult to handle and detection of PB1-F2 in Western blots often resulted in high background. The separation of the PB1-F2 ORF from the PB1 ORF offers the possibility to add a short peptide onto PB1-F2 (V5-tag, FLAG-tag). This would help to detect and localise the protein within cells and may be of use when looking for additional interaction partners of PB1-F2. The stable insertion of PB1-F2 into segment 2 via FMDV 2A showed that influenza A viruses are highly flexible regarding their genome length.

The discovery of a third ORF expressed from segment 2 and the related consequences the removal of the PB1-F2 start codon had on the system influenced the direction of research in the present study (Wise et al., 2009). The comparison of the two PB1-F2 deletion mutants (△AUG and F2-11) showed that the loss of PB1-F2 was not the main factor for attenuation, whereas the loss of PB1-F2 in combination with an increased expression level of N40 was detrimental for the virus. Four major functions of PB1-F2 have been reported so far:

The protein was shown to induce apoptosis in a cell-dependent manner (Chen et al., 2001). It targets the mitochondrial membrane and interacts with two mitochondrial membrane proteins, ANT3 and VDAC1 (Zamarin et al., 2005). Two phosphorylation sites were identified that are critical for the mitochondrial localisation and the apoptotic function (Mitzner et al., 2009). Like other small viral pro-apoptotic proteins, the C-terminus of

PB1-F2 forms an amphipathic α-helix (Gibbs et al., 2003). How PB1-F2 induces apoptosis is not fully understood. One possible mechanism it that apoptosis is induced via the PTPC (Zamarin et al., 2005). It was also suggested that PB1-F2 oligomerises and forms a pore or ion channel in lipid bilayers, which could cause apoptosis (Chanturiya et al., 2004; Henkel et al., 2010). A dependency of BAK/BAX was also reported (McAuley et al., 2010a). However, the induction of apoptosis is restricted to a few viral strains (Chen et al., 2010; McAuley et al., 2010a).

In 2008, a second function was identified. Besides the mitochondrial membrane, PB1-F2 localised to the cytoplasm and nucleus of infected cells and this was connected to an interaction with the polymerase subunit PB1 (Mazur et al., 2008). An involvement of the protein in the regulation of the viral polymerase activity was suggested, however the positive effect was reported to be cell-type and virus-strain specific (Mazur et al., 2008; McAuley et al., 2010b; Chen et al., 2010).

Thirdly, infections with a virus deficient for PB1-F2 were less pathogenic and it was therefore suggested that the protein is a virulence factor (Zamarin et al., 2006). When PB1-F2 was absent, a decrease in inflammation and in the occurrence of secondary bacterial infections was found (McAuley et al., 2007). Amino acid 66 may be of particular interest in this context (Conenello et al., 2007, 2011).

Recent insights revolve mainly around the induction of IFN-β and other cytokines. PB1-F2 was reported to delay or even suppress the level of IFN-β in infected cells (Conenello et al., 2011; Varga et al., 2011). PB1-F2 containing 66S was reported to be more effective in antagonising the immune response. However, when PB1-F2 was deleted by removing the AUG in the PB1-F2 ORF, the expected increase in IFN-β expression did not occur, but the opposite effect was found (Goffic et al., 2010; Varga et al., 2011).

Many of these conclusions were based on findings made with viruses deficient for PB1-F2. However, with the discovery of N40 it became clear that the design of many of these viruses was not optimal as it changed the expression level of N40 (Wise et al., 2009; Chen et al., 2001; Zamarin et al., 2006). The comparison of viruses deficient for PB1-F2 but expressing different levels of N40 (Chapter 3 and 6) revealed that the loss of PB1-F2 alone (rWSN F2-11) was not sufficient to change the phenotype of A/WSN/33 to a great extent. The deletion of both ORFs

(rWSN $\triangle$F2/$\triangle$N40) had some negative effects on viral growth, polymerase activity and pathogenicity. More dramatic effects were seen with a virus that was knocked out for PB1-F2, but showed an increased level of N40 synthesis (rWSN $\triangle$AUG). This virus was attenuated in growth, apoptosis and pathogenicity in mice, and the polymerase showed a bias towards replication in primer extension assays, suggesting a new role for N40 in the viral life cycle. Expression of PB1-F2 in transfected cells showed that some of the above mentioned functions can be associated to the protein directly. PB1-F2 was shown to induce apoptosis possibly by interacting with VDAC1 and ANT3 in the mitochondrial membrane (Zamarin et al., 2005). It was also shown to suppress the induction of IFN-β expression via MAVS proteins (Varga et al., 2011). MAVS proteins were reported to be involved in IFN-β-expression following RIG-I activation and they are also important in the regulation of apoptosis by interacting with VDAC1 (Seth et al., 2005; Xu et al., 2005; Kawai et al., 2005; Meylan et al., 2005; Xu et al., 2010). The assumption seems alluring that PB1-F2 influences both cellular processes by interacting with MAVS, thereby linking and modulating the pathways. However, the role of N40 in this system remains obscure. Viruses only deficient for PB1-F2 show WT levels of apoptosis, but increased levels of N40 attenuated the virus in an so far unknown manner (Chapter 3). Additionally these viruses did not induce IFN-β expression (Varga et al., 2011).

PB1-F2 was reported to localise to the cytoplasm and nucleus and this was connected to an interaction with the polymerase subunit PB1 (Mazur et al., 2008). The domain for this interaction is not known, but it is possible that N40 retained the ability to interact with PB1-F2. The interaction with different partners in the cytoplasm and in the mitochondrial membrane may also be influenced by the conformation of PB1-F2, which was reported to vary depending on the hydrophobicity of the solvent (Chevalier et al., 2010). Also, the amino acid sequence of PB1-F2 in different virus strains could alter the stability of the secondary structure or the binding affinity to different interaction partners, which may explain the reported strain specificity of PB1-F2 on virus induced apoptosis and the regulation of polymerase activity (Chen et al., 2010; McAuley et al., 2010a).

The 5' UTR of segment 2 was shown to be highly complex. It combines elements that regulate the initiation of translation of PB1, PB1-F2 and N40 and it also contains segment-specific packaging signals (Wise et al., 2011).

Some of the effects found in this study and in the studies by Wise et al. showed that the influence of point mutations may not always be selective but they might be highly complex and unpredictable (Wise et al., 2009, 2011). It can be speculated that influenza A viruses code for more than 12 proteins and that fragments of already identified proteins or alternative splicing products may have some regulatory functions. The finding that segment 2 expresses additional N-terminal truncated fragments of PB1 is as intriguing as the observation that they show a different expression level depending on the removed upstream AUG (Figure 6.17). There are also reports about possible 13th or 14th proteins expressed from the influenza A virus genome. Human strains were reported to posses an ORF in the positive-sense orientation in segment 8 encoding a hypothetical transmembrane protein (Baez et al., 1981; Zhirnov et al., 2007). Due to the finding of cytotoxic T cells responding to epitopes derived from this ORF, it has been suggested that the protein is expressed (Clifford et al., 2009). Additionally, the existence of an M2 variant with an alternative ectodomain expressed from the second AUG of mRNA4 from segment 7 was suggested (Wise, personal communication; 2011). Some of these proteins might be more important in humans or in an avian host. This host specificity may be also possible for PB1-F2 and N40. So far, studies of the effect of PB1-F2 on avian hosts are limited. Three amino acid residues were determined to influence on viral pathogenicity in mallard ducks (residues 51, 56 and 87), which are different to the previously detected residue 66 that influences on the virulence in a mammalian host (Marjuki et al., 2010). Future work on PB1-F2 and N40 will be necessary to understand the role of these protein in different hosts and cell types and to define key residues.

7.2 Outlook

The strategy and the design of mutant viruses in order to study a protein or only one aspect of a protein becomes more and more important. The anticipated change of one ORF in segment 2 altered the level of a number of proteins and the effects seen are not always predictable. Also, a single mutation may not change the viral phenotype but the combination with other mutations in the same or other proteins could make a difference. Examples can be found in this work and outside. Ozawa et al. determined in a recent study that amino acids in three proteins influence viral pathogenicity but only

certain combinations had an effect (Ozawa et al., 2011). The amino acid 627 in PB2 is a well known residue that contributes to viral pathogenicity. However, other sites are at least as important. The H1N1 2009 pandemic strain does not contain the lysine residue that is thought to increase viral replication in humans, but amino acid 591 was found to compensate for the lack of lysine at position 627 (Yamada et al., 2010). The search for amino acids that are involved in the degradation of cellular RNA polymerase II showed that a combination of several amino acids is likely (Chapter 4). As an analogy, this seems like a big orchestra and every protein acts as one instrument with the cell as its concert hall. The piece of music played depends on each individual instrument and changing one violin string may change the sound of the piece of music. But it also depends on other instruments as well as on the concert hall. Therefore, changes may not be heard because they are covered by other instruments.

The role of the segment 2 proteins PB1-F2 and N40 seems even more unclear. The reported functions of PB1-F2 are mainly based on studies using the laboratory strain A/PR/8/34 and deletion viruses with an increased level of N40. The results of the work presented here show that the induction of apoptosis and the contribution to viral pathogenicity are not due to PB1-F2 alone, but the balance of PB1-F2, PB1 and N40. What role PB1-F2 plays remains unknown and requires further investigation. A possible new role for N40 was discovered. Although the mechanism is not known, high levels of N40 resulted in a switch from transcription to replication. This could be due to competition for viral and cellular interaction partners between PB1 and N40. Alternatively, N40 may act on the polymerase complex to alter the specificity for the vRNA or cRNA promoter. Additionally, viruses overexpressing N40 were highly attenuated *in vitro* and *in vivo*, interfering with the induction of apoptosis, viral growth and pathogenicity in mice. Further experiments should examine the influence of N40 in different virus strains, in mammalian and avian hosts, using similar approaches to design knockout viruses for PB1-F2 and/or N40. High levels of N40 in a PB1-F2 deficient background were most severe, but the effects could not be clearly addressed to overexpression of N40 alone or if the combination with the loss of PB1-F2 is important. Therefore high levels of N40 in combination with PB1-F2 expression may be studied to dissect the influence of each of the proteins on the virus attenuation. Because the engineering of such a virus is not possible, cells could be infected with a mixture of $\triangle$AUG and

△N40 viruses similar to the experiment explained in Section 6.3 but using higher MOI to increase to possibility that the majority of cells is co-infected with one of the two viruses. Alternatively cells could be transfected with plasmids expressing N40 or PB1-F2 following an infection with WT viruses or △AUG viruses, respectively. However, it is of importance that mutations are chosen in a careful way and that changes are studied in an authentic genetic background avoiding the use of chimeric viruses.

More work will be necessary to fully understand these fascinating viruses and the relationship between the virus and its host, the interaction between viral proteins and host proteins, the influence of the host towards pathogenesis or the importance of a possible hierarchy of events within the host cell. Although Influenza A viruses are one of the most researched viruses, they are still full of surprises and new exciting discoveries are continued to be made. Without question, these new insights will also open new questions: The more you learn, the more you realise how little you know.

Bibliography

Ahmadian, G., Randhawa, J. S., and Easton, A. J. (2000). Expression of the ORF-2 protein of the human respiratory syncytial virus M2 gene is initiated by a ribosomal termination-dependent reinitiation mechanism. *EMBO J*, 19(11):2681–9.

Albariño, C. G., Bird, B. H., Chakrabarti, A. K., Dodd, K. A., Erickson, B. R., and Nichol, S. T. (2011). Efficient rescue of recombinant Lassa virus reveals the influence of S segment noncoding regions on virus replication and virulence. *Journal of Virology*, 85(8):4020–4.

Alberts, R., Srivastava, B., Wu, H., Viegas, N., Geffers, R., Klawonn, F., Novoselova, N., do Valle, T. Z., Panthier, J.-J., and Schughart, K. (2010). Gene expression changes in the host response between resistant and susceptible inbred mouse strains after influenza A infection. *Microbes Infect*, 12(4):309–18.

Alonso-Caplen, F. V., Nemeroff, M. E., Qiu, Y., and Krug, R. M. (1992). Nucleocytoplasmic transport: the influenza virus NS1 protein regulates the transport of spliced NS2 mRNA and its precursor NS1 mRNA. *Genes & Development*, 6(2):255–67.

Amorim, M. J., Bruce, E. A., Read, E. K. C., Foeglein, A., Mahen, R., Stuart, A. D., and Digard, P. (2011). A Rab11- and microtubule-dependent mechanism for cytoplasmic transport of influenza A virus viral RNA. *Journal of Virology*, 85(9):4143–56.

Andersen, J. L., Dehart, J. L., Zimmerman, E. S., Ardon, O., Kim, B., Jacquot, G., Benichou, S., and Planelles, V. (2006). HIV-1 Vpr-induced apoptosis is cell cycle dependent and requires Bax but not ANT. *PLoS Pathogens*, 2(12):e127.

Argos, P. (1988). A sequence motif in many polymerases. *Nucleic Acids Research*, 16(21):9909–16.

Azzeh, M., Flick, R., and Hobom, G. (2001). Functional analysis of the influenza A virus cRNA promoter and construction of an ambisense transcription system. *Virology*, 289(2):400–10.

Baez, M., Zazra, J. J., Elliott, R. M., Young, J. F., and Palese, P. (1981). Nucleotide sequence of the influenza A/duck/Alberta/60/76 virus NS RNA:

conservation of the NS1/NS2 overlapping gene structure in a divergent influenza virus RNA segment. *Virology*, 113(1):397–402.

Beaton, A. R. and Krug, R. M. (1981). Selected host cell capped RNA fragments prime influenza viral RNA transcription in vivo. *Nucleic Acids Research*, 9(17):4423–36.

Beaton, A. R. and Krug, R. M. (1986). Transcription antitermination during influenza viral template RNA synthesis requires the nucleocapsid protein and the absence of a 5' capped end. *Proc Natl Acad Sci USA*, 83(17):6282–6.

Bellini, W. J., Englund, G., Rozenblatt, S., Arnheiter, H., and Richardson, C. D. (1985). Measles virus P gene codes for two proteins. *Journal of Virology*, 53(3):908–19.

Belzacq, A.-S., Vieira, H. L. A., Kroemer, G., and Brenner, C. (2002). The adenine nucleotide translocator in apoptosis. *Biochimie*, 84(2-3):167–76.

Biswas, S. K., Boutz, P. L., and Nayak, D. P. (1998). Influenza virus nucleoprotein interacts with influenza virus polymerase proteins. *Journal of Virology*, 72(7):5493–501.

Biswas, S. K. and Nayak, D. P. (1994). Mutational analysis of the conserved motifs of influenza A virus polymerase basic protein 1. *Journal of Virology*, 68(3):1819–26.

Blaas, D., Patzelt, E., and Kuechler, E. (1982). Identification of the cap binding protein of influenza virus. *Nucleic Acids Research*, 10(15):4803–12.

Blazejewska, P., Koscinski, L., Viegas, N., Anhlan, D., Ludwig, S., and Schughart, K. (2011). Pathogenicity of different PR8 influenza A virus variants in mice is determined by both viral and host factors. *Virology*, 412:36–45.

Boon, A. C. M., deBeauchamp, J., Hollmann, A., Luke, J., Kotb, M., Rowe, S., Finkelstein, D., Neale, G., Lu, L., Williams, R. W., and Webby, R. J. (2009). Host genetic variation affects resistance to infection with a highly pathogenic H5N1 influenza A virus in mice. *Journal of Virology*, 83(20):10417–26.

Bouloy, M., Plotch, S. J., and Krug, R. M. (1978). Globin mRNAs are primers for the transcription of influenza viral RNA in vitro. *Proc Natl Acad Sci USA*, 75(10):4886–90.

Bourmakina, S. V. and García-Sastre, A. (2005). The morphology and composition of influenza A virus particles are not affected by low levels of M1 and M2 proteins in infected cells. *Journal of Virology*, 79(12):7926–32.

Braam, J., Ulmanen, I., and Krug, R. (1983). Molecular model of a eucaryotic transcription complex: functions and movements of influenza P proteins during capped RNA-primed transcription. *Cell*, 34:609–618.

Bridgen, A. and Elliott, R. M. (1996). Rescue of a segmented negative-strand RNA virus entirely from cloned complementary DNAs. *Proc Natl Acad Sci USA*, 93(26):15400–4.

Bruce, E. A., Digard, P., and Stuart, A. D. (2010). The Rab11 pathway is required for influenza A virus budding and filament formation. *Journal of Virology*, 84(12):5848–59.

Bruns, K., Studtrucker, N., Sharma, A., Fossen, T., Mitzner, D., Eissmann, A., Tessmer, U., Röder, R., Henklein, P., Wray, V., and Schubert, U. (2007). Structural characterization and oligomerization of PB1-F2, a proapoptotic influenza A virus protein. *J Biol Chem*, 282(1):353–63.

Bullido, R., Gómez-Puertas, P., Albo, C., and Portela, A. (2000). Several protein regions contribute to determine the nuclear and cytoplasmic localization of the influenza A virus nucleoprotein. *J Gen Virol*, 81(Pt 1):135–42.

Caton, A. J. and Robertson, J. S. (1980). Structure of the host-derived sequences present at the 5' ends of influenza virus mRNA. *Nucleic Acids Research*, 8(12):2591–603.

Cattaneo, R., Kaelin, K., Baczko, K., and Billeter, M. A. (1989). Measles virus editing provides an additional cysteine-rich protein. *Cell*, 56(5):759–64.

Chanturiya, A. N., Basañez, G., Schubert, U., Henklein, P., Yewdell, J. W., and Zimmerberg, J. (2004). PB1-F2, an influenza A virus-encoded proapoptotic mitochondrial protein, creates variably sized pores in planar lipid membranes. *Journal of Virology*, 78(12):6304–12.

Chen, C.-J., Chen, G.-W., Wang, C.-H., Huang, C.-H., Wang, Y.-C., and Shih, S.-R. (2010). Differential localization and function of PB1-F2 derived from different strains of influenza A virus. *Journal of Virology*, 84(19):10051–62.

Chen, W., Calvo, P. A., Malide, D., Gibbs, J., Schubert, U., Bacik, I., Basta, S., O'Neill, R., Schickli, J., Palese, P., Henklein, P., Bennink, J. R., and Yewdell, J. W. (2001). A novel influenza A virus mitochondrial protein that induces cell death. *Nat Med*, 7(12):1306–12.

Chen, Z. and Krug, R. M. (2000). Selective nuclear export of viral mRNAs in influenza-virus-infected cells. *Trends Microbiol*, 8(8):376–83.

Chen, Z., Li, Y., and Krug, R. M. (1999). Influenza A virus NS1 protein targets poly(A)-binding protein II of the cellular 3'-end processing machinery. *EMBO J*, 18(8):2273–83.

Cheng, E. H., Wei, M. C., Weiler, S., Flavell, R. A., Mak, T. W., Lindsten, T., and Korsmeyer, S. J. (2001). BCL-2, BCL-X(L) sequester BH3 domain-only molecules preventing BAX- and BAK-mediated mitochondrial apoptosis. *Mol Cell*, 8(3):705–11.

Chevalier, C., Bazzal, A. A., Vidic, J., Fevrier, V., Bourdieu, C., Bouguyon, E., Goffic, R. L., Vautherot, J.-F., Bernard, J., Moudjou, M., Noinville, S., Chich, J.-F., Costa, B. D., Rezaei, H., and Delmas, B. (2010). PB1-F2 influenza a virus protein adopts a beta-sheet conformation and forms amyloid fibers in membrane environments. *J Biol Chem*, 285:13233–13243.

Child, S. J., Miller, M. K., and Geballe, A. P. (1999). Translational control by an upstream open reading frame in the HER-2/neu transcript. *J Biol Chem*, 274(34):24335–41.

Clifford, M., Twigg, J., and Upton, C. (2009). Evidence for a novel gene associated with human influenza A viruses. *Virol J*, 6:198.

Conenello, G. M. and Palese, P. (2007). Influenza A virus PB1-F2: a small protein with a big punch. *Cell Host & Microbe*, 2(4):207–9.

Conenello, G. M., Tisoncik, J. R., Rosenzweig, E., Varga, Z. T., Palese, P., and Katze, M. G. (2011). A single N66S mutation in the PB1-F2 protein of influenza A virus increases virulence by inhibiting the early interferon response in vivo. *Journal of Virology*, 85(2):652–62.

Conenello, G. M., Zamarin, D., Perrone, L. A., Tumpey, T., and Palese, P. (2007). A single mutation in the PB1-F2 of H5N1 (HK/97) and 1918 influenza A viruses contributes to increased virulence. *PLoS Pathogens*, 3(10):1414–21.

Cox, N. J., Neumann, G., Donis, R. O., and Kawaoka, Y. (2005). Orthomyxoviruses: Influenza. *Topley & Wilson's Microbiology and Microbial Infections*, pages 634–698.

Crescenzo-Chaigne, B. and van der Werf, S. (2007). Rescue of influenza C virus from recombinant DNA. *Journal of Virology*, 81(20):11282–9.

Cuconati, A., Degenhardt, K., Sundararajan, R., Anschel, A., and White, E. (2002). Bak and Bax function to limit adenovirus replication through apoptosis induction. *Journal of Virology*, 76(9):4547–58.

D'Agostino, D. M., Ranzato, L., Arrigoni, G., Cavallari, I., Belleudi, F., Torrisi, M. R., Silic-Benussi, M., Ferro, T., Petronilli, V., Marin, O., Chieco-Bianchi, L., Bernardi, P., and Ciminale, V. (2002). Mitochondrial alterations induced by the p13II protein of human T-cell leukemia virus type 1. Critical role of arginine residues. *J Biol Chem*, 277(37):34424–33.

D'agostino, D. M., Silic-Benussi, M., Hiraragi, H., Lairmore, M. D., and Ciminale, V. (2005). The human T-cell leukemia virus type 1 p13II protein: effects on mitochondrial function and cell growth. *Cell Death Differ*, 12 Suppl 1:905–15.

de Jong, M. D., Simmons, C. P., Thanh, T. T., Hien, V. M., Smith, G. J. D., Chau, T. N. B., Hoang, D. M., Chau, N. V. V., Khanh, T. H., Dong, V. C., Qui, P. T., Cam, B. V., Ha, D. Q., Guan, Y., Peiris, J. S. M., Chinh, N. T., Hien, T. T., and Farrar, J. (2006). Fatal outcome of human influenza A (H5N1) is associated with high viral load and hypercytokinemia. *Nat Med*, 12(10):1203–7.

de Wit, E., Spronken, M. I. J., Vervaet, G., Rimmelzwaan, G. F., Osterhaus, A. D. M. E., and Fouchier, R. A. M. (2007). A reverse-genetics system for Influenza A virus using T7 RNA polymerase. *J Gen Virol*, 88(Pt 4):1281–7.

Deng, T., Engelhardt, O. G., Thomas, B., Akoulitchev, A. V., Brownlee, G. G., and Fodor, E. (2006a). Role of ran binding protein 5 in nuclear import and assembly of the influenza virus RNA polymerase complex. *Journal of Virology*, 80(24):11911–9.

Deng, T., Sharps, J., Fodor, E., and Brownlee, G. G. (2005). In vitro assembly of PB2 with a PB1-PA dimer supports a new model of assembly of influenza A virus polymerase subunits into a functional trimeric complex. *Journal of Virology*, 79(13):8669–74.

Deng, T., Vreede, F. T., and Brownlee, G. G. (2006b). Different de novo initiation strategies are used by influenza virus RNA polymerase on its cRNA and viral RNA promoters during viral RNA replication. *Journal of Virology*, 80(5):2337–48.

Detjen, B. M., Angelo, C. S., Katze, M. G., and Krug, R. M. (1987). The Three Influenza Virus Polymerase (P) Proteins Not Associated with Viral Nucleocapsids in the Infected Cell Are in the Form of a Complex. *Journal of Virology*, 61:1–7.

Dias, A., Bouvier, D., Crépin, T., Mccarthy, A. A., Hart, D. J., Baudin, F., Cusack, S., and Ruigrok, R. W. H. (2009). The cap-snatching endonuclease of influenza virus polymerase resides in the PA subunit. *Nature*, 458(7240):914–8.

Digard, P., Tiley, L., and Elton, D. (2009). Viral Genome Replication: Chapter 9 Orthomyxovirus Genome Transcription and Replication. *Springer US*, pages 163–180.

Doms, R. W., Lamb, R. A., Rose, J. K., and Helenius, A. (1993). Folding and assembly of viral membrane proteins. *Virology*, 193(2):545–62.

Donnelly, M. L., Gani, D., Flint, M., Monaghan, S., and Ryan, M. D. (1997). The cleavage activities of aphthovirus and cardiovirus 2A proteins. *J Gen Virol*, 78 (Pt 1):13–21.

Donnelly, M. L., Luke, G., Mehrotra, A., Li, X., Hughes, L. E., Gani, D., and Ryan, M. D. (2001). Analysis of the aphthovirus 2A/2B polyprotein 'cleavage' mechanism indicates not a proteolytic reaction, but a novel translational effect: a putative ribosomal 'skip'. *J Gen Virol*, 82(Pt 5):1013–25.

Dunn, E. F., Pritlove, D. C., Jin, H., and Elliott, R. M. (1995). Transcription of a recombinant bunyavirus RNA template by transiently expressed bunyavirus proteins. *Virology*, 211(1):133–43.

Ehrhardt, C., Wolff, T., Pleschka, S., Planz, O., Beermann, W., Bode, J. G., Schmolke, M., and Ludwig, S. (2007). Influenza A virus NS1 protein activates the PI3K/Akt pathway to mediate antiapoptotic signaling responses. *Journal of Virology*, 81(7):3058–67.

Eisfeld, A. J., Kawakami, E., Watanabe, T., Neumann, G., and Kawaoka, Y. (2011). RAB11A Is Essential for Transport of the Influenza Virus Genome to the Plasma Membrane. *Journal of Virology*, 85(13):6117–26.

Elliott, R. M. (1989). Nucleotide sequence analysis of the small (S) RNA segment of Bunyamwera virus, the prototype of the family Bunyaviridae. *J Gen Virol*, 70 (Pt 5):1281–5.

Elton, D., Simpson-Holley, M., Archer, K., Medcalf, L., Hallam, R., McCauley, J., and Digard, P. (2001). Interaction of the influenza virus nucleoprotein with the cellular CRM1-mediated nuclear export pathway. *Journal of Virology*, 75(1):408–19.

Emonet, S. F., Seregin, A. V., Yun, N. E., Poussard, A. L., Walker, A. G., de la Torre, J. C., and Paessler, S. (2011). Rescue from cloned cDNAs and in vivo characterization of recombinant pathogenic Romero and live-attenuated Candid #1 strains of Junin virus, the causative agent of Argentine hemorrhagic fever disease. *Journal of Virology*, 85(4):1473–83.

Enami, M., Luytjes, W., Krystal, M., and Palese, P. (1990). Introduction of site-specific mutations into the genome of influenza virus. *Proc Natl Acad Sci USA*, 87(10):3802–5.

Enami, M. and Palese, P. (1991). High-efficiency formation of influenza virus transfectants. *Journal of Virology*, 65(5):2711–3.

Engelhardt, O. G. and Fodor, E. (2006). Functional association between viral and cellular transcription during influenza virus infection. *Rev. Med. Virol.*, 16(5):329–45.

Engelhardt, O. G., Smith, M., and Fodor, E. (2005). Association of the influenza A virus RNA-dependent RNA polymerase with cellular RNA polymerase II. *Journal of Virology*, 79(9):5812–8.

Flick, R. and Hobom, G. (1999a). Interaction of influenza virus polymerase with viral RNA in the 'corkscrew' conformation. *J Gen Virol*, 80 (Pt 10):2565–72.

Flick, R. and Hobom, G. (1999b). Transient bicistronic vRNA segments for indirect selection of recombinant influenza viruses. *Virology*, 262(1):93–103.

Flick, R., Neumann, G., Hoffmann, E., Neumeier, E., and Hobom, G. (1996). Promoter elements in the influenza vRNA terminal structure. *RNA*, 2(10):1046–57.

Flory, E., Kunz, M., Scheller, C., Jassoy, C., Stauber, R., Rapp, U. R., and Ludwig, S. (2000). Influenza virus-induced NF-kappaB-dependent gene expression is mediated by overexpression of viral proteins and involves oxidative radicals and activation of IkappaB kinase. *J Biol Chem*, 275(12):8307–14.

Fodor, E., Devenish, L., Engelhardt, O. G., Palese, P., Brownlee, G. G., and García-Sastre, A. (1999). Rescue of influenza A virus from recombinant DNA. *Journal of Virology*, 73(11):9679–82.

Fodor, E., Poon, L. L. M., Mikulasova, A., Mingay, L. J., and Brownlee, G. G. (2001). Transcription of influenza A virus genes. *International Congress Series*, pages 427–434.

Fodor, E., Pritlove, D. C., and Brownlee, G. G. (1994). The influenza virus panhandle is involved in the initiation of transcription. *Journal of Virology*, 68(6):4092–6.

Fortes, P., Beloso, A., and Ortín, J. (1994). Influenza virus NS1 protein inhibits pre-mRNA splicing and blocks mRNA nucleocytoplasmic transport. *EMBO J*, 13(3):704–12.

Fouchier, R. A. M., Munster, V., Wallensten, A., Bestebroer, T. M., Herfst, S., Smith, D., Rimmelzwaan, G. F., Olsen, B., and Osterhaus, A. D. M. E. (2005). Characterization of a novel influenza A virus hemagglutinin subtype (H16) obtained from black-headed gulls. *Journal of Virology*, 79(5):2814–22.

Fouchier, R. A. M., Schneeberger, P. M., Rozendaal, F. W., Broekman, J. M., Kemink, S. A. G., Munster, V., Kuiken, T., Rimmelzwaan, G. F., Schutten, M., Doornum, G. J. J. V., Koch, G., Bosman, A., Koopmans, M., and Osterhaus, A. D. M. E. (2004). Avian influenza A virus (H7N7) associated with human conjunctivitis and a fatal case of acute respiratory distress syndrome. *Proc Natl Acad Sci USA*, 101(5):1356–61.

Fujii, Y., Goto, H., Watanabe, T., Yoshida, T., and Kawaoka, Y. (2003). Selective incorporation of influenza virus RNA segments into virions. *Proc Natl Acad Sci USA*, 100(4):2002–7.

Gack, M. U., Albrecht, R. A., Urano, T., Inn, K.-S., Huang, I.-C., Carnero, E., Farzan, M., Inoue, S., Jung, J. U., and García-Sastre, A. (2009). Influenza A virus NS1 targets the ubiquitin ligase TRIM25 to evade recognition by the host viral RNA sensor RIG-I. *Cell Host & Microbe*, 5(5):439–49.

Galinski, M. S., Troy, R. M., and Banerjee, A. K. (1992). RNA editing in the phosphoprotein gene of the human parainfluenza virus type 3. *Virology*, 186(2):543–50.

Galluzzi, L., Brenner, C., Morselli, E., Touat, Z., and Kroemer, G. (2008). Viral control of mitochondrial apoptosis. *PLoS Pathogens*, 4(5):e1000018.

García-Sastre, A., Egorov, A., Matassov, D., Brandt, S., Levy, D. E., Durbin, J. E., Palese, P., and Muster, T. (1998). Influenza A virus lacking the NS1 gene replicates in interferon-deficient systems. *Virology*, 252(2):324–30.

García-Sastre, A., Muster, T., Barclay, W. S., Percy, N., and Palese, P. (1994). Use of a mammalian internal ribosomal entry site element for expression of a foreign protein by a transfectant influenza virus. *Journal of Virology*, 68(10):6254–61.

Garcin, D., Pelet, T., Calain, P., Roux, L., Curran, J., and Kolakofsky, D. (1995). A highly recombinogenic system for the recovery of infectious Sendai paramyxovirus from cDNA: generation of a novel copy-back nondefective interfering virus. *EMBO J*, 14(24):6087–94.

Garten, W. and Klenk, H. D. (1983). Characterization of the carboxypeptidase involved in the proteolytic cleavage of the influenza haemagglutinin. *J Gen Virol*, 64 (Pt 10):2127–37.

Geerts-Dimitriadou, C., Goldbach, R., and Kormelink, R. (2011a). Preferential use of RNA leader sequences during influenza A transcription initiation in vivo. *Virology*, 409(1):27–32.

Geerts-Dimitriadou, C., Zwart, M. P., Goldbach, R., and Kormelink, R. (2011b). Base-pairing promotes leader selection to prime in vitro influenza genome transcription. *Virology*, 409(1):17–26.

Gibbs, J. S., Malide, D., Hornung, F., Bennink, J. R., and Yewdell, J. W. (2003). The influenza A virus PB1-F2 protein targets the inner mitochondrial membrane via a predicted basic amphipathic helix that disrupts mitochondrial function. *Journal of Virology*, 77(13):7214–24.

Giorgi, C., Accardi, L., Nicoletti, L., Gro, M. C., Takehara, K., Hilditch, C., Morikawa, S., and Bishop, D. H. (1991). Sequences and coding strategies of the S RNAs of Toscana and Rift Valley fever viruses compared to those

of Punta Toro, Sicilian Sandfly fever, and Uukuniemi viruses. *Virology*, 180(2):738–53.

Giorgi, F. D., Lartigue, L., Bauer, M. K. A., Schubert, A., Grimm, S., Hanson, G. T., Remington, S. J., Youle, R. J., and Ichas, F. (2002). The permeability transition pore signals apoptosis by directing Bax translocation and multimerization. *FASEB J*, 16(6):607–9.

Goffic, R. L., Bouguyon, E., Chevalier, C., Vidic, J., Costa, B. D., Leymarie, O., Bourdieu, C., Decamps, L., Dhorne-Pollet, S., and Delmas, B. (2010). Influenza A virus protein PB1-F2 exacerbates IFN-beta expression of human respiratory epithelial cells. *J Immunol*, 185(8):4812–23.

González, S. and Ortín, J. (1999). Characterization of influenza virus PB1 protein binding to viral RNA: two separate regions of the protein contribute to the interaction domain. *Journal of Virology*, 73(1):631–7.

González, S., Zürcher, T., and Ortín, J. (1996). Identification of two separate domains in the influenza virus PB1 protein involved in the interaction with the PB2 and PA subunits: a model for the viral RNA polymerase structure. *Nucleic Acids Research*, 24(22):4456–63.

Gould, P. S. and Easton, A. J. (2005). Coupled translation of the respiratory syncytial virus M2 open reading frames requires upstream sequences. *J Biol Chem*, 280(23):21972–80.

Gregoriades, A. (1980). Interaction of influenza M protein with viral lipid and phosphatidylcholine vesicles. *Journal of Virology*, 36(2):470–9.

Grimm, D., Staeheli, P., Hufbauer, M., Koerner, I., Martínez-Sobrido, L., Solórzano, A., García-Sastre, A., Haller, O., and Kochs, G. (2007). Replication fitness determines high virulence of influenza A virus in mice carrying functional Mx1 resistance gene. *Proc Natl Acad Sci USA*, 104(16):6806–11.

Hai, R., Schmolke, M., Varga, Z. T., Manicassamy, B., Wang, T. T., Belser, J. A., Pearce, M. B., García-Sastre, A., Tumpey, T. M., and Palese, P. (2010). PB1-F2 expression by the 2009 pandemic H1N1 influenza virus has minimal impact on virulence in animal models. *Journal of Virology*, 84(9):4442–50.

Hale, B. G., Jackson, D., Chen, Y.-H., Lamb, R. A., and Randall, R. E. (2006). Influenza A virus NS1 protein binds p85beta and activates phosphatidylinositol-3-kinase signaling. *Proc Natl Acad Sci USA*, 103(38):14194–9.

Hale, B. G., Randall, R. E., Ortin, J., and Jackson, D. (2008). The multifunctional NS1 protein of influenza A viruses. *Journal of General Virology*, 89(10):2359–2376.

Han, J., Modha, D., and White, E. (1998). Interaction of E1B 19K with Bax is required to block Bax-induced loss of mitochondrial membrane potential and apoptosis. *Oncogene*, 17(23):2993–3005.

Han, J., Sabbatini, P., Perez, D., Rao, L., Modha, D., and White, E. (1996). The E1B 19K protein blocks apoptosis by interacting with and inhibiting the p53-inducible and death-promoting Bax protein. *Genes & Development*, 10(4):461–77.

Hao, L., Sakurai, A., Watanabe, T., Sorensen, E., Nidom, C. A., Newton, M. A., Ahlquist, P., and Kawaoka, Y. (2008). Drosophila RNAi screen identifies host genes important for influenza virus replication. *Nature*, 454(7206):890–3.

Hatta, M., Gao, P., Halfmann, P., and Kawaoka, Y. (2001). Molecular basis for high virulence of Hong Kong H5N1 influenza A viruses. *Science*, 293(5536):1840–2.

Hemerka, J. N., Wang, D., Weng, Y., Lu, W., Kaushik, R. S., Jin, J., Harmon, A. F., and Li, F. (2009). Detection and characterization of influenza A virus PA-PB2 interaction through a bimolecular fluorescence complementation assay. *Journal of Virology*, 83(8):3944–55.

Henkel, M., Mitzner, D., Henklein, P., Meyer-Almes, F.-J., Moroni, A., Difrancesco, M. L., Henkes, L. M., Kreim, M., Kast, S. M., Schubert, U., and Thiel, G. (2010). The proapoptotic influenza A virus protein PB1-F2 forms a nonselective ion channel. *PLoS ONE*, 5(6):e11112.

Henklein, P., Bruns, K., Nimtz, M., Wray, V., Tessmer, U., and Schubert, U. (2005). Influenza A virus protein PB1-F2: synthesis and characterization of the biologically active full length protein and related peptides. *J Pept Sci*, 11(8):481–90.

Herman, R. C. (1986). Internal initiation of translation on the vesicular stomatitis virus phosphoprotein mRNA yields a second protein. *Journal of Virology*, 58(3):797–804.

Herrler, G., Dürkop, I., Becht, H., and Klenk, H. D. (1988). The glycoprotein of influenza C virus is the haemagglutinin, esterase and fusion factor. *J Gen Virol*, 69 (Pt 4):839–46.

Herz, C., Stavnezer, E., Krug, R. M., and Jr, T. G. (1981). Influenza virus, an RNA virus, synthesizes its messenger RNA in the nucleus of infected cells . *Cell*, 26:391–400.

Heynisch, B., Frensing, T., Heinze, K., Seitz, C., Genzel, Y., and Reichl, U. (2010). Differential activation of host cell signalling pathways through infection with two variants of influenza A/Puerto Rico/8/34 (H1N1) in MDCK cells. *Vaccine*, 28(51):8210–8.

Hinshaw, V. S., Olsen, C. W., Dybdahl-Sissoko, N., and Evans, D. (1994). Apoptosis: a mechanism of cell killing by influenza A and B viruses. *Journal of Virology*, 68(6):3667–73.

Hoffmann, E., Mahmood, K., Yang, C.-F., Webster, R. G., Greenberg, H. B., and Kemble, G. (2002). Rescue of influenza B virus from eight plasmids. *Proc Natl Acad Sci USA*, 99(17):11411–6.

Hoffmann, E., Neumann, G., Hobom, G., Webster, R. G., and Kawaoka, Y. (2000a). "Ambisense" approach for the generation of influenza A virus: vRNA and mRNA synthesis from one template. *Virology*, 267(2):310–7.

Hoffmann, E., Neumann, G., Kawaoka, Y., Hobom, G., and Webster, R. G. (2000b). A DNA transfection system for generation of influenza A virus from eight plasmids. *Proc Natl Acad Sci USA*, 97(11):6108–13.

Hoffmann, E. and Webster, R. G. (2000). Unidirectional RNA polymerase I-polymerase II transcription system for the generation of influenza A virus from eight plasmids. *J Gen Virol*, 81(Pt 12):2843–7.

Holsinger, L. J. and Lamb, R. A. (1991). Influenza virus M2 integral membrane protein is a homotetramer stabilized by formation of disulfide bonds. *Virology*, 183(1):32–43.

Holsinger, L. J., Shaughnessy, M. A., Micko, A., Pinto, L. H., and Lamb, R. A. (1995). Analysis of the posttranslational modifications of the influenza virus M2 protein. *Journal of Virology*, 69(2):1219–25.

Honda, A., Mizumoto, K., and Ishihama, A. (2002). Minimum molecular architectures for transcription and replication of the influenza virus. *Proc Natl Acad Sci USA*, 99(20):13166–71.

Honda, A., Okamoto, T., and Ishihama, A. (2007). Host factor Ebp1: selective inhibitor of influenza virus transcriptase. *Genes Cells*, 12(2):133–42.

Honda, A., Uéda, K., Nagata, K., and Ishihama, A. (1988). RNA polymerase of influenza virus: role of NP in RNA chain elongation. *J Biochem*, 104(6):1021–6.

Horimoto, T. and Kawaoka, Y. (2005). Influenza: lessons from past pandemics, warnings from current incidents. *Nat Rev Micro*, 3(8):591–600.

Horvath, C. M., Williams, M. A., and Lamb, R. A. (1990). Eukaryotic coupled translation of tandem cistrons: identification of the influenza B virus BM2 polypeptide. *EMBO J*, 9(8):2639–47.

Hsu, M. T., Parvin, J. D., Gupta, S., Krystal, M., and Palese, P. (1987). Genomic RNAs of influenza viruses are held in a circular conformation in

virions and in infected cells by a terminal panhandle. *Proc Natl Acad Sci USA*, 84(22):8140–4.

Huang, T. S., Palese, P., and Krystal, M. (1990). Determination of influenza virus proteins required for genome replication. *Journal of Virology*, 64(11):5669–73.

Huet, S., Avilov, S., Ferbitz, L., Daigle, N., Cusack, S., and Ellenberg, J. (2010). Nuclear import and assembly of the influenza A virus RNA polymerase studied in live cells by Fluorescence Cross Correlation Spectroscopy. *Journal of Virology*, 84(3):1254–1264.

Hutchinson, E. C., von Kirchbach, J. C., Gog, J. R., and Digard, P. (2010). Genome packaging in influenza A virus. *J Gen Virol*, 91(Pt 2):313–28.

Ikegami, T., Won, S., Peters, C. J., and Makino, S. (2006). Rescue of infectious rift valley fever virus entirely from cDNA, analysis of virus lacking the NSs gene, and expression of a foreign gene. *Journal of Virology*, 80(6):2933–40.

Inglis, S. C., Barrett, T., Brown, C. M., and Almond, J. W. (1979). The smallest genome RNA segment of influenza virus contains two genes that may overlap. *Proc Natl Acad Sci USA*, 76(8):3790–4.

Jackson, D., Killip, M. J., Galloway, C. S., Russell, R. J., and Randall, R. E. (2010). Loss of function of the influenza A virus NS1 protein promotes apoptosis but this is not due to a failure to activate phosphatidylinositol 3-kinase (PI3K). *Virology*, 396(1):94–105.

Jacotot, E., Ferri, K. F., Hamel, C. E., Brenner, C., Druillennec, S., Hoebeke, J., Rustin, P., Métivier, D., Lenoir, C., Geuskens, M., Vieira, H. L., Loeffler, M., Belzacq, A. S., Briand, J. P., Zamzami, N., Edelman, L., Xie, Z. H., Reed, J. C., Roques, B. P., and Kroemer, G. (2001). Control of mitochondrial membrane permeabilization by adenine nucleotide translocator interacting with HIV-1 viral protein rR and Bcl-2. *J Exp Med*, 193(4):509–19.

Jacotot, E., Ravagnan, L., Loeffler, M., Ferri, K. F., Vieira, H. L., Zamzami, N., Costantini, P., Druillennec, S., Hoebeke, J., Briand, J. P., Irinopoulou, T., Daugas, E., Susin, S. A., Cointe, D., Xie, Z. H., Reed, J. C., Roques, B. P., and Kroemer, G. (2000). The HIV-1 viral protein R induces apoptosis via a direct effect on the mitochondrial permeability transition pore. *J Exp Med*, 191(1):33–46.

Jones, J. C., Phatnani, H. P., Haystead, T. A., MacDonald, J. A., Alam, S. M., and Greenleaf, A. L. (2004). C-terminal repeat domain kinase I phosphorylates Ser2 and Ser5 of RNA polymerase II C-terminal domain repeats. *J Biol Chem*, 279(24):24957–64.

Jorba, N., Coloma, R., and Ortín, J. (2009). Genetic trans-complementation establishes a new model for influenza virus RNA transcription and replication. *PLoS Pathogens*, 5(5):e1000462.

Kamps (2006). Influenzareport. page 225.

Karlas, A., Machuy, N., Shin, Y., Pleissner, K.-P., Artarini, A., Heuer, D., Becker, D., Khalil, H., Ogilvie, L. A., Hess, S., Mäurer, A. P., Müller, E., Wolff, T., Rudel, T., and Meyer, T. F. (2010). Genome-wide RNAi screen identifies human host factors crucial for influenza virus replication. *Nature*, 463(7282):818–22.

Kawai, T., Takahashi, K., Sato, S., Coban, C., Kumar, H., Kato, H., Ishii, K. J., Takeuchi, O., and Akira, S. (2005). IPS-1, an adaptor triggering RIG-I- and Mda5-mediated type I interferon induction. *Nat Immunol*, 6(10):981–8.

Keinan, N., Tyomkin, D., and Shoshan-Barmatz, V. (2010). Oligomerization of the mitochondrial protein voltage-dependent anion channel is coupled to the induction of apoptosis. *Mol Cell Biol*, 30(24):5698–709.

Kerr, J. F., Wyllie, A. H., and Currie, A. R. (1972). Apoptosis: a basic biological phenomenon with wide-ranging implications in tissue kinetics. *Br J Cancer*, 26(4):239–57.

Kim, E., Du, L., Bregman, D. B., and Warren, S. L. (1997). Splicing factors associate with hyperphosphorylated RNA polymerase II in the absence of pre-mRNA. *J Cell Biol*, 136(1):19–28.

Kittel, C., Ferko, B., Kurz, M., Voglauer, R., Sereinig, S., Romanova, J., Stiegler, G., Katinger, H., and Egorov, A. (2005). Generation of an influenza A virus vector expressing biologically active human interleukin-2 from the NS gene segment. *Journal of Virology*, 79(16):10672–7.

Kittel, C., Sereinig, S., Ferko, B., Stasakova, J., Romanova, J., Wolkerstorfer, A., Katinger, H., and Egorov, A. (2004). Rescue of influenza virus expressing GFP from the NS1 reading frame. *Virology*, 324(1):67–73.

Knipe, D. M., Howley, P. M., Griffin, D. E., Lamb, R. A., Martin, M. A., Roizman, B., and Straus, S. E. (2001). Fields Virology. *Lippincott Williams & Wilkin*, Forth Edition:2501.

Kobasa, D., Takada, A., Shinya, K., Hatta, M., Halfmann, P., Theriault, S., Suzuki, H., Nishimura, H., Mitamura, K., Sugaya, N., Usui, T., Murata, T., Maeda, Y., Watanabe, S., Suresh, M., Suzuki, T., Suzuki, Y., Feldmann, H., and Kawaoka, Y. (2004). Enhanced virulence of influenza A viruses with the haemagglutinin of the 1918 pandemic virus. *Nature*, 431(7009):703–7.

Kobayashi, M., Toyoda, T., Adyshev, D. M., Azuma, Y., and Ishihama, A. (1994). Molecular dissection of influenza virus nucleoprotein: deletion mapping of the RNA binding domain. *Journal of Virology*, 68(12):8433–6.

Komarnitsky, P., Cho, E. J., and Buratowski, S. (2000). Different phosphorylated forms of RNA polymerase II and associated mRNA processing factors during transcription. *Genes & Development*, 14(19):2452–60.

Kozak, M. (1986). Point mutations define a sequence flanking the AUG initiator codon that modulates translation by eukaryotic ribosomes. *Cell*, 44(2):283–92.

Kozak, M. (1999). Initiation of translation in prokaryotes and eukaryotes. *Gene*, 234(2):187–208.

Kozak, M. (2001). Constraints on reinitiation of translation in mammals. *Nucleic Acids Research*, 29(24):5226–32.

Kretzschmar, E., Buonocore, L., Schnell, M. J., and Rose, J. K. (1997). High-efficiency incorporation of functional influenza virus glycoproteins into recombinant vesicular stomatitis viruses. *Journal of Virology*, 71(8):5982–9.

Krossøy, B., Hordvik, I., Nilsen, F., Nylund, A., and Endresen, C. (1999). The putative polymerase sequence of infectious salmon anemia virus suggests a new genus within the Orthomyxoviridae. *Journal of Virology*, 73(3):2136–42.

Krug, R. M., Broni, B. A., LaFiandra, A. J., Morgan, M. A., and Shatkin, A. J. (1980). Priming and inhibitory activities of RNAs for the influenza viral transcriptase do not require base pairing with the virion template RNA. *Proc Natl Acad Sci USA*, 77(10):5874–8.

Krug, R. M., Yuan, W., Noah, D. L., and Latham, A. G. (2003). Intracellular warfare between human influenza viruses and human cells: the roles of the viral NS1 protein. *Virology*, 309(2):181–9.

Lam, W. Y., Tang, J. W., Yeung, A. C. M., Chiu, L. C. M., Sung, J. J. Y., and Chan, P. K. S. (2008). Avian influenza virus A/HK/483/97(H5N1) NS1 protein induces apoptosis in human airway epithelial cells. *Journal of Virology*, 82(6):2741–51.

Lamb, R. A., Lai, C. J., and Choppin, P. W. (1981). Sequences of mRNAs derived from genome RNA segment 7 of influenza virus: colinear and interrupted mRNAs code for overlapping proteins. *Proc Natl Acad Sci USA*, 78(7):4170–4.

Lamb, R. A., Zebedee, S. L., and Richardson, C. D. (1985). Influenza virus M2 protein is an integral membrane protein expressed on the infected-cell surface. *Cell*, 40(3):627–33.

Laver, W. G., Colman, P. M., Webster, R. G., Hinshaw, V. S., and Air, G. M. (1984). Influenza virus neuraminidase with hemagglutinin activity. *Virology*, 137(2):314–23.

Leahy, M. B., Dessens, J. T., Weber, F., Kochs, G., and Nuttall, P. A. (1997). The fourth genus in the Orthomyxoviridae: sequence analyses of two Thogoto virus polymerase proteins and comparison with influenza viruses. *Virus Research*, 50(2):215–24.

Lei, Y., Moore, C. B., Liesman, R. M., O'connor, B. P., Bergstralh, D. T., Chen, Z. J., Pickles, R. J., and Ting, J. P.-Y. (2009). MAVS-mediated apoptosis and its inhibition by viral proteins. *PLoS ONE*, 4(5):e5466.

Li, F., Feng, L., Pan, W., Dong, Z., Li, C., Sun, C., and Chen, L. (2010). Generation of replication-competent recombinant influenza A viruses carrying a reporter gene harbored in the neuraminidase segment. *Journal of Virology*, 84(22):12075–81.

Li, G., Zhang, J., Tong, X., Liu, W., and Ye, X. (2011). Heat shock protein 70 inhibits the activity of influenza a virus ribonucleoprotein and blocks the replication of virus in vitro and in vivo. *PLoS ONE*, 6(2):e16546.

Li, S., Polonis, V., Isobe, H., Zaghouani, H., Guinea, R., Moran, T., Bona, C., and Palese, P. (1993). Chimeric influenza virus induces neutralizing antibodies and cytotoxic T cells against human immunodeficiency virus type 1. *Journal of Virology*, 67(11):6659–66.

Li, S., Xu, M., and Coelingh, K. (1995). Electroporation of influenza virus ribonucleoprotein complexes for rescue of the nucleoprotein and matrix genes. *Virus Research*, 37(2):153–61.

Li, S. Q., Schulman, J. L., Moran, T., Bona, C., and Palese, P. (1992). Influenza A virus transfectants with chimeric hemagglutinins containing epitopes from different subtypes. *Journal of Virology*, 66(1):399–404.

Li, X. and Palese, P. (1994). Characterization of the polyadenylation signal of influenza virus RNA. *Journal of Virology*, 68(2):1245–9.

Liang, Y., Hong, Y., and Parslow, T. G. (2005). cis-Acting packaging signals in the influenza virus PB1, PB2, and PA genomic RNA segments. *Journal of Virology*, 79(16):10348–55.

Liljeström, P., Lusa, S., Huylebroeck, D., and Garoff, H. (1991). In vitro mutagenesis of a full-length cDNA clone of Semliki Forest virus: the small 6,000-molecular-weight membrane protein modulates virus release. *Journal of Virology*, 65(8):4107–13.

Liu, X., Kim, C. N., Yang, J., Jemmerson, R., and Wang, X. (1996). Induction of apoptotic program in cell-free extracts: requirement for dATP and cytochrome c. *Cell*, 86(1):147–57.

Liu, Y., Garceau, N. Y., Loros, J. J., and Dunlap, J. C. (1997). Thermally regulated translational control of FRQ mediates aspects of temperature responses in the neurospora circadian clock. *Cell*, 89(3):477–86.

Lloyd, R. E., Toyoda, H., Etchison, D., Wimmer, E., and Ehrenfeld, E. (1986). Cleavage of the cap binding protein complex polypeptide p220 is not effected by the second poliovirus protease 2A. *Virology*, 150(1):299–303.

Lowy, R. J. (2003). Influenza virus induction of apoptosis by intrinsic and extrinsic mechanisms. *Int Rev Immunol*, 22(5-6):425–49.

Lu, B., Kemble, G., and Jin, H. (2004). The NS1 gene of influenza a virus supplied from a separate segment is excluded from virion. *International Congress Series*, 1263:439 – 443.

Luk, D., Sánchez, A., and Banerjee, A. K. (1986). Messenger RNA encoding the phosphoprotein (P) gene of human parainfluenza virus 3 is bicistronic. *Virology*, 153(2):318–25.

Luo, G. X., Luytjes, W., Enami, M., and Palese, P. (1991). The polyadenylation signal of influenza virus RNA involves a stretch of uridines followed by the RNA duplex of the panhandle structure. *Journal of Virology*, 65(6):2861–7.

Luytjes, W., Krystal, M., Enami, M., Parvin, J. D., and Palese, P. (1989). Amplification, expression, and packaging of foreign gene by influenza virus. *Cell*, 59(6):1107–13.

Ma, W., Kahn, R. E., and Richt, J. A. (2008). The pig as a mixing vessel for influenza viruses: Human and veterinary implications. *J Mol Genet Med*, 3(1):158–66.

Machado, A. V., Naffakh, N., Gerbaud, S., van der Werf, S., and Escriou, N. (2006). Recombinant influenza A viruses harboring optimized dicistronic NA segment with an extended native 5' terminal sequence: induction of heterospecific B and T cell responses in mice. *Virology*, 345(1):73–87.

Machado, A. V., Naffakh, N., van der Werf, S., and Escriou, N. (2003). Expression of a foreign gene by stable recombinant influenza viruses harboring a dicistronic genomic segment with an internal promoter. *Virology*, 313(1):235–49.

Macken, C., Lu, H., Goodman, J., and Boykin, L. (2001). The value of a database in surveillance and vaccine selection . *International Congress Serie*, pages 103–106.

Marjuki, H., Scholtissek, C., Franks, J., Negovetich, N. J., Aldridge, J. R., Salomon, R., Finkelstein, D., and Webster, R. G. (2010). Three amino acid changes in PB1-F2 of highly pathogenic H5N1 avian influenza virus affect pathogenicity in mallard ducks. *Arch Virol*, 155:925–934.

Marshall, N. F., Peng, J., Xie, Z., and Price, D. H. (1996). Control of RNA polymerase II elongation potential by a novel carboxyl-terminal domain kinase. *J Biol Chem*, 271(43):27176–83.

Marzo, I., Brenner, C., Zamzami, N., Jürgensmeier, J. M., Susin, S. A., Vieira, H. L., Prévost, M. C., Xie, Z., Matsuyama, S., Reed, J. C., and Kroemer, G. (1998). Bax and adenine nucleotide translocator cooperate in the mitochondrial control of apoptosis. *Science*, 281(5385):2027–31.

Matlin, K. S., Reggio, H., Helenius, A., and Simons, K. (1981). Infectious entry pathway of influenza virus in a canine kidney cell line. *J Cell Biol*, 91(3 Pt 1):601–13.

Mayer, D., Molawi, K., Martínez-Sobrido, L., Ghanem, A., Thomas, S., Baginsky, S., Grossmann, J., García-Sastre, A., and Schwemmle, M. (2007). Identification of cellular interaction partners of the influenza virus ribonucleoprotein complex and polymerase complex using proteomic-based approaches. *J Proteome Res*, 6(2):672–82.

Mazur, I., Anhlan, D., Mitzner, D., Wixler, L., Schubert, U., and Ludwig, S. (2008). The proapoptotic influenza A virus protein PB1-F2 regulates viral polymerase activity by interaction with the PB1 protein. *Cell Microbiol*, 10(5):1140–52.

McAuley, J. L., Chipuk, J. E., Boyd, K. L., Velde, N. V. D., Green, D. R., and McCullers, J. A. (2010a). PB1-F2 proteins from H5N1 and 20 century pandemic influenza viruses cause immunopathology. *PLoS Pathogens*, 6(7):e1001014.

McAuley, J. L., Hornung, F., Boyd, K. L., Smith, A. M., McKeon, R., Bennink, J., Yewdell, J. W., and McCullers, J. A. (2007). Expression of the 1918 influenza A virus PB1-F2 enhances the pathogenesis of viral and secondary bacterial pneumonia. *Cell Host & Microbe*, 2(4):240–9.

McAuley, J. L., Zhang, K., and McCullers, J. A. (2010b). The effects of influenza A virus PB1-F2 protein on polymerase activity are strain specific and do not impact pathogenesis. *J Virol*, 84(1):558–564.

McCracken, S., Fong, N., Yankulov, K., Ballantyne, S., Pan, G., Greenblatt, J., Patterson, S. D., Wickens, M., and Bentley, D. L. (1997). The C-terminal domain of RNA polymerase II couples mRNA processing to transcription. *Nature*, 385(6614):357–61.

McCullers, J. A. and Rehg, J. E. (2002). Lethal synergism between influenza virus and Streptococcus pneumoniae: characterization of a mouse model and the role of platelet-activating factor receptor. *J Infect Dis*, 186(3):341–50.

McCullers, J. A., Wang, G. C., He, S., and Webster, R. G. (1999). Reassortment and insertion-deletion are strategies for the evolution of influenza B viruses in nature. *Journal of Virology*, 73(9):7343–8.

McLean, J. E., Datan, E., Matassov, D., and Zakeri, Z. F. (2009). Lack of Bax prevents influenza a virus-induced apoptosis and causes diminished viral replication. *Journal of Virology*, 83(16):8233–46.

Mena, I., Jambrina, E., Albo, C., Perales, B., Ortín, J., Arrese, M., Vallejo, D., and Portela, A. (1999). Mutational analysis of influenza A virus nucleoprotein: identification of mutations that affect RNA replication. *Journal of Virology*, 73(2):1186–94.

Meyers, G. (2003). Translation of the minor capsid protein of a calicivirus is initiated by a novel termination-dependent reinitiation mechanism. *J Biol Chem*, 278(36):34051–60.

Meyers, G. (2007). Characterization of the sequence element directing translation reinitiation in RNA of the calicivirus rabbit hemorrhagic disease virus. *Journal of Virology*, 81(18):9623–32.

Meylan, E., Curran, J., Hofmann, K., Moradpour, D., Binder, M., Bartenschlager, R., and Tschopp, J. (2005). Cardif is an adaptor protein in the RIG-I antiviral pathway and is targeted by hepatitis C virus. *Nature*, 437(7062):1167–72.

Mitzner, D., Dudek, S., Studtrucker, N., Anhlan, D., Mazur, I., Wissing, J., Jänsch, L., Wixler, L., Bruns, K., Sharma, A., Wray, V., Henklein, P., Ludwig, S., and Schubert, U. (2009). Phosphorylation of the influenza A virus protein PB1-F2 by PKC is crucial for apoptosis promoting functions in monocytes. *Cell Microbiol*, 11:1502–1516.

Morris, S. J., Smith, H., and Sweet, C. (2002). Exploitation of the Herpes simplex virus translocating protein VP22 to carry influenza virus proteins into cells for studies of apoptosis: direct confirmation that neuraminidase induces apoptosis and indications that other proteins may have a role. *Arch Virol*, 147(5):961–79.

Mullin, A. E., Dalton, R. M., Amorim, M. J., Elton, D., and Digard, P. (2004). Increased amounts of the influenza virus nucleoprotein do not promote higher levels of viral genome replication. *J Gen Virol*, 85(Pt 12):3689–98.

Muster, T., Ferko, B., Klima, A., Purtscher, M., Trkola, A., Schulz, P., Grassauer, A., Engelhardt, O. G., García-Sástre, A., and Palese, P. (1995). Mucosal model of immunization against human immunodeficiency virus type 1 with a chimeric influenza virus. *Journal of Virology*, 69(11):6678–86.

Muster, T., Guinea, R., Trkola, A., Purtscher, M., Klima, A., Steindl, F., Palese, P., and Katinger, H. (1994). Cross-neutralizing activity against divergent human immunodeficiency virus type 1 isolates induced by the gp41 sequence ELDKWAS. *Journal of Virology*, 68(6):4031–4.

Nagata, K., Kawaguchi, A., and Naito, T. (2008). Host factors for replication and transcription of the influenza virus genome. *Rev. Med. Virol.*, 18(4):247–60.

Naito, T., Momose, F., Kawaguchi, A., and Nagata, K. (2007). Involvement of Hsp90 in assembly and nuclear import of influenza virus RNA polymerase subunits. *Journal of Virology*, 81(3):1339–49.

Nayak, D. P., Balogun, R. A., Yamada, H., Zhou, Z. H., and Barman, S. (2009). Influenza virus morphogenesis and budding. *Virus Research*, 143(2):147–61.

Nemeroff, M. E., Barabino, S. M., Li, Y., Keller, W., and Krug, R. M. (1998). Influenza virus NS1 protein interacts with the cellular 30 kDa subunit of CPSF and inhibits 3'end formation of cellular pre-mRNAs. *Mol Cell*, 1(7):991–1000.

Neumann, G., Castrucci, M. R., and Kawaoka, Y. (1997). Nuclear import and export of influenza virus nucleoprotein. *Journal of Virology*, 71(12):9690–700.

Neumann, G., Feldmann, H., Watanabe, S., Lukashevich, I., and Kawaoka, Y. (2002). Reverse genetics demonstrates that proteolytic processing of the Ebola virus glycoprotein is not essential for replication in cell culture. *Journal of Virology*, 76(1):406–10.

Neumann, G., Fujii, K., Kino, Y., and Kawaoka, Y. (2005). An improved reverse genetics system for influenza A virus generation and its implications for vaccine production. *Proc Natl Acad Sci USA*, 102(46):16825–9.

Neumann, G., Noda, T., and Kawaoka, Y. (2009). Emergence and pandemic potential of swine-origin H1N1 influenza virus. *Nature*, 459(7249):931–939.

Neumann, G., Watanabe, T., Ito, H., Watanabe, S., Goto, H., Gao, P., Hughes, M., Perez, D. R., Donis, R., Hoffmann, E., Hobom, G., and Kawaoka, Y. (1999). Generation of influenza A viruses entirely from cloned cDNAs. *Proc Natl Acad Sci USA*, 96(16):9345–50.

Neumann, G., Zobel, A., and Hobom, G. (1994). RNA polymerase I-mediated expression of influenza viral RNA molecules. *Virology*, 202(1):477–9.

Newcomb, L. L., Kuo, R.-L., Ye, Q., Jiang, Y., Tao, Y. J., and Krug, R. M. (2009). Interaction of the influenza a virus nucleocapsid protein with the viral RNA polymerase potentiates unprimed viral RNA replication. *Journal of Virology*, 83(1):29–36.

Nie, Z., Phenix, B. N., Lum, J. J., Alam, A., Lynch, D. H., Beckett, B., Krammer, P. H., Sekaly, R. P., and Badley, A. D. (2002). HIV-1 protease processes procaspase 8 to cause mitochondrial release of cytochrome c, caspase cleavage and nuclear fragmentation. *Cell Death Differ*, 9(11):1172–84.

Nimmerjahn, F., Dudziak, D., Dirmeier, U., Hobom, G., Riedel, A., Schlee, M., Staudt, L. M., Rosenwald, A., Behrends, U., Bornkamm, G. W., and Mautner, J. (2004). Active NF-kappaB signalling is a prerequisite for influenza virus infection. *J Gen Virol*, 85(Pt 8):2347–56.

Noda, T., Sagara, H., Yen, A., Takada, A., Kida, H., Cheng, R. H., and Kawaoka, Y. (2006). Architecture of ribonucleoprotein complexes in influenza A virus particles. *Nature*, 439(7075):490–2.

Odagiri, T. and Tobita, K. (1990). Mutation in NS2, a nonstructural protein of influenza A virus, extragenically causes aberrant replication and expression of the PA gene and leads to generation of defective interfering particles. *Proc Natl Acad Sci USA*, 87(15):5988–92.

Odagiri, T., Tominaga, K., Tobita, K., and Ohta, S. (1994). An amino acid change in the non-structural NS2 protein of an influenza A virus mutant is responsible for the generation of defective interfering (DI) particles by amplifying DI RNAs and suppressing complementary RNA synthesis. *J Gen Virol*, 75 (Pt 1):43–53.

Olson, A. C., Rosenblum, E., and Kuchta, R. D. (2010). Regulation of influenza RNA polymerase activity and the switch between replication and transcription by the concentrations of the vRNA 5' end, the cap source, and the polymerase. *Biochemistry*, 49(47):10208–15.

O'Neill, R. E., Jaskunas, R., Blobel, G., Palese, P., and Moroianu, J. (1995). Nuclear import of influenza virus RNA can be mediated by viral nucleoprotein and transport factors required for protein import. *J Biol Chem*, 270(39):22701–4.

O'Neill, R. E., Talon, J., and Palese, P. (1998). The influenza virus NEP (NS2 protein) mediates the nuclear export of viral ribonucleoproteins. *EMBO J*, 17(1):288–96.

Osterhaus, A. D., Rimmelzwaan, G. F., Martina, B. E., Bestebroer, T. M., and Fouchier, R. A. (2000). Influenza B virus in seals. *Science*, 288(5468):1051–3.

Ozawa, M., Basnet, S., Burley, L. M., Neumann, G., Hatta, M., and Kawaoka, Y. (2011). Impact of Amino Acid Mutations in PB2, PB1-F2, and NS1 on the Replication and Pathogenicity of Pandemic (H1N1) 2009 Influenza Viruses. *Journal of Virology*, 85(9):4596–601.

Pahl, H. L. (1999). Activators and target genes of Rel/NF-kappaB transcription factors. *Oncogene*, 18(49):6853–66.

Palese, P., Ritchey, M. B., and Schulman, J. L. (1977). Mapping of the influenza virus genome. II. Identification of the P1, P2, and P3 genes. *Virology*, 76(1):114–21.

Palese, P. and Schulman, J. L. (1976). Mapping of the influenza virus genome: identification of the hemagglutinin and the neuraminidase genes. *Proc Natl Acad Sci USA*, 73(6):2142–6.

Pattnaik, A. K. and Wertz, G. W. (1991). Cells that express all five proteins of vesicular stomatitis virus from cloned cDNAs support replication, assembly, and budding of defective interfering particles. *Proc Natl Acad Sci USA*, 88(4):1379–83.

Pauli, E.-K., Schmolke, M., Wolff, T., Viemann, D., Roth, J., Bode, J. G., and Ludwig, S. (2008). Influenza A virus inhibits type I IFN signaling via NF-kappaB-dependent induction of SOCS-3 expression. *PLoS Pathogens*, 4(11):e1000196.

Pekosz, A., He, B., and Lamb, R. A. (1999). Reverse genetics of negative-strand RNA viruses: closing the circle. *Proc Natl Acad Sci USA*, 96(16):8804–6.

Percy, N., Barclay, W. S., García-Sastre, A., and Palese, P. (1994). Expression of a foreign protein by influenza A virus. *Journal of Virology*, 68(7):4486–92.

Perez, J. T., Varble, A., Sachidanandam, R., Zlatev, I., Manoharan, M., García-Sastre, A., and Tenoever, B. R. (2010). Influenza A virus-generated small RNAs regulate the switch from transcription to replication. *Proc Natl Acad Sci USA*, 107(25):11525–11530.

Phatnani, H. P. and Greenleaf, A. L. (2006). Phosphorylation and functions of the RNA polymerase II CTD. *Genes & Development*, 20(21):2922–36.

Pichlmair, A., Schulz, O., Tan, C. P., Näslund, T. I., Liljeström, P., Weber, F., and e Sousa, C. R. (2006). RIG-I-mediated antiviral responses to single-stranded RNA bearing 5'-phosphates. *Science*, 314(5801):997–1001.

Pinto, L. H., Holsinger, L. J., and Lamb, R. A. (1992). Influenza virus M2 protein has ion channel activity. *Cell*, 69(3):517–28.

Pleschka, S., Jaskunas, R., Engelhardt, O. G., Zürcher, T., Palese, P., and García-Sastre, A. (1996). A plasmid-based reverse genetics system for influenza A virus. *Journal of Virology*, 70(6):4188–92.

Plotch, S., Bouloy, M., Ulmanen, I., and Krug, R. (1981). A unique cap(m7GpppXm)-dependent influenza virion endonuclease cleaves capped RNAs to generate the primers that initiate viral RNA transcription. *Cell*, 23:847–58.

Poon, L. L., Pritlove, D. C., Fodor, E., and Brownlee, G. G. (1999). Direct evidence that the poly(A) tail of influenza A virus mRNA is synthesized by reiterative copying of a U track in the virion RNA template. *Journal of Virology*, 73(4):3473–6.

Powell, M., Napthine, S., Jackson, R., Brierley, I., and Brown, T. (2008a). Characterization of the termination-reinitiation strategy employed in the expression of influenza B virus BM2 protein. *RNA*, 14(11):2394–2406.

Powell, M. L., Brown, T. D. K., and Brierley, I. (2008b). Translational termination-re-initiation in viral systems. *Biochem. Soc. Trans*, 36(Pt 4):717–22.

Powell, M. L., Leigh, K. E., Pöyry, T. A. A., Jackson, R. J., Brown, T. D. K., and Brierley, I. (2011). Further characterisation of the translational termination-reinitiation signal of the influenza B virus segment 7 RNA. *PLoS ONE*, 6(2):e16822.

Presti, R. M., Zhao, G., Beatty, W. L., Mihindukulasuriya, K. A., da Rosa, A. P. A. T., Popov, V. L., Tesh, R. B., Virgin, H. W., and Wang, D. (2009). Quaranfil, Johnston Atoll, and Lake Chad viruses are novel members of the family Orthomyxoviridae. *Journal of Virology*, 83(22):11599–606.

Pringle, C. R. (1996). Virus taxonomy 1996 - a bulletin from the Xth International Congress of Virology in Jerusalem. *Arch Virol*, 141(11):2251–6.

Pritlove, D. C., Poon, L. L., Fodor, E., Sharps, J., and Brownlee, G. G. (1998). Polyadenylation of influenza virus mRNA transcribed in vitro from model virion RNA templates: requirement for 5' conserved sequences. *Journal of Virology*, 72(2):1280–6.

Racaniello, V. R. and Baltimore, D. (1981). Cloned poliovirus complementary DNA is infectious in mammalian cells. *Science*, 214(4523):916–9.

Racine, T. and Duncan, R. (2010). Facilitated leaky scanning and atypical ribosome shunting direct downstream translation initiation on the tricistronic S1 mRNA of avian reovirus. *Nucleic Acids Research*, 38(20):7260–72.

Radecke, F., Spielhofer, P., Schneider, H., Kaelin, K., Huber, M., Dötsch, C., Christiansen, G., and Billeter, M. A. (1995). Rescue of measles viruses from cloned DNA. *EMBO J*, 14(23):5773–84.

Ramakrishnan, M. A., Gramer, M. R., Goyal, S. M., and Sreevatsan, S. (2009). A Serine12Stop mutation in PB1-F2 of the 2009 pandemic (H1N1) influenza A: a possible reason for its enhanced transmission and pathogenicity to humans. *J Vet Sci*, 10(4):349–51.

Rice, C. M., Levis, R., Strauss, J. H., and Huang, H. V. (1987). Production of infectious RNA transcripts from Sindbis virus cDNA clones: mapping of lethal mutations, rescue of a temperature-sensitive marker, and in vitro mutagenesis to generate defined mutants. *Journal of Virology*, 61(12):3809–19.

Ritchey, M. B., Palese, P., and Schulman, J. L. (1976). Mapping of the influenza virus genome. III. Identification of genes coding for nucleoprotein, membrane protein, and nonstructural protein. *Journal of Virology*, 20(1):307–13.

Robb, N. C., Smith, M., Vreede, F. T., and Fodor, E. (2009). NS2/NEP protein regulates transcription and replication of the influenza virus RNA genome. *J Gen Virol*, 90(Pt 6):1398–407.

Roberts, A., Kretzschmar, E., Perkins, A. S., Forman, J., Price, R., Buonocore, L., Kawaoka, Y., and Rose, J. K. (1998a). Vaccination with a recombinant vesicular stomatitis virus expressing an influenza virus hemagglutinin provides complete protection from influenza virus challenge. *Journal of Virology*, 72(6):4704–11.

Roberts, P. C. and Compans, R. W. (1998). Host cell dependence of viral morphology. *Proc Natl Acad Sci USA*, 95:5746–5751.

Roberts, P. C., Lamb, R. A., and Compans, R. W. (1998b). The M1 and M2 proteins of influenza A virus are important determinants in filamentous particle formation. *Virology*, 240(1):127–37.

Robertson, J. S., Schubert, M., and Lazzarini, R. A. (1981). Polyadenylation sites for influenza virus mRNA. *Journal of Virology*, 38(1):157–63.

Rodriguez, A., Pérez-González, A., Hossain, M. J., Chen, L.-M., Rolling, T., Pérez-Breña, P., Donis, R., Kochs, G., and Nieto, A. (2009). Attenuated Strains of Influenza A Viruses Do Not Induce Degradation of RNA Polymerase II. *Journal of Virology*, 83(21):11166–74.

Rodriguez, A., Pérez-González, A., and Nieto, A. (2007). Influenza virus infection causes specific degradation of the largest subunit of cellular RNA polymerase II. *Journal of Virology*, 81(10):5315–24.

Rogers, G. N. and Paulson, J. C. (1983). Receptor determinants of human and animal influenza virus isolates: differences in receptor specificity of the H3 hemagglutinin based on species of origin. *Virology*, 127(2):361–73.

Rogers, G. N., Pritchett, T. J., Lane, J. L., and Paulson, J. C. (1983). Differential sensitivity of human, avian, and equine influenza A viruses to a glycoprotein inhibitor of infection: selection of receptor specific variants. *Virology*, 131(2):394–408.

Rolling, T., Koerner, I., Zimmermann, P., Holz, K., Haller, O., Staeheli, P., and Kochs, G. (2009). Adaptive mutations resulting in enhanced polymerase activity contribute to high virulence of influenza A virus in mice. *Journal of Virology*, 83(13):6673–80.

Rose, N. F., Marx, P. A., Luckay, A., Nixon, D. F., Moretto, W. J., Donahoe, S. M., Montefiori, D., Roberts, A., Buonocore, L., and Rose, J. K. (2001). An effective AIDS vaccine based on live attenuated vesicular stomatitis virus recombinants. *Cell*, 106(5):539–49.

Rose, N. F., Roberts, A., Buonocore, L., and Rose, J. K. (2000). Glycoprotein exchange vectors based on vesicular stomatitis virus allow effective boosting and generation of neutralizing antibodies to a primary isolate of human immunodeficiency virus type 1. *Journal of Virology*, 74(23):10903–10.

Ruigrok, R. W., Calder, L. J., and Wharton, S. A. (1989). Electron microscopy of the influenza virus submembranal structure. *Virology*, 173(1):311–6.

Ryan, M. D. and Drew, J. (1994). Foot-and-mouth disease virus 2A oligopeptide mediated cleavage of an artificial polyprotein. *EMBO J*, 13(4):928–33.

Ryan, M. D., King, A. M., and Thomas, G. P. (1991). Cleavage of foot-and-mouth disease virus polyprotein is mediated by residues located within a 19 amino acid sequence. *J Gen Virol*, 72 (Pt 11):2727–32.

Sakaguchi, A., Hirayama, E., Hiraki, A., ichi Ishida, Y., and Kim, J. (2003). Nuclear export of influenza viral ribonucleoprotein is temperature-dependently inhibited by dissociation of viral matrix protein. *Virology*, 306(2):244–53.

Sánchez, A. B. and de la Torre, J. C. (2006). Rescue of the prototypic Arenavirus LCMV entirely from plasmid. *Virology*, 350(2):370–80.

Schägger, H. (2006). Tricine-SDS-PAGE. *Nat Protoc*, 1(1):16–22.

Scheel, I., Aldrin, M., Frigessi, A., and Jansen, P. A. (2007). A stochastic model for infectious salmon anemia (ISA) in Atlantic salmon farming. *Journal of the Royal Society, Interface / the Royal Society*, 4(15):699–706.

Schnell, M. J., Foley, H. D., Siler, C. A., McGettigan, J. P., Dietzschold, B., and Pomerantz, R. J. (2000). Recombinant rabies virus as potential live-viral vaccines for HIV-1. *Proc Natl Acad Sci USA*, 97(7):3544–9.

Schnell, M. J., Mebatsion, T., and Conzelmann, K. K. (1994). Infectious rabies viruses from cloned cDNA. *EMBO J*, 13(18):4195–203.

Schroeder, S. C., Schwer, B., Shuman, S., and Bentley, D. (2000). Dynamic association of capping enzymes with transcribing RNA polymerase II. *Genes & Development*, 14(19):2435–40.

Schultz-Cherry, S., Dybdahl-Sissoko, N., Neumann, G., Kawaoka, Y., and Hinshaw, V. S. (2001). Influenza virus ns1 protein induces apoptosis in cultured cells. *Journal of Virology*, 75(17):7875–81.

Schultz-Cherry, S. and Hinshaw, V. S. (1996). Influenza virus neuraminidase activates latent transforming growth factor beta. *Journal of Virology*, 70(12):8624–9.

Scull, M. A. and Rice, C. M. (2010). A big role for small RNAs in influenza virus replication. *Proceedings of the National Academy of Sciences*, pages 1–2.

Seth, R. B., Sun, L., Ea, C.-K., and Chen, Z. J. (2005). Identification and characterization of MAVS, a mitochondrial antiviral signaling protein that activates NF-kappaB and IRF 3. *Cell*, 122(5):669–82.

Shapira, S. D., Gat-Viks, I., Shum, B. O. V., Dricot, A., de Grace, M. M., Wu, L., Gupta, P. B., Hao, T., Silver, S. J., Root, D. E., Hill, D. E., Regev, A., and Hacohen, N. (2009). A physical and regulatory map of host-influenza interactions reveals pathways in H1N1 infection. *Cell*, 139(7):1255–67.

Shapiro, G. I. and Krug, R. M. (1988). Influenza virus RNA replication in vitro: synthesis of viral template RNAs and virion RNAs in the absence of an added primer. *Journal of Virology*, 62(7):2285–90.

Shaw, M. L. (2009). Henipaviruses Employ a Multifaceted Approach to Evade the Antiviral Interferon Response. *viruses*, 1(3):1190–1203.

Shimizu, S., Narita, M., and Tsujimoto, Y. (1999). Bcl-2 family proteins regulate the release of apoptogenic cytochrome c by the mitochondrial channel VDAC. *Nature*, 399(6735):483–7.

Shimizu, T., Takizawa, N., Watanabe, K., Nagata, K., and Kobayashi, N. (2011). Crucial role of the influenza virus NS2 (NEP) C-terminal domain in M1 binding and nuclear export of vRNP. *FEBS Letters*, 585(1):41–6.

Shinya, K., Ebina, M., Yamada, S., Ono, M., Kasai, N., and Kawaoka, Y. (2006). Avian flu: influenza virus receptors in the human airway. *Nature*, 440(7083):435–6.

Shirakata, Y. and Koike, K. (2003). Hepatitis B virus X protein induces cell death by causing loss of mitochondrial membrane potential. *J Biol Chem*, 278(24):22071–8.

Shoshan-Barmatz, V., Keinan, N., Abu-Hamad, S., Tyomkin, D., and Aram, L. (2010). Apoptosis is regulated by the VDAC1 N-terminal region and by VDAC oligomerization: release of cytochrome c, AIF and Smac/Diablo. *Biochim Biophys Acta*, 1797(6-7):1281–91.

Silva, E. V. P. D., da Rosa, A. P. A. T., Nunes, M. R. T., Diniz, J. A. P., Tesh, R. B., Cruz, A. C. R., Vieira, C. M. A., and Vasconcelos, P. F. C. (2005). Araguari virus, a new member of the family Orthomyxoviridae: serologic, ultrastructural, and molecular characterization. *Am J Trop Med Hyg*, 73(6):1050–8.

Simons, J. F., Hellman, U., and Pettersson, R. F. (1990). Uukuniemi virus S RNA segment: ambisense coding strategy, packaging of complementary strands into virions, and homology to members of the genus Phlebovirus. *Journal of Virology*, 64(1):247–55.

Simpson-Holley, M., Ellis, D., Fisher, D., Elton, D., McCauley, J., and Digard, P. (2002). A Functional Link between the Actin Cytoskeleton and Lipid Rafts during Budding of Filamentous Influenza Virions. *Virology*, 301:212–225.

Skehel, J. J., Bayley, P. M., Brown, E. B., Martin, S. R., Waterfield, M. D., White, J. M., Wilson, I. A., and Wiley, D. C. (1982). Changes in the conformation of influenza virus hemagglutinin at the pH optimum of virus-mediated membrane fusion. *Proc Natl Acad Sci USA*, 79(4):968–72.

Skehel, J. J. and Wiley, D. C. (2000). Receptor binding and membrane fusion in virus entry: the influenza hemagglutinin. *Annu Rev Biochem*, 69:531–69.

Smith, G. J. D., Naipospos, T. S. P., Nguyen, T. D., de Jong, M. D., Vijaykrishna, D., Usman, T. B., Hassan, S. S., Nguyen, T. V., Dao, T. V., Bui, N. A., Leung, Y. H. C., Cheung, C. L., Rayner, J. M., Zhang, J. X., Zhang, L. J., Poon, L. L. M., Li, K. S., Nguyen, V. C., Hien, T. T., Farrar, J., Webster, R. G., Chen, H., Peiris, J. S. M., and Guan, Y. (2006). Evolution and adaptation of H5N1 influenza virus in avian and human hosts in Indonesia and Vietnam. *Virology*, 350(2):258–68.

Smith, G. J. D., Vijaykrishna, D., Bahl, J., Lycett, S. J., Worobey, M., Pybus, O. G., Ma, S. K., Cheung, C. L., Raghwani, J., Bhatt, S., Peiris, J. S. M., Guan, Y., and Rambaut, A. (2009). Origins and evolutionary genomics of the 2009 swine-origin H1N1 influenza A epidemic. *Nature*, 459(7250):1122–5.

Song, M. M. and Shuai, K. (1998). The suppressor of cytokine signaling (SOCS) 1 and SOCS3 but not SOCS2 proteins inhibit interferon-mediated antiviral and antiproliferative activities. *J Biol Chem*, 273(52):35056–62.

Srivastava, B., Błazejewska, P., Hessmann, M., Bruder, D., Geffers, R., Mauel, S., Gruber, A. D., and Schughart, K. (2009). Host genetic background strongly influences the response to influenza a virus infections. *PLoS ONE*, 4(3):e4857.

Stacey, S. N., Jordan, D., Williamson, A. J., Brown, M., Coote, J. H., and Arrand, J. R. (2000). Leaky scanning is the predominant mechanism for translation of human papillomavirus type 16 E7 oncoprotein from E6/E7 bicistronic mRNA. *Journal of Virology*, 74(16):7284–97.

Starr, R., Willson, T. A., Viney, E. M., Murray, L. J., Rayner, J. R., Jenkins, B. J., Gonda, T. J., Alexander, W. S., Metcalf, D., Nicola, N. A., and Hilton, D. J. (1997). A family of cytokine-inducible inhibitors of signalling. *Nature*, 387(6636):917–21.

Stertz, S. and Shaw, M. L. (2011). Uncovering the global host cell requirements for influenza virus replication via RNAi screening. *Microbes Infect*, 13:516–525.

Subbarao, E. K., Kawaoka, Y., and Murphy, B. R. (1993a). Rescue of an influenza A virus wild-type PB2 gene and a mutant derivative bearing a site-specific temperature-sensitive and attenuating mutation. *Journal of Virology*, 67(12):7223–8.

Subbarao, E. K., London, W., and Murphy, B. R. (1993b). A single amino acid in the PB2 gene of influenza A virus is a determinant of host range. *Journal of Virology*, 67(4):1761–4.

Sugrue, R. J., Belshe, R. B., and Hay, A. J. (1990). Palmitoylation of the influenza A virus M2 protein. *Virology*, 179(1):51–6.

Szewczyk, B., Laver, W. G., and Summers, D. F. (1988). Purification, thioredoxin renaturation, and reconstituted activity of the three subunits of the influenza A virus RNA polymerase. *Proc Natl Acad Sci USA*, 85(21):7907–11.

Takada, S., Shirakata, Y., Kaneniwa, N., and Koike, K. (1999). Association of hepatitis B virus X protein with mitochondria causes mitochondrial aggregation at the nuclear periphery, leading to cell death. *Oncogene*, 18(50):6965–73.

Takizawa, T., Matsukawa, S., Higuchi, Y., Nakamura, S., Nakanishi, Y., and Fukuda, R. (1993). Induction of programmed cell death (apoptosis) by influenza virus infection in tissue culture cells. *J Gen Virol*, 74 (Pt 11):2347–55.

Taniguchi, T., Palmieri, M., and Weissmann, C. (1978). A Qbeta DNA-containing hybrid plasmid giving rise to Qbeta phage formation in the bacterial host [proceedings]. *Ann Microbiol (Paris)*, 129 B(4):535–6.

Taubenberger, J. K. and Morens, D. M. (2006). 1918 Influenza: the mother of all pandemics. *Emerging Infect Dis*, 12(1):15–22.

Taylor, R. C., Cullen, S. P., and Martin, S. J. (2008). Apoptosis: controlled demolition at the cellular level. *Nat Rev Mol Cell Biol*, 9(3):231–41.

Tiley, L. S., Hagen, M., Matthews, J. T., and Krystal, M. (1994). Sequence-specific binding of the influenza virus RNA polymerase to sequences located at the 5' ends of the viral RNAs. *Journal of Virology*, 68(8):5108–16.

Toyoda, T., Adyshev, D. M., Kobayashi, M., Iwata, A., and Ishihama, A. (1996). Molecular assembly of the influenza virus RNA polymerase: determination of the subunit-subunit contact sites. *J Gen Virol*, 77 (Pt 9):2149–57.

Trifonov, V. and Rabadan, R. (2009). The Contribution of the PB1-F2 protein to the fitness of Influenza A viruses and its recent evolution in the 2009 Influenza A (H1N1) pandemic virus. *PLoS Curr*, 1:RRN1006.

van Riel, D., Munster, V. J., de Wit, E., Rimmelzwaan, G. F., Fouchier, R. A. M., Osterhaus, A. D. M. E., and Kuiken, T. (2006). H5N1 Virus Attachment to Lower Respiratory Tract. *Science*, 312(5772):399.

Varga, Z. T., Ramos, I., Hai, R., Schmolke, M., García-Sastre, A., Fernandez-Sesma, A., and Palese, P. (2011). The Influenza Virus Protein PB1-F2 Inhibits the Induction of Type I Interferon at the Level of the MAVS Adaptor Protein. *PLoS Pathogens*, 7(6):1–16.

Verreck, F. A. W., de Boer, T., Langenberg, D. M. L., Hoeve, M. A., Kramer, M., Vaisberg, E., Kastelein, R., Kolk, A., de Waal-Malefyt, R., and Ottenhoff, T. H. M. (2004). Human IL-23-producing type 1 macrophages promote but IL-10-producing type 2 macrophages subvert immunity to (myco)bacteria. *Proc Natl Acad Sci USA*, 101(13):4560–5.

Volchkov, V. E., Volchkova, V. A., Muhlberger, E., Kolesnikova, L. V., Weik, M., Dolnik, O., and Klenk, H. D. (2001). Recovery of infectious Ebola virus from complementary DNA: RNA editing of the GP gene and viral cytotoxicity. *Science*, 291(5510):1965–9.

Vreede, F., Chan, A., Sharps, J., and Fodor, E. (2009). Mechanisms and functional implications of the degradation of host RNA polymerase II in influenza virus infected cells. *Virology*, 396:125–134.

Vreede, F. T. and Brownlee, G. G. (2007). Influenza virion-derived viral ribonucleoproteins synthesize both mRNA and cRNA in vitro. *Journal of Virology*, 81(5):2196–204.

Vreede, F. T., Jung, T. E., and Brownlee, G. G. (2004). Model suggesting that replication of influenza virus is regulated by stabilization of replicative intermediates. *Journal of Virology*, 78(17):9568–72.

Wagner, E., Engelhardt, O. G., Gruber, S., Haller, O., and Kochs, G. (2001). Rescue of recombinant Thogoto virus from cloned cDNA. *Journal of Virology*, 75(19):9282–6.

Watanabe, T., Watanabe, S., Shinya, K., Kim, J. H., Hatta, M., and Kawaoka, Y. (2009). Viral RNA polymerase complex promotes optimal growth of 1918 virus in the lower respiratory tract of ferrets. *Proc Natl Acad Sci USA*, 106(2):588–92.

Wharton, S. A., Belshe, R. B., Skehel, J. J., and Hay, A. J. (1994). Role of virion M2 protein in influenza virus uncoating: specific reduction in the rate of membrane fusion between virus and liposomes by amantadine. *J Gen Virol*, 75 (Pt 4):945–8.

Whittaker, G., Bui, M., and Helenius, A. (1996). The role of nuclear import and export in influenza virus infection. *Trends Cell Biol*, 6(2):67–71.

Wiley, D. C., Skehel, J. J., and Waterfield, M. (1977). Evidence from studies with a cross-linking reagent that the haemagglutinin of influenza virus is a trimer. *Virology*, 79(2):446–8.

Wise, H. M., Barbezange, C., Jagger, B. W., Dalton, R. M., Gog, J. R., Curran, M. D., Taubenberger, J. K., Anderson, E. C., and Digard, P. (2011). Overlapping signals for translational regulation and packaging of influenza A virus segment 2. *Nucleic Acids Research*, 39(17):7775–7790.

Wise, H. M., Foeglein, A., Sun, J., Dalton, R. M., Patel, S., Howard, W., Anderson, E. C., Barclay, W. S., and Digard, P. (2009). A complicated message: Identification of a novel PB1-related protein translated from influenza A virus segment 2 mRNA. *Journal of Virology*, 83(16):8021–31.

Wolff, T., O'Neill, R. E., and Palese, P. (1998). NS1-Binding protein (NS1-BP): a novel human protein that interacts with the influenza A virus nonstructural NS1 protein is relocalized in the nuclei of infected cells. *Journal of Virology*, 72(9):7170–80.

Wurzer, W. J., Planz, O., Ehrhardt, C., Giner, M., Silberzahn, T., Pleschka, S., and Ludwig, S. (2003). Caspase 3 activation is essential for efficient influenza virus propagation. *EMBO J*, 22(11):2717–28.

Xu, L.-G., Wang, Y.-Y., Han, K.-J., Li, L.-Y., Zhai, Z., and Shu, H.-B. (2005). VISA is an adapter protein required for virus-triggered IFN-beta signaling. *Mol Cell*, 19(6):727–40.

Xu, Y., Zhong, H., and Shi, W. (2010). MAVS protects cells from apoptosis by negatively regulating VDAC1. *Mol Cell Biochem*.

Yamada, H., Chounan, R., Higashi, Y., Kurihara, N., and Kido, H. (2004). Mitochondrial targeting sequence of the influenza A virus PB1-F2 protein and its function in mitochondria. *FEBS Letters*, 578(3):331–6.

Yamada, S., Hatta, M., Staker, B. L., Watanabe, S., Imai, M., Shinya, K., Sakai-Tagawa, Y., Ito, M., Ozawa, M., Watanabe, T., Sakabe, S., Li, C., Kim, J. H., Myler, P. J., Phan, I., Raymond, A., Smith, E., Stacy, R., Nidom, C. A., Lank, S. M., Wiseman, R. W., Bimber, B. N., O'Connor, D. H., Neumann, G., Stewart, L. J., and Kawaoka, Y. (2010). Biological and structural characterization of a host-adapting amino acid in influenza virus. *PLoS Pathogens*, 6(8):e1001034.

Yasuda, J., Bucher, D. J., and Ishihama, A. (1994). Growth control of influenza A virus by M1 protein: analysis of transfectant viruses carrying the chimeric M gene. *Journal of Virology*, 68(12):8141–6.

Ye, Q., Krug, R. M., and Tao, Y. J. (2006). The mechanism by which influenza a virus nucleoprotein forms oligomers and binds rna. *Nature*, 444(7122):1078–82.

Yuan, P., Bartlam, M., Lou, Z., Chen, S., Zhou, J., He, X., Lv, Z., Ge, R., Li, X., Deng, T., Fodor, E., Rao, Z., and Liu, Y. (2009). Crystal structure of an avian influenza polymerase PA(N) reveals an endonuclease active site. *Nature*, 458(7240):909–13.

Zaid, H., Abu-Hamad, S., Israelson, A., Nathan, I., and Shoshan-Barmatz, V. (2005). The voltage-dependent anion channel-1 modulates apoptotic cell death. *Cell Death Differ*, 12(7):751–60.

Zamarin, D., García-Sastre, A., Xiao, X., Wang, R., and Palese, P. (2005). Influenza virus PB1-F2 protein induces cell death through mitochondrial ANT3 and VDAC1. *PLoS Pathogens*, 1(1):e4.

Zamarin, D., Ortigoza, M. B., and Palese, P. (2006). Influenza A virus PB1-F2 protein contributes to viral pathogenesis in mice. *Journal of Virology*, 80(16):7976–83.

Zebedee, S. L., Richardson, C. D., and Lamb, R. A. (1985). Characterization of the influenza virus M2 integral membrane protein and expression at the infected-cell surface from cloned cDNA. *Journal of Virology*, 56(2):502–11.

Zell, R., Krumbholz, A., Eitner, A., Krieg, R., Halbhuber, K.-J., and Wutzler, P. (2007). Prevalence of PB1-F2 of influenza A viruses. *J Gen Virol*, 88(Pt 2):536–46.

Zhang, J., Li, G., and Ye, X. (2010a). Cyclin T1/CDK9 interacts with influenza A virus polymerase and facilitates its association with cellular RNA polymerase II. *Journal of Virology*, 84(24):12619–27.

Zhang, S., Wang, J., Wang, Q., and Toyoda, T. (2010b). Internal initiation of influenza virus replication of viral RNA and complementary RNA in vitro. *J Biol Chem*, 285(52):41194–201.

Zhirnov, O. P., Konakova, T. E., Wolff, T., and Klenk, H.-D. (2002a). NS1 protein of influenza A virus down-regulates apoptosis. *Journal of Virology*, 76(4):1617–25.

Zhirnov, O. P., Ksenofontov, A. L., Kuzmina, S. G., and Klenk, H. D. (2002b). Interaction of influenza A virus M1 matrix protein with caspases. *Biochemistry Mosc*, 67(5):534–9.

Zhirnov, O. P., Poyarkov, S. V., Vorob'eva, I. V., Safonova, O. A., Malyshev, N. A., and Klenk, H. D. (2007). Segment NS of influenza A virus contains an additional gene NSP in positive-sense orientation. *Dokl Biochem Biophys*, 414:127–33.

Zobel, A., Neumann, G., and Hobom, G. (1993). RNA polymerase I catalysed transcription of insert viral cDNA. *Nucleic Acids Research*, 21(16):3607–14.